



PACIFIC EARTHQUAKE ENGINEERING RESEARCH CENTER

Guidelines for Nonlinear Analysis of Bridge Structures in California

Ady Aviram

University of California, Berkeley

Kevin R. Mackie

University of Central Florida, Orlando

Božidar Stojadinović

University of California, Berkeley

1. Report No. 2008/03		2. Government Accession No.		3. Recipient's Catalog No.	
4. Title and Subtitle Guidelines for Nonlinear Analysis of Bridge Structures in California			5. Report Date August 2008		
			6. Performing Organization Code		
7. Author(s) Ady Aviram, Kevin R. Mackie, and Božidar Stojadinović			8. Performing Organization Report No. UCB/PEER 2008/03		
9. Performing Organization Name and Address Pacific Earthquake Engineering Research Center 325 Davis Hall MC 1792 University of California Berkeley, CA 94720			10. Work Unit No. (TRAIS)		
			11. Contract or Grant No. 65A0215		
12. Sponsoring Agency Name and Address California Department of Transportation Engineering Service Center 1801 30 th St., West Building MS-9 Sacramento, CA 95807			13. Type of Report and Period Covered Technical report; does not expire		
			14. Sponsoring Agency Code 06681		
15. Supplementary Notes This study was sponsored by the Pacific Earthquake Engineering Research Center's Program of Applied Earthquake Engineering Research of Lifelines Systems supported by the California Department of Transportation, the California Energy Commission, and the Pacific Gas and Electric Company.					
16. Abstract <i>The Guidelines for Nonlinear Analysis of Bridge Structures in California</i> presents a collection of practical and readily implementable recommendations for the modeling and analysis of highway bridges and overpasses subjected to earthquake ground motions. The specifications are applicable for Ordinary Standard Bridges in California as defined according to Caltrans Seismic Design Criteria (SDC) 2004. The main emphasis of the document is the implementation of nonlinear analysis procedures intended primarily to estimate seismic demand on critical bridge components and systems. These guidelines are not intended for evaluation of bridge system or component capacity. An extended literature review of the current engineering practice and code criteria for bridge design, modeling, and analysis was carried out concurrently throughout this document, focusing on design documents such as SDC 2004, BDS 2000, BDS 2003, ATC-32, MTD 20-1, AASHTO LRFD Specifications, 3 rd edition, to guarantee consistency with the proposed modeling guidelines and recommendations. The modeling guidelines and recommendations presented in this report are expected to ensure that accurate nonlinear modeling techniques are employed by Caltrans engineers and that PEER researchers realistically model typical Caltrans bridge systems and details. Bridge components that require special modeling considerations and nonlinear characterization are identified in this document, establishing specific criteria for the level of modeling sophistication required to estimate seismic demand with sufficient accuracy. Several incompatibilities or inconsistencies between SAP2000 and OpenSees finite element software analysis tools were investigated to identify underlying causes and to reduce possible analysis errors while using a particular structural analysis tool. Numerous recommendations for linear and nonlinear analysis of bridge structures appropriate for any structural analysis program, as well as specific details on the use of SAP2000 software for such analysis, are presented. Simultaneously, a general review and definitions related to structural dynamics, applicable to both linear and nonlinear analysis, are presented throughout.					
17. Key Words Bridges Reinforced concrete Finite element modeling Nonlinear analysis		18. Distribution Statement Unlimited			
19. Security Classif. (of this report) Unclassified	20. Security Classif. (of this page) Unclassified	21. No. of Pages 218		22. Price	

Guidelines for Nonlinear Analysis of Bridge Structures in California

Ady Aviram

Department of Civil and Environmental Engineering
University of California, Berkeley

Kevin R. Mackie

Department of Civil and Environmental Engineering
University of Central Florida, Orlando

Božidar Stojadinović

Department of Civil and Environmental Engineering
University of California, Berkeley

PEER Report 2008/03
Pacific Earthquake Engineering Research Center
College of Engineering
University of California, Berkeley

August 2008

ABSTRACT

The Guidelines for Nonlinear Analysis of Bridge Structures in California presents a collection of practical and readily implementable recommendations for the modeling and analysis of highway bridges and overpasses subjected to earthquake ground motions. The specifications are applicable for Ordinary Standard Bridges in California as defined according to Caltrans Seismic Design Criteria (SDC) 2004. The main emphasis of the document is the implementation of nonlinear analysis procedures intended primarily to estimate seismic demand on critical bridge components and systems. These guidelines are not intended for evaluation of bridge system or component capacity.

An extended literature review of the current engineering practice and code criteria for bridge design, modeling, and analysis was carried out concurrently throughout this document, focusing on design documents such as SDC 2004, BDS 2000, BDS 2003, ATC-32, MTD 20-1, AASHTO LRFD Specifications, 3rd edition, to guarantee consistency with the proposed modeling guidelines and recommendations.

The modeling guidelines and recommendations presented in this report are expected to ensure that accurate nonlinear modeling techniques are employed by Caltrans engineers and that PEER researchers realistically model typical Caltrans bridge systems and details. Bridge components that require special modeling considerations and nonlinear characterization are identified in this document, establishing specific criteria for the level of modeling sophistication required to estimate seismic demand with sufficient accuracy.

Several incompatibilities or inconsistencies between SAP2000 and OpenSees finite element software analysis tools were investigated to identify underlying causes and to reduce possible analysis errors while using a particular structural analysis tool. Numerous recommendations for linear and nonlinear analysis of bridge structures appropriate for any structural analysis program, as well as specific details on the use of SAP2000 software for such analysis, are presented. Simultaneously, a general review and definitions related to structural dynamics, applicable to both linear and nonlinear analysis, are presented throughout.

ACKNOWLEDGMENTS

This study was sponsored by the Pacific Earthquake Engineering Research Center's Program of Applied Earthquake Engineering Research of Lifelines Systems supported by the California Department of Transportation, the California Energy Commission, and the Pacific Gas and Electric Company.

This work made use of the Earthquake Engineering Research Centers Shared Facilities supported by the National Science Foundation, under award number EEC-9701568 through the Pacific Earthquake Engineering Research Center (PEER). Any opinions, findings, and conclusions or recommendations expressed in this material are those of the authors and do not necessarily reflect those of the National Science Foundation.

The authors gratefully acknowledge extensive comments and extraordinarily helpful feedback provided by Caltrans engineers, particularly Thomas Shantz, Mark Mahan, Steve Mitchell, Don Lee and Paul Chung.

CONTENTS

ABSTRACT	iii
ACKNOWLEDGMENTS	iv
TABLE OF CONTENTS	v
LIST OF FIGURES	ix
LIST OF TABLES	xi
1 INTRODUCTION	1
1.1 Scope	1
1.2 Applicability of Nonlinear Analysis	2
1.3 Model Dimension.....	4
1.4 Nonlinear Behavior	5
2 BRIDGE MODELING	7
2.1 Bridge Geometry	7
2.1.1 Compilation of General Characteristics	7
2.1.2 Coordinate System	8
2.1.3 Node and Element Definition	9
2.2 Material and Mass Properties.....	10
2.2.1 Material Properties	10
2.2.2 Translational Mass	11
2.2.3 Mass Moment of Inertia	12
2.3 Superstructure Modeling.....	13
2.3.1 Superstructure Elements	13
2.3.2 Superstructure Effective Section Properties.....	14
2.4 Cap Beam Modeling	15
2.5 Modeling of Pier Columns	18
2.5.1 General Considerations	18
2.5.2 Column Effective Section Properties	20
2.5.3 Column Moment-Curvature Analysis	21
2.5.4 Column Nonlinear Behavior	24
2.5.5 Uncoupled Plastic Hinge.....	26

2.5.6	Interaction PMM Hinge	29
2.5.7	Fiber Hinge	32
2.5.8	NL-Link	36
2.6	Boundary Conditions	39
2.6.1	Soil-Structure Interaction.....	39
2.6.2	Column Supports.....	40
2.6.3	Superstructure End Restraints.....	42
2.7	Abutment Modeling.....	43
2.7.1	Importance	43
2.7.2	Abutment Geometry and Behavior	44
2.7.3	Abutment Models.....	45
2.8	Other Issues	50
2.8.1	Damping.....	50
2.8.2	P- Δ Effects	54
2.8.3	Expansion Joints and Restrainers.....	55
3	BRIDGE ANALYSIS	57
3.1	General Considerations	57
3.2	Modal Analysis	60
3.3	Free Vibration Test	62
3.4	Static Analysis for Gravity Loads.....	63
3.5	Equivalent Static Analysis (ESA).....	64
3.6	Nonlinear Static Pushover Analysis (POA).....	65
3.6.1	Limiting Displacement Value	66
3.6.2	Pushover Load Cases	66
3.6.3	Force Pattern	67
3.6.4	Verification of Pushover Curve	70
3.7	Linear Dynamic Analysis—Response Spectrum Analysis (RSA).....	71
3.7.1	Purpose of RSA Procedure.....	71
3.7.2	Limitations of RSA Procedure.....	72
3.7.3	Acceleration Response Spectrum (ARS) Curves.....	73
3.7.4	Modal Combination Rule.....	74

3.7.5	Orthogonal Effects	74
3.7.6	RSA Using SAP2000	76
3.8	Dynamic Analysis—Time History Analysis (THA).....	78
3.8.1	Purpose of THA Procedure	79
3.8.2	Solution Methods	79
3.8.3	Time Integration Methods.....	81
3.8.4	Ground Motion Characterization	83
3.8.5	THA Using SAP2000.....	84
3.8.6	Analysis of Results.....	86
4	CONCLUSIONS.....	87
4.1	Project Goals and Objectives	87
4.2	Summary of Modeling Guidelines	88
4.3	Pending Aspects	90
	REFERENCES.....	93
	APPENDIX A.....	A-1
	APPENDIX B	B-1

LIST OF FIGURES

Fig. 2.1	Coordinate systems and degrees of freedom	9
Fig. 2.2	Rotational mass of superstructure	12
Fig. 2.3	Rotational mass of column bent.....	13
Fig. 2.4	Cap beam twist.....	17
Fig. 2.5	Expected reduction in cap beam twist displayed in pushover curve	17
Fig. 2.6	Location of column top and superstructure nodes	18
Fig. 2.7	Local deformation capacity in column bents	20
Fig. 2.8	Moment-curvature relation	22
Fig. 2.9	Idealized moment-curvature relation for static and dynamic analysis.....	22
Fig. 2.10	Pushover curves for 2D and 3D analysis using different plastic hinge options in SAP2000	25
Fig. 2.11	Column section with biaxial symmetry: simplification for moment-curvature analysis.....	29
Fig. 2.12	Fiber distribution along circular cross section	33
Fig. 2.13	Assignment of fiber hinge to plastic hinge zone.....	34
Fig. 2.14	Nonlinear parameters for NL-Link using plastic Wen model	37
Fig. 2.15	Hysteretic behavior of the NL-Link using multi-linear plastic model.....	38
Fig. 2.16	Modeling scheme of flexible foundation with adequate lateral soil resistance	41
Fig. 2.17	Modeling scheme of flexible foundation with partial lateral restraint.....	42
Fig. 2.18	Effect of superstructure end restraints in single and multi-column bent bridges	43
Fig. 2.19	Abutment components	44
Fig. 2.20	Roller abutment model.....	46
Fig. 2.21	General scheme of the simplified abutment model.....	47
Fig. 2.22	Series system for the longitudinal abutment response.....	47
Fig. 2.23	General scheme of the spring abutment model.....	48
Fig. 2.24	Damping estimation under free vibration test.....	52
Fig. 3.1	Principal modes of vibration for a multi-column bent, double-span bridge	61
Fig. 3.2	Force-deformation (P-d) or moment-rotation (M- θ) relation for bridge structure under pushover loading.....	66

Fig. 3.3	Tributary mass	62
Fig. 3.4	Force patterns for pushover analysis according to tributary mass.....	69
Fig. 3.5	Typical pushover response curve.....	70
Fig. 3.6	Rayleigh damping used for direct-integration time history analysis	85
Fig. 4.1	Summary of structural components and modeling aspects.....	89

LIST OF TABLES

Table 1.1	Components modeling.....	6
Table 2.1	Capabilities and limitations of nonlinear models for column plastic hinge in SAP2000	24
Table 2.2	Nonlinear models for column plastic hinge in SAP2000	24
Table 2.3	Summary of required values from M- ϕ analysis	27
Table 2.4	Stiffness coefficients defined in the analysis manual of SAP2000	36
Table 3.1	Analysis types applicable to Caltrans bridges	59
Table 3.2	Summary of Newmark's methods modified by delta factor.....	81
Table 4.1	Summary of main aspects of analysis procedures for Standard Ordinary bridges	90

1 Introduction

1.1 SCOPE

The Guidelines for Nonlinear Analysis for Bridge Structures in California presents a collection of general recommendations for the modeling and analysis of highway bridges and overpasses subjected to earthquake ground motions, required for the design or evaluation of the capacity and ductility of critical bridge components and systems.

The specifications and guidelines presented throughout the document are applicable for Ordinary Standard Bridges as defined according to the 2004 Caltrans Seismic Design Criteria (SDC), Section 1.1. Some general recommendations can be extended to Ordinary Nonstandard Bridges and Important Bridges, where more rigorous and advanced nonlinear analysis is required due to geometric irregularities of the bridge structure, including curves and skew, long spans or significant total length, multiple expansion joints, massive substructure components, or unstable soil conditions. For these special cases, the design engineer must exercise judgment in the application of these recommendations and refer to additional resources in situations beyond the intended scope of this document.

The introductory chapter identifies the relevance and importance of nonlinear analysis procedures in bridge structures, including the advantages and drawbacks over simpler linear analysis. The different types of nonlinearities to be incorporated in the analytical bridge model are described briefly, with a list of the critical components of the structure that require detailed inelastic modeling to guarantee a desired level of accuracy. The appropriate model dimension (2D or 3D) recommended for the application of nonlinear analysis procedures is also justified in detail.

The second chapter, titled *Bridge Modeling*, establishes a set of recommendations for the simplification of the geometry of the structure, definition of elements and materials, and the

assignment of mass and boundary conditions, among others. A thorough explanation is presented that addresses the minimum requirements in the modeling of the plastic hinge zone in column bents. The nonlinear behavior of bridge abutments and foundations, as well as expansion joints integrated along the superstructure is discussed briefly.

The third chapter, titled *Bridge Analysis*, specifies the procedures and parameters used to simulate the seismic demand on the bridge structure in the form of imposed static and dynamic forces or displacements. The chapter provides an adequate and detailed methodology that allows the design engineer to conduct modal, gravity load, pushover, response spectra, and time history analysis, as well as to analyze the resulting response data of the bridge. References are provided to other resources for the use of response spectrum curves, selection and scaling of ground motions, and definition of additional parameters required for the different nonlinear analysis types.

The guidelines document presents ample recommendations for linear and nonlinear analysis of bridge structures appropriate for any structural analysis program, as well as specific details on the use of SAP2000 for such procedures. Additionally, a general review and definitions related to structural dynamics, applicable to both linear and nonlinear analysis, are presented throughout.

The emphasis of the present document is the implementation of nonlinear analysis procedures used primarily for the estimation of the demand on a bridge structure, not the evaluation of its capacity for design purposes. The design engineer must determine the appropriate methods and level of refinement necessary to analyze each bridge structure on a case-by-case basis. This document is intended for use on bridges designed by and for the California Department of Transportation, reflecting the current state of practice at Caltrans. This document contains references specific and unique to Caltrans and may not be applicable to other parties, either institutional or private.

1.2 APPLICABILITY OF NONLINEAR ANALYSIS

The seismic demands on a bridge structure subjected to a particular ground motion can be estimated through an equivalent analysis of a mathematical model that incorporates the behavior of the superstructure, piers, footing, and soil system. To achieve confident results for a variety of earthquake scenarios, the idealized model should properly represent the actual geometry,

boundary conditions, gravity load, mass distribution, energy dissipation, and nonlinear properties of all major components of the bridge.

If a simple linear elastic model of a bridge structure is used, the corresponding analysis will only accurately capture the static and dynamic behavior of the system when stresses in all elements of the bridge do not exceed their elastic limit. Beyond that demand level, the forces and displacements generated by a linear elastic analysis will differ considerably from the actual force demands on the structure. Such a linear model will fail to represent many sources of inelastic response of the bridge including the effects of the surrounding soil according to its strain level, cyclic yielding of structural components, opening and closing of superstructure expansion joints, engagement, yielding and release of restrainers, and the complex nonlinear abutment behavior.

Nonlinear modeling and analysis allows more accurate determination of stresses, strains, deformations, forces, and displacements of critical components, results that can then be utilized for the final design of the bridge subsystems or evaluation of the bridge global capacity and ductility.

However, the precise definition of material and geometric nonlinearities in the model is a delicate task, as the resulting response values are generally highly sensitive to small variations in the input parameters. To obtain an accurate representation of the nonlinear behavior of the bridge structure, it is necessary for the design engineer to have a clear understanding of basic nonlinear analysis concepts to correctly follow the recommendations offered in the present document. A final verification of selected response parameters will be necessary at the end of the analysis to evaluate the reliability of the results by a comparison to an expected range of response, estimated previously following the recommendations of Section 3.6.4.

Unfortunately, the additional level of sophistication of the nonlinear model will also increase the computational effort required for the analysis, as well as the difficulty in the interpretation of results. The accurate estimation of the peak demand and response of the bridge structure under dynamic excitation will require the use of a large suite of ground motions, and will therefore further increase the complexity level of the analysis process and size of the output information. The present guidelines for nonlinear analysis were established by pursuing a balance between model complexities and the corresponding gain in accuracy of the results. The level of refinement in the definition of materials, elements, and sections of all major components was calibrated based on the stability of the result values.

In general, the modeling assumptions should be independent of the computer program used to perform the static and dynamic analysis; however, mathematical models are often limited by the capabilities of the computer program utilized. Therefore, the present guidelines include recommendations and limitations in the modeling and analysis of bridges by *SAP2000 Nonlinear*, a general purpose, three-dimensional structural analysis program, commonly used by Caltrans. These recommendations can be adapted accordingly for the use of other structural analysis software.

The definition of the analysis guidelines was carried out through a rigorous comparison of nonlinear analysis results obtained from several Ordinary Standard Caltrans bridge models to obtain a wide range of bridge geometries and cross sections, using different structural analysis programs such as OpenSees by UC Berkeley, SAP2000 NL by CSI, X-Section by Caltrans, Xtract by Imbsen, among others.

1.3 MODEL DIMENSION

A three-dimensional (3D) model of the structural system is required to capture the response of the entire bridge system and individual components under specific seismic demand characteristics. The interaction between the response in the orthogonal bridge directions and the variation of axial loads in column bents throughout the analysis are captured more accurately in a 3D model. This enables correct evaluation of the capacity and ductility of the system under seismic loads or displacements applied along any given direction, not necessary aligned with the principal axis of the bridge.

If the primary modes of the structure are highly correlated due to special mass distribution or geometry characteristics, they will significantly affect the dynamic response of the bridge, which must then be represented adequately through a three-dimensional model. Since the modal contribution is a key aspect in bridge analysis, and since the ground motions applied in a time history analysis are decomposed into three orthogonal directions and applied at an angle with respect to the principal axes of the bridge, a global analysis of the system is required.

A two-dimensional (2D) model consisting of plane frames or cantilevers will fail to capture the particular geometric characteristics of the entire bridge and the interaction between structural subsystems. The actual distribution of forces among critical components of the bridge is determined according to their relative stiffness. The flexibility of the superstructure in the

transverse direction, the relative stiffness of the column bents according to their heights and cross-sectional properties, and the abutment characteristics are imperative aspects to consider in the analysis that cannot be modeled correctly using a two-dimensional model.

The use of combinations rules for the interaction of responses in orthogonal directions to estimate the maximum demand on critical bridge components are applicable only for linear elastic structures, and could result in significant errors when extrapolated to the inelastic range. Particularly in the case of special bridge systems with irregular geometry, curved or skewed, with multiple transverse expansion joints, massive substructure components, and foundations supported by soft soil, the dynamic response characteristics exhibited are not necessarily obvious beforehand and may not be captured in a separate subsystem analysis. According to Section 5.2 of SDC 2004, for structures supported on highly non-uniform soils, a separate analysis of each individual frame is recommended in addition to the conventional three-dimensional multi-frame analysis.

Local analysis of an individual component or subsystem may be used to assess the critical values of their strength and ductility capacity and provide a general approximation of the expected range of response of the entire bridge system. If desired, local analysis is performed in the transverse and longitudinal directions for bridge column cross sections with biaxial symmetry, following the recommendations of Sections 5.3–5.5 of SDC 2004. Local analysis fails to capture the interaction between different components or subsystems of the bridge, and could therefore result in significant errors in the estimation of the demand on the analyzed component.

1.4 NONLINEAR BEHAVIOR

Two categories of nonlinear behavior are incorporated in the bridge model to properly represent the expected response under moderate to intense levels of seismic demand. The first category consists of inelastic behavior of elements and cross sections due to nonlinear material stress-strain relations, as well as the presence of gaps, dampers, or nonlinear springs in special bridge components. The second category consists of geometric nonlinearities that represent second-order or P- Δ effects on a structure, as well as stability hazard under large deformations, where the equilibrium condition is determined under the deformed shape of the structure. The second nonlinearity category is incorporated directly in the analysis algorithm.

The following table summarizes the recommended criteria for inelastic modeling of the primary elements comprising an Ordinary Standard Bridge structure. If the modeling criteria chosen by the design engineer diverge from the present guidelines, i.e., a certain component is modeled as linear elastic instead of nonlinear; the resulting level of accuracy and reliability of the analysis will decrease considerably. The specific modeling methodology for each component will be explicitly detailed and clarified in Chapter 2.

Table 1.1 Component modeling.

Component	Linear-Elastic	Nonlinear
Superstructure	X	
Column–plastic hinge zone		X
Column–outside plastic hinge zone	X	
Cap beam	X	
Abutment– transverse		X
Abutment–longitudinal		X
Abutment–overturning		X
Abutment– gap		X
Expansion joints		X
Foundation springs	X	
Soil-structure interaction	X	

2 Bridge Modeling

2.1 BRIDGE GEOMETRY

2.1.1 Compilation of General Characteristics

The following information is required for the modeling of the basic bridge structural geometry:

- Total length of the bridge (L_{Total})
- Number of spans and length of each superstructure span
- Total superstructure width ($W_{superstructure}$)
- Superstructure cross-sectional geometry
- Number and clear height of each column bent (H_{col})
- Column cross-sectional dimension in the direction of interest (D_c)
- Distance from column top to center of gravity of superstructure ($D_{c.g.}$)
- Length of cap beam to centroid of column (L_{cap})
- Cap beam width (B_{cap})
- Location of expansion joints
- Support details for boundary conditions

The definition of the individual behavior of major bridge components entails the following data:

- Concrete material properties for concrete of superstructure (f'_c, E_c)
- Concrete and reinforcing steel material properties ($\sigma-\epsilon$) of column bents
- Reinforcement details of column bent cross section
- Foundation soil geotechnical properties
- Abutment general geometry
- Number and properties of abutment bearing pads
- Size of expansion joints

2.1.2 Coordinate System

The coordinate system used for the modeling and analysis of the bridge is shown in Figure 2.1. The global X-axis is in the direction of the chord connecting the abutments, denoted as the longitudinal direction; the global Y-axis is orthogonal to the chord in the horizontal plane, representing the transverse direction; while the global Z-axis defines the vertical direction of the bridge. For the analysis and design of elements of the bridge using two-noded elements, a local coordinate system is used, as shown in Figure 2.1.

It is recommended that the orientation of all frame elements in a bridge structure without a skew coincides with the positive direction of the global axis; namely, the coordinate of node i of the frame will be smaller than node j . In the case of bridge structures with skew supports, the orientation of the superstructure elements should coincide with the skew coordinates, not the global axis. The nomenclature for twist or torsion, as well as axial force or deformation of an element will be denoted as the *direction 1-1* or axial direction. Shear forces and deformations, as well as moments and rotations will be specified as *directions 2-2* or *3-3* (see Fig. 2.1).

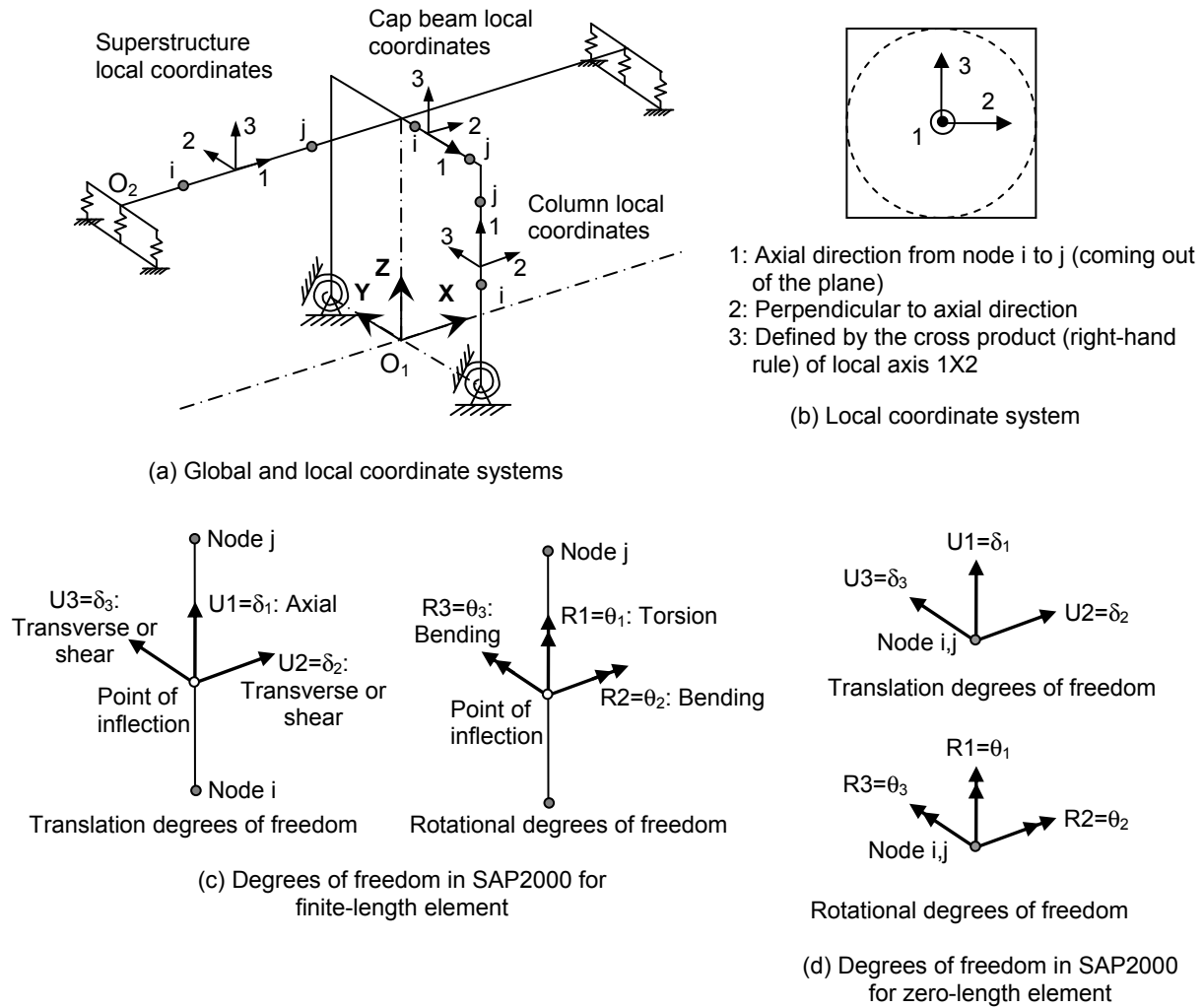


Fig. 2.1 Coordinate systems and degrees of freedom.

2.1.3 Node and Element Definition

For the seismic analysis of highway bridges it is customary to use three-dimensional beam-column elements (line or frame elements) with corresponding cross-sectional properties, to represent the superstructure and the components of the bents (columns and cap beams). The geometry, nodes, and connectivity of the elements in the model will be determined according to plans, following the recommendations of this chapter. The present guidelines document focuses on the three-dimensional spine model of the bridge structure with line elements located at the centroid of the cross section, following the alignment of the bridge; however, some of the

recommendations offered in the document can be extended to three-dimensional shell or frame grillage models of the bridge.

ATC-32 (1996) suggests that a minimum of three elements per column and four elements per span shall be used in a linear elastic model. However, it is recommended for all analysis cases that the superstructure, cap beam, and column bents be discretized using a minimum of five elements of equal length, except for spans with intermediate hinges or expansion joints. In such cases, the nodes of the superstructure must coincide with the location of those special links.

This discretization helps approximate the distributed (translational) mass of the bridge components with lumped masses at the nodes between segments, generated automatically by SAP2000 (see Section 2.1.3). The additional assignment of rotational mass of the superstructure is required in the model, as well as of the columns, when a global torsional mode is excited under certain dynamic conditions (see Section 2.2.3). The use of fewer (displacement-based) elements, even for the linear elastic superstructure element, could result in loss of accuracy in the mass formulation, and therefore is discouraged unless distributed mass properties can be specified. The nodes lie along the line of the geometric centroids of the bridge's components, and are assigned a translational and rotational mass corresponding to the tributary mass associated with each node, according to Section 2.2.

2.2 MATERIAL AND MASS PROPERTIES

2.2.1 Material Properties

The expected material strength and stress-strain (σ - ϵ) relation should be used for unconfined and confined concrete, as well as reinforcing steel, to more accurately capture the bridge's capacity and behavior. The reinforcement details of the piers and other major bridge components are required. The properties of normal weight Portland Cement Concrete should be applied according to Section 3.2.6 of SDC 2004, and the Mander et al. (1988) model is to be used to represent the uniaxial stress-strain behavior for unconfined and confined concrete. It is recommended that the concrete tensile strength for both confined and unconfined concrete be included. The tensile strength is estimated by ACI 318 as $f_t = 7.5\sqrt{f'_c}$ (psi) for normal weight concrete, defined with an initial Modulus of Elasticity E_c according to Section 3.2.6 of SDC 2004. The initial stiffness of RC columns can be significantly altered due to the tensile resistance of uncracked concrete fibers between cracks, denoted as tension-stiffening of a section.

When a moment-curvature ($M-\phi$) analysis is to be carried out for the concrete column (see Section 2.5.3), the properties of the steel longitudinal and transverse reinforcement are to be used according to Sections 3.2.2 and 3.2.3 of SDC 2004 Guidelines for Steel ASTM A-706. The steel material model with symmetric behavior in tension and compression assumes an initial elastic behavior up to yield, a yield plateau, followed by a strain-hardening region. The onset of strain hardening and the reduced ultimate tensile strain defining the point of fracture are defined according to bar size for each column cross section. According to SDC 2004, Sections 3.2.3, the yield stress F_y and ultimate stress F_u for all bar sizes are to be taken as 68 and 95 ksi, respectively.

The definition of the $\sigma-\epsilon$ relation in SAP2000 must be carried out with a sufficient number of points in the curve to capture the nonlinear behavior of the material, specifically the degradation of strength beyond the elastic or yield point in confined and unconfined concrete, and the variation in the strain-hardening slope in the reinforcing steel.

The material and mass properties for all load cases other than seismic should be selected to comply with the AASHTO LRFD Specifications, 3rd edition.

2.2.2 Translational Mass

The weight of normal concrete is specified by SDC 2004 Section 3.2.6 as $w=143.96 \text{ lb/ft}^3$ (2286.05 kg/m^3) and therefore a mass of $\rho_{R/C}=4.471 \text{ lb-sec}^2/\text{ft}^4$ ($233.03 \text{ kg-sec}^2/\text{m}^4$) is to be used when specifying material properties for confined and unconfined concrete. It is desired to approximate all bridge elements with a distributed mass along their length. However, the program SAP2000, as well as other analysis software packages, automatically calculates the translational mass of all longitudinal elements in the three global directions of the bridge (longitudinal, transverse, and vertical) and assigns them as lumped mass at each node, based on tributary lengths. To approximate the distributed mass with lumped masses, a sufficient number of nodes and segments are to be defined, with a minimum recommended of 5 segments per superstructure span and column bent (see Section 2.1.3).

2.2.3 Mass Moment of Inertia

Additional assignment of rotational mass (mass moment of inertia) is required for the superstructure and the column bents of a spine model of the bridge, since it is not generated automatically in SAP2000. The assignment of superstructure rotational mass helps represent with greater accuracy the dynamic response and fundamental modes of the bridge associated with the transverse direction. The rotational moment of inertia of the superstructure shall be assigned according to the following (see Fig. 2.2):

$$M_{XX} = \frac{Md_w^2}{12} = \frac{(m/L)L_{trib}d_w^2}{12} \quad (1.1)$$

Where:

- M_{XX} Rotational mass of superstructure, assigned as lumped mass in axial direction $I-I$ or global $X-X$ (R1)
- M Total mass of superstructure segment, tributary to the node
- m/L Mass of superstructure per length ($\rho_{R/C} A_{superstructure}$)
- L_{trib} Tributary length according to node definition
- d_w Superstructure width, which can be taken as average of bottom and top flanges

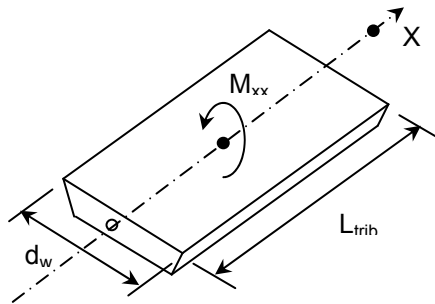


Fig. 2.2 Rotational mass of superstructure.

The global torsional mode of the entire bridge, defined in Section 3.2 (see Fig. 3.1), must be captured accurately through a correct mass definition. The torsional mode is generally not dominant for most real structures with realistic abutment model and boundary conditions. However, if such mode of deformation is a dominant and primary mode of response that significantly affects the seismic behavior of the entire structure, an additional rotational mass assignment is required for the column bents, according to the following (see Fig. 2.3):

$$M_{ZZ} = \frac{1}{2} M R_{col}^2 = \frac{(m/L) L_{trib} D_c^2}{8} \quad (1.2)$$

Where:

- M_{ZZ} Rotational mass of column, assigned as lumped mass in local direction *I-I* or global direction *Z-Z* (R3)
- M Total mass of column segment, tributary to the node
- R_{col} Half of the average column dimension equivalent to the radius of circular columns
- m/L Mass of column per length ($\rho_{R/C} A_{col}$)
- L_{trib} Tributary length according to node definition
- D_c Column dimension, which can be taken for cross sections with biaxial symmetry as the average of the transverse and longitudinal dimensions

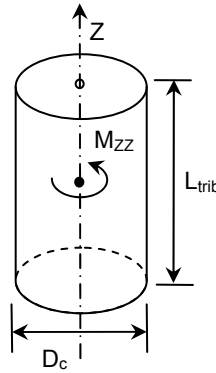


Fig. 2.3 Rotational mass of column bent.

2.3 SUPERSTRUCTURE MODELING

2.3.1 Superstructure Elements

The superstructure elements will be modeled as linear-elastic beam-column elements with material properties corresponding to cracked reinforced concrete. No nonlinearities are considered for the superstructure elements for an overall analysis of the bridge, since other elements such as the columns and abutments are designed to undergo inelastic excursions, while the superstructure is protected by a capacity design and is expected to remain in the elastic range of response. The elevation (node height) of the superstructure frame elements will be defined at the elevation of the superstructure centroid, H_{super} (as shown in Fig. 2.6).

The superstructure frame properties for a box-girder cross section can be defined in SAP2000 as a General Property or as a Section Designer (SD Section). If the General Property is used, the values of the cross-sectional area (A), torsional constant (J), moments of inertia (I_{22} and I_{33}), shear areas (A_{v2} and A_{v3}), elastic and plastic section moduli (S_{22} , S_{33} , Z_{22} , and Z_{33}), and radii of gyration (r_{22} and r_{33}) in the vertical and transverse directions of the superstructure, are to be specified. These values must be estimated accurately using a separate spreadsheet or program based on elementary solid mechanics theory, assuming multiply-connected thin-walled section subjected to axial load, bending, shear, and torsion (Ugural and Fenster 1995).

The shear area of the superstructure must also be approximated accurately, since elastic shear deformations are included in the stiffness computation of the bridge in SAP2000. Incorrect specification of the shear area will significantly alter the superstructure's modes of deformation. The area of the box-girder webs can be used to compute the shear area in the vertical direction, while for the transverse direction the average area of the top and bottom flanges can be used. The shear coefficients can be determined from SD Section in SAP2000 or the principles of Timoshenko's beam theory (Timoshenko 1969).

If the SD Section by SAP2000 is used, the program will automatically calculate the cross-sectional properties, according to the specified geometry of the superstructure and columns. A solid rectangular cross section defined with total depth and width of the superstructure should not be used, since it will overestimate the mass and stiffness of the bridge's superstructure, and alter the results for the modal, linear, and nonlinear analysis cases.

2.3.2 Superstructure Effective Section Properties

Elastic analysis assumes a linear relationship between deformation and strength. Concrete members exhibit nonlinear response even before reaching an idealized yield strength limit. Section properties, flexural rigidity $E_c I$, and torsional rigidity $G_c J$, shall reflect the cracking that occurs before the limit state is reached. The effective moments of inertia I_{eff} and J_{eff} shall be used to obtain realistic values for the structure's period and the seismic demands generated from the analysis.

I_{eff} in box girder superstructures is dependent on the extent of cracking and the effect of the cracking on the element's stiffness. I_{eff} for conventionally reinforced concrete box girder sections can be estimated between $0.5I_g$ – $0.75I_g$, according to SDC 2004, Section 5.6.1.2. The

lower and upper bounds represent lightly and heavily reinforced sections, respectively. The location of the pre-stressing steel's centroid and the direction of bending have a significant impact on how cracking affects the stiffness of pre-stressed members. Multi-modal analyses are incapable of capturing the variations in stiffness caused by moment reversal. Therefore, no stiffness reduction is recommended for pre-stressed concrete box girder sections ($I_{\text{eff}}=I_g$), as specified by SDC 2004, Section 5.6.1.2.

Reductions to I_g similar to those specified for box girders can be used for other superstructure types and cap beams. A more refined estimate of I_{eff} based on $M-\phi$ analysis may also be required for lightly reinforced girders and precast elements.

A reduction of the torsional moment of inertia is not required for bridge superstructures that meet the Ordinary Bridge requirements in Section 1.1 of SDC 2004 and do not have a high degree of in-plane curvature. For special bridges, the torsional constant J_{eff} can be taken to be $0.20J_g$. The non-reduced properties of the cross section are used to model axial stiffness (A_g) and transverse shear stiffness (A_v).

ATC-32 (1996) recommends that the effective box girder stiffness be reduced because of shear lag effects near the piers. The stiffness in these regions is based on an effective width that is no greater than the width of the column plus twice the cap beam depth. If this width is nearly the entire width of the superstructure, no reduction in stiffness due to shear lag is required in the model.

Pre-stress forces will be assigned to the superstructure elements only when nonlinear behavior is expected for the superstructure. However for all Ordinary Caltrans bridges, cracked elastic behavior can be assumed for seismic conditions.

2.4 CAP BEAM MODELING

The cap beam is a concrete element connecting the superstructure and the column bents, helping a multi-column bent bridge resist, through frame action, lateral loads or displacements applied primarily in the transverse direction of the bridge. For single-column bent bridges, the cap beam is built to facilitate the connection of the bent to the superstructure and reinforce the joint. The Bridge Modeler feature available in latest versions of SAP2000 resolves many of the issues regarding cap beam modeling discussed in the present section.

In the case of multi-column bent bridges, an elastic element representing the cap beam should be modeled as a frame element with a solid rectangular cross section with dimensions according to plans. The material properties used for this element include the Modulus of Elasticity E_c , Weight w_c , and Mass $\rho_{R/c}$ of reinforced concrete, as defined by SDC 2004, Section 3.2.6. The definition of a σ - ϵ relationship of the concrete material, as well as other properties, is not required for this elastic element.

The cap beam is connected through rigid or moment connections to the superstructure since both elements are usually constructed monolithically without joints. The use of joint constraints between column top nodes, representing node slaving or a rigid diaphragm perpendicular to the Global Z direction, will produce an overestimation of the bridge's stiffness, primarily in the transverse direction. The flexibility of the cap beam should be accounted for in the model, instead of joint constraints, if sufficient design details are specified for such an element. Since the concrete superstructure and cap beam are cast simultaneously into a single element, the superstructure's flexural stiffness enhances the torsional stiffness of the cap beam. The actual dimensions of the cap beam-superstructure system resisting torsion are greater than the cross-sectional dimensions of the cap beam element exclusively. The torsional constant of the cap beam J should therefore be modified by an amplification factor C by applying Property Modifiers to that value, as follows (see Fig. 2.4):

$$J_{eff} = J_g \times C \quad (2.1)$$

Where:

- C Torsional constant amplification factor, determined with a minimum value in the order of 10^2
- J_{eff} Effective torsional resistance of the cap beam
- J_g Torsional resistance of the cap beam gross cross section, calculated automatically by SAP2000 according to cross section geometry

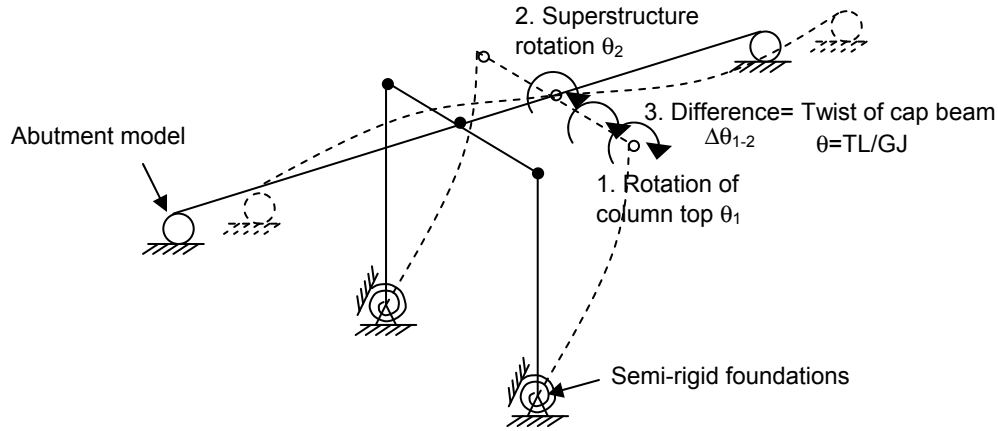


Fig. 2.4 Cap beam twist.

In order to model the correct torsional stiffness of the cap beam-superstructure system, it is necessary to verify that the cap beam twist, which is the difference between the column top rotation and the superstructure rotation, has reduced to 5% of its original value obtained without amplification factors (see Fig. 2.5). The value of the C factor should be adjusted accordingly by multiples of 10 until reaching the desired value of the cap beam twist and approximating rigid element behavior.

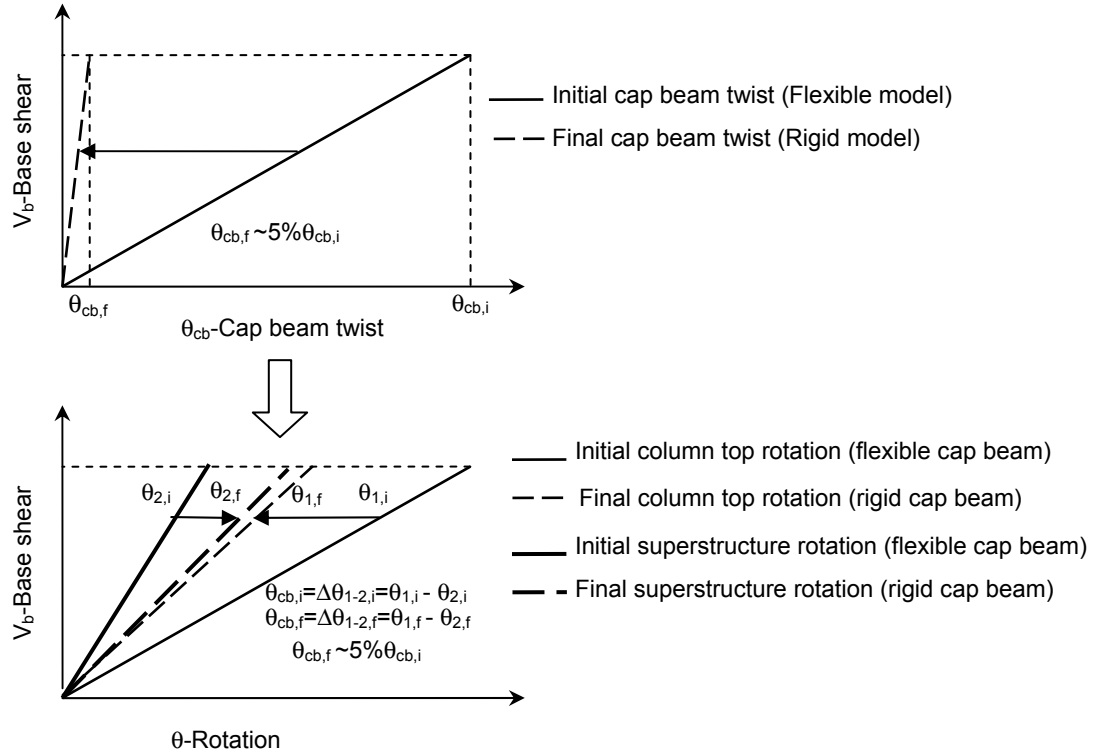


Fig. 2.5 Expected reduction in cap beam twist displayed in elastic pushover curve.

The additional torsional stiffness provided by the modification factor to the cap beam will reduce the cap beam twist and produce an increase in column-top fixity to the superstructure and consequently in the lateral stiffness of the bridge in the longitudinal direction. As a result of this modeling assumption, the load demand and inelastic base shear will increase, while a reduction in the displacement capacity and ductility of the bridge will take place simultaneously. This behavior and additional effects will more accurately approximate the actual response of the bridge under loads in the longitudinal and transverse directions.

2.5 MODELING OF PIER COLUMNS

2.5.1 General Considerations

According to the bridge geometry described in specific plans and Section 3.1 of SDC 2004, the foundation of the bridge column will be defined at the level of base fixity. The clear height of the column H_{col} is to be taken according to Figure 3.3 of SDC 2004 Guidelines. The top of the column will be defined at a distance of $D_{c.g.}$ (difference between the bottom flange or slab and the vertical centroid of the superstructure cross section) above the clear height of the bridge column, as shown in Figure 2.6:

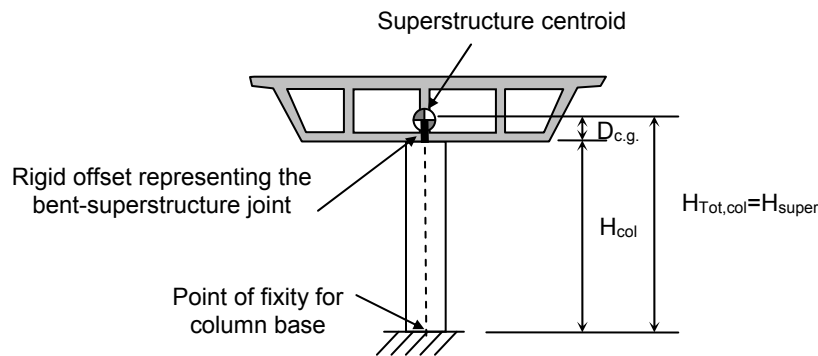


Fig. 2.6 Location of column top and superstructure nodes.

Inelastic three-dimensional beam-column elements are used to model the column and shaft for each of the piers in the bridge. A beam-column element connects each of the nodes at the geometric centroid of the column cross section, using a minimum of five elements to model the column, according to Section 2.1.3.

It is recommended to define a separate segment at the column top with the length $D_{c.g.}$ defined above, representing the portion of the column embedded in the bent cap. An end (rigid)

offset should be assigned in SAP2000 to the column top with a length of $D_{c.g.}$. The offset should be specified with a rigid-zone factor of 1.0 to account for the high stiffness provided by the joint.

The local ductility or displacement capacity of the column bent is idealized according to Section 3.1.3 of SDC 2004 with one or two cantilever segments, representing bending of the column bents in single or double curvature, according to the boundary conditions provided at the top and bottom of the element. The relative rigidity of the superstructure with respect to the column, determined by the aspect ratio (span length to column height), the cross section of the elements, the overall geometry of the bridge, and the soil-structure interaction properties, will play a key role in defining these boundary conditions. In addition, for multi-column bent bridges, the rigidity of the bent cap will also have a significant influence on the degree of frame action. Section 2.2 of SDC 2004 describes the effect of foundation type and flexibility, as well as cap beam properties on the force-deformation relation of column bents (see Section 2.7 of the present guidelines).

The idealized cantilever models assume the formation of plastic hinges at the end of each segment near the point of fixity of the column. The curvature of the column increases linearly with height from the point of inflection (zero moment) to the point of fixity (maximum moment). In the plastic hinge zone, the plastic moment and curvature are assumed constant, as seen in Figure 2.7 or Section 3.1.3 of SDC 2004. The length of the plastic hinge in the column will be approximated following Section 7.6.2 of SDC 2004 and should be introduced into the model as a separate segment at the column bottom and top. A preliminary linear static analysis of the bridge model in both the transverse and longitudinal directions of the bridge (see Section 3.5) allows the determination of the moment distribution between the top and bottom hinges and the possible locations where plastic hinges may form. For the case of loading in the transverse direction of the bridge, it is expected that plastic hinges will develop at both the column top and bottom, if a rotational restraint detail is provided at the base of the columns, due to frame action in multi-column bent bridges. In single-column bent bridges with long-span superstructure, plastic hinges are most likely to develop at the column bottom due to cantilever action in the transverse direction. According to the boundary conditions and torsional restraint of the superstructure ends provided by the abutment system, double curvature could develop in the column bents of single-column bents bridges for loading in the transverse direction, forming plastic hinges at both column top and bottom. For loading in the longitudinal direction of the bridge, the behavior of single and multi-column bent bridges is similar and equally governed by the degree of

foundation fixity and frame action through the superstructure. The plastic hinge zone is assigned an inelastic model according to Section 2.5.3, while the rest of the element outside the plastic hinge is assigned an elastic frame element with a solid cross section, according to its geometry, using effective section properties (see Section 2.5.2).

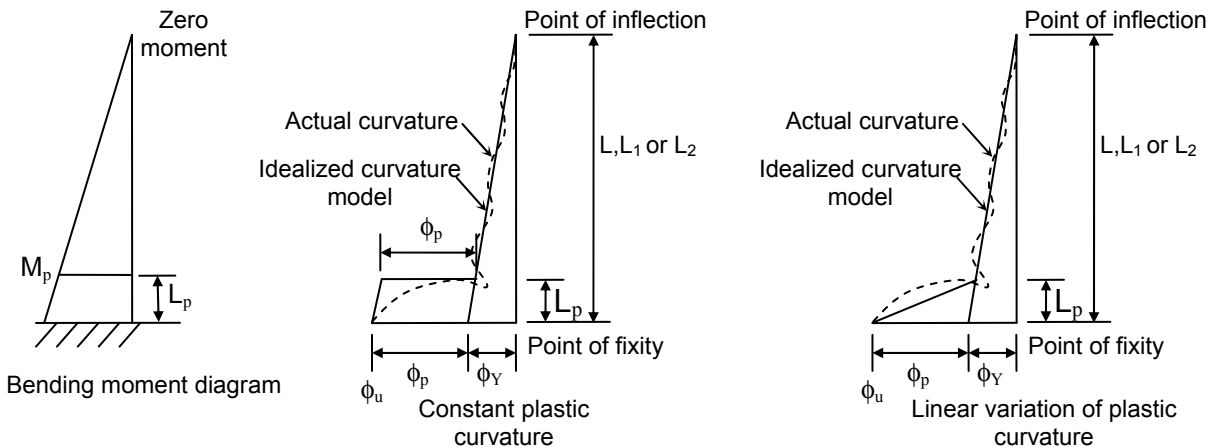


Fig. 2.7 Local deformation capacity in column bent.

2.5.2 Column Effective Section Properties

For column bents designed as ductile members according to SDC 2004, the cracked flexural stiffness I_{eff} should be used, estimated from Figure 5.3 of SDC 2004 based on the level of axial load and transverse reinforcement, or from the initial slope of the $M-\phi$ curve between the origin and the point designating the first reinforcement bar yield (ϕ_y, M_y). Assuming the level of axial load is derived from the column dead load, equation 5.1 from SDC 2004 defines I_{eff} as follows:

$$I_{eff} = \frac{M_y}{E\phi_y} \quad (2.2)$$

The use of the effective cross-sectional properties is a common practice recommended by the ACI 318-2005 building code, anticipating the development of cracking in reinforced concrete girders and columns due to gravity and wind loads. After several cycles of motion due to lateral loads such as wind pressure or earthquake ground motion, the inflection point in column bents oscillates with respect to its original location. Therefore, for seismic analysis, the effective inertia of the column is used for the entire length of the element.

The torsional stiffness of concrete members is greatly reduced after the onset of cracking. The torsional moment of inertia for columns is reduced according to the following:

$$J_{eff} = 0.2J_g \quad (2.3)$$

Where:

- J_{eff} Effective torsional resistance of the column
- J_g Torsional resistance of the column gross cross section, calculated automatically by SAP2000 according to cross section geometry

In SAP2000 the calculation of the bridge's stiffness automatically accounts for shear deformation, using the shear area properties of the elements' cross section. According to Section 3.6 of SDC 2004, a reduction to the gross area of the column due to the combined effects of flexure and axial load is carried out to estimate the expected shear capacity of ductile concrete elements such as column bents. Since a reduction in the axial capacity of the column is not likely, the axial stiffness of the column is obtained using the area properties of the gross section. It is therefore recommended to introduce a property modifier factor to the shear area of the column elements gross section in SAP2000, according to the following:

$$A_{v,eff} = 0.8A_{v,g} \quad (2.4)$$

Where:

- $A_{v,eff}$ Effective shear area of the column
- $A_{v,g}$ Shear area of the column gross cross section, calculated automatically by SAP2000 according to cross section geometry or defined by user as a General Property

2.5.3 Column Moment-Curvature Analysis

The plastic moment capacity of all ductile concrete members of the bridge, particularly column bents, shall be calculated by moment-curvature ($M-\phi$) analysis based on expected material properties, according to Section 3.3.1 of SDC 2004. Moment-curvature analysis derives the curvatures associated with a range of moments for a cross section subjected to monotonic loading, based on the principles of strain compatibility and equilibrium of forces. The $M-\phi$ curve can be idealized with an elastic-perfectly-plastic response to estimate the plastic moment capacity of a member's cross section; however, a bilinear model accounting for strain hardening of steel is preferred (see Fig. 2.8). The elastic portion of the idealized curve should pass through the point marking the first reinforcing bar yield and the expected nominal moment capacity, M_{ne}

representing the limit of elastic behavior when the concrete strain ϵ_c reaches 0.003. The idealized plastic moment capacity is obtained by balancing the areas between the actual and the idealized $M-\phi$ curves beyond the first reinforcing bar yield point, as shown in Figure 2.8.

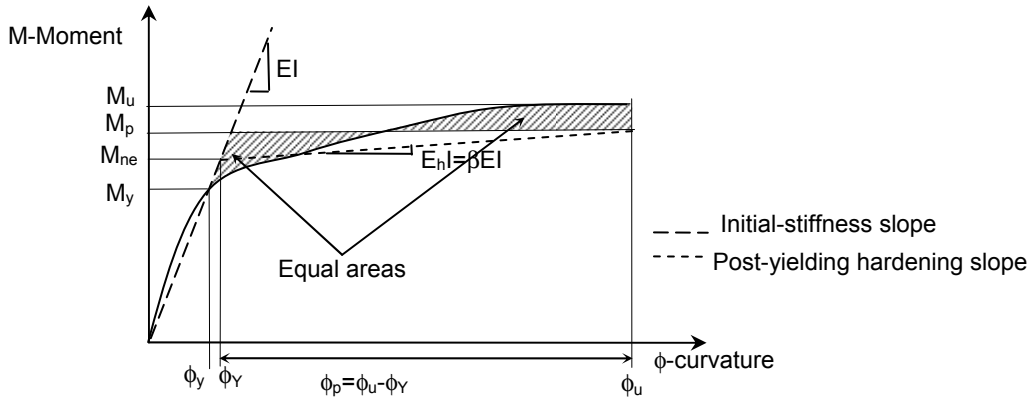


Fig. 2.8 Moment-curvature relation.

The values corresponding to the yield point (ϕ_y, M_y) , nominal point (ϕ_Y, M_{ne}) , ultimate capacity (ϕ_u, M_u) , plastic capacity (ϕ_u, M_p) and curvature ductility $(\mu_\phi = \phi_u / \phi_y)$, are computed based on an $M-\phi$ analysis of the column under a certain level of axial load. For this calculation, the use of programs such as X-Section by Caltrans, Xtract by Imbsen, or SD-Section by SAP, are recommended. The resulting bilinear models considered for static and dynamic analysis are presented in Figure 2.9 and discussed in more detail in Section 2.5.3.

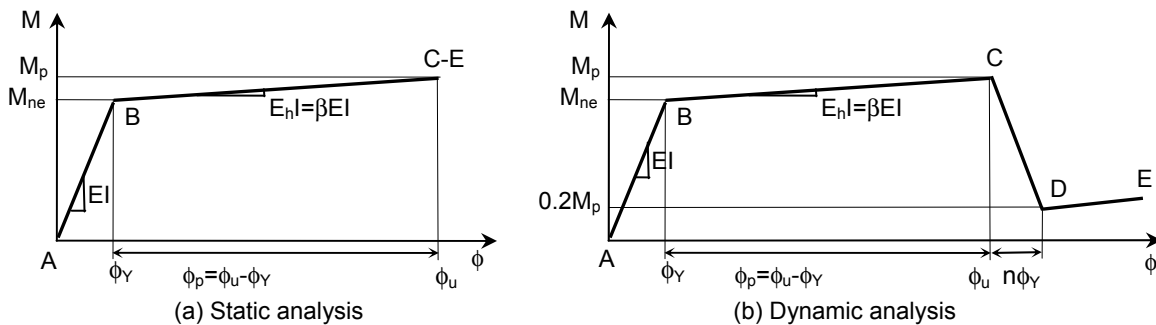


Fig. 2.9 Idealized moment-curvature relation for static and dynamic analysis.

The following considerations are taken into account for the moment-curvature analysis:

- The basic level of axial load for the column top will be defined as the dead load on the column, including superstructure tributary and self weights. For the column bottom, the

column self weight is included as well. If the difference between the axial load at the column top and bottom is less than 10%, a further simplification can be made by assuming the same axial load for both locations. The dead load corresponds generally to a ratio P/P_n of the column between 0.05 and 0.35, where P_n is the nominal bearing capacity of the cross section, estimated according to ACI 318 as $f'_c A_g$.

- Fluctuations in the column axial load will occur due to vertical excitation and frame action during a seismic event represented by static lateral loads or dynamic analysis caused by ground motions. The maximum range of column axial load is typically estimated between $(-)0.05P_n$ in tension and $(+)0.15P_n$ in compression. This range must be verified in future research of bridge structures under combined horizontal and vertical excitation using an acceptable and realistic abutment model. Two additional moment-curvature curves should be obtained for these two levels of column axial load. These moment-curvature curves will be used in the definition of the Interaction PMM Hinge for the corresponding level of column axial load. The SAP2000 program automatically interpolates between these limiting levels of axial loads.
- The column cross section must be represented in the analysis with a sufficient number of fibers and include the correct dimensions and reinforcement of the cross section.
- The expected material strength and stress-strain (σ - ϵ) relation for concrete and steel is used according to chapter 3 of SDC 2004 and Section 2.2.1 of the present document.
- The failure of the cross section will be defined as fracture of the steel rebar when reaching the Ultimate Strain ϵ_{su} or the crushing of confined concrete at ϵ_{cu} . According to Section 3.2.2 of SDC 2004, if the moment-curvature relationship includes strength degradation, the Ultimate Strain limit is used, ϵ_{su} . Otherwise, the Reduced Ultimate Strain Limit, ϵ_{suR} , is used to compute the M - ϕ curve.
- Plastic capacity M_p is defined by balancing the areas between the actual and the idealized M - ϕ curves beyond the yield point, as defined in Section 3.3.1 of SDC 2004.
- The plastic curvature ϕ_p is defined between the ultimate and yield curvatures $\phi_p = \phi_u - \phi_Y$ and the ductility capacity of the column $\mu_c = \phi_u / \phi_Y$, as shown in Figure 2.7.
- The moment-curvature analysis of column cross sections with biaxial symmetry must be repeated for strong and weak axis bending under gravity axial load and other specified levels of axial load.

2.5.4 Column Nonlinear Behavior

The nonlinearity and hysteretic behavior in the column is idealized through discrete plastic hinge models, assigned to pre-determined locations of the column, as described in Section 2.5.1. These models require an approximate plastic hinge length to convert plastic curvature to plastic rotation, defined in Section 7.6.2 of SDC 2004. Several modeling options can be employed in SAP2000 to represent the behavior of the column plastic hinge. Some of the main capabilities and limitations of these nonlinear models for column plastic hinge are presented in Table 2.1.

Table 2.1 Capabilities and limitations of nonlinear models for column plastic hinge in SAP2000.

Nonlinear Option	Coupled behavior M2-M3	Axial-moment interaction: P-M2-M3	Degrading behavior	Ductility estimation	Numerical stability	Low computational effort
<i>Uncoupled Hinge M2,M3</i>			X	X		X
<i>Interaction PMM Hinge</i>	X	X	X	X		X
<i>Fiber PMM Hinge</i>	X	X	X		X	
<i>NL-link- Plastic Wen</i>					X	X
<i>NL-link- Multi-Linear Plastic</i>			X	X	X	X

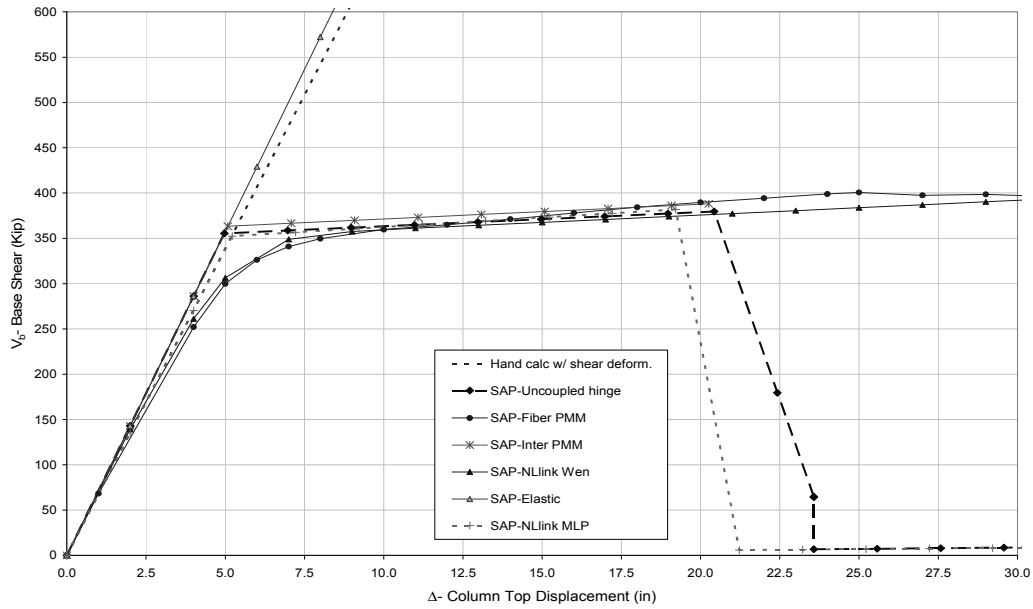
Based on the features presented in Table 2.1 and the observations of the following sections, the use of these nonlinear models for column plastic hinge is recommended for the following analysis types:

Table 2.2 Nonlinear models for column plastic hinge in SAP2000.

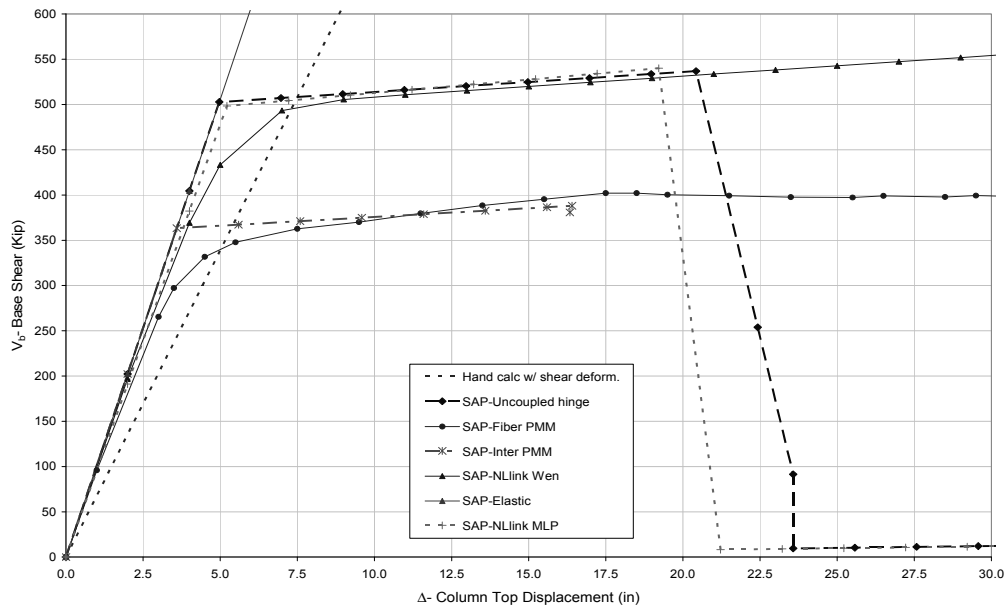
Nonlinear Option ¹	2D Pushover Analysis (L or T directions)	3D Pushover Analysis (Simultaneous L and T directions)	Dynamic 2D (THA with L,V or T,V components)	Dynamic 3D (THA-Simultaneous L,T and V components)
<i>Uncoupled Hinge M2,M3</i>	X			
<i>Interaction PMM Hinge</i>	X	X		
<i>Fiber PMM Hinge</i>	X	X	X	X
<i>NL-link- Plastic Wen</i>	X		X	
<i>NL-link- Multi-Linear Plastic</i>	X		X	

¹ The applicability, limitations, and modeling recommendations for each nonlinear hinge option are presented in detail in the following sections.

The results for 2D and 3D pushover analysis for a typical column bent are presented in Figure 2.10, where an overestimation of the plastic capacity (Fig. 2.10b) is clearly observed when the loading direction does not align with the principle axis of the bridge and an uncoupled model is used.



(a)



(b)

Fig. 2.10 Pushover curves for 2D and 3D analysis using different plastic hinge options in SAP2000: (a) longitudinal or transverse pushover and (b) 45° pushover.

The NL-link and the uncoupled hinge models are defined for a unique level of axial load, corresponding to the column dead load, thus failing to represent the variation of the column capacity and ductility that occur due to the fluctuation of column axial load during different loading conditions of the bridge. Therefore, a plastic hinge model which does not capture the axial-moment interaction properly will result in significant inaccuracy when axial load fluctuations control the capacity. These models are therefore limited to simple preliminary 2D analysis of the bridge.

A fiber model (Fiber PMM in SAP2000) as well as an idealized moment-rotation model for different axial load levels (Interaction PMM Hinge in SAP2000) will enable the correct evaluation of the column behavior under an applied curvature and axial strain to the cross section. Therefore, the use of these models is recommended for three-dimensional static and dynamic analysis. Other computational aspects related to convergence and numerical stability during dynamic analysis cause difficulties in the use of the interaction PMM hinge model for such analysis.

2.5.5 Uncoupled Plastic Hinge

2.5.5.1 General Characteristics

The column plastic hinge can be modeled in SAP2000 as a lumped plasticity model, using the uncoupled hinge in the direction of bending M2, as well as M3, corresponding to local axis 2-2 and 3-3 (transverse and longitudinal directions of the bridge, respectively). In each orthogonal bending direction, the longitudinal and transverse properties of the column cross section must be taken into account. The column axial dead load is used including superstructure tributary and self weight. A separate moment-curvature analysis must be carried out to determine the yield capacity M_y , nominal capacity M_{ne} , plastic capacity M_p , and ultimate capacity M_u of the column, as well as the rotations (θ) or curvatures (ϕ) related to those values, in both directions of the column (with a total of 12 values, summarized in Table 2.3).

Table 2.3 Summary of required values from M- ϕ analysis.

Level	Transverse Direction (M2)		Longitudinal Direction (M3)	
	M-Moment	ϕ -Curvature	M-Moment	ϕ -Curvature
Yield	$M_{y,T}$	$\phi_{y,T}$	$M_{y,L}$	$\phi_{y,L}$
Nominal	$M_{ne,T}$	$\phi_{y,T}$	$M_{ne,L}$	$\phi_{y,L}$
Plastic	$M_{p,T}$	$\phi_{p,T}$	$M_{p,L}$	$\phi_{p,L}$
Ultimate	$M_{u,T}$	$\phi_{u,T}$	$M_{u,L}$	$\phi_{u,L}$

The elastic stiffness of the column section is used until the nominal M_{ne} is reached and nonlinear behavior is assumed to develop. The elastic period of the structure is not altered with the definition and assignment of the uncoupled hinge. The unloading behavior of the model follows the slope of the structure's elastic stiffness, and permanent deformations are computed accordingly. The nonlinear behavior is defined through a normalized moment-rotation (M- θ) or moment-curvature (M- ϕ) relation with possible degrading behavior. The uncoupled hinge can be used for linear static analysis, nonlinear static analysis (pushover), as well as nonlinear time history analysis with direct integration. As mentioned in Section 2.5.3, the use of this model however, is not recommended for dynamic or three-dimensional static analysis.

2.5.5.2 Hinge Definition

1. Define normalized moment-rotation (M- θ) or moment-curvature (M- ϕ) relation with the corresponding plastic hinge length in the displacement control parameters and type boxes, for both directions of bending (positive and negative), for which symmetry can be used for simplification. The definition of the nonlinear behavior must include the following points, normalized with respect to yield point (with M_{ne} as the scale factor SF for the moment- 1st column, and θ_Y (or ϕ_Y) as the scale factor SF for the rotation (or curvature)- 2nd column). Figure 2.8 presents two options for the M- ϕ curve used for this model, with the following points:
 - A (zero load), defined automatically in the program.
 - B (yield point), for which M_{ne} and θ_Y (or ϕ_Y) shall be used (introduce value 1.0 for both table columns).
 - C (ultimate capacity point), for which M_p and θ_p (or ϕ_p) shall be used instead of M_u and θ_u (or ϕ_u), in order to avoid an overestimation of the column plastic capacity and

bridge base shear. The ratio of C to B points shall be taken as M_p/M_{ne} and θ_p/θ_Y , respectively. The corresponding hardening slope is approximately $(E_{sh}/2)/E_{s.}$, representing the expected behavior and ductility of the column.

- D (degraded capacity), which can be taken as 20% of the column plastic capacity M_p .
 - E (failure point), for which it is recommended to have a greater value than point D (positive ultimate slope) for numerical stability.
2. Define the scaling parameters for moment and rotation as M_{ne} and θ_Y in radians (or ϕ_Y in units of 1/Length).
 3. Repeat steps 1 and 2 for the orthogonal direction.

2.5.5.3 Observations

1. Uncoupled behavior in each orthogonal direction results in a significant overestimation of column strength for 3D analysis (40% in the case of pushover at 45°), even in the case of circular symmetry of the cross section. A bias factor between 0.7 and 1.0 can be taken in order to reduce the strength values resulting in a 3D analysis of the bridge.
2. Convergence problems occur in SAP2000 after yielding during nonlinear time history analysis, possible solutions for which are:
 - Divide the plastic hinge zone into smaller discrete elements, with an additional rotational mass assigned to the nodes. The arbitrary value of this mass should be relatively small, not greater than $1e^{-3}$, to avoid overestimating the existing mass of the structure, but rather provide an artificial tool for numerical stability during the analysis algorithm.
 - The recommended degrading slope defined for the moment-rotation or moment-curvature relationship of the hinge should be in the order of the elastic stiffness. Since the elastic properties of the hinge are not defined, but rather calculated automatically in SAP2000 through the elastic section, the definition of the degrading stiffness is determined iteratively by the user. The value of the degrading slope is increased progressively by the user until convergence or stable response of the bridge is achieved, which can be monitored, e.g., through displacement time history plots.
3. The uncoupled plastic hinge fails to adjust the capacity and ductility of the column according to the fluctuation in column axial load, expected during a static pushover or

dynamic analysis. The use of such plastic hinge model is not recommended when large variations of column axial load occur.

2.5.6 Interaction PMM Hinge

2.5.6.1 General Characteristics

The column plastic hinge can be modeled in SAP2000 as a lumped plasticity model, using the Interaction PMM Hinge. The applicability and limitations of the Interaction PMM Hinge are similar to those of uncoupled hinge, except for its consideration of coupled behavior of the column in both orthogonal bending directions. The configuration of the column cross section must be taken into account in a separate moment-curvature analysis and interaction diagram, carried out to determine the nominal capacity M_{ne} , plastic capacity M_p , and ultimate capacity M_u of the column, as well as the rotations (θ) or curvatures (ϕ) related to those values, in discrete bending directions of the column. In the case of circular symmetry of the column cross section, only one $M-\theta$ or $M-\phi$ relation is required for each level of axial load, while the use of a minimum of three curves is recommended for asymmetrical column-bent configuration (transverse, longitudinal, and a 45° directions) as seen in Figure 2.11.

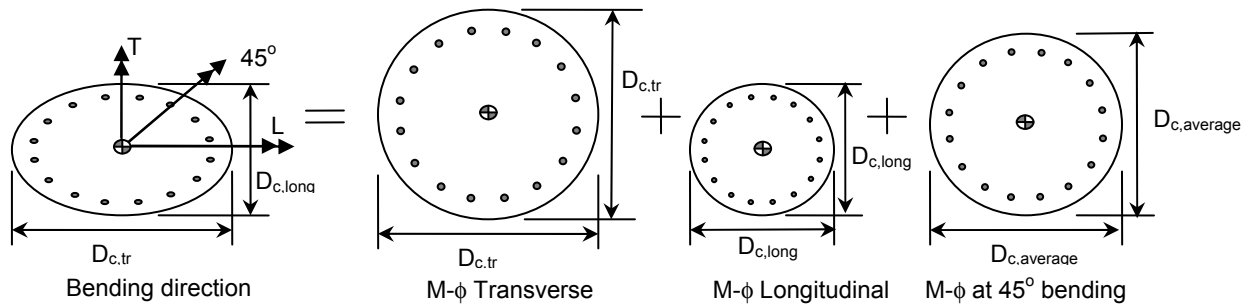


Fig. 2.11 Column section with biaxial symmetry: simplification for moment-curvature analysis.

The elastic stiffness of the column section is used until the yield point or nominal moment M_{ne} when nonlinear behavior is developed. The elastic period of the structure is not altered with the definition and assignment of the Interaction PMM Hinge. The unloading behavior of the model from a yielded state follows the slope of the elastic stiffness of the structure, and permanent deformations are computed accordingly. The nonlinear behavior is defined through a normalized moment-rotation ($M-\theta$) or moment-curvature ($M-\phi$) relation with

possible degrading behavior. The Interaction PMM Hinge can be used for linear static analysis, nonlinear static analysis (pushover), as well as nonlinear time history analysis with direct integration. Due to convergence difficulties during time history analysis, the use of this model is limited to static analysis.

2.5.6.2 Hinge Definition

1. Define normalized moment-rotation ($M-\theta$) or moment-curvature ($M-\phi$) relation for several levels of axial load P of the column, for all directions of bending considered. For simplification, the column axial dead load can be considered as a basic load, including superstructure tributary and self weight. Additional levels of axial load should be considered as well, with a range between the minimum and maximum values of the fluctuation of column axial load. This range can be roughly determined through a preliminary pushover analysis of the bridge, using the basic level of axial load (dead load) to define the behavior of the plastic hinge. A more accurate range of column axial load can be determined from a series of time history analysis including vertical excitation; however, this analysis type is not recommended for a nonlinear bridge model using the Interaction PMM Hinge. Once the maximum axial loads are established, additional moment-curvature analysis are carried out and incorporated into the refined model. A minimum of three levels of axial load are required, corresponding to the minimum, maximum, and dead load expected on the column bent. In SAP2000 tension and compression loads must have a positive and a negative value, respectively. Symmetry options can be used as well for simplification of hinge description.
2. Define the scaling parameters for moment and rotation as M_{ne} and θ_Y in radians (or ϕ_Y in units of 1/Length).
3. The definition of the nonlinear behavior in each bending direction must include the following points (see Fig. 2.8) normalized with respect to nominal point, with M_{ne} as the scale factor SF for the moment— 1st column, and θ_Y (or ϕ_Y) as the scale factor SF for the rotation (or curvature)— 2nd column.
 - A (zero loading), automatically generated by the program.
 - B (yield point), for which M_{ne} and θ_Y (or ϕ_Y) shall be used (introduce value 1.0 for both table columns).

- C (ultimate capacity point), for which M_p and θ_p (or ϕ_p) shall be used instead of M_u and θ_u (or ϕ_u), in order to avoid an overestimation of the column plastic capacity and bridge base shear. The ratio of C to B points shall be taken as M_p/M_{ne} and θ_p/θ_Y , respectively. The corresponding hardening slope is approximately $(E_{sh}/2)/E_s$, representing the expected behavior and ductility of the column.
 - D (degraded capacity), which can be taken as 20% of the column plastic capacity M_p .
 - E (failure point), for which it is recommended to have a greater value than point D (positive ultimate slope) for numerical stability.
4. Define scale factors for maximum axial capacity, and principal bending moments M2 and M3 (transverse and longitudinal global direction of the bridge, respectively).
 5. Define normalized interaction diagram P-M2-M3 between the axial load and bending moments M2 and M3, using Xtract, X-Section or SD-Section (without reduction factors or steel hardening). Positive values of axial load represent tension, while negative are for compression capacities of the column.

2.5.6.3 Observations

1. The estimation of the strength of the column in the nonlinear range during pushover at 45° and other 3D analysis is more accurate using the Interaction PMM Hinge than the uncoupled hinge, and therefore the former model is recommended for static analysis in 3D. An overestimation of the strength of the column cross section outside the plastic hinge is still present in SAP2000 up to yield point for 3D analysis, for which a bias factor of 0.8–1.0 can be used to reduce the column capacity.
2. The Interaction PMM Hinge will automatically adjust the capacity of the column according to the fluctuation in column axial load, expected during a static pushover or dynamic analysis, and will therefore provide more accurate results.
3. Convergence problems occur in SAP2000 after yielding during nonlinear time history analysis, similar to those of the uncoupled hinge, for which similar approaches can be taken (see Section 2.5.4).

2.5.7 Fiber Hinge

2.5.7.1 General Characteristics

The column plastic hinge can be modeled with greater accuracy using the fiber hinge option in SAP2000. The fiber hinge computes a moment-curvature relation in any bending direction for varying levels of axial load throughout a static or dynamic analysis. This interaction between biaxial moment and axial force, and the distribution of inelastic action throughout the section is obtained automatically by assigning particular stress-strain (σ - ϵ) relationships to individual discretized fibers in the cross section. The stress-strain relationships correspond to unconfined concrete, confined concrete, and longitudinal steel reinforcement.

The fiber hinge model is a lumped plasticity model with a characteristic length L_p , assigned to an elastic element at a specific point (see Section 2.5.1). The use of this model can be extended to modal analysis, nonlinear static (pushover), and nonlinear time history analysis with direct integration. The fiber model can represent the loss of stiffness caused by concrete cracking, yielding of reinforcing steel due to flexural yielding, and strain hardening. It is successful in representing degradation and softening after yielding; however pinching and bond slip are not included in the present model. Shear and torsion behaviors of the cross section are represented elastically.

The definition of each fiber in the cross section of the pier columns and shafts includes the area, centroid coordinates, and material type, for which a stress-strain relation was defined previously. For a bridge reinforced concrete column, the definition of the σ - ϵ relation with degrading material strength is defined separately for confined concrete, unconfined concrete, and steel (see Section 2.2.1).

2.5.7.2 Fiber Definition

1. Define the stress-strain σ - ϵ relation separately for confined concrete (core—Mander 1988), unconfined concrete (cover—Mander 1988), and reinforcing steel (ASTM A706), according to Section 2.2.1 of the present guidelines document, and scale the values for stress σ by the factor M_p/M_u . If the unscaled σ - ϵ values are used, these ultimate stress values will result in a base shear V_b corresponding to ultimate moment M_u , not plastic moment M_p . These results for base shear or other column capacities can then be scaled

down by the factor M_p/M_u to capture the column's plastic capacity, according to SDC 2004.

2. Create the fiber hinge as a user-defined displacement control (ductile) model, with a characteristic length of L_p or $L_p/2$, according to step 4.
3. Define the area, coordinates, and material type for each fiber of the column cross section, including those corresponding to the cover, the core, and reinforcing steel. A circular patch can be generated through a separate spreadsheet and copied into SAP2000, to represent the radial distribution of fibers, in a circular cross section, using as an example the following scheme:

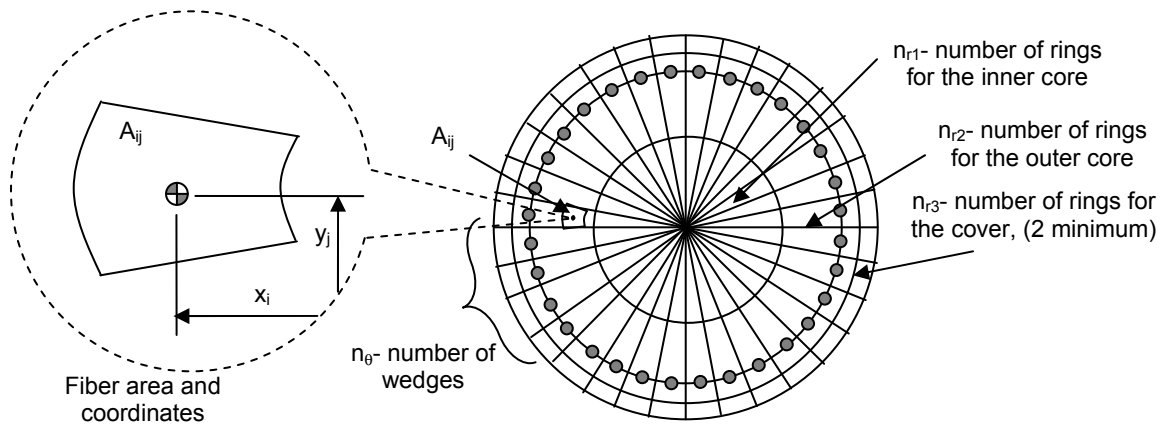


Fig. 2.12 Fiber distribution along circular cross-section.

The concrete fibers must be placed at the geometric centroid of the concrete areas, as shown in Figure 2.12. When more than one longitudinal bar is lumped at a location, the steel fibers must also be placed at the centroid of the bar bundle or specified separately at their actual location.

A sufficient number of fibers are required to represent the cross section configuration with enough accuracy and obtain values for the hinge area and moment of inertias within 5% of the column gross section properties. The number of fibers defined for the inner core can be reduced for computation efficiency, since the cross-sectional behavior in flexure is controlled by the outer rings and fibers. This reduction can be carried out by reducing the number of wedges and rings used for the core. The number of wedges for the outer core and cover can be taken as the number of steel bundles or bars, for simplicity, thus assisting the definition of the steel fibers.

The recommendations for column cross section fiber discretization provided by Eberhard and Berry (PEER Annual Meeting 2006) can be used for this purpose.

4. Assign the fiber hinge to the plastic hinge zone of the column element. The location of the plastic hinge can be assumed at mid-height of the hinge zone, under the assumption of constant plastic curvature ϕ_p throughout the plastic hinge zone length L_p . Two equivalent options can be used arbitrarily for this assignment (see Fig. 2.13), producing similar results:

- Option A: 1 fiber hinge assigned at the plastic hinge location (mid-height of plastic zone) with a segment length $L=L_p$.
- Option B: 2 segments, each with a fiber hinge at the plastic hinge location with $L=L_p/2$., assigned to the mid-height of the plastic hinge zone.

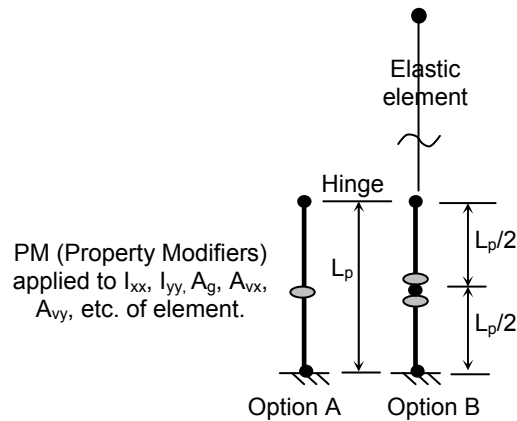


Fig. 2.13 Assignment of fiber hinge to plastic hinge zone.

2.5.7.3 Observations

1. The uncoupled hinge and Interaction PMM Hinge defined above are rigid-plastic, hence the stiffness of the more flexible element corresponding to the elastic column controls the response in the elastic range. However, since both the nonlinear fiber model and the elastic column have finite stiffness, the resulting column stiffness is a series stiffness of the two components. The use of the fiber hinge in SAP2000 results in a very flexible model with a first mode period T_1 greater than the expected $T_{1, \text{elastic}}$, corresponding to the elastic column alone. To achieve the target period, Property Modifiers or gross-section scale factors are determined iteratively and assigned to the column segment in the plastic hinge zone. A uniform factor in the order of 1.0–3.0, applied to the gross area A_g , shear

area A_v , and gross inertia I_g of the column, is found to result in the correct first mode period T_1 . This procedure is illustrated explicitly in Appendix A.

2. The correct implementation of the fiber hinge using other analysis programs can be achieved by using a rigid-plastic nonlinear behavior of the fiber model in series with an elastic column section or by moving the location of the plastic hinge to a point with a distance L_p above the fixed base of the column. Higher-order elements can also predict the correct elastic stiffness (Scott and Fenves 2006).
3. The use of unscaled stress values will result in a base shear V_b of the bridge corresponding to ultimate moment M_u , not plastic moment M_p . To correct the results, the stress values in σ - ϵ curves for concrete and steel can be scaled to $SF=M_p/M_u$. The strain values ϵ should not be scaled.
4. The steeply descending branch of the stress-strain curve defined in the material models for confined and unconfined concrete could produce problems converging to an equilibrium solution. For this reason, a shallower descending slope can be used instead, taking into consideration the imprecision introduced into the determination of deformation capacity of the cross section after reaching maximum strength.
5. In the computation of the capacity in a nonlinear static analysis (pushover) in SAP2000, an extrapolation of stress values after the failure point (E) is computed without strength degradation, which results in infinite ductility of the column. A separate estimation of the ductility capacity can be carried out following Section 3.1.3 of SDC 2004 and Section 3.6 of the present document.
6. The fiber hinge model will automatically adjust the bending capacity of the column in any direction according to the fluctuation in column axial load, expected during a static pushover or dynamic analysis, and will therefore provide more accurate results.
7. The use of the fiber hinge model for nonlinear time history analysis (direct integration) requires high computational effort. In the case of 2D analysis, where the uncoupled hinge and interaction PMM hinge are applicable, the use of these simpler models is recommended instead of the fiber model.
8. For a 45° pushover or 3D analysis in SAP2000, the strength of the elastic column outside the plastic hinge zone is still overestimated by 40%. A small bias factor in the order of 0.8–1.0 can be used to reduce the column capacities in a coupled 3D analysis.

2.5.8 NL-Link

2.5.8.1 General Characteristics

The use of the plastic nonlinear link (link/support element) as a model of the plastic hinge zone is recommended for 2D static and dynamic analysis. The uncoupled behavior of the link in both orthogonal directions in the linear and nonlinear range can be defined using several options, such as Plastic Wen and Multi-linear Plastic, among others. The elastic behavior of the column within the plastic hinge zone in the axial, transverse, and torsional directions are maintained equivalent to those of the elastic column outside the hinge. If a zero-length link is used, these properties remain fixed and no further definition is required. For a finite length link, specific stiffness coefficients should be used, according to the SAP2000 Analysis Manual (see Table 2.4). The nonlinear behavior of the NL-Link is defined solely in the flexural bending direction of the column.

Table 2.4 Stiffness coefficients defined in analysis manual of SAP2000.

k_1 - Axial (U1)	k_2, k_3 - Translation (U2, U3)	k_4 - Torsion (R1)	K_5, k_6 - Flexure (R2, R3)
EA/L	$12EI/L^3$	GJ/L	EI/L

In the case of an NL-link with finite length, a constant plastic curvature ϕ_p is assumed throughout the plastic hinge length, as well as the location of shear deformation or inflection point at mid-height $L_p/2$ of the hinge for degrees of freedom U2 and U3 (transverse translation). A separate moment-curvature analysis must be carried out previously to determine the yield point, maximum, and plastic capacity.

2.5.8.2 Definition of NL-Link: Plastic-Wen

1. Define the elastic stiffness for degrees of freedom U1 through R1 (see Fig. 2.1) and damping in the order of $\zeta=5\%$ for linear analysis cases, as required in SAP2000.
2. For degrees of freedom R2 and R3, corresponding to the flexural bending of the column, define the linear and nonlinear stiffness as the effective elastic stiffness (k_5, k_6 with I_{eff}

according to Section 2.5.2), nominal strength (M_{ne}), post-yield stiffness $(E_{sh}/2)/E_s$, and a yield exponent ($r=2$) (see Fig. 2.14).

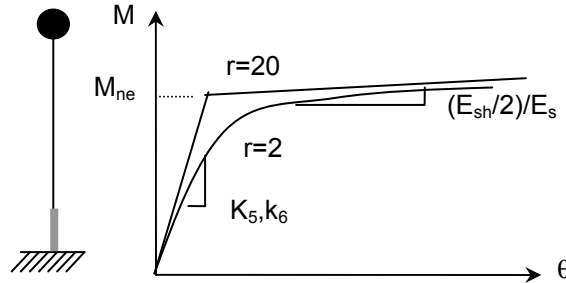


Fig. 2.14 Nonlinear parameters for NL-Link using plastic Wen model.

2.5.8.3 Observations for NL-Link: Plastic-Wen

1. Cyclic behavior of the columns is represented by elastic unloading and reloading following the elastic stiffness (equivalent to the initial inelastic stiffness for degrees of freedom R2 and R3) and the backbone curve in Figure 2.13.
2. No degrading behavior is defined and infinite ductility of the column is obtained. A separate estimation of the actual ductility capacity can be carried out according to SDC 2004, Section 3.1.4.
3. Uncoupled behavior in each orthogonal direction results in a significant overestimation of strength for 3D analysis, which in the case of pushover at 45° is in the order of 40%. Bias factors between the value of 1.0–1.4 can be used to correct the results of the column capacity in a 3D analysis. The use of the NL-Link in a 2D analysis solely is therefore recommended.

2.5.8.4 Definition of NL-Link: Multi-Linear Plastic

1. Define the elastic stiffness for degrees of freedom U1 through R1 (see Fig. 2.1) and damping in the order of $\zeta=5\%$ for linear analysis cases, as required in SAP2000.
2. For degrees of freedom R2 and R3, corresponding to the flexural bending of the column, define the linear stiffness as the effective elastic stiffness (k_5, k_6 with I_{eff} according to Section 2.5.2), and a damping coefficient in the order of $\zeta=5\%$.

- For degrees of freedom R2 and R3 specify kinematic hysteretic behavior and symmetric moment-rotation $M-\theta$ relation with a minimum of 3 points defined as follows: Origin or zero load $(0,0)$, nominal point (θ_Y, M_{ne}) , and ultimate capacity defined instead as plastic capacity and ultimate rotation (θ_u, M_p) . The resulting slope will approximate the expected hardening slope $(E_{sh}/2)/E_s$ of the reinforced concrete column.
- Specify degrading behavior as additional points in the $M-\theta$ relation for estimation of ductility capacity. The values beyond the last point specified in the $M-\theta$ curve are extrapolated and the use of a final positive slope is recommended to avoid convergence problems.

2.5.8.5 Observations for NL-Link: Multi-Linear Plastic

- Cyclic behavior of the columns is represented by elastic unloading and reloading following the backbone curve defined by the moment-rotation relation (see Fig. 2.15).
- As for the Plastic Wen link, uncoupled behavior in each orthogonal direction result in a significant overestimation of strength for 3D analysis, which in the case of pushover at 45o is in the order of 40%. Bias factors between the value of 1.0–1.4 can be used to correct the result of the column capacity in a 3D analysis. The use of the NL-Link in a 2D analysis solely is therefore recommended.

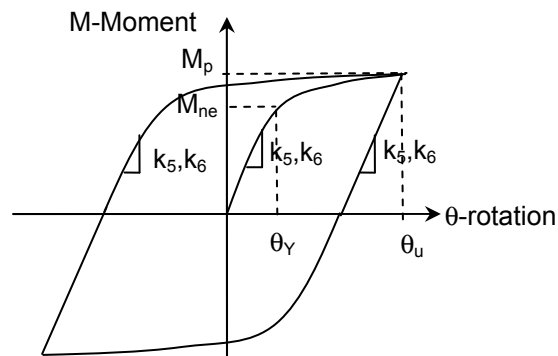


Fig. 2.15 Hysteretic behavior of NL-Link using multi-linear plastic model.

2.6 BOUNDARY CONDITIONS

2.6.1 Soil-Structure Interaction

The dynamic interaction between the soil and the pile shaft of bridge foundations has a significant effect on the seismic response of bridges. Soil-structure interaction is usually classified into kinematic and inertial effects. Kinematic interaction is the modification of the free-field ground motion by the presence of the massless foundation, while the inertial soil-structure interaction is caused by the deformation of the soil by the time-varying inertia induced forces developed in the foundation.

Although it is impractical to include all the effects of the soil and foundation on the earthquake response of a bridge, the design engineer should recognize that soil-structure interaction introduces flexibility and energy dissipation into the system compared with an assumption of a rigid or pinned support. The stiffness and damping properties of a foundation depend on the characteristics of the soil, piles, and the connections between the piles and the pile cap. The group effects of the large number of piles in bridge foundations can significantly affect the dynamic properties (Section 4.2.2 of ATC 32).

According to geotechnical specifications, in the case of Ordinary Standard bridge structures with normal soil conditions, the underlying soil can be assumed rigid and soil-structure interaction neglected. In such cases, the column foundation may still be considered to have semi-rigid behavior through the assignment of a rotational spring if a reduction in the cross section is specified for the column base (see Section 2.6.2). For non-conventional soil conditions in Ordinary Standard bridges, a semi-rigid connection will be defined for the column base, according to Section 2.6.2. Soil-structure interaction should always be considered in the analysis of Nonstandard and Important bridge structures, especially very rigid systems with short natural periods. For such cases, it is also expected that the modal damping ratios of the soil system differ significantly from the remaining structure, with values in the range of 15–20% compared to 3–5%, respectively. The assumptions of classical damping are no longer appropriate for combined soil-structure systems with different damping levels, requiring an adjustment in the modal damping definition through substructure method (Chopra 2006).

Section 4.2.2 of ATC 32 provides general guidelines for the consideration of soil-structure interaction effects in the modeling of bridge structures. Section 17 of BDS 2000 offers

a series of recommendations for the design of buried reinforced concrete structure representing a composite soil-structure interaction system.

2.6.2 Column Supports

The definition of boundary conditions in a structural system is a key factor in the assemblage of its stiffness matrix, thus affecting both the static and dynamic behavior of the structure. The boundary conditions must be assigned correctly through simplified and realistic models of the abutments and foundation system of the bridge to correctly approximate the ductility capacity and seismic demand on major structural components. In a dynamic analysis of the bridge, the modal periods and mode shapes, as well as other related properties are greatly affected by such assignment.

Depending on the details of the foundations, a pinned, semi-rigid, or fixed connection should be specified at the column base. If a reduction in the column base (built hinge) is detailed in the plans of multi-column bent bridges, a completely pinned connection can be used for simplicity (restraints on degrees of freedom U1, U2, and U3 corresponding to translation). In such cases, a rigid connection between the column top and the superstructure is also specified to maintain the stability of the bridge under transverse loads. For single-column bent bridges, the stability of the structure in the transverse direction is obtained through an idealized fixed connection at the column base and a rigid connection between the superstructure and column bent top. Such boundary conditions must be verified with the geotechnical data for the site and assigned to the model through joint restraints at the column base.

However, since the actual bridge system is more complex, its displacement capacity is affected by components other than the ductile members within the frame, mainly the flexibility of the column bent foundations. This feature is included in the model to represent the realistic boundary conditions of the system, according to Section 2.2.4 of SDC 2004, using either the uncoupled hinge or the zero-length NL-Link in SAP2000 for the model (see Sections 2.5.4 or 2.5.7 of the present document, respectively). In the case of flexible foundations with appropriate lateral restraint, a pinned connection is specified at the column base through joints restraints at the degrees of freedom U1, U2, and U3 corresponding to translation, while the linear or nonlinear behavior of the foundations is introduced at the degrees of freedom corresponding to

rotations R2 and R3 (see Fig. 2.16). The effective height of the column should also be adjusted to the idealized location of column fixity.

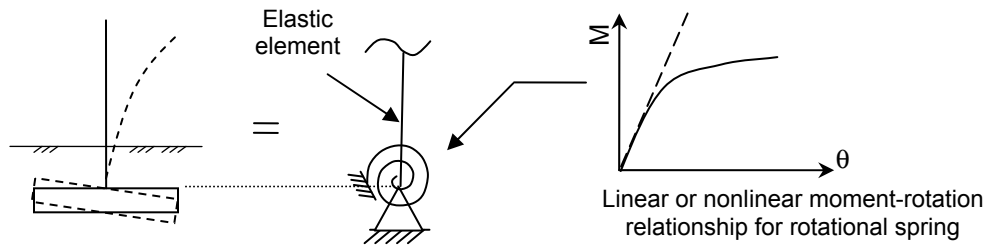


Fig 2.16 Modeling scheme of flexible foundations with adequate lateral soil resistance.

The increase in the rotational stiffness and the corresponding degree of semi-rigidity of the column base will produce an upward shift in the point of inflection of the column under lateral load or deformation. This shift in the inflection point will modify and redistribute the rotational demand on the column between the top and bottom sections. It will also produce an overall increase in base shear, a reduction in the displacement ductility capacity of the bridge, and could significantly modify other response parameters of the bridge. Therefore, the estimation of the column base degree of semi-rigidity must be made with caution.

A similar modeling approach can be taken for the translational degrees of freedom. If such foundation response is expected in the longitudinal, transverse, or vertical directions (see Fig. 2.17), the column base can be modeled as a semi-rigid connection using elastic or nonlinear springs. In general, the parameters used for the assignment of semi-rigid column bases are defined according to the geotechnical specifications for the site. The assigned boundary conditions or springs must guarantee the stability of the bridge model in any direction to carry out the analysis successfully. The geometrical properties of the column cross section at the transition point between the foundation footing or piles and the column bent are also considered in the model.

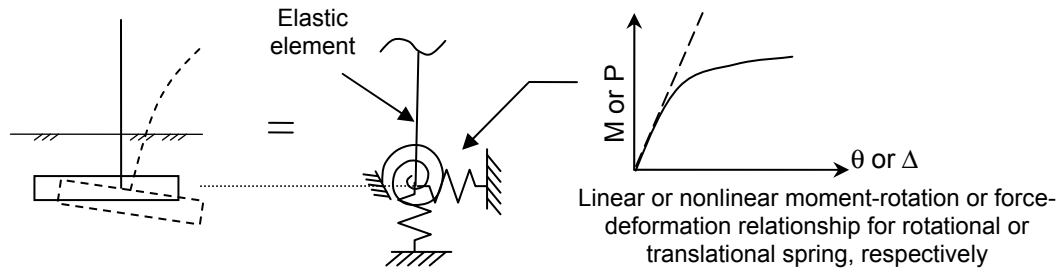


Fig. 2.17 Modeling scheme of flexible foundations with partial lateral restraint.

Torsional restraints in the degree of freedom R1 should not be specified for the column base with an idealized pinned connection, specifically in the case of single-column bent bridges, where the torsional modes of the structure could be significantly impacted (see Fig. 3.1 in Section 3.2). Section 5.3 of ATC 32 provides some additional recommendations for foundation modeling.

2.6.3 Superstructure End Restraints

When using the simplified or spring abutment models (see Section 2.7), the connection between the superstructure and the abutment model at each deck end is modeled as a rigid connection. The idealized translational and overturning properties of the superstructure-abutment system are defined in the abutment model, following the recommendations of Section 2.7.

For a preliminary bridge model without complex abutment models used for the verification of basic analysis results (see Section 3.6.4), a roller boundary condition is defined at each end of the superstructure, i.e., a vertical restraint at degree of freedom U3 is specified, representing a simple vertical support provided by these elements. No torsional restraint is defined at the ends of the superstructure at degree of freedom R1. In this simplified preliminary model, a single-column bent bridge will resist the lateral loads or displacements in the transverse direction of the bridge through cantilever action, developed since no significant rotational restraint at the column top is provided by the superstructure. The torsional release at the superstructure ends has a smaller effect on the transverse response of a multi-column bent bridge, since frame action will always be generated between the column bents and the cap beam, thus obtaining double curvature in the columns and a possible formation of plastic hinges at the column top and base (see Fig. 2.18).

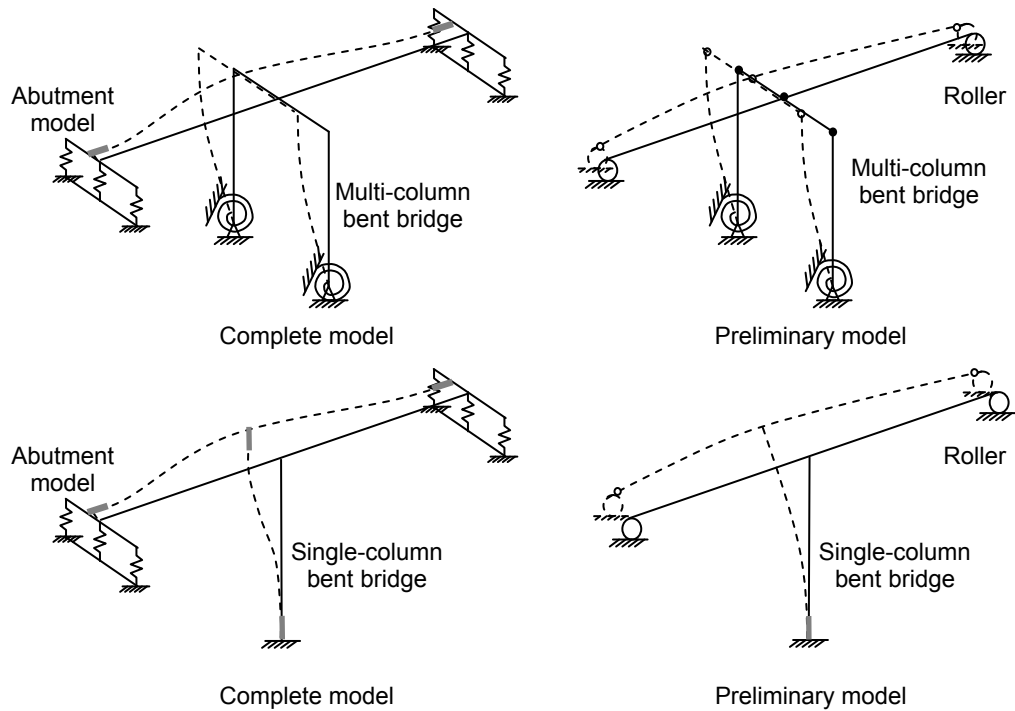


Fig 2.18 Effect of superstructure end restraints in single- and multi-column bent bridges.

2.7 ABUTMENT MODELING

2.7.1 Importance

Abutments are earth-retaining systems designed to provide unimpeded traffic access to and from the bridge. Abutments also provide an economical means of resisting bridge inertial loads developed during ground excitations. Abutment walls are traditionally designed following principles for free-standing retaining walls based on active and passive earth pressure theories. However, such pressure theories are invalid for abutment walls during seismic events when inertial loading from the massive bridge structure induces higher than anticipated passive earth pressure conditions (Lam and Martin 1986).

Abutment behavior, soil-structure interaction, and embankment flexibility have been found by post-earthquake reconnaissance reports to significantly influence the response of an entire bridge system under moderate to strong intensity ground motions. Specifically for Ordinary Standard bridge structures with short spans and relatively high superstructure stiffness, the embankment mobilization and the inelastic behavior of the soil material under high shear

deformation levels dominate the response of the bridge and the intermediate column bents (Kotsoglou and Pantazopouloi 2006).

The proper evaluation of the dynamic characteristics and response of abutment systems under transverse and longitudinal excitations is the main focus of many ongoing research studies. The findings of these studies will also play an important role in predicting the functionality of the bridge following an earthquake.

2.7.2 Abutment Geometry and Behavior

The different components of a typical seat-type abutment system are presented in Figure 2.19. Some of the typical abutment types used for highway bridges are classified by ATC 32 and include pile cap, stub, stub “L”, cantilever, cantilever “L”, spill-trough, and rigid frame abutments (see Fig. 5.1 of ATC 32). These abutments are alternatively categorized as seat and diaphragm abutment types, according to Chapter 7 of SDC 2004. Munfakh (1990) and Schnore (1990) discuss the advantages and disadvantages of various types of walls and abutments.

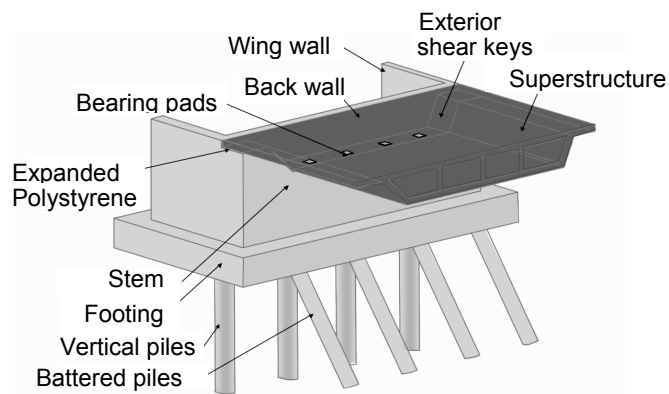


Fig. 2.19 Abutment components (Megally, Silva, and Seible 2002).

A realistic abutment model should represent all major resistance mechanisms and components, including an accurate estimation of their mass, stiffness, and nonlinear hysteretic behavior. Values of embankment critical length and participating mass were suggested by many research studies in order to quantify the embankment mobilization. Among them are Kotsoglou and Pantazopouloi (2006), Zhang and Makris (2002), and Werner (1994). The consideration of the abutment system participating mass has a critical effect on the mode shapes and consequently the dynamic response of the bridge, captured primarily through time history analysis. The load

pattern specified for a pushover analysis of the bridge is also adjusted due to this additional mass, modifying the force-deformation results of the system considerably. Due to the high sensitivity of the bridge response to the magnitude of the abutment mass, additional research is needed to standardize the modeling recommendations for Caltrans bridges. In addition, soil-structure interaction behind the abutment walls and due to the abutment foundations is also an important aspect affecting the abutment system behavior that requires further investigation.

2.7.3 Abutment Models

The choice of abutment models has a profound effect on the response of the bridge, especially the end spans closest to the abutments. Chapter 5 of ATC 32 presents several aspects of the modeling and design of different foundation types including bridge abutments, as well as pile footings, spread footings, cast-in-place column shafts, and cast-in-place pile shafts. Section 7.8 of SDC 2004 provides the backbone curves for seat and diaphragm abutment types for the longitudinal direction and discusses certain modeling limitations for the transverse direction. Three abutment models were implemented in this study to investigate the sensitivity of the global seismic response of the bridge to abutment modeling.

2.7.3.1 Roller Abutment

The roller abutment model consists of a simple boundary condition module that applies single point constraints against displacement in the vertical direction (vertical support), as seen in Figure 2.20. This model can be used to provide a lower-bound estimate of the longitudinal and transverse resistance of the bridge, captured through a pushover analysis (see Section 3.6). The response of this simple bridge model is dominated by the formation of plastic hinges and the ductility capacity of the column bents. These columns will act either as a cantilever or a frame, according to their connectivity and relative stiffness in each direction of the bridge. If a rotational restraint about the superstructure longitudinal axis is specified for such a model to represent the overturning resistance of the abutment, a possible overestimation of the bridge's overall strength and underestimation of its ductility can occur, specifically for single-column bents bridges. The actual response of the bridge will lie between this restrained and

unrestrained rotational degree of freedom. A proper nonlinear bridge model, nonetheless, should include as a minimum the roller abutment approach.

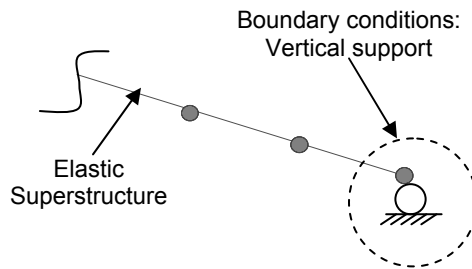


Fig. 2.20 Roller abutment model.

2.7.3.2 Simplified Abutment

The simplified abutment model, developed for the purpose of this project, consists of a simplification of the spring abutment model (see Section 2.7.3.3). The general scheme of the simplified model is presented in Figure 2.21.

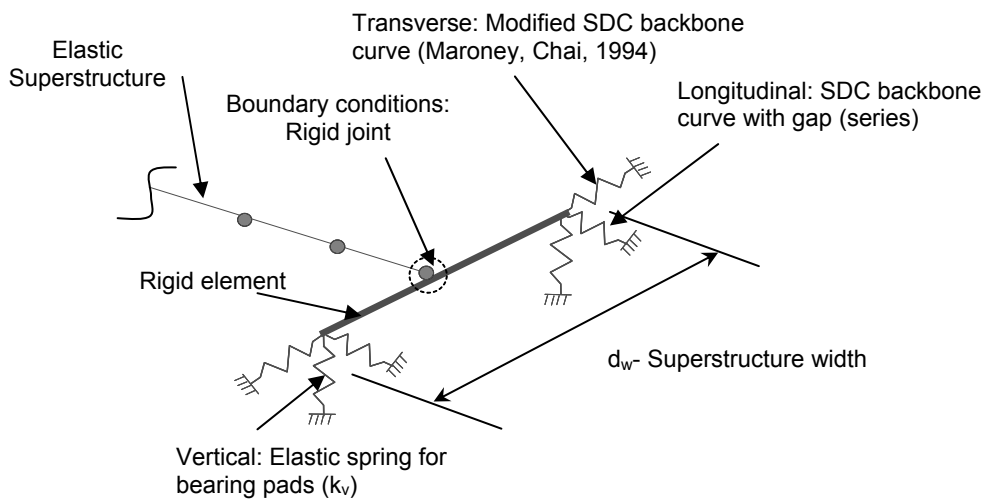


Fig 2.21 General scheme of the simplified abutment model.

The simplified abutment model consists of a rigid element of length d_w (superstructure width), connected through a rigid joint to the superstructure centerline, with defined longitudinal, transverse and vertical nonlinear response at each end. In the longitudinal direction, a series system is defined (see Fig. 2.22), consisting of a rigid element with shear and moment releases, a gap element with boundary conditions at each end allowing only longitudinal translation and a zero-length. The zero-length element is assigned an elastic-perfectly-plastic (EPP) backbone

curve with abutment stiffness (K_{abt}) and ultimate strength (P_{bw}) obtained from Section 7.8.1 of SDC 2004. The longitudinal response defined for the simplified abutment model accounts only for the gap and the embankment fill response, where passive pressures are produced by the abutment back wall. The shear resistance of the bearing pads is ignored.

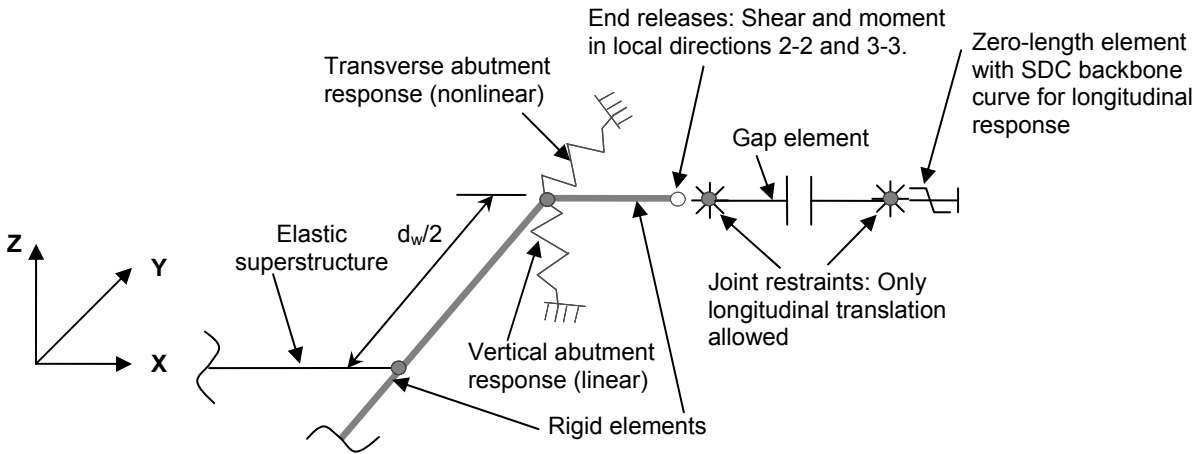


Fig. 2.22 Series system for the longitudinal abutment response.

In the transverse direction, a zero-length element is defined at each end of the rigid link with an assigned elastic-perfectly-plastic (EPP) backbone curve representing the backfill, wing wall, and pile system response. The abutment stiffness (K_{abt}) and back wall strength (P_{bw}) obtained for the longitudinal direction from Section 7.8 of SDC 2004 are modified using factors corresponding to wall effectiveness (C_L) of $2/3$ and participation coefficients (C_W) of $4/3$ (Maroney and Chai 1994). The wing wall length can be assumed to be $1/2$ – $1/3$ of the back wall length. The resistance of the brittle shear keys and distributed bearing pads is ignored in this model. The resulting force-displacement response in the longitudinal and transverse directions of a bridge example using this abutment model is presented in Appendix A of the document.

In the vertical direction, an elastic spring is defined at each end of the rigid link, with a stiffness corresponding to the bearing pads stiffness k_v . The distribution of the bearing pads and the vertical embankment stiffness is not accounted for in the mode, assuming rigid soil conditions.

2.7.3.3 Spring Abutment

A more complex abutment model was developed by Mackie and Stojadinović (2006) that includes sophisticated longitudinal, transverse, and vertical nonlinear abutment response, as well as a participating mass corresponding to the concrete abutment and mobilized embankment soil. A general scheme of this abutment module, denoted as spring abutment model, is presented in Figure 2.23.

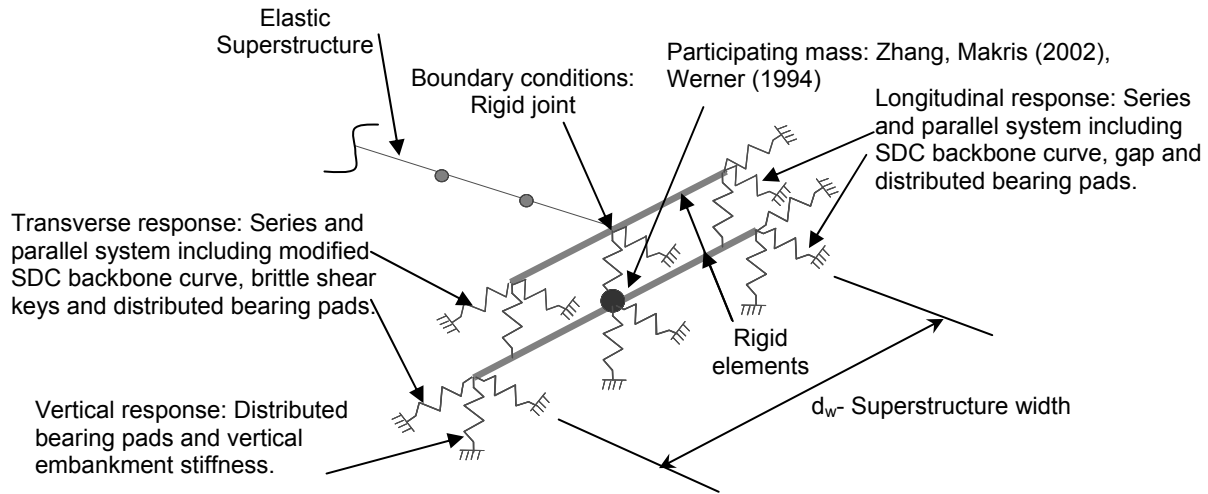


Fig. 2.23 General scheme of spring abutment model.

The longitudinal response is based on the system response of the elastomeric bearing pads, gap, abutment back wall, abutment piles, and soil backfill material. Prior to impact or gap closure, the superstructure forces are transmitted through the elastomeric bearing pads to the stem wall, and subsequently to the piles and backfill, in a series system. After gap closure, the superstructure bears directly on the abutment back wall and mobilizes the full passive backfill pressure. A system of zero-length elements representing each element of the abutment is used to approximate their combined behavior. The abutment stiffness (K_{abt}) and ultimate strength (P_{bw}) are obtained from equations 7.43 and 7.44 of SDC 2004. The number and distribution of the bearing pads is defined according to the number and location of the girders in the box, with plan and thickness dimensions according to plans or specifications. The yield and ultimate displacement of the bearings are assumed to be at 150% and 300% of the shear strain. A dynamic coefficient of friction of 0.40 for neoprene on concrete is used, guaranteeing shear that failure occurs prior to sliding of the bearing pads. The abutment stiffness and

strength are represented by placing a system of zero-length elements at each of the two extreme bearing pad locations to account for rotation of the superstructure about the vertical bridge axis. The combined stiffness and strength of the bearing pads must be taken into account in the model. The properties of the two spring systems are, therefore, determined to represent the combined behavior of all abutment components. The spring system may be used at each bearing pad location at the expense of making the model more complex without a substantial increase in accuracy of the analysis. However, such complex modeling may be required if the geometry of bearings and/or size of the gap differ along the joint between the bridge superstructure and the abutment.

The transverse response is based on the system response of the elastomeric bearing pads, exterior concrete shear keys, abutment piles, wing walls, and back-fill material. The bearing pad model discussed above is used with uncoupled behavior with respect to the longitudinal direction. The constitutive model of the exterior shear keys is derived from experimental tests (Megally et al. 2002). The ultimate shear key strength is assumed to be 30% of the superstructure dead load, according to equation 7.47 of SDC 2004. A hysteretic material with trilinear response backbone curve is used with two hardening and one softening stiffness values. The initial stiffness is a series-system stiffness of the shear and flexural response of a concrete cantilever with shear key dimensions. The hardening and softening branches are assumed to have magnitudes of 2.5% of the initial stiffness. The transverse stiffness and strength of the backfill, wing wall and pile system is calculated using a modification of the SDC procedure for the longitudinal direction. Wing wall effectiveness (C_L) and participation coefficients (C_W) of $2/3$ and $4/3$ are used, according to Maroney and Chai (1994). The abutment stiffness (K_{abt}) and back wall strength (P_{bw}) obtained for the longitudinal direction from Section 7.8 of SDC 2004 are modified using the above coefficients. The wing wall length can be assumed $1/2$ – $1/3$ of the back wall length. The bearing pads and shear keys are assumed to act in parallel. This combined bearing pad- shear key system acts in series with the transverse abutment stiffness and strength. The resulting force-displacement response in the longitudinal and transverse directions of a bridge example using this abutment model is presented in Appendix A of the document.

The vertical response of the abutment model includes the vertical stiffness of the bearing pads in series with the vertical stiffness of the trapezoidal embankment, obtained from Zhang

and Makris (2001). The abutment is assumed to have a nominal mass proportional to the superstructure dead load at the abutment.

2.8 OTHER ISSUES

2.8.1 Damping

2.8.1.1 Definitions

Damping is an energy-dissipation mechanism that results in the decay of motion in a vibrating linear or nonlinear system under exciting forces or imposed deformations. Material damping refers to the energy dissipation by deformation of a continuous medium, and radiation damping is the attenuation of vibration amplitudes due to wave dispersion over a large area or volume. Structural damping in a bridge structure can therefore be defined as the energy dissipation in the assembled bridge system that includes material damping in the structural components, inelastic cyclic behavior of the members, frictional losses at contact interfaces and connections, and radiation damping in the supporting soil and abutments. For Standard Ordinary Bridges, the effect of radiation damping can be neglected due to small skew and short spans.

The most commonly used mechanism for representing energy dissipation is viscous damping, which assumes the existence of dissipative forces that are a function of velocity. These equivalent viscous damping forces are intended to model the energy dissipation within the linear elastic limit of the structural system. The nonlinearity of this damping property is not considered explicitly in dynamic analysis (Chopra 2006). Equivalent viscous damping ratios in each mode of vibration are construed as mathematical representations of real energy-dissipation mechanisms. For most soils and structures, however, energy is dissipated hysteretically, that is, by yielding or plastic straining of the material.

The uniform distribution of damping in a system is called classical damping, and such systems possess the same natural modes as those of the undamped systems. The general form of the damping matrix is square diagonal; the equations of motion are damping uncoupled and classical modal analysis is applicable to such systems. Conversely, when significant material and component differences cause an uneven distribution of damping in the complete bridge structure, the system damping is referred to as non-classical. The equations of motion for such structures are damping coupled in the modal coordinate system, since the damping matrix is non-diagonal.

These systems are not amenable to classical modal analysis and they do not possess the same natural modes as the undamped system.

Active damping refers to energy dissipation of the system by external means, such as controlled actuators, while passive damping refers to energy dissipation within the structure by add-on damping devices such as isolators, by structural joints and supports, or by internal damping of structural members.

2.8.1.2 Determination of Damping Properties

In a simple linear system, the vibration properties (natural periods), mode shapes, and modal damping ratios can be determined by forced harmonic or free vibration tests. Figure 2.24 illustrates the procedure for determining the damping coefficient in a structure through a free vibration test. An initial displaced shape is imposed on the structure and then released. The decay of motion of a monitored point in the structure, called the logarithmic decrement, is used to estimate classical damping for a linear system or a nonlinear system undergoing deformation cycles in the elastic range of response. The oscillation of the structure occurs about its original position. In the case of a nonlinear system undergoing excursions into the inelastic range, the permanent displacements recorded can be used to estimate the total (classical and non-classical) damping in the system through nonlinear action, for a certain level of displacement ductility.

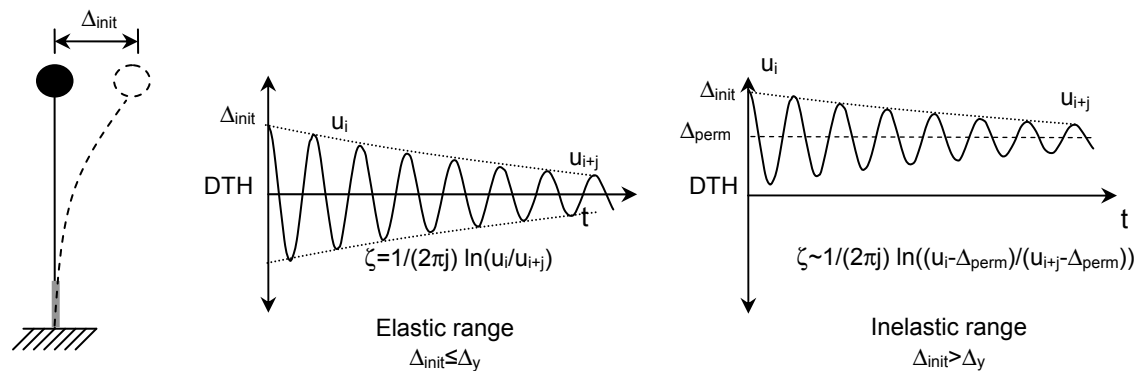


Fig. 2.24 Damping estimation under free vibration test.

In massive, complex, or yielding structures such as bridges, it is impractical to determine or verify the damping properties experimentally. In the design of a new structure, the measurement of damping and other dynamic properties is also impractical. Also, the total hysteretic damping in a nonlinear system depends on the characteristics of the ground motion or

dynamic excitation. Different damping results will be produced for different system configurations and dynamic loading. Therefore, an estimation of the modal damping coefficients that account for all energy-dissipating mechanisms in the response of a bridge system cannot be determined accurately, and typical values are then used based on measurements or estimated data from similar structures.

2.8.1.3 Recommended Damping Coefficients

The recommended damping values (Newmark 1982) for reinforced concrete bridges with considerable cracking undergoing small deformation or subjected to low intensity ground motion is estimated at 3–5% of critical. For bridges with a pre-stressed superstructure (without complete loss in pre-stress), the estimated damping coefficient is increased to about 5–7% of critical. For a yielding bridge structure, the hysteretic behavior and structural damage occurring in ductile components due to severe seismic conditions is estimated at 7–10% of critical, for bridges with both pre-stressed and conventionally reinforced concrete superstructure.

Typically, a 5% damping ratio is used in design codes. Section 2.1.5 of SDC 2004 requires the use of a 5% damped elastic acceleration response spectra (ARS) curves for Ordinary Standard concrete bridges for the estimation of earthquake forces. In studies of “flexible” reinforced concrete structures founded on firm materials, the combination of 5% viscous damping and effective stiffness corresponding to the stiffness at yield have been found to be appropriate when using a linear response spectrum to estimate peak nonlinear displacement response (ATC 32).

Higher damping ratios up to 10% of critical (SDC 2004) may be anticipated and justified by the design engineer for bridges with the following characteristics:

- Short bridges with a total length less than 300 ft (90 m)
- Three spans or less
- Normal or slight skew (less than 20°)
- Continuous superstructure without hinges or expansion joints
- Abutments designed for sustained soil mobilization (except for seat type abutment with backwalls intended to fuse, or abutments designed to respond in a flexible manner)
- Heavy influence of energy dissipation at the abutments

Seed et al. (1984) recommended the use of a viscous damping ratio of 8 to 20% for abutment fills with cohesionless soils in which the maximum shear strain ranges between 0.05 to 5%, respectively. The design spectrum must be modified for these higher levels of damping.

2.8.1.4 Modeling of Damping in SAP2000

Material damping coefficients can be specified in SAP2000 when defining material properties, and used in dynamic analyses ($0 < \rho < 1$). By default these coefficients are equal to zero. Alternatively, additional or total damping coefficients can be specified for each analysis case. Modal damping ratios are required for response-spectrum (see Section 3.7) and modal time-history (not recommended) analyses. For direct-integration time-history analyses (Section 3.8), viscous (velocity-proportional) damping is required, defined through mass- and stiffness-proportional components. Hysteretic proportional damping is used for steady-state and power-spectral-density analyses (not necessary for bridge analysis).

For each nonlinear-type of Link/Support Property, uncoupled linear effective-damping coefficients can be specified as well, one for each of the internal springs (by default, these coefficients are equal to zero). The linear effective damping represents the total viscous damping for the Link/Support element that is used for response-spectrum analyses, for linear and periodic time-history analyses, and for frequency-dependent analyses. The actual nonlinear properties are ignored for these types of analysis using the Link/Support Property. Effective damping is used instead to represent energy dissipation due to nonlinear damping, plasticity, or friction. For response-spectrum and linear modal time-history analysis, the effective damping values are converted to modal damping ratios assuming proportional damping and ignoring the modal cross-coupling damping terms. These effective modal-damping values are added to other modal damping ratios specified directly.

A linear analysis based on effective-damping properties could significantly overestimate or underestimate the amount of damping present in the structure. The recommended damping ratios to be used are specified in Section 2.9.1.2. It is recommended to specify Rayleigh (mass and stiffness proportional) damping coefficients directly in the dynamic analysis cases of the bridge structure (transient analysis), which requires the definition of the first two modal periods of the system. A modal analysis must be conducted previously, according to Section 3.2. The same damping ratio (according to Section 2.9.1.2) is used for both the first and second modal

periods when defining the parameters of linear and nonlinear transient analysis cases, unless additional information concerning modal damping is available.

The additional hysteretic damping is developed through the nonlinear models of yielding bridge components; specifically column bent plastic hinges (see Section 2.5.4). Nonlinear time-history analysis does not use the effective damping values defined for elastic cases, since it accounts for energy dissipation in the elements directly, including the effects of modal cross-coupling. The accuracy of the resulting dynamic response and total system damping depends directly on the proficiency of those nonlinear models in representing the realistic element behavior.

2.8.2 P- Δ Effects

The dynamic effects of column axial loads acting through large lateral displacements, otherwise known as P- Δ or second-order effects, is included in several analysis cases of the bridge model. The consideration of P- Δ effects helps identify the structural instability hazard of the bridge by capturing the degradation of strength and amplification of the seismic demand on the column bents, caused by the relative displacement between the column top and bottom.

During a pushover analysis, the degradation of strength is noted with the increase of lateral displacements of the column top, thus providing an accurate estimate of the actual capacity and base shear of the bridge (see Section 3.6). A softening behavior with a constant slope is observed in the force-displacement curve. During time history analysis, P- Δ effects play an important role in capturing the peak displacements of a yielding system, where a significant amplification of the response is generally expected for an adequate set of ground motions (see Section 3.8).

In SAP2000 2 types of geometric nonlinearities are available for nonlinear static (pushover) analysis and nonlinear time history analysis case using the direct integration method. These nonlinearities are the P- Δ and large displacements effects. For both geometric nonlinearities, the strains are still assumed to be small in all elements. P- Δ effects are computed by solving the equilibrium equations of the system taking into partial consideration the deformed configuration of the structure. In the P- Δ transformation tensile forces tend to resist the rotation of elements and stiffen the structure, while compressive forces tend to enhance the rotation of the elements and destabilize the structure. Large displacements analysis considers all equilibrium

equations in the deformed geometrical configuration of a structure undergoing large deformations, particularly large strains and rotations. This transformation requires more iteration than the P- Δ transformation and is sensitive to convergence tolerances established by the user.

For typical bridges, the P- Δ option is adequate, particularly when material nonlinearity dominates the nonlinear behavior. Section 4.2 of SDC 2004 provides a conservative limit for Ordinary Standard bridges meeting the specified ductility requirements to ignore P- Δ effects in static analysis. For Nonstandard and Special bridges, P- Δ effects should always be considered. The large displacement option is used for structures undergoing significant deformation and for buckling analysis, therefore it is not recommended for typical bridge analysis.

2.8.3 Expansion Joints and Restrainers

The opening and closing of expansion joints between segments of a bridge's superstructure introduce nonlinearities and discontinuities that affect the load path and hence the dynamic response of bridges. Section 4.2.2 of ATC 32 provides general guidelines for the modeling of bridges with expansion joints and restrainers, as well as recommendations for the selection of input ground motions to be used in the analysis. The expansion joints and restrainers can be modeled in SAP2000 using the Gap, Hook, or Multi-Linear Plastic special Link/Support to model the nonlinear spring elements.

3 Bridge Analysis

3.1 GENERAL CONSIDERATIONS

Following the completion of the modeling phase of the bridge structure, including geometry, elements, cross sections, materials, masses, boundary conditions, and sources of nonlinear behavior, the structural model must be evaluated to comply with the stiffness and period requirements in Section 7.1.1 and 7.1.2 of the SDC 2004 guidelines. Subsequently, the seismic analysis of the bridge is carried out to determine the force and deformation demands on the structural system and its individual components. The evaluation of the capacity of the bridge structure for design purposes is not the main emphasis of the present document.

The extent of the nonlinear behavior recommended for a particular bridge model depends on the classification and importance, the level of geometric, structural, and geotechnical irregularity, as well as the performance level required for the structure. Since great computational and analytical effort is required to perform nonlinear dynamic analysis, the analysis procedures for Ordinary Standard bridges can be simplified in some cases using linear models and static analysis procedures.

Dynamic analysis of a bridge model can only estimate the complex response of a structure to an earthquake, since inherent uncertainties in the specification of the ground motion, soil-structure interaction effects, and the expected linear or nonlinear behavior of structural components can produce significant inaccuracies in the analysis results. These uncertainties are generally accounted for in the design process through demand amplification and capacity reduction factors. However, additional engineering criteria must be applied to recognize fundamental sources of error in the analysis and verify the results through a simplified structural model and analysis procedures.

According to Sections 4.1.7 and 4.2 of ATC 32, Section 5.2 of SDC 2004 and the findings of the present document, the following recommendations are provided for the selection of the analysis type to be carried out for Caltrans bridges, classified according to Seismic Design Criteria Memo To Designers 20-1, January 1999 (MTD 20-1). The applicability and limitations of each analysis type is described in detail in the remaining sections of this chapter.

- Equivalent static analysis (ESA, see Section 3.5) is considered an appropriate analytical tool for estimating the response of Ordinary Standard bridges with properties specified in Section 5.2.1 of SDC 2004.
- Linear elastic dynamic analysis (RSA, see Section 3.7) is recommended for the estimation of the structural response of all bridge types for which behavior is essentially elastic.
- Nonlinear static analysis (pushover, see Section 3.6) allows for a more realistic determination of the interaction of critical components and the evaluation of the bridge strength and deformation capacity. It accounts for the redistribution of internal actions as components respond inelastically, and therefore provides a better measure of behavior than elastic analysis procedures. It is a recommended procedure for establishing actual strength and displacement capacities for all bridge types.
- Dynamic analysis is recommended for all bridges, except one- and two-span structures without intermediate expansion joints and with small or no skew, where static analysis is sufficient.
- The use of nonlinear models in dynamic analysis is required for Important Bridges and highly irregular bridges (Ordinary Nonstandard bridges). Elastic dynamic analysis can be used otherwise, using modal spectral analysis (RSA, see Section 3.7).
- Nonlinear dynamic behavior can be appropriately represented using nonlinear time history analysis- direct integration formulation (THA, see Section 3.8). Time history analysis using modal superposition or nonlinear response spectrum analysis procedures are not recommended for the evaluation of the dynamic response of highly nonlinear structures (see Sections 3.7.2 and 3.8.2).
- The proper evaluation of the maximum response of bridge structures due to dynamic excitation can only be carried out using an adequate suite of earthquake ground motions and reasonable criteria to estimate the variance in the results (see Section 3.8.4).

- For Important Bridges, the dynamic analysis should be supplemented with a static inelastic analysis (pushover) to evaluate local demands on yielding members.

The following table presents the acceptable and recommended analysis procedures for each bridge type according to its importance and irregularity classification, based on the criteria presented in ATC 32, SDC 2004, and the present document. The design engineer must apply the appropriate criteria in choosing the type of analysis and the parameters required on a case-by-case basis, according to the recommendations presented above and the limitations of each methodology described in this chapter.

Table 3.1 Analysis types applicable to Caltrans bridges.

Bridge Classification	Nonlinear Static		Dynamic		
	Equivalent Static Analysis (ESA)	Incremental Static Analysis (Pushover)	Response Spectrum Analysis (RSA)-Linear	Time History Analysis (THA)- Direct integration	
				Linear	Nonlinear
Ordinary Standard	A	R	A	A	A
Ordinary Nonstandard	N	R	A	A	R
Important	N	R	A	A	R

N: Not acceptable analysis type

A: Acceptable analysis type

R: Acceptable and strongly recommended analysis type, not necessarily comprehensive

The applicability of several analytical methods including the single-mode spectral method, the multi-mode spectral method, and elastic and nonlinear time-history analysis has also been discussed in other related references. Criteria for the choice of an appropriate method for analysis of bridge structures in the transverse direction are proposed (Isakovic, Fischinger, and Fajfar 1999).

Section 3.5 of ATC 32 and MTD 20-1 present a short discussion on a performance-based approach to bridge structures, including a general characterization of performance levels including Life-Safety Performance, Damage-Reduction Performance, and Functionality Performance. The seismic demand levels for the response spectrum and time history analysis cases can be determined accordingly and a capacity-design approach is recommended for certain bridge types. For Ordinary Bridges, the estimated local demands for functional evaluation should be a fraction of those determined for the safety-evaluation earthquake. For Important Bridges,

the safety evaluation is supplemented by a functional evaluation. For the functional evaluation, the same analysis procedures are applied, except that the capacity design check is not required.

3.2 MODAL ANALYSIS

The dynamic characteristics of a bridge structure are explicitly portrayed through modal analysis procedures. The frequencies at which vibrations naturally occur and the mode shapes assumed by the bridge are determined analytically, based on the mass, stiffness, and damping properties of the system. These modal results, specifically modal periods, are the main parameters used for response spectrum analysis (see Section 3.7) and time history analysis (Section 3.8). Such procedures allow a realistic evaluation of the seismic demand and the corresponding structural response of the bridge, through an acceleration spectra or ground motion simulation. Modal pushover analysis is not considered for Ordinary Standard bridges, since the natural modes of the structure generally present low correlation (see Section 3.6 and Appendix A.2).

Since bridges are complex structural systems, they are particularly prone to seismic demand amplification due to specific ground motion excitation characteristics. These resonance effects can cause premature or unanticipated failure. To account for these hazardous situations in the design process, modal analysis procedures can be conducted iteratively to obtain the dynamic characteristics of the bridge for different stages of damage. The correct determination of the dynamic properties of a designed bridge structure can also assist in the detection of invisible structural damage after a seismic event, obtained specifically from the variation or lengthening of its modal periods, which is evaluated experimentally.

The principal modes of deformation of an Ordinary Standard bridge structure generally include the transverse and longitudinal translation of the bridge, the global torsion of the bridge and superstructure, and several modes of flexural deformation of the superstructure, primarily in the vertical direction or simple in-plane bending (see Fig. 3.1).

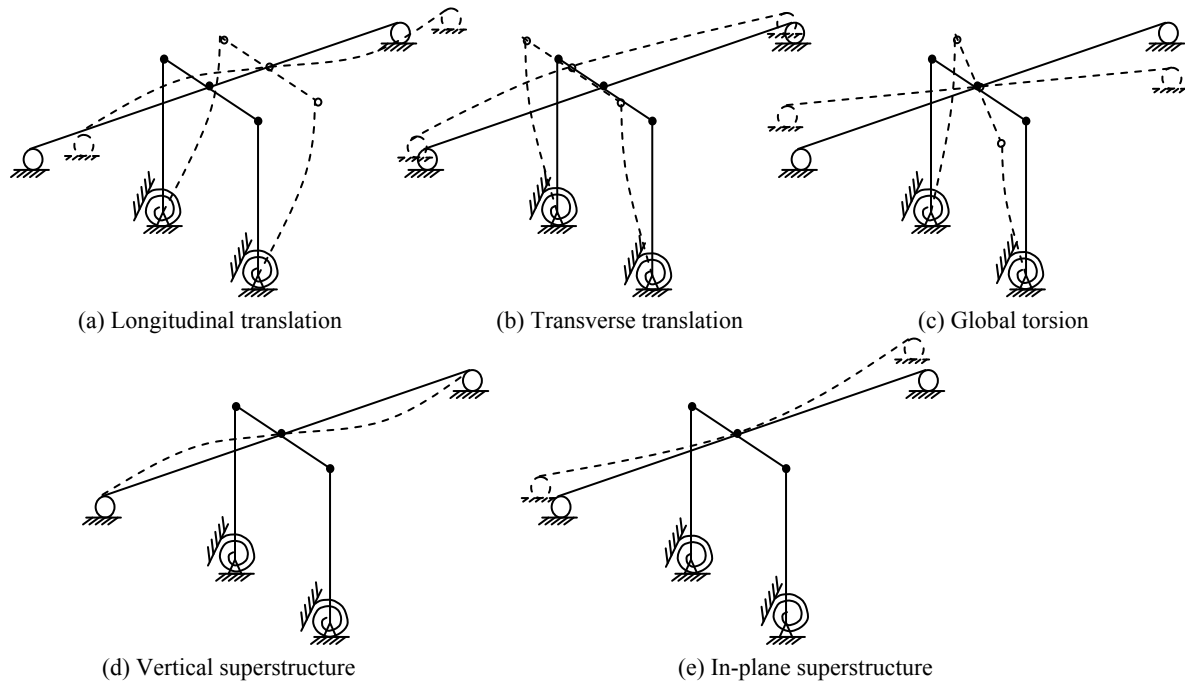


Fig. 3.1 Principal modes of deformation for a multi-column bent, double-span bridge.

The modal analysis can be carried out for Ordinary Standard bridge systems in SAP2000 through an Eigenvector analysis or Ritz-vector modes analysis. Eigenvector analysis determines the undamped elastic mode shapes and frequencies of the system, while Ritz-vector analysis seeks to find modes that are excited by a particular loading. Ritz-vectors representative of the expected vibration modes of a structure can provide a good basis when used for response spectrum or time history analyses that are based on modal superposition (Wilson, Yuan, and Dickens 1982). However, modal time history analysis is not recommended for bridge structures, since it does not account for all model nonlinearities (see Section 3.8). Ritz modes are only representative of the selected Ritz shapes and may be biased compared to the eigenmodes.

The use of Ritz modes for a modal analysis is recommended for the bridge when a distributed gravity load or wind load pattern is of concern for the bridge. For such cases, AASHTO LRFD, 3rd edition, is applicable for determining the initial force vector. For Ordinary Bridge Structures, defined by SDC 2004 as with a total span length smaller than 300 ft and conventional traffic loads, the modal results using Eigenvector analysis and Ritz modes in SAP2000 are similar when the initial load vector is not specified or when typical gravity loading conditions are used instead. For Special Bridge Structures, both Eigenvector analysis and Ritz

modes analysis should be conducted on the bridge to evaluate the dynamic response of the bridge due to free-vibration and special load patterns on the bridge.

The parameters to be specified in the Eigenvector modal analysis case are the number of modes to be found, a convergence tolerance, and the frequency range of interest, which should not be limited. For the Ritz vector modes, the additional parameters to be specified are the starting load vectors, which indicate the spatial distribution of the dynamic load vector, and the number of generation cycles performed for each starting load vector. The generation cycle is the static solution or displacement vector obtained by a recurrence relationship where the mass matrix is multiplied by the previously obtained Ritz vector and used as the load vector. The Ritz vectors are orthogonalized using standard eigensolution techniques.

SAP2000 conducts a linear modal analysis based on the elastic properties of the elements, defined with effective cross section properties to account for concrete cracking. However, it is also possible to perform a modal analysis to approximate the post-earthquake (damaged) dynamic characteristics of the bridge under P- Δ effects. This is achieved by using the resulting stiffness at the end of a nonlinear analysis case (pushover or nonlinear direct-integration time history analysis) instead of the initial stiffness defined under unstressed conditions.

3.3 FREE VIBRATION TEST

A free vibration test is generally performed on an experimental specimen to verify its dynamic properties such as modal damping and natural frequencies. The test is carried out by imposing an initial deformation on the system, within the expected elastic range of response, and then releasing it and allowing it to vibrate without any forced excitation (see Section 2.8.1.2). The decay of motion, as well as the duration of each cycle will allow determining the damping and vibration frequencies of the system (see Sections 2.1, 2.2 of Chopra 2006). To capture the response of a specific mode, the initial deformed shape must coincide with the corresponding mode shape of the structure (see Chapter 9 of Chopra 2006).

A free vibration test can also be performed on the analytical model of the bridge and used to verify the dynamic properties of the system prior to conducting pushover, response spectrum or time history analysis procedures. However, most of the results of the free vibration test must be known previously in order to properly conduct this analysis type. Therefore, a significant insight into the structural system behavior will not be gained through such an analysis procedure.

The mode shapes of the bridge must be obtained previously through a modal analysis (see Section 3.2), as well as the yield displacement of the structure (or the column bent in a specific direction), determined according to Section 3.1.3 of SDC 2004. The damping in the system must be estimated as well for the transient analysis procedure (see Section 2.8.1.3 and Section 3.8.5.3). Nevertheless, the free vibration test can be used to verify that dynamic analysis is properly executed in the structural analysis program used for the bridge.

In SAP2000, a free vibration test is performed on a complete bridge model through a time history analysis (transient analysis) with zero initial conditions, by specifying a unitary impulse time history function to excite the structure and obtain an initial deformed shape. The duration of the impulse must be shorter than 25% of the first mode period. The duration of the entire time history duration can be equal to 10 times the first mode elastic period of the bridge to capture a sufficient number of vibration cycles and observe the decay of motion. The impulse will allow the structure to vibrate freely after the initial excitation with respect to its original undeformed position. A predefined load pattern corresponding to the mode shape of interest is used to excite that particular mode of the structure (see Section 3.6.3 for a similar procedure), while the remaining parameters for the time history analysis are defined according to Section 3.8.5. To achieve a displacement of the structure within its elastic range of response, the scale factor for the unit impulse must be iterated upon. P- Δ geometric nonlinearities are not considered in the analysis, since second-order effects are not expected to occur under small displacements of the structure.

3.4 STATIC ANALYSIS FOR GRAVITY LOADS

The static analysis of dead, live, impact, wind, earth pressure, and other loading conditions is carried out following the specifications of AASHTO LRFD Specifications, 3rd edition. The load combination factors between these load cases are defined accordingly. The seismic analysis of Ordinary Standard bridges is conducted in accordance with Section 2.1.4 of SDC 2004. The combination of seismic analysis results and analysis results obtained from vertical live load or additional dead load corresponding to the weight of the pavement and other nonstructural components of the bridge should not be done for Ordinary Standard bridges. In the case of Nonstandard and Important bridges, a case-by-case determination is required of the effect of such vertical loads on the seismic behavior of these bridge systems.

For Ordinary Standard bridges, some gravity loads in the form of self weight of major structural components, such as the superstructure, column bents, cap beam and abutments are considered in the bridge model for seismic analysis. In SAP2000, the self weight of the bridge is calculated automatically by assigning a load factor of 1 to the dead load case, after the correct specification of the volumetric weight and mass of each material, and an accurate estimation of the cross-sectional area of all modeled components. The remaining tributary dead load of the bridge, corresponding to the pavement or other permanent nonstructural elements, is not considered for seismic analysis.

The definition of the self-weight of the structure is a key element in the assemblage of the mass matrix, thus controlling the dynamic behavior and demand of the system. The load pattern in the pushover analysis (see Section 3.6) is directly related to the mass assignment, and the pushover is carried out considering the dead load on the structure. P-delta effects are also incorporated into the model correspondingly, affecting both static and dynamic analysis results.

Section 2.1.3 of SDC 2004 establishes an equivalent static vertical load applied to the superstructure to estimate the effects of vertical acceleration on the bridge superstructure for Ordinary Standard bridges where the site peak rock acceleration is 0.6g or greater. Section 7.2.2 of SDC 2004 establishes that if such vertical acceleration is considered, a separate analysis of the superstructure nominal capacity is therefore required based on a uniformly applied vertical force equal to 25% of the dead load applied upward and downward. The boundary condition for the superstructure ends is assumed pinned in the vertical direction, for such a load case. However, since the seismic analysis of Ordinary Standard bridges is carried out assuming an elastic superstructure section (see Section 2.3), these additional effects of gravity load, vertical acceleration, and pre-stress are not of interest.

3.5 EQUIVALENT STATIC ANALYSIS (ESA)

According to Section 5.2 of SDC 2004, Equivalent Static Analysis (ESA) can be used to estimate displacement demands for structures where a more sophisticated dynamic analysis will not provide additional insight into its behavior. It is considered to be best suited for structures or individual frames with well-balanced spans and uniformly distributed stiffness where the response can be captured by a predominant translational mode of vibration. According to ATC

32, this procedure should be limited to one- and two-span structures without intermediate expansion joints and with small or no skew.

The seismic demand is assumed as an equivalent static horizontal force applied to individual frames. The total applied force is determined as the product of the spectral acceleration obtained from the 5% damped Acceleration Response Spectra (ARS) curves (see Section 3.7) and the tributary weight. The total horizontal force is applied at the vertical center of mass of the superstructure and distributed horizontally in proportion to the mass distribution.

3.6 NONLINEAR STATIC- PUSHOVER ANALYSIS (POA)

Pushover analysis is a static, nonlinear procedure in which the magnitude of the structural loading is incrementally increased in accordance with a predefined reference load pattern. With the increase in the magnitude of the loading, weak links and failure modes of the bridge structure are determined. The goal of the static pushover analysis is to evaluate the overall strength, typically measured through base shear V_b , yield, and maximum displacement δ_y and δ_u , as well as the ductility capacity μ_c of the bridge structure. Since the objective is to capture the actual behavior of the structure, pushover analysis is performed using the expected material properties of modeled members. The pushover analysis can examine the sequence of limit states, formation of plastic hinges, and redistribution of forces throughout the structure, with the increment of the lateral loads or displacement demand. The pushover curve (force vs. deformation) of the bridge also allows identifying any softening behavior of the entire structure due to material strength degradation or P- Δ effects.

The pushover analysis procedure applied to the bridge structure follows the recommendations of Section 3 of ATC-32 and the present section that define the force-deformation behavior, as shown in Figure 3.2. The values assigned to each of these points vary, according to the type of member and nonlinear model used (see Section 2.5 of the present document).

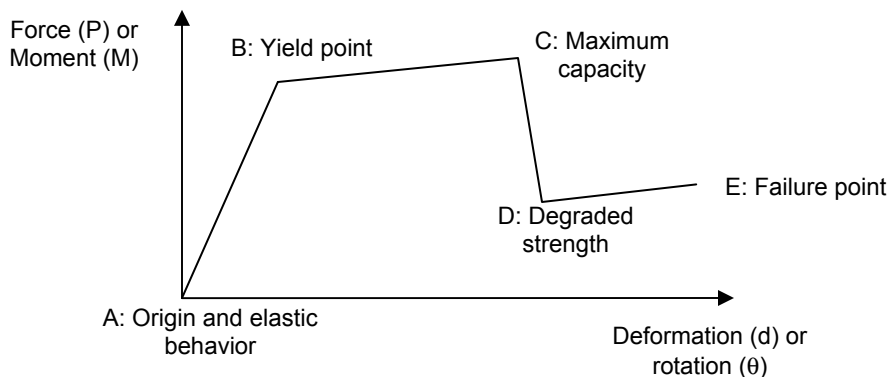


Fig. 3.2 Force-deformation (P-d) or moment-rotation (M-θ) relation for pushover hinge.

3.6.1 Limiting Displacement Value

The pushover analysis of the bridge is conducted as a displacement controlled method to a specified limiting displacement value to capture the softening behavior of the structure by monitoring the displacement at a point of reference, such as one of the column's top nodes or the center of the superstructure span. The maximum displacement specified for the reference point (calculated in SAP) exceeds the ultimate displacement calculated for the column in Section 3.1.3 of SDC 2004 by about 50–100%, i.e. $\Delta_{\max}=(1.5-2.0)\Delta_c$. If degrading behavior is specified or assigned to one or more elements of the bridge, this limiting displacement value allows capturing the failure point in the pushover curve. Section 4.4.5.2 of FEMA 350 for building analysis specifies a limiting displacement value of 1.50 times the ultimate displacement calculated.

3.6.2 Pushover Load Cases

In SAP2000 more than one pushover load case can be run in the same analysis or a pushover load case can start from the final conditions of another pushover load case, previously run in the same session. The lateral pushover load cases conducted on the bridge structure are specified to start from the final conditions of the gravity pushover, where the dead load of the bridge superstructure is fully applied.

The lateral load pushover analysis is conducted in several directions, including longitudinal, transverse, and at an angle α with respect to the principal directions or axes of the

bridge. The values for maximum displacements are computed for each direction of analysis, in accordance with the structural system considered; however, it can be taken as Δ_{\max} for simplification (see Section 3.6.1). For bridges that are asymmetrical with respect to a plane perpendicular to the applied lateral loads, the lateral loads or displacement must be applied in both the positive and negative directions, and the maximum forces and deformations obtained from both directions used for design.

The pushover analysis at an angle α allows the evaluation of the proper interaction between the capacity and stiffness of the bridge along its principal axis. This analysis produces valid results only when column plastic hinges are modeled with nonlinear options including Interaction PMM Hinge and Fiber hinge. For all other nonlinear models of the plastic hinges in SAP2000, an overestimation of the base shear is produced, in the order of 40%, due to the incorrect mathematical formulation of the resultant of the cross section capacities in each orthogonal direction. The combination of pushover analysis cases in orthogonal directions is therefore not recommended for Standard Ordinary bridges; instead, pushover analysis at an angle α is used.

3.6.3 Force Pattern

SAP2000 allows the force pattern used in the pushover analysis to be based on a uniform acceleration in a specified direction, a specified mode shape, or a user-defined static load case. If a uniform acceleration is applied, the force pattern will be automatically assigned by SAP2000, proportional to the translational mass distribution in the corresponding direction. If a mode shape is used instead, modal analysis results corresponding to the longitudinal and transverse translation of the bridge (see Section 3.2) are to be assigned to the corresponding load case (longitudinal or transverse pushover, respectively). The results from Eigenvector or Ritz vector modes can be interchangeably used.

However, the pushover analysis combining different mode-shape force patterns is not necessary for Ordinary Standard bridges with negligible skew supports or significantly different column heights. The natural modes of such structures generally exhibit low correlation and the higher modes generally do not contribute significantly to the overall response of the bridge due to low mass participation factors (see Appendix A.2). However, pushover analysis using a force pattern derived from a combination of mode shapes should be considered in the cases of

Nonstandard Ordinary or Important bridges, where high correlations develop between the natural modes due to geometric and other irregularities. The criteria for the choice of an appropriate force pattern for pushover analysis of bridge structures including more than one mode shape are proposed by Isakovic, Fischinger, and Fajfar (1999).

If a user-defined force pattern is used for the bridge structure, a separate static load case will be defined in each direction of analysis, where the total pushover force or base shear should be distributed between the column top nodes and the superstructure ends at the connection with the abutments, according to the tributary translational mass assigned to each node. The participating mass of the abutments is defined in Section 2.8 of the present document, while the tributary mass of each column top will be determined based on tributary length of the superstructure and half the column height.

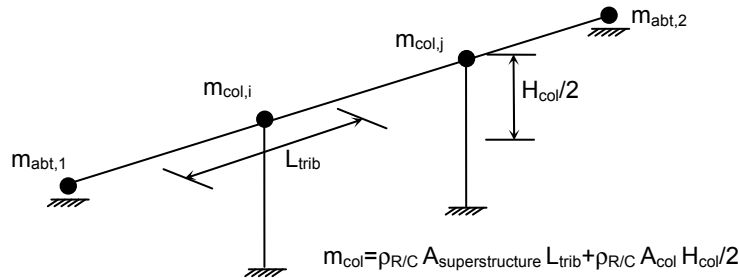


Fig. 3.3 Tributary mass.

The user-defined force pattern for the pushover analysis will be based on the ratio of the tributary mass at each point to the total mass of the bridge as follows: $F_i = m_i / \sum m_i$, where m_i is the tributary mass at either the abutment or the column top node.

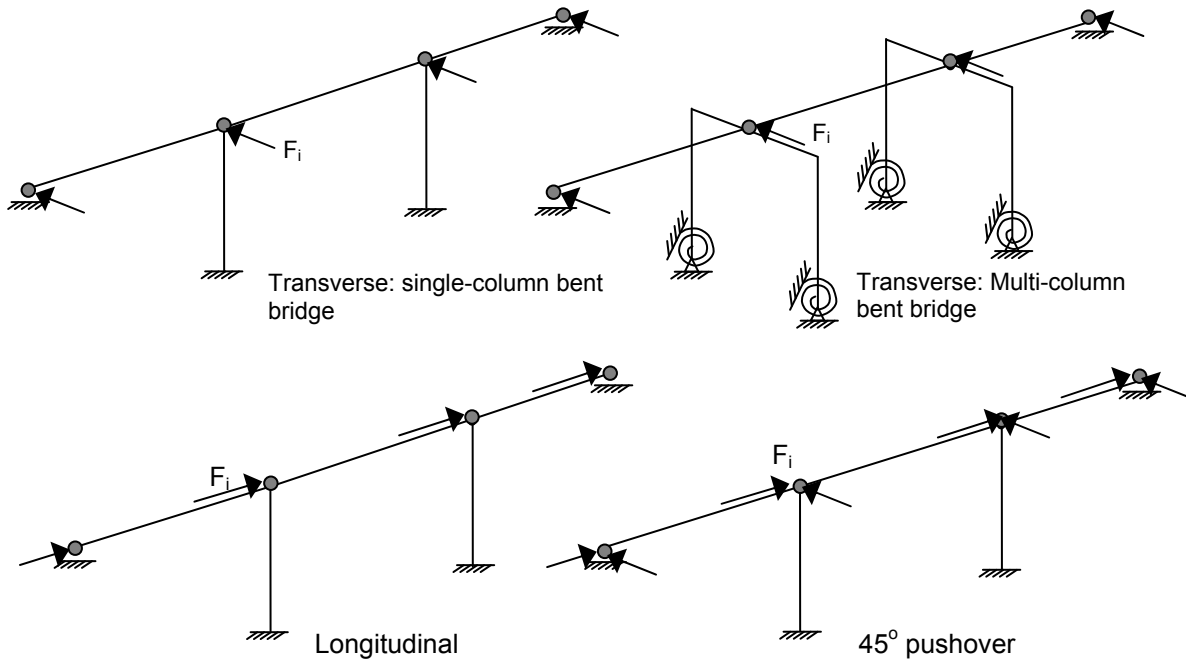


Fig. 3.4 Force pattern for pushover analysis.

The pushover analysis simulates inertial forces through the application of static nodal forces at the column top or superstructure ends. The load pattern presented above for the transverse direction takes into consideration the distribution of the translational mass throughout the bridge. However, the rotational mass of the superstructure is not considered in the analysis. In the case of single column bent bridges or Nonstandard bridges with significant skew, the rotational mass could play an important role in the demand conditions. The rotational mass could be modeled for those special bridges with a distributed torque applied to the superstructure elements.

Additional parameters that influence the results of a pushover analysis in the transverse bridge direction have been identified, including the ratio between the stiffness of the superstructure and that of the bents, eccentricity, the ratio between the torsional and translational stiffnesses of the bridge, and the type of constraints at the abutments (Isakovic, Fishinger, and Fajfar 1999). The effect of some of these parameters on the results of a pushover analysis of Standard Ordinary bridges have not been investigated in the present guidelines document.

3.6.4 Verification of Pushover Curve

At the completion of the analysis phase, the pushover curve is obtained (see Fig. 3.5), where the total base shear and displacement capacity of the bridge are determined. A quick check of the base shear values should be conducted to verify the results of the pushover analysis, according to the number and capacity of the plastic hinges expected to form in each direction of loading, the free height of column bents, the ductility capacity calculated as per Section 3.1 of SDC 2004, and the estimated abutment backbone curves. In addition to the pushover curve, the sequence of hinge formation can also be obtained in SAP2000 by displaying the deformed shape on a step-by-step basis, where hinges will appear when yielded and the rotational demand can be established for each one through the additional tables provided.

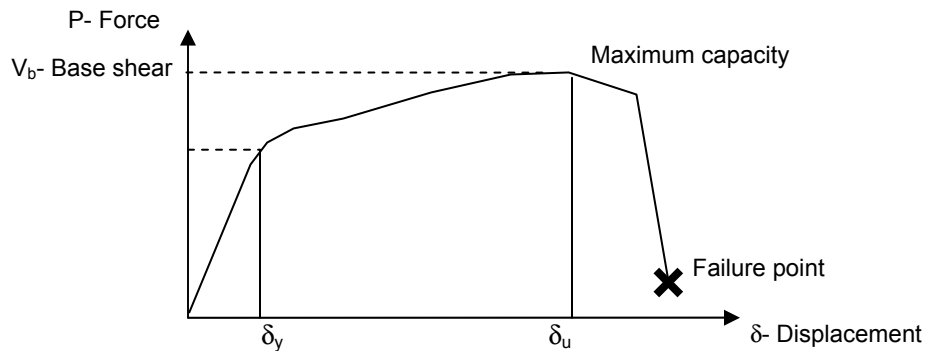


Fig. 3.5 Typical pushover curve.

The capacity spectrum curve can also be obtained in SAP2000. The magnitude of the earthquake and the damping information can be modified interactively. The performance point for a given set of values is defined by the intersection of the capacity curve (green) and the single demand spectrum curve (yellow). It is also possible to record the capacity and demand curves and to convert the pushover curve to acceleration-displacement response spectrum format (known as ADRS format, see pages 8–12 in ATC-40).

3.7 DYNAMIC ANALYSIS—RESPONSE SPECTRUM ANALYSIS (RSA)

3.7.1 Purpose of RSA Procedure

The response spectrum analysis (RSA) is an elastic seismic analysis procedure that generally results in reasonable response values for the predicted design motions, displacements and member forces in structural systems that remain essentially elastic under earthquake excitation. The method involves the previous calculation of the maximum values of the displacements and member forces in each mode using smooth design spectra, obtained as the average of several earthquake motions, and accounting for the maximum credible earthquake (MCE) expected for the site.

For each natural mode considered for the system, static analysis is conducted for the entire structure under a set of equivalent earthquake forces. The resulting modal static response is then multiplied by the spectral ordinate (displacement, pseudo-velocity, or pseudo-acceleration) to obtain the peak modal response. Such procedure therefore reduces the dynamic analysis to a series of static analysis and avoids the lengthy computation required from a response history analysis of a multi-degree of freedom system (see Section 3.8). The RSA is still considered a dynamic analysis procedure since it makes use of the vibration properties of the structure, including the natural periods, modes, and modal damping ratios, as well as the dynamic characteristics of the ground motions considered.

According to Section 2.2 and 5.2.2 of SDC 2004, when ESA (see Section 3.5) is inadequate, the displacement demand on the Ordinary Standard bridges can be estimated through the RSA procedure (see Section 3.7), including the effects of soil or foundation flexibility (see Section 2.6 of the guidelines). The internal forces obtained from the RSA method can be used in design only for bridge structures that remain elastic throughout the analysis. Several limitations are identified in the RSA procedure (see Section 3.7.2), thus recommending its use only for Ordinary Standard Bridges. This procedure fails to accurately approximate the nonlinear response of a complex three-dimensional structural system, and therefore for the case of Standard bridges with significant nonlinear action, Nonstandard or Important bridges, time history analysis (see Section 3.8) should be conducted as well to verify and enhance the RSA results.

3.7.2 Limitations of RSA Procedure

The limitations of the response spectrum method can result in notable inaccuracies for nonlinear analysis of multi-degree of freedom structures in comparison with the response history analysis result, some of which could be removed by future development of the procedure. However, the RSA results are generally considered accurate enough for structural design applications. A few of the limitations of the RSA are summarized as follows:

- The modal superposition method is restricted to linear elastic analysis. RSA is an elastic dynamic analysis where the structural demand is defined based on an elastic spectrum; however, it will produce stresses in some elements exceeding their elastic limit. The estimated force and displacement demand could vary significantly from the actual values due to sources of nonlinearity which are not captured in the analysis.
- The equivalent earthquake forces determined using the RSA procedure may at times seriously underestimate or overestimate the site-specific ground motion characteristics.
- The peak values of drifts, stresses, element forces and base shear obtained for each mode in the response spectrum procedure are not produced at the same time. Certain combination rules may result in significant inaccuracy when computing the modal contribution to the total response.
- A plot of a dynamic displaced shape has little meaning, since each displacement is an estimation of the maximum value, which is always a positive number. Drift values are used instead to estimate the damage to structural and nonstructural elements; however, these values cannot be computed directly from the peak displacement values.
- Stresses and element force computation can be overestimated using RSA, since the distribution of forces and energy dissipation in the bridge components due to inelastic action is ignored in such procedure. This overestimation could result in a highly conservative design with unnecessary over-strength (Section 4.2.2 of ATC 32).
- Design considerations for the combined effect of different element forces such as axial force, shear, and bending moment must account for the relative signs of the force values in each mode and will usually result in errors, since the peak values for each force can occur at a different time.

- The estimation of the peak base shear for a three-dimensional structure is carried out by a repeated RSA procedure applied at different angles with respect to the principal axes of the bridge.

Wilson (1998) presents a series of recommendations on reducing such inaccuracies in the computation of several of the demand parameters and design values mentioned above. Additional limitations were identified in ATC 32, Section 3.1 related to the ARS curves generated for Caltrans bridges, among them considerations regarding earthquake intensity, damage potential, near-source effects, hazardous soil conditions, accuracy of soil-amplification spectral ratios, spectral shapes and duration of output motions.

3.7.3 Acceleration Response Spectrum (ARS) Curves

As specified in Section 2.2.1 of SDC 2004, the horizontal mean spectral acceleration used for bridge analysis is selected from an elastic acceleration response spectra (ARS) curve, based on the recommendations of Caltrans Geotechnical Services (GS). GS will recommend a standard ARS curve, a modified standard ARS curve, or a site-specific ARS curve that includes the effect of local soil conditions and distance to the nearest faults, all developed assuming a 5% damping coefficient. A reduction factor, R_D can be applied to the 5% damped ARS curves, according to Section 2.1.5 of SDC 2004, to adjust the displacement demand of the bridge if a higher damping coefficient is anticipated for the structure. The Standard ARS curves for California are included in Appendix B of SDC 2004, and Section 6.1.2 of SDC 2004 provides information regarding the modified ARS curves and site specific ARS curves.

The Caltrans SDC 2004 specifications use the concept of a maximum credible earthquake (MCE) and define the seismic loading for typical bridges for a variety of soil conditions in terms of ARS curves. The elements of the ARS curves are the maximum expected acceleration at bedrock or rock-like material due to the maximum credible earthquake (factor A), a smoothed, normalized 5% damped elastic acceleration response spectra on rock (factor R), and soil amplification spectral ratio (factor S).

3.7.4 Modal Combination Rule

The modal combination rules are intended for use when the excitation is characterized by a smooth response or design spectrum, obtained as the average of numerous ground motions. The most conservative method used to estimate the peak structural response values (displacements or forces) is the sum of the absolute of the modal response values (ABS). This approach assumes that all the maximum modal values occur at the same time, thus highly overestimating the actual peak response. Another common approach is the square root of the sum of the squares (SRSS) of the maximum modal values (Rosenblueth 1951), which assumes that all of the maximum modal values are statistically independent. This approach provides satisfactory results for well-separated natural frequencies. However, for three-dimensional structures such as bridges, in which a large number of frequencies are closely spaced, the SRSS approach does not yield adequate results.

The complete quadratic combination (CQC) rule for modal combination (Wilson, Der Kiureghian, and Bayo 1981) overcomes the limitations of the SRSS method and is recommended for Caltrans bridge analysis using the RSA procedure. The CQC rule provides satisfactory results for a wide spread of structures with natural frequencies that are well-separated or closely-spaced (associated to the several frames in the bridge model) by recognizing the relative sign of the terms in the modal response and adding an additional cross-term to the summation, thus eliminating the errors in the SRSS method. The CQC method takes into account the statistical coupling between closely-spaced modes caused by modal damping. Increasing the modal damping increases the coupling between closely-spaced modes. If the damping is zero for all modes, this method degenerates to the SRSS method.

3.7.5 Orthogonal Effects

It has been established (Penzien and Watabe 1975) that motions that take place during an earthquake event have one principal direction that is difficult to determine. In addition to the motion in the principal direction, orthogonal motions with a lower intensity can occur simultaneously. Because of the complex nature of three-dimensional wave propagation, statistical independence is generally assumed between the orthogonal motions. Based on these

findings, the conventional seismic design criterion is that the structure must equally resist earthquake ground motions of a given intensity from all possible directions.

According to Chapter 2 of SDC 2004, the dynamic analysis intended to represent the linear response of Caltrans bridges to the MCE is performed through a single response spectrum procedure defined for a specific site. Separate RSA analyses are carried out for simplicity along an arbitrarily defined set of global axis of the bridge: The longitudinal direction (L), usually selected as a chord between the two abutments and the transverse direction (T), orthogonal to the first. Section 2.1.2 of SDC 2004 defines the maximum earthquake demand as the combination of 100% of the response in the longitudinal direction and 30% of the transverse, or vice versa. In each direction of analysis (T or L), the maximum response is computed separately through modal superposition, as defined in Section 3.7.4. The number of degrees of freedom and the number of modes considered in the analysis shall be sufficient to capture at least 90% mass participation in the longitudinal and transverse directions, according to Section 5.2.2 of SDC 2004.

Section 4.2.2 of ATC 32 recognizes some potential shortcomings of the combination rule presented by SDC 2004 and recommends the use of 40% of the orthogonal response quantities instead of 30%, to include the effects of vertical earthquake loading and better approximate the critical earthquake effects. However, these percentage combination rules are empirical and could still underestimate the design forces in certain members, producing a member design which is relatively weak in one direction.

For Ordinary Standard Bridges which are regular structures with clearly defined principal directions, the combination of forces in orthogonal directions (using 100% of the response in one direction and 30 or 40% in the orthogonal direction) yields approximately the same results as the SRSS combination method for orthogonal responses, and is an acceptable procedure. In each orthogonal direction of analysis, the maximum response is computed separately through modal superposition (see Section 3.7.4). However, for complex three- dimensional structures such as Nonstandard or curved bridges, the principal direction producing the critical earthquake response is not apparent.

An additional method is suggested in Section 2.1.2 of SDC 2004 for the determination of the maximum seismic response, consisting of the application of the ground motion along the principal axes of individual components. In such a method, the ground motion must be applied at a sufficient number of angles to capture the maximum deformation of all critical components. This approach can be used to determine the maximum stresses and deformations for Nonstandard

and curved bridges. The modal superposition of the response quantities in each direction of analysis is carried out according to Section 3.7.4.

The two methods described above ignore the vertical input motions and require great computational effort and several runs to establish the critical response. Section 4.2.2 of ATC 32 recommends an alternative approach consisting of a three-dimensional analysis using 100% of the maximum input motions in the vertical and horizontal directions, which can be all distinct. A single analysis is carried out for this three-directional input, with responses combined using an appropriate statistical combination rule such as the CQC applied to the required end-product. The end-product consists of a modal combination of the response quantities computed in each direction, carried out according to Section 3.7.4. The common practice of calculating responses in orthogonal directions and then using a vector combination is not recommended. This approach is independent of the reference system and therefore the resulting structural members design will equally resist earthquake motions from all possible directions. For such alternative analysis enough modes should be included in the model to provide 90% of the participating mass in the horizontal directions and 75% in the vertical direction, representing the significant modes of vibration of the entire bridge structure. The CQC method for combining orthogonal responses is recommended for response spectrum analysis, since it resolves many of the shortcomings of the orthogonal combination rules (using 100% of the response in one direction and 30 or 40% in the orthogonal direction).

The approach presented by Menun and Der Kiureghian (1998) as the CQC3 method for the combination of the effects of orthogonal spectrum was evaluated successfully on bridge-like components in a building-type structure (Menun and Der Kiureghian 2000). In this approach, envelopes for seismic response vectors are established according to the orientation of the principal axes of the structure. This method has been found (Wilson 1998) to produce realistic results for building structures and been adopted by several buildings codes. The applicability of this approach for bridge structures is currently under investigation.

3.7.6 RSA Using SAP2000

Response- spectrum analysis is performed in SAP2000 using mode superposition (Wilson and Butten 1982). SAP2000 automatically accounts for the elastic properties of the structure and ignores the nonlinearities defined for the geometry or materials of the bridge. The earthquake

ground acceleration in each direction is defined by a digitized response–spectrum curve of pseudo–spectral acceleration response versus period of the structure. The accelerations can be specified in three directions; however, a single positive result is produced for each response quantity, including displacements, forces, and stresses. A user’s reference system can be defined for the directions of ground accelerations.

The response-spectrum curve chosen should reflect the damping that is present in the structure being modeled. During the analysis, SAP2000 automatically adjusts the response-spectrum curve from the defined damping value to the actual damping present in the model. The damping in the structure affects the shape of the response-spectrum input curve and the amount of statistical coupling between the modes for certain modal combination rules (CQC). The damping in the structure is modeled using uncoupled modal damping with specific damping ratios defined for each mode.

The modal damping is obtained from three different sources in the analysis which are added together to obtain the total damping in the bridge:

1. Modal damping from each response-spectrum analysis case which can be constant for all modes, linearly interpolated by period or frequency, or mass and stiffness proportional.
2. Composite modal damping from the materials: Material damping is converted automatically to composite modal damping, ignoring cross-coupling between the modes.
3. Effective damping from the Link/Support elements with linear effective-damping coefficients specified and ignoring cross-coupling between the modes.

For every given direction of acceleration, the maximum displacements, forces, and stresses are computed throughout the structure for each of the vibration modes. These modal values for a given response quantity are combined to produce a single positive result for the given direction of acceleration using the CQC modal combination rule, which is the default and recommended procedure. Other combination rules are also available.

For each displacement, force, or stress quantity in the structure, modal combination produces a single, positive result for each direction of acceleration. These directional values for a given response quantity are combined to produce a single, positive result through the recommended (and default) SRSS directional combination rule. This method is invariant with respect to coordinate system, and as described in Section 3.7.5, the results for any choice of reference system are the same.

The response spectrum analysis output includes:

- Modal damping and ground accelerations acting in each direction for every mode.
- Modal amplitudes or multipliers of the mode shapes that contribute to the displaced shape of the structure for each direction of acceleration.
- Modal correlation symmetric matrix showing the coupling factors assumed between closely spaced modes.
- Base reactions: Total forces and moments about the global origin at the supports needed to resist the inertia forces due to response spectrum loading and reported for each individual mode and loading direction. The total response-spectrum reactions are reported after performing modal combination and directional combination.

3.8 DYNAMIC ANALYSIS—TIME HISTORY ANALYSIS (THA)

3.8.1 Purpose of THA Procedure

Due to the limitations of the response spectrum analysis procedure to approximate the dynamic nonlinear response of a complex three-dimensional structural bridge systems, nonlinear time-history analysis is strongly recommended instead. Nonlinear time history analysis accounts for the nonlinearities or strength degradation of different elements of the bridge, as well as the load pattern or ground motion intensity and characteristics used during a nonlinear dynamic analysis. Nonlinear time history analysis also allows determining the effect of added energy-dissipation devices in structural systems.

The loading in a time history analysis is foundation displacement or ground motion acceleration, not externally applied loads at the joints or members of the structure. The design displacements are not established using a target displacement, but instead are determined directly through dynamic analysis using suites of ground motion records. Inertial forces are produced in the structure when the structure suddenly deforms due to ground motion and internal forces are produced in the structural members. As described in Section 3.2, each bridge structure possesses different predominating mode shapes and frequencies, which are excited according to the ground motion characteristics and intensity. The calculated bridge response is highly sensitive to those characteristics of individual ground motions.

For complex three-dimensional structures such as curved bridges, the direction of the earthquake that produces the maximum stresses, in a particular member or at a specified point, is not apparent. For all bridge types time history analysis must therefore be performed using several

different earthquake motions at various input angles to assure that all the significant modes are excited and the critical earthquake direction is captured, producing the peak response and estimating accurately the seismic demand on the structure. Another approach is to use a larger suite of earthquake ground motion records of three components at one angle of input. The selection, scaling and application of ground motions to the bridge structure's analytical model will be carried out according to the recommendations of Section 3.8.4.

Since seismic motions can excite the higher frequencies of the structure, neglecting higher modes of the bridge system could introduce a significant error in the dynamic analysis results. According to Section 5.2.2 of SDC 2004, the number of degrees of freedom and the number of modes considered in the analysis shall be sufficient to capture at least 90% mass participation in the longitudinal and transverse directions.

The main disadvantage of the time history analysis method is the high computational and analytical effort required and the large amount of output information produced. During the analysis, the capacity of the main bridge components is evaluated as a function of time, based on the nonlinear behavior determined for the elements and materials. This evaluation is carried out for several input ground motions applied at different angles, and the response of the structure is recorded at every time step. Despite these challenges, the evaluation of the capacity using the THA method at each time step produces superior results, since it allows for redistribution of internal forces within the structure. Each member is therefore not designed for maximum peak values, as required by the response spectrum method, but for the actual forces produced in the structure during dynamic excitation. The recent development of computer hardware has allowed to reduce the required computational time and made it more practical to run many time history analyses for complex bridge structures. In addition, the seismic demand can be estimated through statistical approximations, using the mean and standard deviation values of joint displacements and element forces to determine the peak response expected for the structure.

3.8.2 Solution Methods

The most general approach for the solution of the dynamic response of structural systems is the direct numerical integration of the dynamic equilibrium equations at a discrete point in time. This analysis is initiated at the undisturbed static condition of the structure and repeated for the

duration of the ground motion input with equal time increments to obtain the complete structural response time history under a specific excitation.

There exist a large number of accurate, higher-order, multi-step methods that have been developed for the numerical solution of the differential equations. However, in real bridge systems the differential equations of motion involving displacement, velocity and acceleration cannot be considered as smooth functions due to the nonlinear hysteresis of most structural materials, friction forces developed between contacting surfaces, and buckling of elements. Therefore, only single-step methods are recommended for the solution of the equations of motions of bridge structures.

The step-by-step solution methods attempt to satisfy dynamic equilibrium at discrete time steps and may require iteration, especially when nonlinear behavior is developed in the structure and the stiffness of the complete structural system must be recalculated due to degradation of strength and redistribution of forces. Different numerical techniques have been studied by numerous researchers and are generally classified as either explicit or implicit integration methods. Important considerations for the proper selection of the integration method for a particular structure are the stability and accuracy of the results, as well as algorithm noise which are spurious oscillations created by the algorithm.

Direct explicit integration methods are very fast, since they do not require iteration within each time step. They allow any type of damping and nonlinearity in the model; however, they require very small time steps to obtain stable results and will therefore produce larger and unnecessary output data. Direct implicit integration of the differential equations of motion require iteration at each time step to achieve equilibrium, and are computationally demanding, solving large sparse matrices. They also allow any type of damping and nonlinearity in the structural model, and additionally tolerate larger time steps due to unconditional stability in the results using certain parameters. Among the implicit integration methods are the Newmark family and the α -method of Hilber Hughes and Taylor, recommended for bridge time history analysis.

Modal solution of the equation of motion is also possible for linear elastic systems and result in some cases in reduced computational effort and accuracy in the analysis results. However, modal-superposition solution should not be used for bridge analysis when nonlinear behavior is expected to develop in the structure. A modal-superposition type of nonlinear time-history analysis is available in SAP2000 (fast nonlinear analysis (FNA)). FNA only accounts for

nonlinear behavior defined in the Link/Support elements, ignoring geometric and material nonlinearities, and therefore the use of such analysis type for bridge structures is discouraged.

The use of frequency-domain solution methods for dynamic analysis is also available and is highly effective for harmonic types of loads such as mechanical vibrations, sea-waves and wind. The use of such methods is restricted to linear systems and present major disadvantages for the solution of structures under non-periodic random earthquake excitation.

3.8.3 Time Integration Methods

The common incremental solution methods using single-step, implicit, and stable procedures recommended for nonlinear structures subjected to seismic motion are presented in the present section. A brief discussion regarding their applicability for bridge analysis and limitations is also offered.

3.8.3.1 Newmark's Family of Methods

Newmark's family of single-step integration methods (Newmark 1959) have been commonly applied to the dynamic analysis of many practical engineering structures under both blast and seismic loading. In addition, it has been modified and improved by many other researchers. A large number of different numerical integration methods are possible by just specifying different integration parameters for the Newmark method. A few of the most commonly used integration methods are summarized in the following table (Wilson 1998).

Table 3.2 Summary of Newmark's methods modified by δ factor.

Method	γ	β	δ	Stability	Accuracy
Central Difference	0.5	0	-	Conditional ($\Delta t/T_{\min} < 0.3183$)	Excellent (small Δt)
Linear Acceleration	0.5	0.167	-	Conditional ($\Delta t/T_{\min} < 0.5513$)	Very good (small Δt)
Average Acceleration	0.5	0.25	-	Unconditional ($\Delta t/T_{\min} = \infty$)	Good (small Δt), no numerical energy dissipation
Modified Average Acceleration	0.5	0.25	$\Delta T/\pi$	Unconditional ($\Delta t/T_{\min} = \infty$)	Good (small Δt), numerical energy dissipation (large Δt)

The average (constant) acceleration method is the most robust method to be used for the step-by-step dynamic analysis of large complex structural systems in which a large number of short periods are present, due the unconditional stability of the algorithm. The modified average acceleration method was introduced to reduce the numerical errors and damp out the indefinite large oscillation of the short-period mode shapes produced in the average acceleration method during the solution procedure. The modified method introduces a δ factor to increase the short-period stiffness proportional damping and numerically dissipate the energy of the oscillating structure; however, it also generates a minimum error in the long-period response.

Since computer models of large real structures normally contain a large number of modes with periods smaller than the integration time step that can produce indefinite oscillation, it is essential to select a numerical integration method that is unconditional for all time steps and displays a desirable level of numerical damping. The modified average acceleration method is therefore a general procedure that can be used for the nonlinear dynamic analysis of bridge structure.

3.8.3.2 Wilson θ -Method

The general Newmark's methods can be made unconditionally stable by the introduction of a θ factor to the time step and external loading, defined as the Wilson θ -method (Wilson 1973). For $\theta=1.0$, Newmark's methods are not modified. The use of the θ factor tends to numerically damp out the high modes of the system and therefore will introduce important errors in complex structures where the higher mode response is imperative. Also, dynamic equilibrium is not satisfied exactly at every time step, and therefore the use of this method is discouraged for such structures.

3.8.3.3 Hilber-Hughes-Taylor α Method (HHT)

The Hilber-Hughes-Taylor (HHT) integration scheme (Hilber, Hughes, and Taylor 1977) is an implicit, unconditionally stable method with numerical damping properties to reduce higher mode oscillation, while achieving second-order accuracy (error proportional to Δt^2) when used to solve the ordinary differential equations of motion. The method makes use of an alpha (α) parameter ranging from $(-1/3)$ to 0, instead of the β and γ parameters in the Newmark method.

The smaller the value of α , the more damping is induced in the numerical solution. The choice of $\alpha = 0$ leads to the trapezoidal method (average acceleration method) with no numerical damping.

The HHT method is a general improvement to the Newmark modified average acceleration method. However, the α factors cannot be predicted as easily as the δ factor for the modal damping ratio in the use of the stiffness proportional damping method (modified average acceleration method). Also, it does not solve the fundamental equilibrium equation at every time step, and in some cases it results in higher computational effort. Therefore, both procedures are considered to have similar performance in the solution of nonlinear dynamic analysis of bridge structures and are currently implemented in many structural analysis software.

3.8.4 Ground Motion Characterization

New criteria for the selection and scaling of ground motions used for linear and nonlinear time history analysis of buildings and bridge structures is currently being developed under the PEER Lifelines program. The hazard and intensity levels of the input earthquake excitation shall also be defined according to the established criteria. Three components of the ground motion including the parallel, perpendicular and vertical to the fault, will be used to conduct the time history analysis of the bridge. To determine the critical response of the bridge, nonlinear time history analysis must be conducted using a large suite of ground motions or by applying few records at different angles with respect to the principal axes of the bridge (longitudinal and transverse). The PEER Lifelines program shall establish the preferred procedure required to adequately capture critical bridge response. In the case of bridge structures with negligible skew, the orientation of the input ground motion parallel to the principal axis of the bridge is likely to produce the maximum response.

For building analysis, the selection of suites of ground motion acceleration histories is currently carried out according to the recommendations of Section 2.6.2 of FEMA-273 and Section 4.4.6 FEMA-350. A minimum of three pairs of ground motion records are used in the analysis, where each ground motion corresponds to the hazard level appropriate to the desired performance objective and consists of two orthogonal components of the record. The envelope of the three records is used to compute the maximum response of the bridge. If seven ground motions are used in the analysis, the median value of response obtained from the different records is used to estimate the peak response of the bridge. The analysis of a three-dimensional

building model under multi-directional excitation is carried out following Section 3.2.7 of FEMA-273 using simultaneously imposed pairs of earthquake ground motion records along the horizontal axes of the building. The effects of torsion are also considered according to Section 3.2.2.2 of FEMA-273.

3.8.5 THA Using SAP2000

3.8.5.1 General Considerations

Direct integration for the solution of the differential equations of motion is available in SAP2000 for linear and nonlinear time history analysis. For linear analysis, modal superposition can be used instead with greater efficiency than the direct integration method. When using direct integration for nonlinear transient analysis, all types of nonlinearities (material, geometric) are considered in the algorithm.

A nonlinear direct-integration time-history analysis can be initiated from zero initial conditions (unloaded structure) or continued from a nonlinear static analysis (pushover) or another direct-integration time-history nonlinear analysis. The geometric nonlinearity is taken as the previous analysis case. For the analysis of undamaged bridge structures, nonlinear time history analysis is conducted including only the effects of gravity loads, according to Section 3.4.

3.8.5.2 Time Integration Methods and Parameters

The same time-integration parameters and considerations are available for linear and nonlinear time history analysis. Direct integration results are extremely sensitive to time-step size, and therefore the analysis should be repeated with decreasing time-step until convergence.

The time-integration methods available in SAP2000 include the Newmark's family of methods, Wilson, HHT, Collocation, and Chung and Hulbert. As recommended in Section 3.8.3, Newmark's average acceleration, modified average acceleration or HHT methods shall be used for seismic analysis. If convergence problems occur during nonlinear analysis, the HHT method is used initially with an α value of (-1/3) to get an approximate solution. The analysis is then repeated with decreasing time step sizes and α values to achieve greater accuracy in the results.

3.8.5.3 Damping

The damping in direct-integration time-history analysis is modeled using a full damping matrix including cross coupling modal damping terms obtained from the following two sources:

1. Proportional damping from the analysis case: Damping matrix applied to the entire structure calculated as a linear combination of the stiffness and mass matrices (Rayleigh damping, see Fig. 3.6). Stiffness and mass proportional damping coefficients are specified directly or by equivalent fractions of critical modal damping at the first two modal periods. The stiffness proportional damping is linearly proportional to frequency and is related to the deformations within the structure. It can excessively damp out low period components of the oscillation. Stiffness proportional damping uses the current, tangent stiffness of the structure at each time step. Therefore, a yielding element has less damping than an elastic element, and a gap element has stiffness-proportional damping when it is closed. Mass proportional damping is linearly proportional to period. It is related to the motion of the structure and can excessively damp out long period components.
2. Proportional damping from the materials: Stiffness and mass proportional damping coefficients can be specified for individual materials. Larger coefficients can be used for soil materials than for steel or concrete. For linear direct-integration time-history analysis, the linear effective damping for the Link/Support elements is also used.

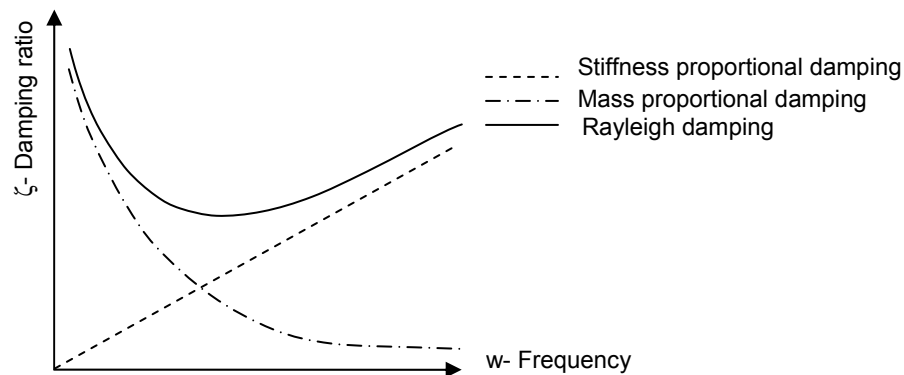


Fig. 3.6 Rayleigh damping used for direct-integration time history analysis.

3.8.6 Analysis of Results

As a result of the large computational requirements it can take a significant amount of time to solve structural systems with just a few hundred degrees of freedom. In addition, artificial or numerical damping must be added to most incremental solution methods in order to obtain stable solutions. Because the numerical model accounts directly for effects of material and geometric inelastic response, the calculated deformations and internal forces are only reasonable approximations of those expected during the applied earthquake motion. For this reason, engineers must be very careful in the interpretation of the results. The results of the analysis are to be checked using the applicable acceptance criteria of Section 5.3 of ATC 32. The calculated displacements and internal forces are compared directly with the acceptance values for the applicable performance level.

The criteria used are for the determination of forces and deformations of bridge structures under nonlinear dynamic analysis will be similar to the recommendations of Section 4.4.6 of FEMA 350. The response quantities shall be computed as follows:

1. If less than seven pairs of ground motion records are used to perform the analyses, each response quantity shall be taken as the maximum value obtained from any of the analyses.
2. If seven or more pairs of ground motion records are used to perform the analyses, the median value (value exceeded by 50% of the analyses in the suite) of each of the response quantities computed from the suite of analyses may be used as the demand.

4 Conclusions

4.1 PROJECT GOALS AND OBJECTIVES

The primary objective of this project was to develop practical guidelines for nonlinear analysis of bridge structures that will assist practicing engineers in the implementation of nonlinear methods for bridge design and analysis during everyday practice. The project was intended as a collaborative effort between university researchers and practicing bridge designers so as to be more readily implemented in practice.

The recommendations developed in the document will ensure that accurate nonlinear modeling techniques are employed by Caltrans and that PEER researchers realistically model typical Caltrans bridge details. Bridge components that require special modeling considerations and nonlinear characterization are identified in the guidelines document, establishing specific criteria for the level of sophistication required. Several incompatibilities or inconsistencies between SAP2000 and OpenSees were investigated for the reduction of possible errors during the analysis using a particular structural analysis program. The bridge models developed for this study using SAP2000 and OpenSees structural analysis programs can be presently used to investigate issues of ground motion selection and scaling. The OpenSees and SAP2000 input files, as well as the ground motion data, are available through the “Additional Files” link for this report at the PEER publications website: http://peer.berkeley.edu/publications/peer_reports/reports_2008/

An extended literature review of the current engineering practice and code criteria for bridge design, modeling, and analysis was carried out concurrently throughout the project, reviewing primarily documents such as SDC 2004, BDS 2000, BDS 2003, ATC-32, MTD 20-1, AASHTO LRFD Specifications, 3rd edition, and others, to guarantee consistency in the proposed recommendations. Additional documentation regarding building modeling and analysis was reviewed as well, such as FEMA 273, FEMA 350, FEMA 356, among others, to compare the

criteria used for building and bridge design. The recommendations of the present guidelines document must be verified to comply with the findings of NCHRP Report 472 pertaining to bridge modeling and design philosophy.

4.2 SUMMARY OF GUIDELINES

The primary modeling aspects of the major components of a Standard Ordinary Bridge, discussed in detail throughout *Bridge Modeling*, Chapter 2 of the guidelines document, are summarized in the following figure:

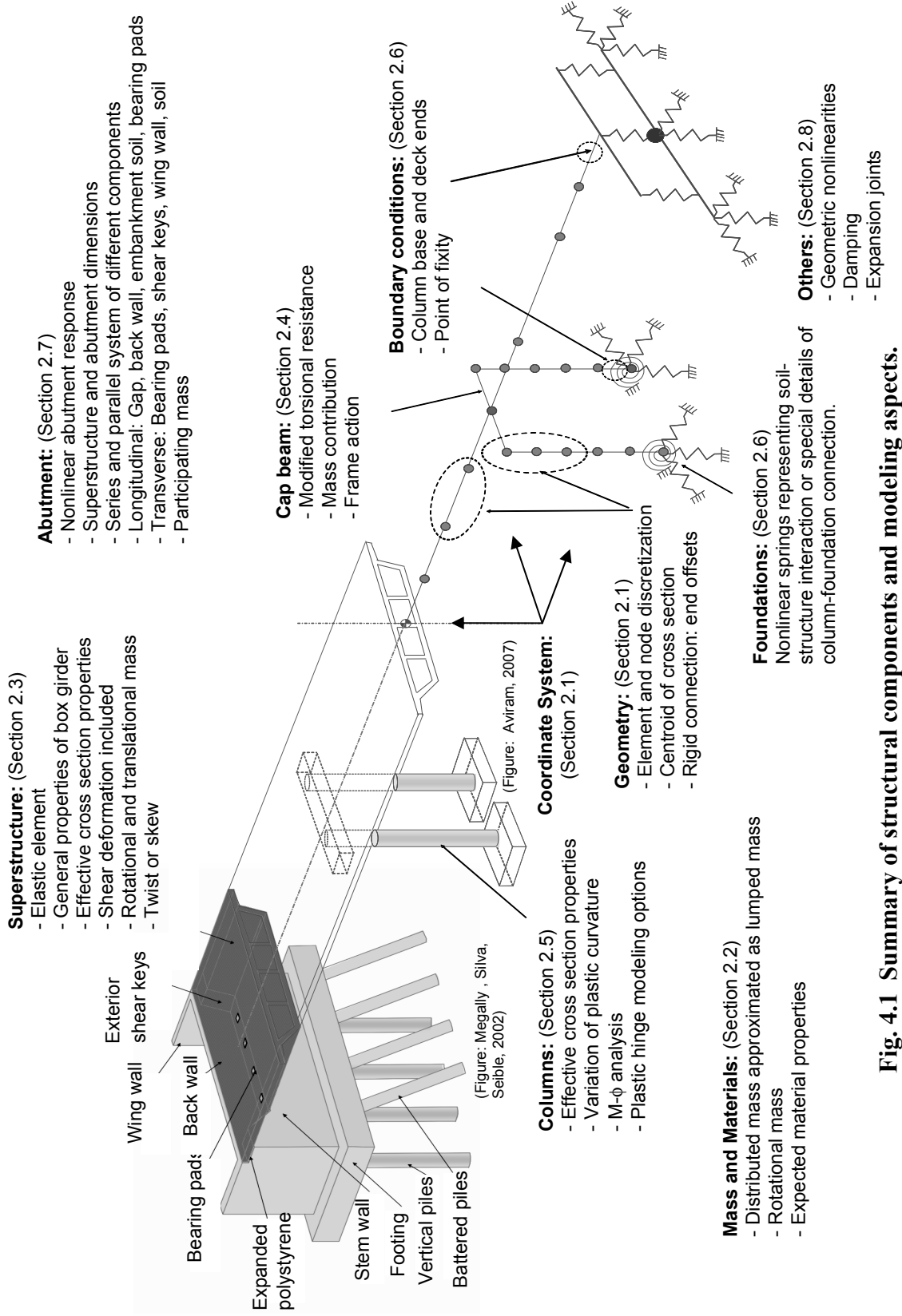


Fig. 4.1 Summary of structural components and modeling aspects.

The different aspects regarding the analysis of Standard Ordinary bridges are presented in Chapter 3 of the document, *Bridge Analysis*, including all the relevant procedures and parameters used to simulate the seismic demand on the system in the form of imposed static and dynamic forces or displacements. Additional references are provided regarding the use of response spectrum curves, selection and scaling of ground motions, as well as interpretation of different analysis results. The following table summarizes the main aspects of the different analysis types presented in the document.

Table 4.1 Summary of main aspects of analysis procedures for Standard Ordinary bridges.

Analysis Procedure	Section	Static analysis	Dynamic properties	Linear	Nonlinear	Computational difficulty	Seismic considerations
Modal	3.2		X	X			
Free Vibration	3.3		X	X		X	
Gravity	3.4	X		X			
Equivalent Static	3.5	X			X		X
Pushover	3.6	X			X		
Response Spectra	3.7	X	X	X		X	X
Time History	3.8		X	X	X	X	X

4.3 PENDING ASPECTS

Due to the extensive scope of this project and subsequent (or subsequently discovered) complexities involved in the modeling and analysis of bridge structures with greater geometric irregularities or high degree of nonlinear action, several aspects of the project require further comprehensive investigation. It is strongly recommended to further research these topics that can later be extended to address modeling and analysis issues of Ordinary Nonstandard and Important bridges.

Among the pending issues of the project related to the modeling of bridge structures are the following:

- Modeling of different abutment types including complex and updated backbone curves for the longitudinal, transverse, and vertical response of the abutments, participating mass of the adjacent soil, and associated damping properties of the system. The new criteria should be in agreement with the findings of ongoing investigations.

- Soil-structure interaction effects for the abutments and column foundations, as well as the effect of nonlinear foundation springs and degree of semi-rigidity of column bases on the overall seismic demand and structural response of the bridge.
- Effect of severe geometric irregularities in bridges including long and numerous spans, curves and skew.
- Definition of column plastic hinge fiber model required to accurately determine the residual displacements of bridge structures produced due to moderate and severe dynamic excitations.
- Modeling of superstructure inelastic behavior and its effect on the bridge's overall structural response. Section 4.3.2 of SDC 2004 establishes capacity design criteria to guarantee the superstructure is essentially elastic under seismic conditions; however, the implications of the superstructure's inelastic behavior should be investigated.
- Modeling of expansion joints and restrainers between superstructure spans.
- Among the pending aspects of the project related to the analysis of Ordinary Standard bridges are the following:
 - Considerations of superstructure torsion and rotational inertia effects in pushover analysis for a spine model of the bridge. These effects are automatically incorporated into the analysis for certain assignment types of the pushover force pattern for three-dimensional shell or solid elements in SAP2000.
 - Consideration of abutment participating mass in pushover analysis force pattern.
 - Applicability of using a force pattern including more than one mode shapes for pushover analysis of Standard Ordinary bridges.
 - Verification of the range of axial load in bridge columns for moment-curvature analysis.
 - Identification of the intensity level for which nonlinear analysis of the bridge structure is required.
 - Development of an approximate formula to verify the pushover curve in each loading direction of the bridge, according to the appropriate ductility estimation and abutment model used.
 - Specification of seismic demand for dynamic linear and nonlinear analysis, including the selection and scaling of ground motions, and the imposed orientation of the components of each record.

- Applicability and specification of multi-support excitation and displacement-driven time history analysis for long-span or irregular bridge structures.
- Determination and verification of bias factors for all analysis types between the latest version of SAP2000 and OpenSees, specifically bias factors for nonlinear time history analysis using a larger suite of ground motions with different intensity levels.
- Determination of the adequacy of the NL-Link (MLP) model with restrained abutment model for nonlinear time history analysis.

REFERENCES

- American Association of State Highway and Transportation Officials (2002). *AASHTO Standard Specifications for Highway Bridges*. 17 edition. AASHTO, Washington, D.C.
- ACI 318 (2005). *Building Code Requirements for Structural Concrete and Commentary*. ACI Committee 318. American Concrete Institute, Michigan.
- ATC/MCEER. (2001). *Recommended LRFD guidelines for the seismic design of highway bridges*. ATC Report No. ATC-49a. Applied Technology Council and Multidisciplinary Center for Earthquake Engineering joint venture.
- ATC (1996). *Improved seismic design criteria for California bridges: provisional recommendations*. ATC Report No. ATC-32. Applied Technology Council.
- Berry, M., and Eberhard, M. (2003). *Performance Models for Flexural Damage in Reinforced Concrete Columns*. Report No. 2003/18. Pacific Earthquake Engineering Research Center, University of California, Berkeley.
- Borzognia, Y., and Bertero, V.V., editors (2004). *Earthquake Engineering: From Engineering Seismology to Performance-Based Engineering*. CRC Press.
- Bozorgzadeh, A., Megally, S., Restrepo, J.I., and Ashford, S.A. (2006). Capacity Evaluation of Exterior Sacrificial Shear Keys of Bridge Abutments. *Journal of Bridge Engineering*. 11(5):555–565.
- Caltrans (1989). *Bridge Design Aids 14-1*. California Department of Transportation, Sacramento, California, Sacramento, California.
- Caltrans (2000). *Caltrans Bridge Design Specifications*. California Department of Transportation, Sacramento, California.
- Caltrans (1999). *Seismic Design Criteria 1.1*. California Department of Transportation, Sacramento, California.
- Caltrans (1999). *Seismic Design Criteria Memo To Designers 20-1 (MTD 20-1)*. California Department of Transportation, Sacramento, California.
- Caltrans (2004). *Caltrans Seismic Design Criteria version 1.3*. California Department of Transportation, Sacramento, California.

- Carballo, J.E, Cornell, C.A. (2000). *Probabilistic seismic demand analysis: Spectrum matching and design*. Reliability of Marine Structures Report No. RMS-41. Dept. of Civil and Envir. Engineering, Stanford University, California.
- Chopra, A.K. and Goel, R.K. (2001). *A Modal Pushover Analysis Procedure to Estimate Seismic Demands for Buildings*. Report No. 2001/03. Pacific Earthquake Engineering Research Center, University of California, Berkeley.
- Chopra, A.K. (2006). *Dynamics of Structures: Theory and Applications to Earthquake Engineering*. 3rd edition. Prentice Hall, New Jersey.
- CSI (2005). *CSI Analysis Reference Manual for SAP200, ETABS, and SAFE*. Computers and Structures, Inc. Berkeley, California.
- CSI (2005). *SAP2000- Linear and Nonlinear Static and Dynamic Analysis and Design of Three-Dimensional Structures: Basic Analysis Reference Manual*. Computers and Structures, Inc. Berkeley, California.
- CSI (2007). Technical Papers and Support. http://www.csiberkeley.com/support_technical_papers.html. Web site. Computers and Structures.
- Eberhard, M.O., and Marsh, M.L. (1997). Lateral-load response of a Reinforced Concrete Bridge. *Journal of Structural Engineering*, 123(4): 451–460.
- Fajfar, P., Vidic, T., and Fischinger, M. (1990). A measure of earthquake motion capacity to damage medium-period structures. *Soil Dynamics and Earthquake Engineering*, 9(5): 236–242.
- Fajfar, P., Gaspersic, P., and Drobnic, D. (1997). A simplified nonlinear method for seismic damage analysis of structures. In *Proceedings of the International Workshop on Seismic Design Methodologies for the Next Generation of Codes*, June 24–27, 1997, Bled, Slovenia.
- FEMA-273. (1996). *NEHRP guidelines for the seismic rehabilitation of buildings*. Report No. FEMA-273. Federal Emergency Management Agency, Washington D.C.
- FEMA-302. (1997). *NEHRP recommended provisions for seismic regulations for new buildings and other structures*. Report No. FEMA-302. Federal Emergency Management Agency, Washington D.C.
- FEMA-350. (July 2000b). *Recommended seismic design criteria for new steel moment-frame buildings*. Report No. FEMA-350. Federal Emergency Management Agency, Washington D.C.

- FEMA-356. (2000a). *Prestandard and commentary for the seismic rehabilitation of buildings*. Report No. FEMA-356. Federal Emergency Management Agency, Washington D.C.
- Fenves, G.L., and Ellery, M. (1998). *Behavior and failure analysis of a multi-frame highway bridge in the 1994 Northridge earthquake*. Technical Report 08, Pacific Earthquake Engineering Research Center.
- Gardoni, P., Der Kiureghian, A., and Mosalam, K.M. (2002). *Probabilistic models and fragility estimates for bridge components and systems*. PEER Report 2002/13. Pacific Earthquake Engineering Research Center, University of California, Berkeley.
- Gazetas, G., and Mylonakis, G. (1998). Seismic soil-structure interaction: New evidence and emerging issues. *Geotechnical Special Publication*, volume 2, pages 1119–1174. ASCE.
- Goel, R.K., and Chopra, A.K. (1997). Evaluation of bridge abutment capacity and stiffness during earthquakes. *Earthquake Spectra*, 13(1):1–23.
- Hachem, M.M., Mahin, S.A., and Moehle, J.P. (2003). *Performance of circular reinforced concrete bridge columns under bidirectional earthquake loading*. Technical Report 06, Pacific Earthquake Engineering Center.
- Hilber, H. M., Hughes, T. J. R., and Taylor, R. L. (1977). Improved numerical dissipation for time integration algorithms in structural dynamics. *Earthquake Engineering & Structural Dynamics*, 5:283–292.
- Hose, Y., Silva, P., and Seible, F. (2000). Development of a performance evaluation database for concrete bridge components and systems under simulated seismic loads, *Earthquake Spectra*, 16(2): 413–442.
- Hutchinson, T.C., Chai, Y.H., Boulanger, R.W., and Idriss, I.M. (2004). Inelastic seismic response of extended pile-shaft-supported bridge structures. *Earthquake Spectra*, 20(4):1057–1080.
- Inel, M., and Aschheim, M.A. (2004). Seismic Design of Column of Short Bridges Accounting for Embankment Flexibility. *Journal of Structural Engineering*. 130(10): 1515–1528.
- Isakovic, T., Fischinger, M., and Fajfar, P. (1999). The seismic response of reinforced concrete single-column-bent viaducts designed according to Eurocode 8/2. *European Earthquake Engineering*. 13(1): 3–18.
- Jalayer, F. (2003). *Direct probabilistic seismic analysis: implementing non-linear dynamic assessments*. PhD Dissertation, Stanford University, Stanford, California.

- Johnson, N., Saiidi, M., and Sanders, D. (2006). *Large-scale experimental and analytical seismic studies of a two-span reinforced concrete bridge system*. Technical Report 02, Center for Civil Engineering Earthquake Research.
- Karim, K.R., and Yamazaki, F. (2001). Effect of earthquake ground motions on fragility curves of highway bridge piers based on numerical simulation. *Earthquake Engineering and Structural Dynamics*, 30(12): 1839–1856.
- Kent, D.C., and Park, R. (1971). Flexural members with confined concrete. *Journal of Structural Engineering*, 97(ST7): 1969–1990.
- Kotsoglu, A., and Pantazopoulou, S. (2006). Modeling of Embankment Flexibility and Soil-Structure Interaction in Integral Bridges. *Proceedings of First European Conference on Earthquake Engineering and Seismology*. September 3–8, 2006. Geneva, Switzerland.
- Kramer, S.L. (1996). *Geotechnical Earthquake Engineering*. Prentice Hall.
- Krawinkler, H. (2002). A general approach to seismic performance assessment. In *Proceedings of the International Conference on Advances and New Challenges in Earthquake Engineering Research*, August 19–20, 2002, Hong Kong.
- Lam, I., and Martin, G.R. (1986). *Seismic design of highway bridge foundations*. U.S. Dept. of Transportation, Federal Highway Administration, Research, Development, and Technology.
- Mackie, K., and Stojadinović, B. (2001). Probabilistic seismic demand model for California highway bridges. *Journal of Bridge Engineering*, 6(6): 468–481.
- Mackie, K., and Stojadinović, B. (2002a). Optimal probabilistic seismic demand model for typical highway overpass bridges. In *Proceedings of the 12th European Conference on Earthquake Engineering*, September 9–13, 2002, London. Elsevier Science Ltd.
- Mackie, K., and Stojadinović, B. (2002b). Design parameter sensitivity in probabilistic seismic demand models. In *Proceedings of the 7th US National Conference on Earthquake Engineering*, July 21–25, 2002, Boston, Massachusetts.
- Mackie, K., and Stojadinović, B. (2002c). Relation between probabilistic seismic demand analysis and incremental dynamic analysis. In *Proceedings of the 7th US National Conference on Earthquake Engineering*, July 21–25, 2002, Boston, Massachusetts.
- Mackie, K., and Stojadinović, B. (2003). *Seismic demands for performance-based design of bridges*. PEER Report No. 2003/16. Pacific Earthquake Engineering Research Center, University of California, Berkeley.

- Mackie, K., and Stojadinović, B. (2006). Seismic Vulnerability of Typical Multi-Span California Highway Bridges. *Proceedings of the Fifth National Seismic Conference on Bridges and Highways*. September 18–20, 2006. San Francisco.
- Mackie, K.R. (2004). *Fragility-based seismic decision making for highway overpass bridges*. Ph.D. Dissertation. Dept. of Civil and Environmental Engineering, University of California, Berkeley.
- Mander, J.B., Priestley, M.J.N., and Park, R. (1988). Theoretical stress-strain model for confined concrete. *Journal of the Structural Engineering*, 114(ST8): 1804–1826.
- Maroney, B.H., and Chai, Y.H. (1994). Seismic design and retrofitting of reinforced concrete bridges. *Proceedings of 2nd International Workshop, Earthquake Commission of New Zealand*, Queenstown.
- Mazzoni, S., Fenves, G.L., and Smith, J.B. (2004). *Effects of local deformations on lateral response of bridge frames*. Technical report, University of California, Berkeley.
- McCallen, D.B., and Romstad, K.M. (1994). Dynamic analyses of a skewed, short-span box-girder overpass. *Earthquake Spectra*, 10(4):729–755.
- McKenna, F., and Fenves, G.L. (2000). An object-oriented software design for parallel structural analysis. *Proceedings of the 2000 Structures Congress & Exposition: Advanced Technology in Structural Engineering*, May 8–10, 2000, Philadelphia, Pennsylvania.
- McKenna, F., Fenves, G.L., Scott, M.H., and Jeremić, B. (2000). Open system for earthquake engineering simulation. <http://opensees.berkeley.edu>.
- Medina, R., Krawinkler, H., and Alavi, B. (2001). Seismic drift and ductility demands and their dependence on ground motions. *Proceedings of the US-Japan Seminar on Advanced Stability and Seismicity Concepts for Performance-Based Design of Steel and Composite Structures*, July 23–27, 2001, Kyoto, Japan.
- Megally, S. et al. (2003). Response of sacrificial shear keys in bridge abutments to simulated seismic loading. *Proceedings of FIB 2003 Symposium on Concrete Structures in Seismic Regions*.
- Menun, C., and Der Kiureghian, A. (1998). A Replacement for the 30 % Rule for Multicomponent Excitation. *Earthquake Spectra*, Vol. 13, Number 1.
- Menun, C., and Der Kiureghian, A. (2000). Envelopes for Seismic Response Vectors. *Journal of Structural Engineering*, April 2000, pp 467–481.

- Moore, J.E., Kiremidjian, A., and Chiu, S. (2000). *Seismic risk model for a designated highway system: Oakland/San Francisco Bay Area*. PEER Report No. 2002/02. U.S.-Japan
- Munfakh, G.A. (1990). Innovative earth retaining structures: selection, design & performance. *Proceedings, Conference on Design and Performance of Earth Retaining Structures*. American Society of Civil Engineers, Ithaca, New York.
- Neuenhofer, A., and Filippou, F.C. (1998). Geometrically nonlinear flexibility-based frame finite element. *Journal of Structural Engineering*, 124(6): 704–711.
- OpenSees. <http://opensees.berkeley.edu>. Web page.
- Panagiotakos, T.B., and Fardis, M.N. (2001). Deformations of reinforced concrete members at yielding and ultimate. *ACI Structural Journal*, 98(2): 135–148.
- PEER Strong Motion Catalog. <http://peer.berkeley.edu/smcat>. Web page.
- Penzien, J., and Watabe, M. (1975). Characteristics of 3-D Earthquake Ground Motions. *Earthquake Engineering & Structural Dynamics*, Vol. 3, pp. 365–373.
- Priestly, M.J.N., Seible, F., and Calvi, G.M. (1996). *Seismic Design and Retrofit of Bridges*. John Wiley & Sons, Inc., New York.
- Scapone, E., Filippous, F.C., and Taucer, F.F. (1996). Fiber beam-column model for non-linear analysis of R/C frames 1. Formulation. *Earthquake Engineering and Structural Dynamics*, 25:711–725.
- Schnore, A.R. (1990). Selecting retaining wall type and specifying proprietary retaining walls in NYSDOT practice. *Proceedings, Conference on Design and Performance of Earth Retaining Structures*. American Society of Civil Engineers, pp. 119–124, Ithaca, New York.
- Scott, M.H., and Fenves, G.L. (2006). Plastic hinge integration methods for force-based beam-column elements. *Journal of Structural Engineering*, 132(2):244–252.
- Seed, H.B., Wong, R.T., Idriss, I.M, and Tokimatsu, K. (1984). *Moduli and damping factors for dynamic analyses of cohesionless soils*. Earthquake Engineering Research Center Report No. UCB/EERC 84/14. University of California, Berkeley.
- Shin, H., Ilankathara, M., Arduino, P., Kutter, B.L., and Kramer, S.L. (2006). Experimental and numerical analysis of seismic soil-pile-structure interaction of a two-span bridge. *Proceedings of the 8th National Conference on Earthquake Engineering*, paper No. 1649, April 18–22, 2006, San Francisco, California.
- Shome, N., Cornell, C.A., Bazzurro, P., and Carballo, J.E. (1998). Earthquakes, records, and nonlinear responses. *Earthquake Spectra*, 14(3): 467–500.

- Shome, N., and Cornell, C.A. (1999). *Probabilistic seismic demand analysis of nonlinear structures*. Reliability of Marine Structures Report No. RMS-35, Dept. of Civil and Envir. Engineering, Stanford University, California.
- Silva, J.M.M., and Maia, N.M.M. (1999). *Modal analysis and testing*. Kluwer Academic Publishers, Boston.
- Silva, P., Megally, S., and Seible, F. (2001). Seismic performance of sacrificial shear keys. *Proceedings of the 6th Caltrans Seismic Research Workshop Program*. June 12–13. Sacramento, California.
- Sommerville, P., and Collins, N. (2002). *Ground Motion Time Histories for the I880 bridge, Oakland*. PEER Methodology Testbeds Project. Pacific Earthquake Engineering Research Center, University of California, Berkeley and URS Corporation, Pasadena, CA.
- Sommerville, P., and Collins, N. (2002). *Ground Motion Time Histories for Van Nuys Building*. PEER Methodology Testbeds Project. Pacific Earthquake Engineering Research Center, University of California, Berkeley and URS Corporation, Pasadena, CA.
- Sun, C.T., and Lu, Y.P. (1995). *Vibration damping of structural elements*. PTR Prentice Hall, New Jersey.
- Timoshenko, S. P., and Goodier, J. N. (1969). *Theory of elasticity*. 3rd edition. McGraw-Hill, New York.
- Travasarou, T., Bray, J.D., and Abrahamson, N.A. (2003). Empirical attenuation relationship for Arias Intensity. *Journal of Earthquake Engineering and Structural Dynamics*, 32(7): 1133–1155.
- USGS. National Seismic Hazard Mapping Project Zip Code Look-up for Ground Motion Values. <http://eqint.cr.usgs.gov/eq/html/zipcode.shtml>. Web page.
- Vamvatsikos, D. and Cornell, C.A. (2002). Incremental dynamic analysis. *Earthquake Engineering and Structural Dynamics*, 31(3): 491–512.
- Veletsos, A.S. (1977). Dynamics of structure-foundation systems. *Structural and Geotechnical Mechanics*.
- Werner, S. D. (1994). Study of Caltrans' seismic evaluation procedures for short bridges. *Proceedings of the 3rd Annual Seismic Research Workshop*. Sacramento, California.
- Werner, S.D., Taylor, C.E., Sungbin, C., Lavoie, J-P., Huyck, C.K., Eitzel, C., Eguchi, R.T., and Moore, J.E. (2004). New developments in seismic risk analysis of highway systems.

- Proceedings of the 13th World Conference on Earthquake Engineering*, August 1–6 2004, Vancouver, Canada.
- Wilson, E. L., Der Kiureghian, A., and Bayo, E. R. (1981). A Replacement for the SRSS Method in Seismic Analysis. *Earthquake Engineering & Structural Dynamics*, Vol. 9, pp. 187–192.
- Wilson, E.L. (1998). *Three Dimensional Static and Dynamic Analysis: A physical Approach with emphasis on Earthquake Engineering*. 2nd edition. Computer and Structures, Inc. Berkeley, California.
- Wilson, E.L., Yuan, M.W., and Dickens, J.M. (1982). Dynamic Analysis by Direct Superposition of Ritz Vectors. *Earthquake Engineering and Structural Dynamics*, 10: 813-821.
- Worden, K., and Tomlinson, G.R. (2001). *Nonlinearity in structural dynamics: detection, identification and modeling*. Institute of Physics Pub., Philadelphia.
- Yamazaki, F., Onishi, J., and Tayama, S. (1998). Damage estimation of highway structures due to earthquakes. *Proceedings of Third China-Japan-US Trilateral Symposium on Lifeline Earthquake Engineering*, August 1998. Kunming China.
- Yashinsky, M., and Ostrom, T. (2000). Caltrans' new seismic design criteria for bridges. *Earthquake Spectra*, 16(1): 285–307.
- Zhang, J., and Makris, N. (2002). Kinematic response functions and dynamic stiffnesses of bridge embankments. *Earthquake Engineering & Structural Dynamics*, 31(11):1933–1966.
- Zhang, J., and Makris, N. (2002). Seismic response analysis of highway overcrossings including soil-structure interaction. *Earthquake Engineering & Structural Dynamic*, 31(11):1967–1991.

Appendix A: Comparison between SAP2000 and OpenSees Results

The appendix presents the methodology employed for the elaboration of the guidelines document and the comparison between the SAP2000 and OpenSees programs used for bridge nonlinear structural analysis. The appendix provides several examples and results of the comparison between SAP2000 and OpenSees, including a simple cantilever column analysis, restrained/unrestrained boundary conditions and abutment behavior, as well as the displacement time history results of all bridge structures analyzed in the study. The regression coefficients relating peak displacements and a ground motion intensity measure obtained through nonlinear time history analysis are tabulated for reference. Bias factors for nonlinear time history analysis computed between OpenSees and SAP2000 program are presented, using three different procedures. A brief discussion concerning several aspects of the dynamic analysis results is offered at the end of the appendix.

Note: The OpenSees and SAP2000 input files, as well as the ground motion data, are available through the “Additional Files” link for this report at the PEER publications website: http://peer.berkeley.edu/publications/peer_reports/reports_2008/

A.1 METHODOLOGY EMPLOYED

The current project was carried out in several stages to progressively advance toward the development of relevant and detailed guidelines for the modeling and analysis of Ordinary Standard bridges.

Phase I

The first stage consisted of a basic analysis and comparison between SAP2000 and OpenSees models of typical bridges classified as Ordinary bridges, with simple boundary conditions and

elastic behavior. A total of 6 bridges (instead of 4 initially selected) with different geometries and column cross sections were considered for the analysis (see Table A.1), as well as a simple model of a cantilever column bent, corresponding to the Route 14 bridge. The models were created based on existing construction drawings, supplied by Caltrans.

Table A.1 Summary of bridge properties used in the analysis.

Bridge	Type	No. Spans	Length (ft)	Width (ft)	No. Cols	Col. Diam. (ft)	Col. Height (ft)	Super. Depth (ft)	Cap Beam Dim. (ft)
Route 14	Multi-Col.	2	286 (145+141)	53.7	2	5.42	37.9	5.74	7.55x5.74
La Veta	Multi-Col.	2	299 (155+145)	75.5	2	5.58	25.4	6.23	7.55x6.23
Adobe	Multi-Col.	2	203 (103+100)	41.0	2	4.00	26.6	4.10	7.00x4.10
LADWP	Multi-Col.	3	262 (78+106+78)	41.6	4	4.49	25.6	4.27	6.56x4.27
MGR	Single-Col.	3	366 (110x2+146)	42.3	2	6.00	39.1	6.23	-
W180-N168	Single-Col.	4	674 (143x2+194x2)	41.2	3	6.00	26.4	7.74	-

The bridges analyzed were reinforced concrete bridges with box-girder superstructure and typical column bent details. The first four bridges of Table A.1 consist of Ordinary Standard Bridges and the last two are Ordinary Nonstandard bridges with simple geometric regularity. Expected material properties and effective section properties were used to carry out modal analysis and linear elastic pushover analysis. The differences between SAP2000 and OpenSees results were evaluated using the modal periods and shapes, as well as the elastic stiffness in both longitudinal and transverse directions of the bridges. Results from this comparison assisted in the formulation of the guideline recommendations for geometry, boundary conditions, section properties, materials, and mass assignment.

The nonlinear behavior of the column plastic hinge was thoroughly studied using a cantilever model to determine the applicability and limitations of the different modeling options available in SAP2000 for different analysis types. The cantilever model used for the comparison of the nonlinear options for modeling column plastic hinges in the SAP2000 and OpenSees programs consists of a single-degree-of-freedom system, i.e., a single element corresponding to a typical column bent cross section with a fixed base and a lumped mass at the top. The cross-sectional properties of the Route 14 bridge column bent were selected for the analysis, where the lumped mass used corresponded to the tributary mass of the superstructure

self-weight. The resulting elastic periods of the cantilever model were therefore similar to those of the entire Route 14 bridge structure, representing realistic dynamic properties of the system.

Modal, nonlinear pushover, as well as linear and nonlinear time history analyses were carried out for this cantilever model. The pushover analysis consisted of loading in the transverse, longitudinal and diagonal directions of the bridge to study the three-dimensional response of the bridge model. The time history analysis was performed using three ground motions with longitudinal, transverse, and vertical components, selected by Caltrans engineers from the PEER ground motion database to represent low, moderate, and high hazard seismic levels. The ground motions were scaled using different factors (but no greater than 3.0) to evaluate the nonlinear behavior of the columns and determine the stability and accuracy of the models under extreme dynamic loading conditions. The characteristics of these records are presented in Table A.2.

Table A.2 Characteristics of time histories used in stage 1 of project.

Earthquake	M_w	Station	Abbrev.	Dist. (km)	Mechanism
Loma Prieta, 1989/10/17	6.9	APEEL 2 - Redwood City	A02	43.2	Reverse/Oblique
Imperial Valley, 1979/10/15	6.5	Brawley Airport	H-BRA	10.4	Strike-Slip
Kocaeli, Turkey 1999/08/17	5.5	Mecidiyekoy	MCD	53.4	Strike-Slip

This approach in the first phase of the project allowed establishing recommendations for the use of different nonlinear options for the column plastic hinge zone, identifying important discrepancies between OpenSees and SAP2000 results for different analysis types, and developing possible approaches for the resolution of such inconsistencies.

Phase II

The implementation of the Fiber model and the NL-Link Multi-Linear Plastic model was completed in the preliminary analysis of the second phase of the project for all the bridges using simple boundary conditions for the superstructure ends. These boundary conditions consisted of merely vertical support to allow unrestrained lateral translation of the bridge and consider the nonlinearity of the column plastic hinge separately. The comparison between

SAP2000 and OpenSees of these models was carried out using modal, nonlinear pushover, and nonlinear time history analysis results. For the dynamic loading, an extended set of ground motions was used for SAP2000 and OpenSees models, as presented in Table A.3.

Table A.3 Ground motion sets used in SAP2000 and OpenSees bridge model Phase II, preliminary analysis.

Ground Motion Set	Reference	No. records	SAP2000	OpenSees
Caltrans (A02,H-BRA,MCD)	-	3	X	X
I880n (normal)	Sommerville and Collins, 2002	20	X	X
I880p (parallel)	Sommerville and Collins, 2002	20	-	X
VN	Sommerville and Collins, 2002	20	-	X
Total		63	23	63

The I880n record set was selected to carry out the time history comparison of the 6 selected bridge models using SAP2000 and OpenSees programs, assuming that the orientation (of the longitudinal axis) of the bridge is normal or perpendicular to the fault. The same records were also used in OpenSees considering the parallel orientation of the bridge with respect to the fault (I880p). The I880 set was used from the PEER ground motion database for the analysis of the I-880 highway bridge in Oakland, California (Somerville, Collins, 2002), which suffered a partial collapse during the 1989 Loma Prieta earthquake and was later heavily retrofitted. The set contains ground motions corresponding to strike-slip faulting with near-fault directivity effects. The general characteristics of the ground motions are presented in Table A.4.

Table A.4 Characteristics of I880 time history catalog.

Earthquake	M_w	Station	Abbrev.	Dist. (km)	Mechanism
Coyote Lake, 1979/6/8	5.7	Coyote Lake Dam abutment	cclyd	4.0	Strike-Slip
		Gilroy #6	gil6	1.2	
Parkfield, 1966/6/27	6.0	Temblo	temb	4.4	Strike-Slip
		Array #5	cs05	3.7	
		Array #8	cs08	8.0	
Livermore, 1980/1/27	5.5	Fagundes Ranch	fgnr	4.1	Strike-Slip
		Morgan Territory Park	mgnp	8.1	
Morgan Hill, 1984/4/24	6.2	Coyote Lake Dam abutment	clyd	0.1	Strike-Slip
		Anderson Dam Downstream	andd	4.5	
		Halls Valley	hall	2.5	
Loma Prieta, 1989/10/17	6.9	Los Gatos Presentation Center	lgpc	3.5	Reverse/Oblique
		Saratoga Aloha Ave	srtg	8.3	
		Corralitos	cor	3.4	
		Gavilan College	gav	9.5	
		Gilroy historic	gilb	11.0	
		Lexington Dam abutment	lex1	6.3	
Kobe, Japan, 1995/1/17	6.9	Kobe JMA	kobj	0.5	Strike-Slip
Tottori, Japan, 2000/10/6	6.6	Kofu	ttr007	10.0	Strike-Slip
		Hino	ttrh02	1.0	
Erzincan, Turkey, 1992/3/13	6.7	Erzincan	erzi	1.8	Strike-Slip

Due to the high computational effort required to conduct nonlinear time history analysis using SAP2000 program, the ground motion catalog was limited to 23 ground motions. Additional ground motions were used in the OpenSees bridge models from the Van Nuys record set (VN) used for the PEER Center VN testbed, to represent diverse directivity effects and faulting types. The characteristics of the VN ground motion set are presented in Table A.5.

Table A.5 Characteristics of VN time history catalog.

Earthquake	M _w	Station	Abbrev.	Dist. (km)	Mechanism
North Palm Springs 1986/7/8	6.0	Palm Springs Airport	plma	9.6	Reverse/Oblique
		Palm Springs Airport, reversed components	plmb	9.6	
Northridge 1994/1/17	6.7	Encino, Ventura Blvd. #1	env1	17.7	Reverse
		Encino, Ventura Blvd. #9	env9	17.9	
		North Hollywood, Lankershim Blvd. #1	nhl2	18.4	
		Van Nuys, Sherman Way #1	vns1	12.8	
		Van Nuys - Sherman Circle #1	vns1	12.8	
		Woodland Hills, Oxnard Street #4	whox	20.0	
		Canoga Park, Topanga Canyon Blvd.	cnpk	17.7	
		Sepulveda VA Hospital - ground	spva	9.2	
		Van Nuys - 7-Story Hotel	vnuy	11.3	
		Arleta, Nordhoff Fire Station	nord	9.4	
		Northridge, Roscoe #1	nrr1	13.7	
		Sun Valley, 13248 Roscoe Blvd.	rosc	10.8	
San Fernando 1971/2/9	6.6	Los Angeles, 14724 Ventura Blvd.	sf253	16.3	Reverse
		Los Angeles, 15910 Ventura Blvd.	sf461	16.2	
		Los Angeles, 15250 Ventura Blvd.	sf466	16.4	
		Glendale, Muni. Bldg., 633 E. Broadway	glen	18.8	
		Van Nuys - 7-Story Hotel	vnuy	9.5	
Whittier Narrows 1987/10/1	6.0	Cal Tech, Brown Athletic Building	athl	16.6	Reverse

A uniform scale factor of 2.0 was applied to all motions to guarantee the development of nonlinear action in the bridge columns. The plastic hinge zone was modeled in OpenSees and SAP2000 using a fiber model that included around 160 concrete and reinforcing steel fibers, according to the recommendations of Eberhard and Berry, 2006. An additional model using the NL-Link element with Multi-Linear Plastic nonlinear behavior was also used in SAP2000, which failed to converge under severe seismic conditions. The self-weight of the bridges was considered in the time history analysis.

The analysis of the time history results for all 6 bridges was carried out relating peak displacements of a monitored point of the bridge to an established intensity measure (IM) for each record (see Fig. A.1). The monitored point in the bridge model selected was the intersection point between the superstructure and column top centerline, while the intensity

measure chosen was the peak ground velocity (PGV). The PGV is an intensity measure which is period-independent and therefore all 6 bridges made use of the same values. A natural log fit was used for the data and the results were plotted in both the linear and logarithmic scale. The parameters of the natural logarithmic regression $\ln(PGV) = \beta_1 + \beta_2 \ln \Delta$ or equivalently $PGV = e^{\beta_1} \Delta^{\beta_2}$ were established for all bridge models with roller abutments.

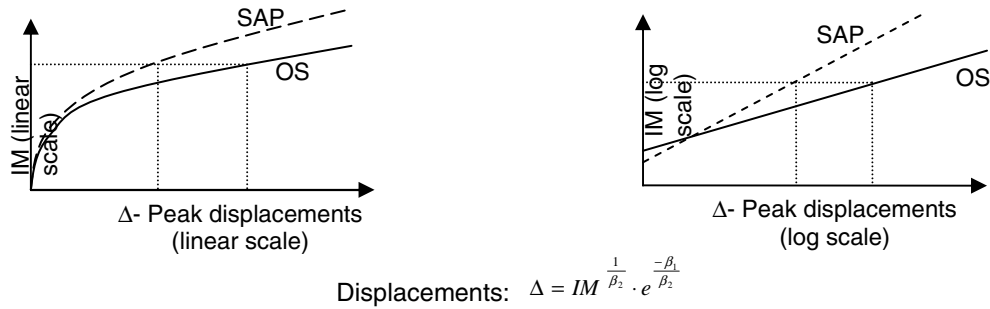


Fig. A.1 Time history analysis results scheme Phase II.

In the second phase of the project several superstructure boundary conditions were examined as well for the Route 14 bridge structure and modeled in SAP2000 and OpenSees. These conditions included a roller abutment, simplified abutment, and spring abutment models (see Section 2.7). The effect of the nonlinear behavior and modeling assumptions for the abutment model was carefully analyzed through a parametric study of transverse and longitudinal pushover curves, as well as nonlinear time history analysis using the complete set of ground motions selected for the project. Additional parameters were established for the natural log fit of the peak displacements results of the different Route 14 bridge models in terms of intensity measure. The NL-Link element with Multi-Linear Plastic behavior was also analyzed using the roller and simplified abutment models, which displayed higher computational efficiency than the fiber model in SAP2000. Reliable bias factors between SAP2000 and OpenSees time history results and their dispersion have not been established yet, since a larger catalog of ground motions and different geometric configurations and cross sections are required for such a purpose. However, important observations were obtained regarding several modeling and analysis aspects of major bridge components, specifically column plastic hinge and abutment nonlinear behavior. Certain discrepancies and inconsistencies between SAP2000 and OpenSees results for different analysis cases, revealed during stages 1 and 2 of the project, are presented below in Section A.2 of this appendix.

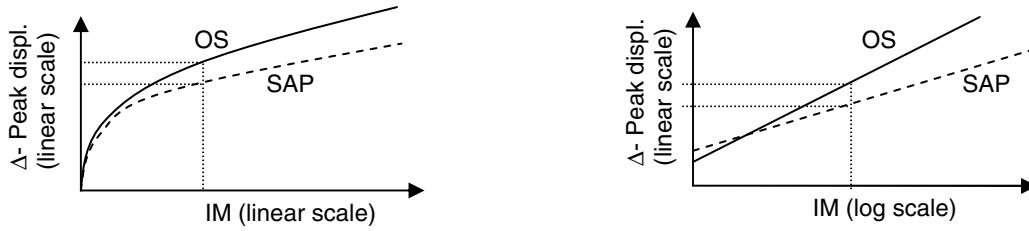
Phase III

An additional series of nonlinear time history analysis was carried out in the third and final stage of the project, using the complete ground motions suite (63 records) presented in Table A.3 for all 6 bridges. Two types of bridges were distinguished, including short bridges where abutment nonlinear response could control the overall bridge behavior and long bridges, where the abutment model can be simplified to reduce the modeling and computational effort. The selected abutment types used for each bridge used in SAP2000 and OpenSees fiber models are presented in Table A.6.

Table A.6 Abutment model used for nonlinear time history analysis Phase III.

Bridge	Length (ft)	Classification	Roller	Simplified
Route 14	286	Short		X
La Veta	299	Short		X
Adobe	203	Short		X
LADWP	262	Short		X
MGR	366	Long	X	
W180-N168	674	Long	X	

The analysis of the time history results for all 6 bridges was repeated relating peak displacements of a monitored point of the bridge to an intensity measure for each record, defined as the spectral displacement at the first mode period ($S_{d,T1}$). The first mode period used was the average of the SAP2000 and OpenSees modal analysis results. The monitored point in the bridge model selected was the intersection point between the superstructure and column top centerline, used in the preliminary analysis of the project's second phase. A natural log fit was used for the data, and the results were plotted in both the linear and logarithmic scale. The parameters of the natural logarithmic regression $\ln(\Delta) = \beta_1 + \beta_2 \ln(S_{d,T1})$ or equivalently $\Delta = e^{\beta_1} S_{d,T1}^{\beta_2}$ were established for all bridge models with fiber model and abutment type according to Table A.6. This time, the regression was carried out in terms of the demand values $S_{d,T1}$.



$$\text{Displacements: } \Delta = e^{\beta_1} S_{d,T1}^{\beta_2}$$

Fig. A.2 Time history analysis results scheme Phase III.

Three levels of seismic hazard were defined to compute the bias factors between SAP2000 and OpenSees results for nonlinear time history analysis. The low, moderate and high seismic hazard levels were defined as the 50%, 10%, and 2% in 50-years probabilities of exceedance for a seismically active zone in California such as Berkeley (zip code 94704). The probabilistic uniform hazard curves provided by USGS (see Fig. A.2) were used to obtain the elastic spectral displacements ($S_{d,elastic}$) corresponding to the first mode period of each bridge, for each hazard level (see Table A.7).

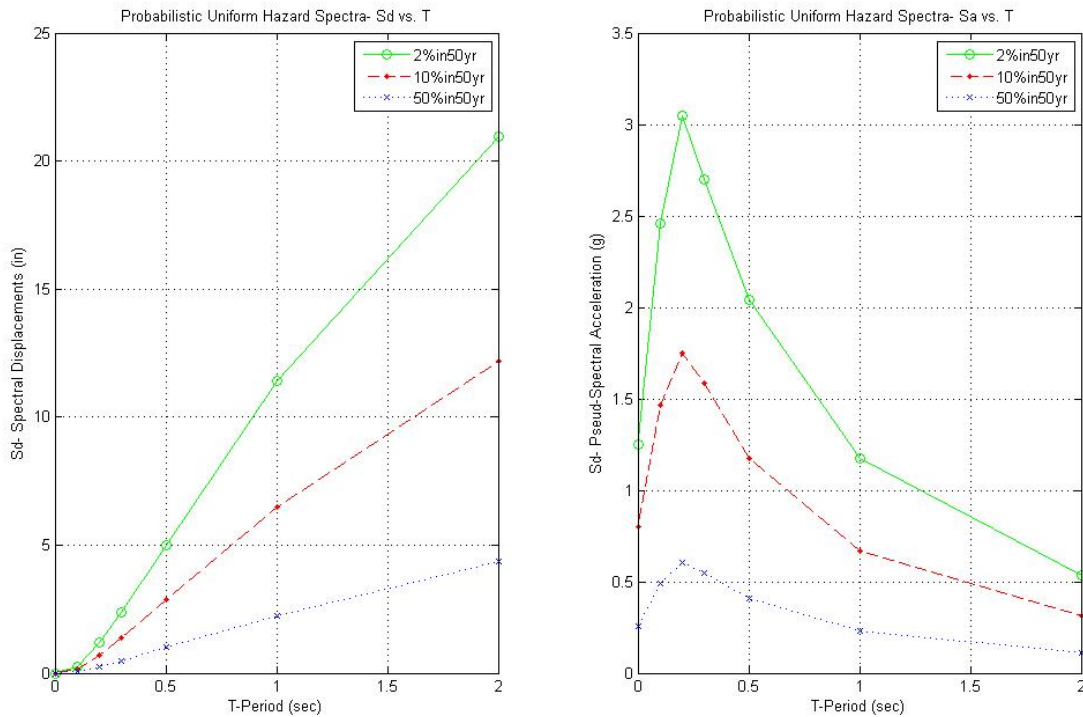


Fig. A.3 Probabilistic uniform hazard spectrum for Berkeley, California.

Table A.7 1st mode period elastic spectral displacements ($S_{d,elastic,T1}$) for each bridge.

		$S_{d,elastic,T1}$ (in) for different hazard levels		
Bridge	$T_{1,ave}$ (sec)	Low- 50% in 50 yr PE	Moderate- 10% in 50 yr PE	High- 2% in 50 yr PE
Route 14	1.87	4.09	11.45	19.73
Adobe	1.66	3.64	10.26	17.73
LADWP	0.87	1.92	5.56	9.76
La Veta	1.18	2.63	7.53	13.15
MGR	2.31	5.02	13.94	23.93
W180-N168	1.55	3.41	9.63	16.68

These values can be used to compute the desired bias factors between SAP2000 and OpenSees for the elastic range, moderate inelastic, and significant inelastic response of the bridges. However, due to safety factors, over-strength and a conservative design approach, the response of the bridges analyzed remained essentially elastic, even under strong seismic excitation. The computation of the bias factors can be carried out according to the following scheme:

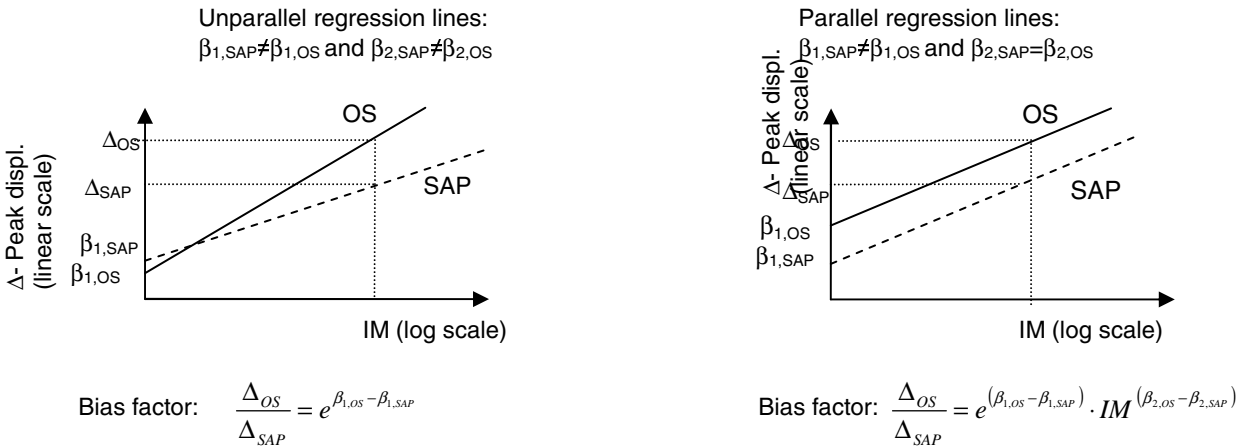


Fig. A.4 Computational scheme for bias factors between SAP2000 and OpenSees nonlinear time history analysis results Phase III, method 1.

The natural logarithmic regression was carried out for peak displacements results (Δ) not exceeding by more than 20% the spectral displacement $S_{d,elastic,T1}$ defined for the high hazard level (corresponding to the 2% in 50 years probability of exceedance level) of each bridge. This range was selected in this study to represent a reasonable demand limit expected during the lifetime of a Standard Ordinary bridge structure. The bias factors, computed using the described methodology (method 1), are presented at the end of Appendix A.

An additional bias factor computation was carried out through a pair-wise comparison between SAP2000 and OpenSees nonlinear time history analysis results for each ground motion, in the longitudinal, transverse, and diagonal directions of the bridge. The average of the ratio between OpenSees and SAP2000 results was obtained for the low, moderate, and high hazard levels, as defined above (method 2). The dispersion of the data was computed as well. A natural log regression was carried out relating the bias obtained for every ground motion to the intensity levels, according to the following scheme (method 3). The bias factor corresponding to the low, moderate, and hazard levels was computed using the new set of regression coefficients. The results of this bias factor computational scheme for the short and long bridge types (methods 2 and 3) are also presented at the end of Appendix A.

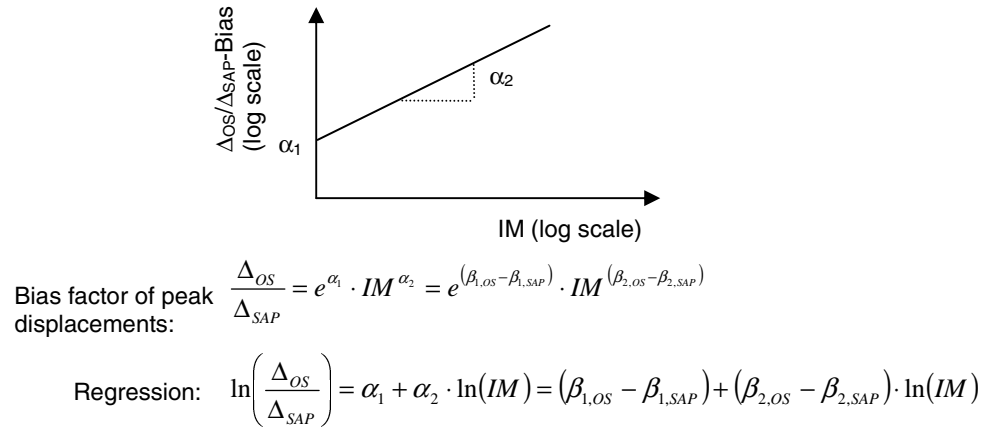


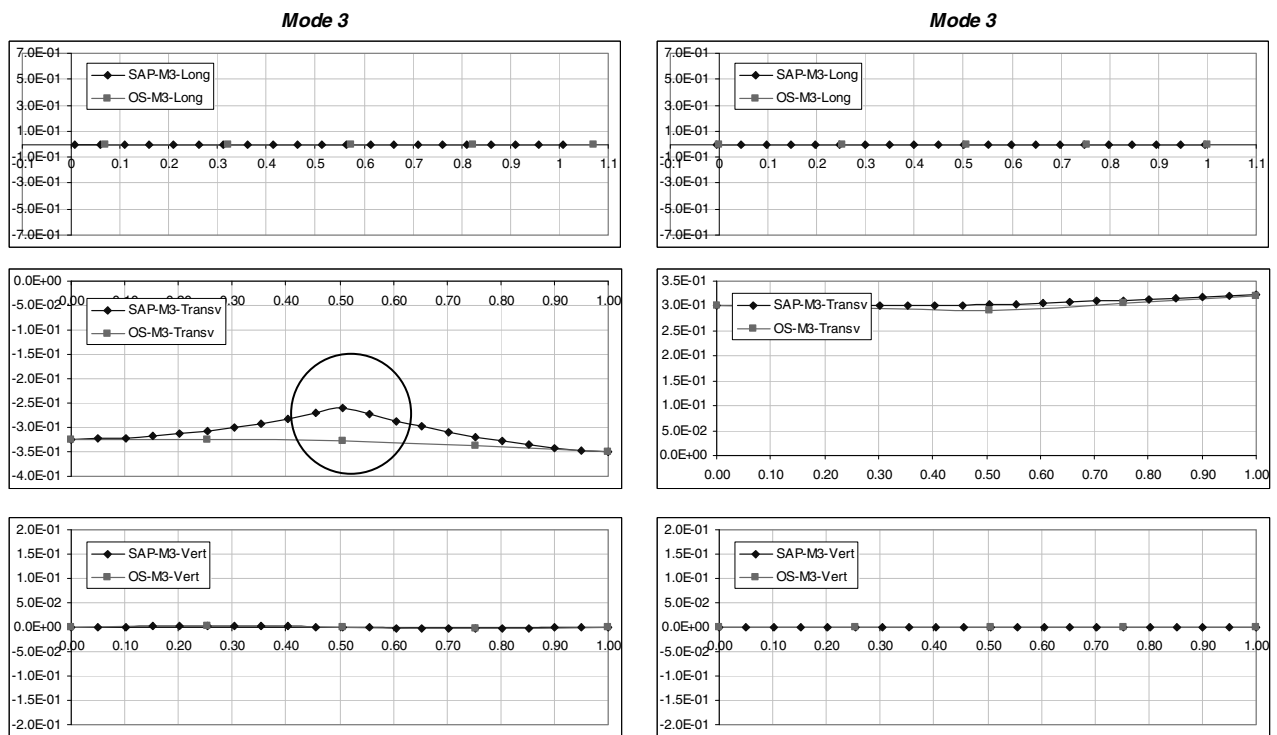
Fig. A.5 Computational scheme for regression of bias factors in terms of intensity measure for pair-wise comparison between OpenSees and SAP2000 NL THA displacements results Phase III, method 3.

The final stage of the project also consisted of the development of specific guidelines for the modeling and analysis of Ordinary Standard bridge models using SAP2000 and structural analysis software, utilizing the results of the previous stages of the project and related literature. Many of the recommendations are applicable or can be easily extended for Ordinary Nonstandard and Important bridges, as specifically defined throughout the document.

A.2 ANALYSIS OF RESULTS

Shear Deformation:

The mode shapes for bridge Route 14 are computed in SAP2000. A kink in the superstructure is observed despite continuity of the element, since the shear area of the superstructure is not accounted for properly. The correct stiffness of the superstructure and mode shapes of the bridge are obtained for a correct shear area of all cross sections, since shear deformation is automatically included in SAP2000 calculations.



Original model: Shear area of superstructure ignored.

Corrected model: Shear area of superstructure specified properly

Fig. A.6 Effect of superstructure shear area.

Cross-sectional analysis:

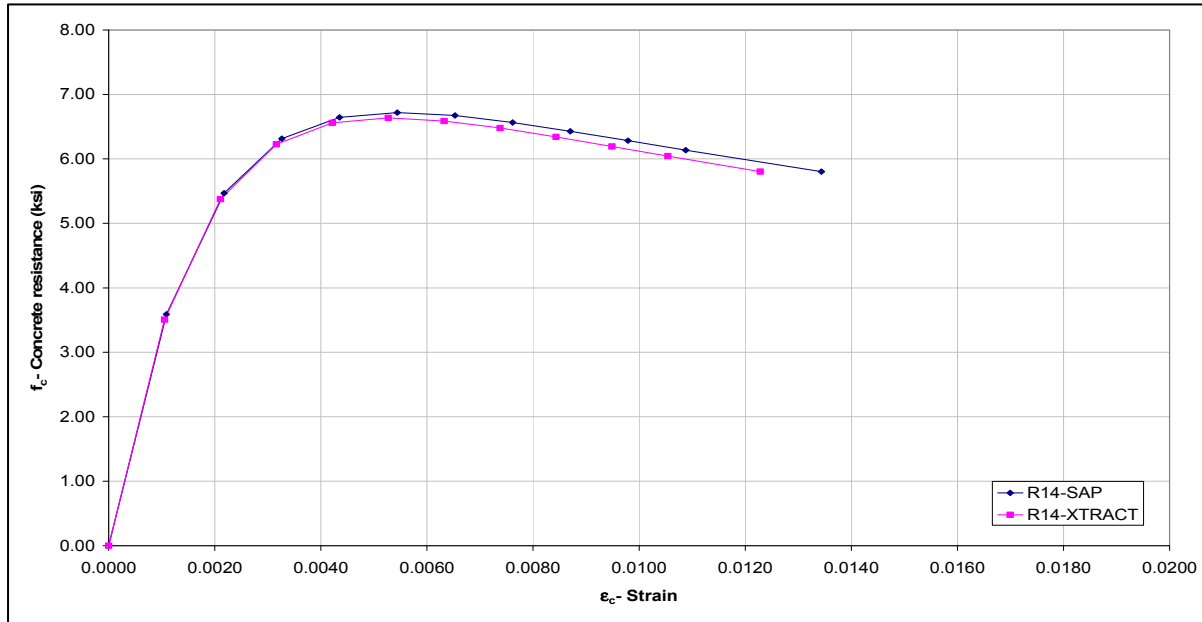


Fig. A.7 Comparison of confined concrete σ - ϵ relationship (Mander model) using SAP2000-SDSection and Xtract by Imbsen (Route 14 column).

XTRACT:

$$f_{cc}^* = 6.64 \text{ ksi}, \epsilon_{cc} = 5.27e^{-3}$$
$$f_{cu}^* = 5.80 \text{ ksi}, \epsilon_{cu} = 12.25e^{-3}$$

SAP:

$$f_{cc} = 6.72 \text{ ksi}, \epsilon_{cc} = 5.44e^{-3}$$
$$f_{cu} = 5.81 \text{ ksi}, \epsilon_{cu} = 13.4e^{-3}$$

Route 14 column: Comparison of moment-curvature curve obtained from SAP2000-SDSection and Xtract by Imbsen

Considerations for Moment-Curvature:

- Dead axial load $P=1247 \text{ K}$ ($7.5\%_c A_g$)
- Expected material strength for concrete and steel
- Failure defined as fracture of rebar or crushing of concrete confinement
- Reduced ultimate strain in steel stress-strain relation ϵ_{suR}
- Plastic capacity M_p defined by balancing the areas between the actual and the idealized M - ϕ curves beyond the yield point.

XTRACT:

$M_y=126,256$ K-in, $\phi_y=6.37e^{-5}$
 $M_u=197,900$ K-in, $\phi_u=7.509e^{-4}$ (concrete crushing)
 $M_p=179,000$ K-in, $\phi_{y-ideal}=9.0e^{-5}$
 $\mu_\phi=11.8$

$I_{crack}=0.56I_g$ (SDC-2004)

Displacement Capacity

$L_p=50.6$ in (0.75D), $H=37.93$ ft
 $\theta_p=(\phi_u-\phi_y)L_p=0.035$ rad
 $\Delta_y=H^2\phi_y/3=4.4$ in, $\Delta_p=\theta_p(H-l_p/2)=15.0$ in, $\Delta_u=19.4$ in,
 $\mu_\delta=4.4$

SAP:

$M_y=127,969$ K-in, $\phi_y=6.37e^{-5}$
 $M_u=203,260$ K-in, $\phi_u=6.928e^{-4}$ (concrete crushing)
 $M_p=185,190$ K-in, $\phi_{y-ideal}=9.218e^{-5}$
 $\mu_\phi=10.9$

$I_{crack}=0.569I_g$

Displacement Capacity

$L_p=50.6$ in (0.75D), $H=37.93$ ft
 $\theta_p=(\phi_u-\phi_y)L_p=0.032$ rad
 $\Delta_y=H^2\phi_y/3=4.4$ in, $\Delta_p=\theta_p(H-l_p/2)=13.8$ in, $\Delta_u=18.2$ in,
 $\mu_\delta=4.1$

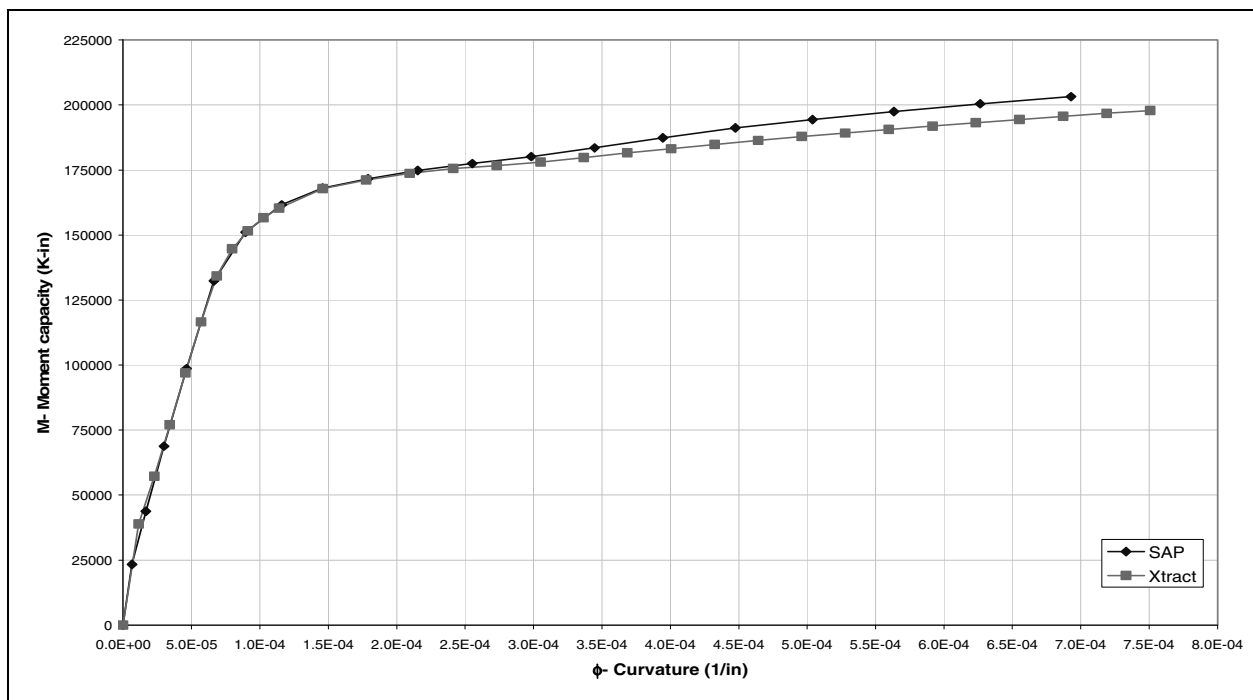


Fig. A.8 Comparison of moment-curvature analysis using SAP2000-SDSection and Xtract by Imbsen (Route 14 column).

Both SAP2000 and Xtract programs use the Mander model with the same input parameters to compute stress-strain relationship for confined concrete of a typical reinforced concrete column bent; however, they result in a 10% difference in the ultimate strain, automatically calculated in both programs. These differences are also reflected in the moment-curvature analysis results of the cross section for ultimate capacity. If the same ultimate concrete strain values were used in both programs, the ultimate capacity and ductility of the cross section, obtained from moment-curvature analysis, would probably coincide. Due to fiber configuration,

the ductility capacity of the resulting Xtract model of the column cross section is about 10% higher than the SAP2000 model results.

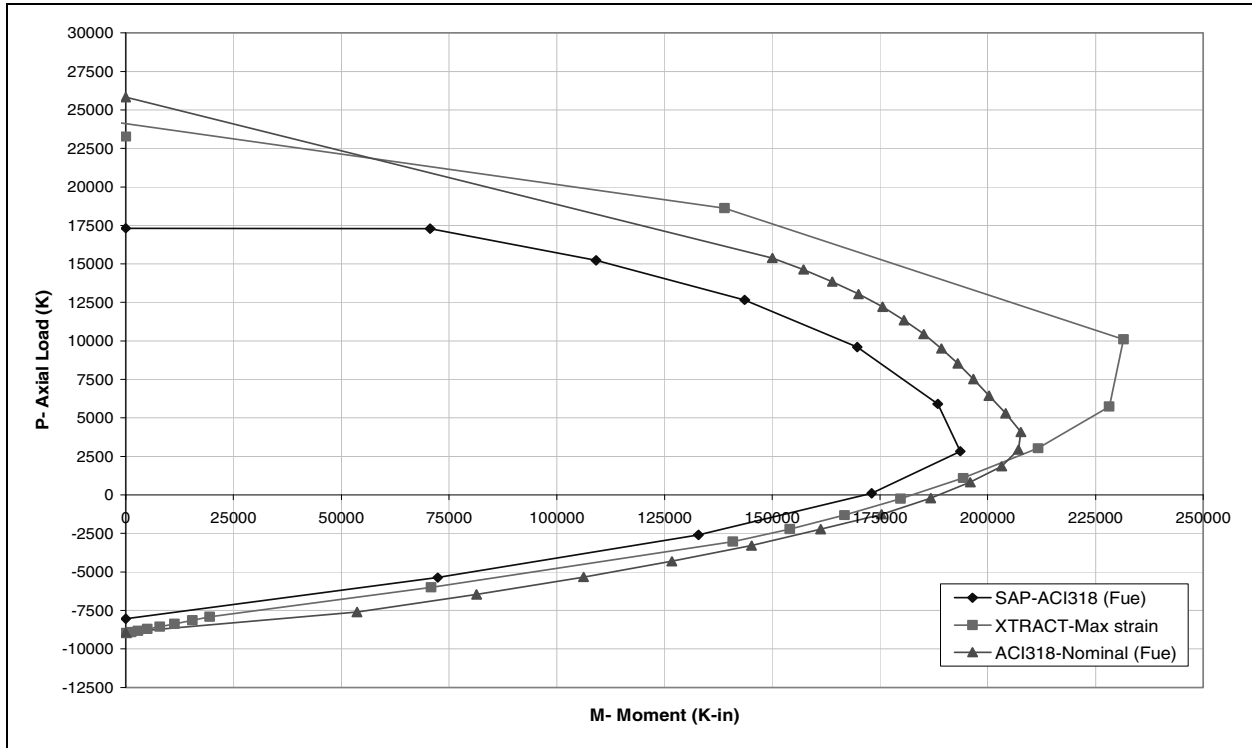


Fig. A.9 Comparison of interaction diagram obtained from SAP2000-SDSection, Xtract by Imbsen, and hand calculations following ACI-318 (Route 14 column).

The results of the interaction diagram obtained using the three sources display significant differences in the balance point and ultimate capacity in compression of a typical column bent cross section. Despite similar stress-strain relationship for steel, confined and unconfined concrete materials, the three sources for computing the interaction diagram representing ultimate capacity without reduction factors probably differ due the use of different maximum concrete and steel stress and strain values for such computation. However, in the typical range of axial load on the column bents of 5–10% in tension and 15–20% in compression, the overall differences between the results are on the order of only 10%. These sources for calculating the interaction diagram for bridge column bents are therefore considered acceptable and the differences can be ignored.

Cantilever Model

A comparison of linear and nonlinear pushover curves between the different nonlinear options for column plastic hinge in SAP2000 and OpenSees fiber model are presented below for the cantilever model of Route 14 column bent. All the different options for modeling the column plastic hinge in SAP2000 can be used for a two-dimensional nonlinear static analysis using the corresponding recommendations, since the different curves display similar initial stiffness, yielding point and maximum base shear. The ductility capacity of some of the ductile models (such as the fiber and NL Link-Wen) require a separate estimate, since the stress or strength values beyond the failure point are extrapolated automatically in SAP2000, even if degradation of strength is built into the material model.

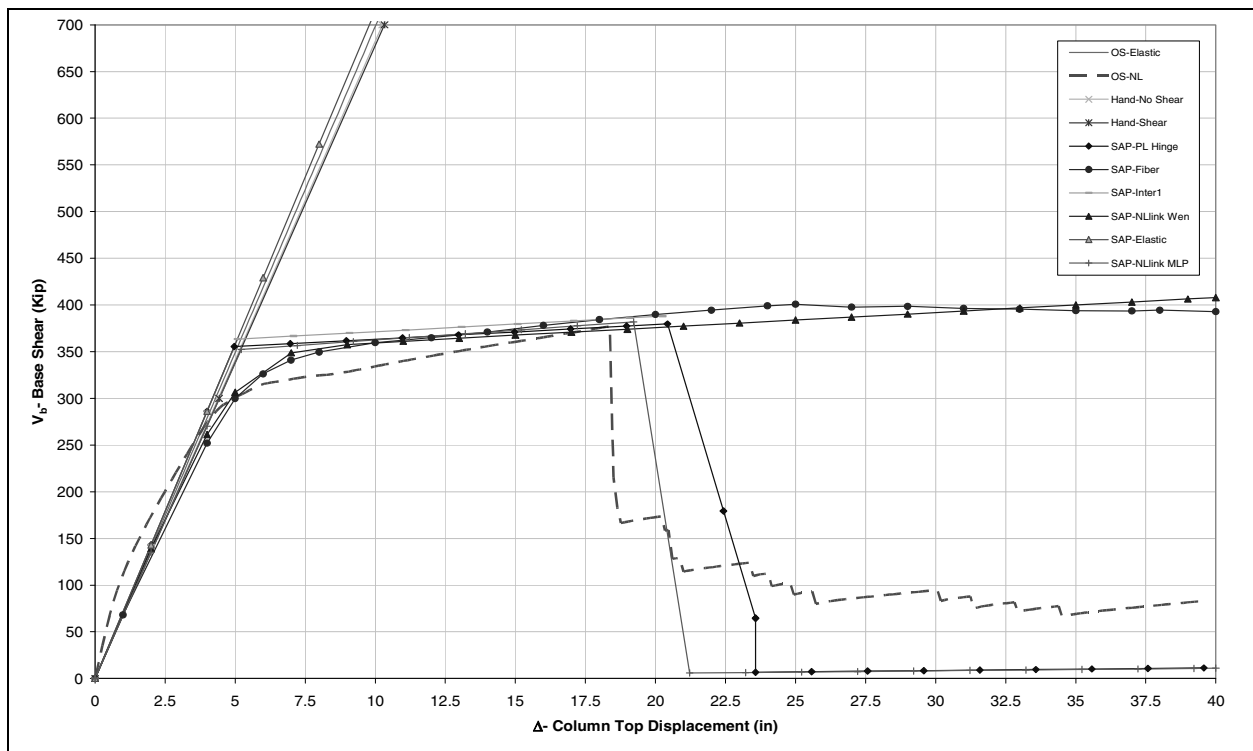


Fig. A.10 Pushover curve of cantilever column, orthogonal directions of bridge (X or Y axis).

The results for pushover analysis at an angle (45° in this case) are displayed below. Due to the overestimation in stiffness and strength of some of the models (produced by an unnecessary vectorial sum of the capacity in the orthogonal directions), some of the plastic hinge models for the column bent should not be used for a three-dimensional analysis. Among these are the NL-link and the uncoupled plastic hinge. The remaining models can be used for three-

dimensional analysis, accounting for smaller overestimation of initial stiffness and strength, as well as observing other limitations specified in the guidelines.

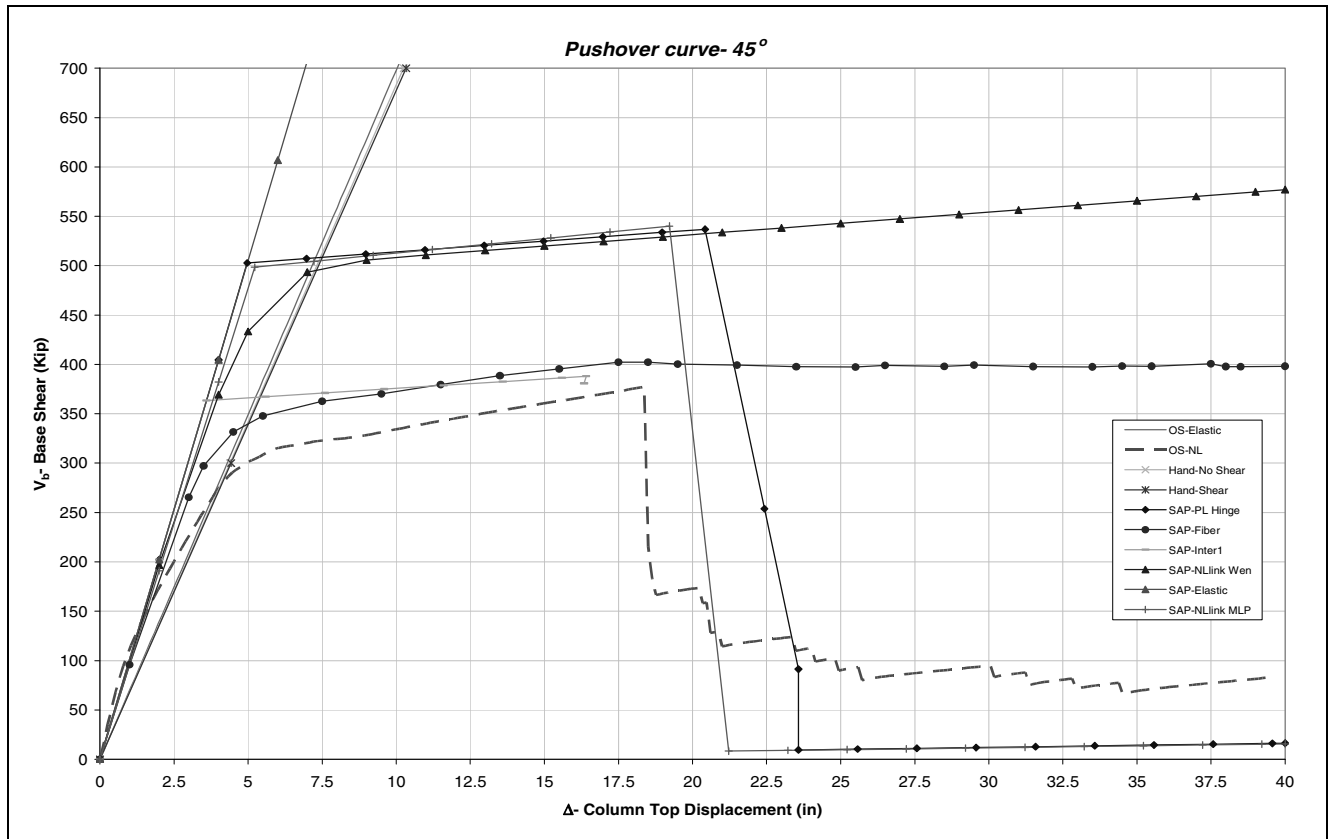
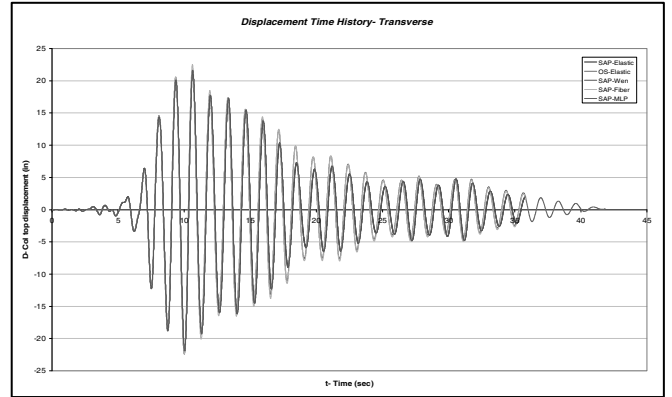
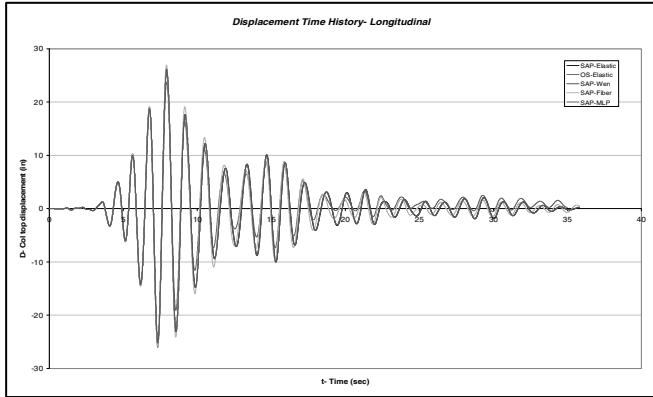


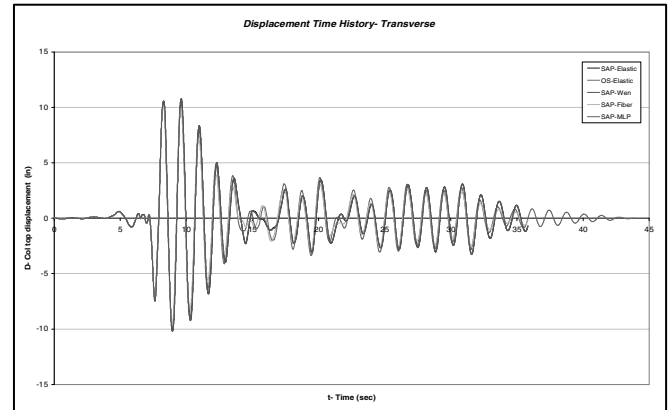
Fig. A.11 Pushover curve for 45° angle push of cantilever column in SAP2000.

Comparison of displacement time histories results between nonlinear options for column plastic hinge in SAP2000 and OpenSees fiber model (linear elastic time history analysis). The displacement time histories and peak displacements obtained from linear time history analysis match within 5-10% between OpenSees fiber model and the different models in SAP2000 for the three ground motions selected by Caltrans design engineers.

Loma Prieta A02, SF=2.25



Imperial Valley\H-BRA, SF=2.5



Kocaeli\MCD, SF=15

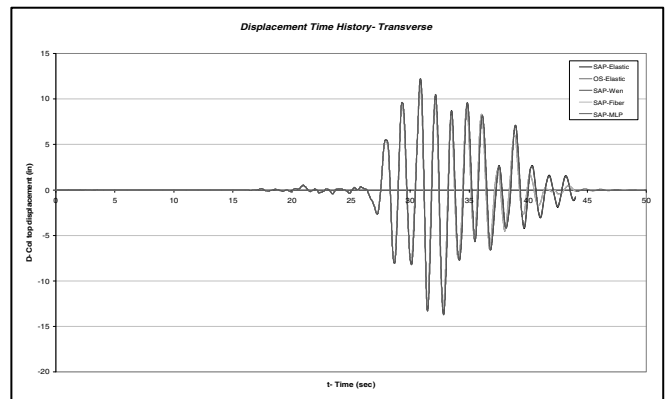
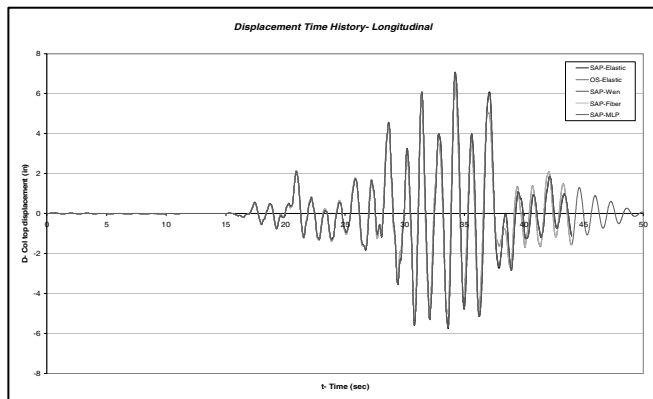


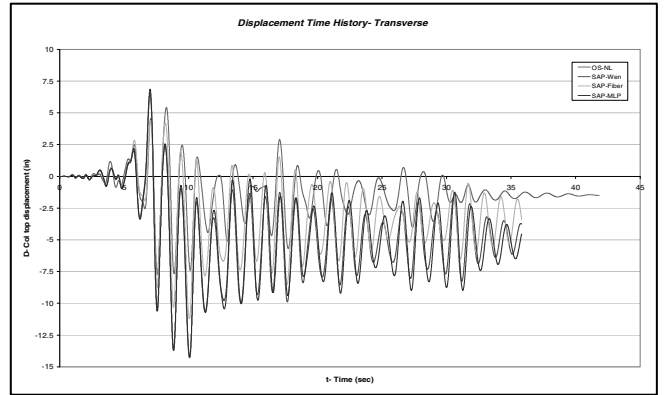
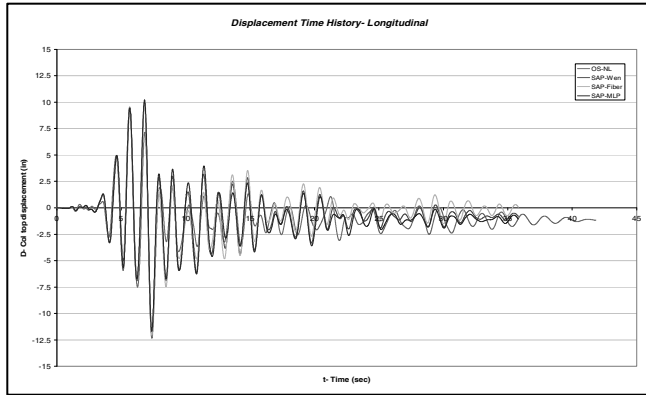
Fig. A.12 Displacement time history analysis results for cantilever column, elastic range.

Table A.8 Differences (%) in peak displacements of SAP2000 models with respect to OpenSees fiber model: nonlinear time history analysis.

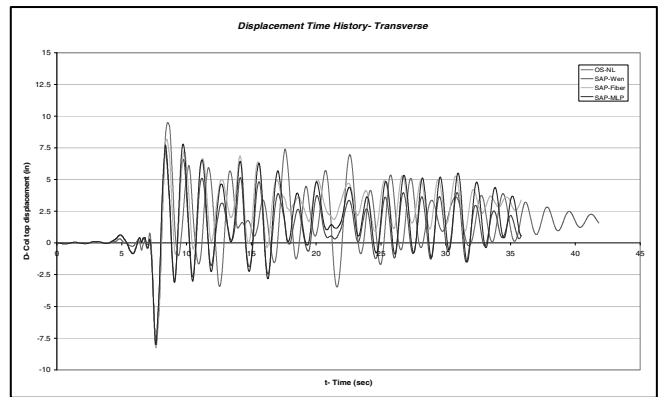
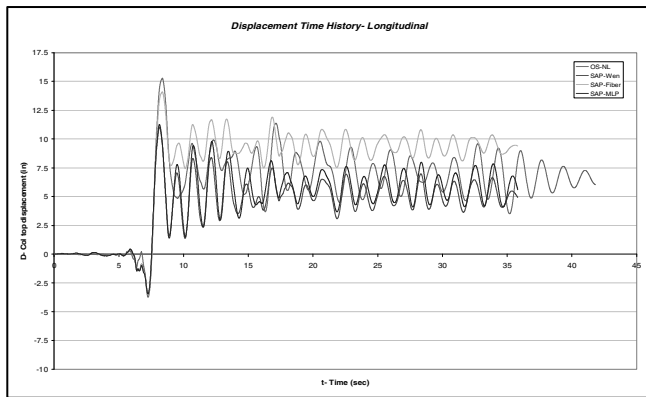
GM	Direc.	SAP		
		Fiber	MLP/Wen	Elastic
1	L	-5	3	3
	T	0	2	2
2	L	13	10	10
	T	5	1	-1
3	L	0	8	8
	T	0	5	6
Average		2	5	5

Comparison of displacement time histories results between nonlinear options for column plastic hinge in SAP2000 and OpenSees fiber model (nonlinear time history analysis). The displacement time histories and peak displacements obtained from nonlinear time history analysis differ significantly between the OpenSees fiber model and the different models in SAP2000 for the three ground motions selected by Caltrans design engineers.

Loma Prieta A02, SF=2.25



Imperial Valley\H-BRA, SF=2.5



KOCAELI\MCD, SF=15

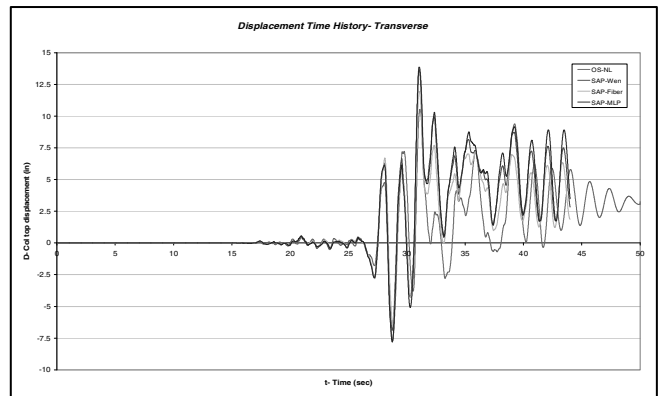
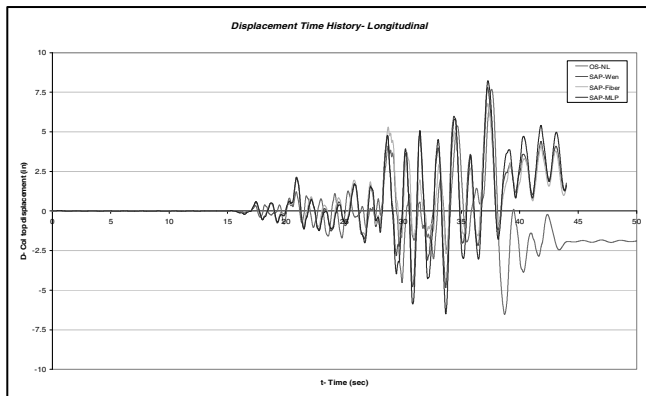


Fig. A.13 Displacement time history analysis results of cantilever column, inelastic range.

Table A.9 Differences (%) in peak displacements of SAP2000 models with respect to OpenSees fiber model: nonlinear time history analysis.

GM	Direc.	SAP		
		Fiber	MLP	Wen
1	L	-2	-5	-3
	T	43	82	83
2	L	-8	-27	-28
	T	-15	-19	-23
3	L	-11	8	1
	T	13	33	31
Average		3	12	10

Damping and Free Vibration Test of Cantilever

A free vibration test of a cantilever column was carried out in OpenSees to illustrate the procedure for damping estimation. Route 14 column cross section and dimensions were used, where the following initial displacements were imposed:

- Elastic response: $\Delta_{init}=2$ in ($\Delta_y=4.4$ in)
- Inelastic response: $\Delta_{init}=17.6$ in ($\mu_d=4$)

The decay of motion was used to estimate classical damping for linear and nonlinear elements for the elastic range of response. Permanent displacement used to estimate the total (classical) damping in the system through nonlinear action in column, for a displacement ductility of 4 and free vibration. The actual damping in nonlinear system depends also on ground motion characteristics, and therefore different damping results can be expected for different column configurations and excitations.

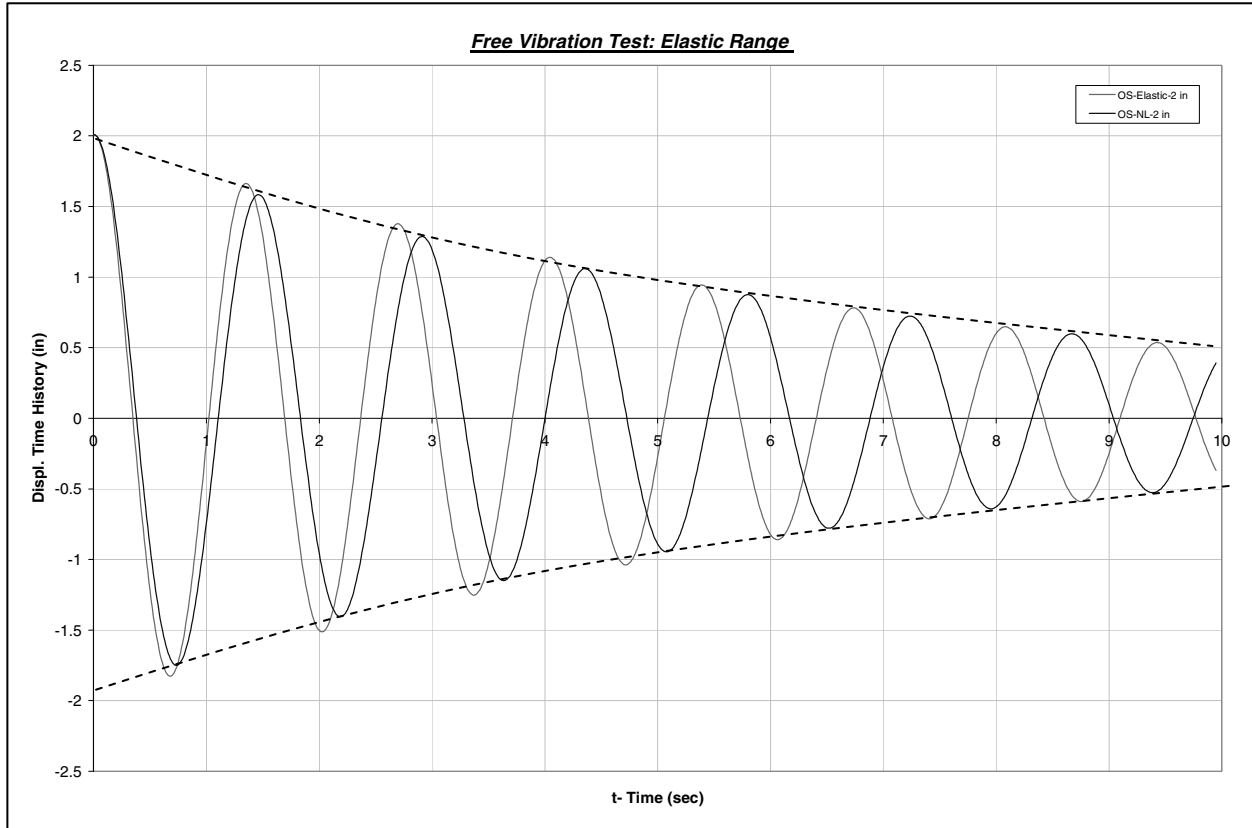


Fig. A.14 Free vibration test of a cantilever in elastic range of response.

Decay of motion: $\zeta = 1/(2\pi j) \ln(u_i/u_{i+j})$

Elastic range of response: $\Delta_{init} = 2 \text{ in} < \Delta_y = 4.4 \text{ in}$

- Elastic model: (T_1 -cracked=1.34 sec): $\zeta = 1/(2\pi 6) \ln(1.648/0.531) = \mathbf{3\%}$ (assigned classical damping)
- Nonlinear model (T_1 -uncracked=0.96 sec): $\zeta = 1/(2\pi 5) \ln(1.571/0.597) = \mathbf{3\%}$ (assigned classical damping)

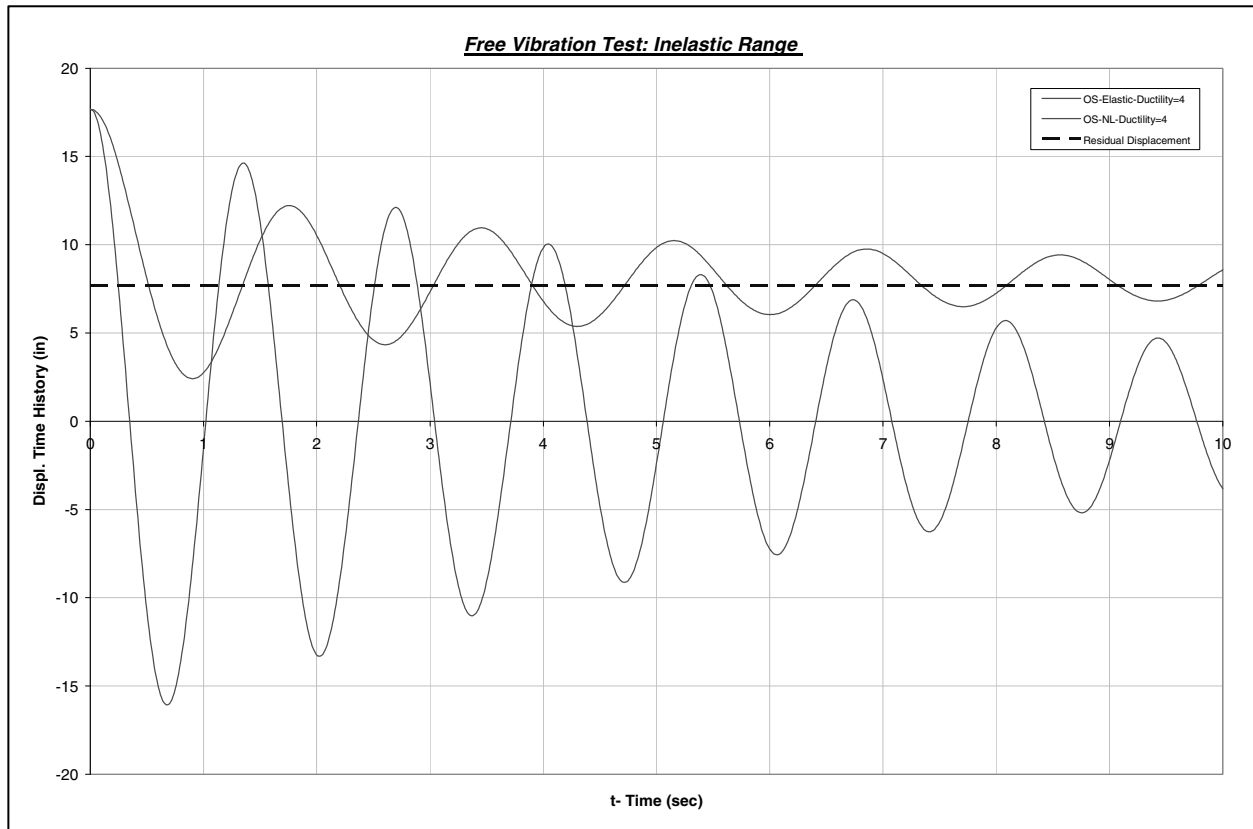


Fig. A.15 Free vibration test of a cantilever in inelastic range of response.

Inelastic range of response: $\Delta_{init}=17.6$ ($\mu_d=4$)

- Elastic model: $\zeta=1/(2\pi 7) \ln(17.6/4.67)=3\%$ (**assigned classical damping=3%**)
- Nonlinear element: permanent deformation $\Delta_{res}=7.71$ in, $\zeta=1/(2\pi 5) \ln((17.6-7.71)/(9.42-7.71))=5.6\%$ (**total damping**)

Ductility Estimation Based on Plastic Curvature Assumption

The displacement ductility capacity of a single column-bent bridge was determined for the longitudinal and transverse directions of the structure, following the procedure of Section 3.1.3 of SDC 2004, which assumes a constant plastic curvature throughout the column plastic hinge length. A similar procedure was applied for a linear variation of the plastic curvature and the results compared to the pushover analysis results of the bridge, implemented in OpenSees. The bridge model in OpenSees was modeled using a distributed plasticity fiber model of the column and expected material strength. Several boundary conditions for the superstructure ends were examined to observe the effect of superstructure torsional restraints on the ductility and strength of the bridge in a pushover analysis.

The results of this analysis showed that the assumption of constant curvature along the plastic hinge length resulted in a good estimation of overall ductility in the transverse direction, while for the longitudinal direction, the results were between the constant and linearly varying plastic curvature. The plastic hinge length was determined according to Section 7.6.2 of SDC 2004, based on constant plastic curvature assumption.

Data:

- Column: circular section. Diameter 6.0 ft.
- Longitudinal reinforcement: 40#11 (1.72%)
- Transverse reinforcement: hoops #8@5.9" (0.80%)
- Dead load: $P=1795$ K ($8.6\% f'_c A_g$)
- Concrete compressive strength: $f'_c=5$ ksi

Moment Capacity:

$M_y=143,500$ K-in, $M_u=179,500$ K-in
 $M_p \approx \text{ave}\{M_y, M_u\} = \mathbf{161,500}$ K-in

Curvature Ductility:

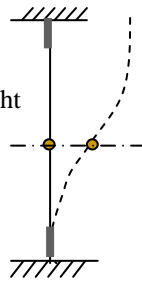
$\phi_y=8.73e-5$ 1/in, $\phi_u=7.77e-4$ 1/in
 $\phi_p=6.90e-4$ 1/in, $\mu_\phi=\mathbf{8.9}$

Moment-curvature analysis for MGR column:

Ductility Estimation for MGR Bridge: Longitudinal Direction

Assumption:

Fixed base, fixed column top (due to superstructure and frame action)
 $L_{p1}=L_{p2}$: Point of inflection at mid-height
 $(P_{top} \sim P_{bottom}$: approximate results)

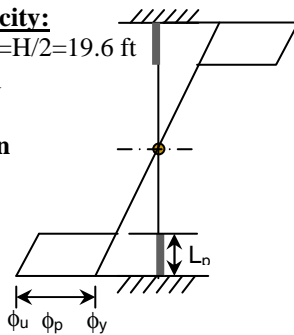


Base Shear:

$V_{b-Col} = (2M_p/H_{Tot}) = \mathbf{688.05}$ K $< \phi V_n = 1220.67$ K
 (1.77 times stronger: Flexural-critical column)
 $V_{b-Bridge} = 2(\text{col's}) \times (2M_p/H_{Tot}) = \mathbf{1376.1}$ K

1. Displacement Capacity:

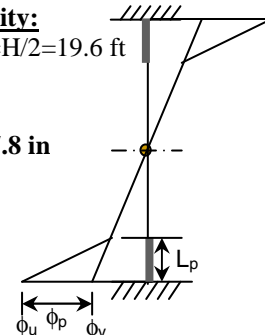
$L_p = 51.9$ in ($0.72D$), $H' = H/2 = 19.6$ ft
 $\theta_p = (\phi_u - \phi_y)L_p = 0.036$ rad
 $\Delta_y = 2H'^2\phi_y/3 = \mathbf{3.2}$ in
 $\Delta_p = 2\theta_p(H' - l_p/2) = \mathbf{15.0}$ in
 $\Delta_u = 18.2$ in, $\mu_d = \mathbf{5.7}$



1. Constant plastic curvature

2. Displacement Capacity:

$L_p = 51.9$ in ($0.72D$), $H' = H/2 = 19.6$ ft
 $\theta_p = (\phi_u - \phi_y)L_p = 0.036$ rad
 $\Delta_y = 2H'^2\phi_y/3 = \mathbf{3.2}$ in
 $\Delta_p \sim 2 \frac{(1/2)}{3} \theta_p (H' - l_p/3) = \mathbf{7.8}$ in
 $\Delta_u = 11.0$ in, $\mu_d = \mathbf{3.4}$



2. Linear variation of curvature over plastic hinge length

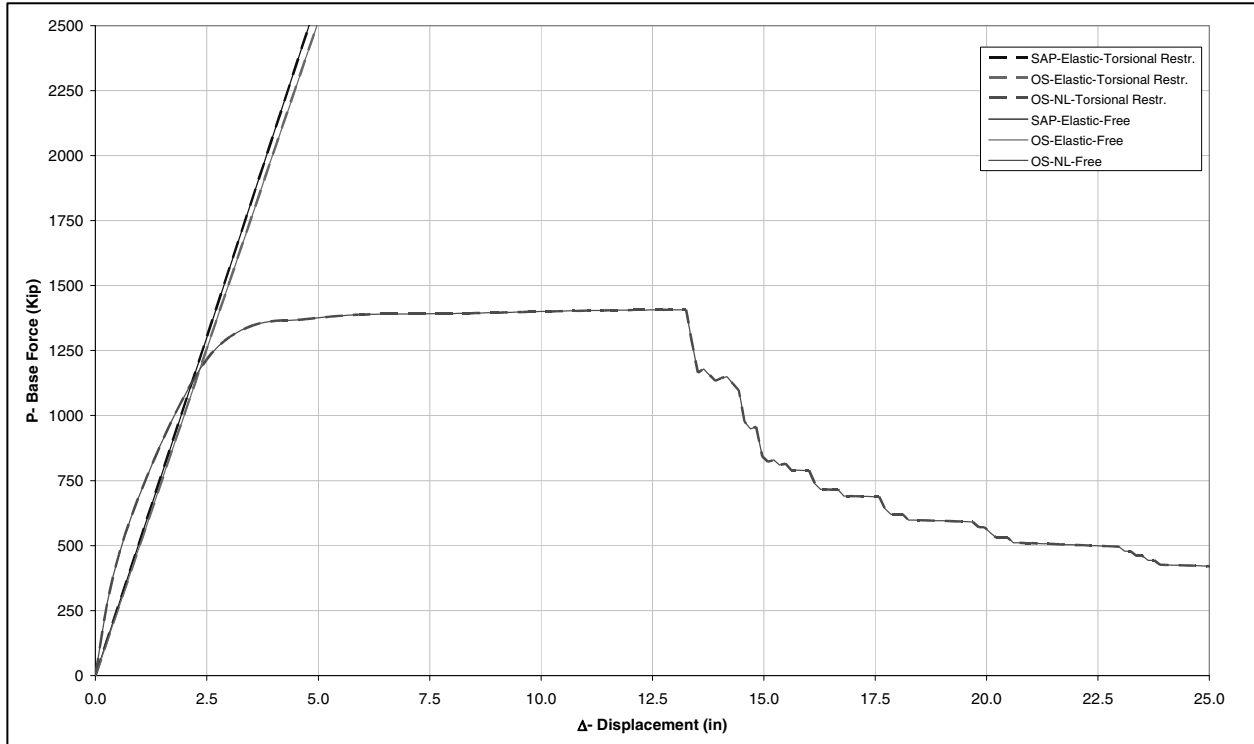
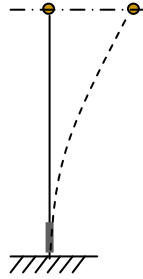


Fig. A.16 Pushover analysis results in longitudinal direction: Same with or without superstructure torsional restraints at abutment. $V_b=1390$ K, $\Delta_y=3.2$ in, $\Delta_u=13.3$ in, $\mu_d=4.2$.

Ductility estimation of MGR Bridge: Transverse direction

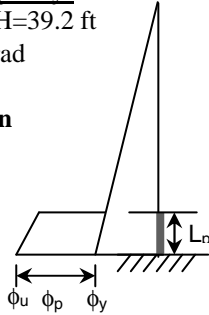
Assumption:
Fixed base, free end.



Base Shear:
 $V_{b-Col} = (M_p/H_{Tot}) = 344.0 \text{ K} < \phi V_n = 1555.6 \text{ K}$
 (4.52 times stronger: Flexural- critical column)
 $V_{b-Bridge} = 2 \text{ (col's)} \times (M_p/H_{Tot}) = 688.0 \text{ K}$

1. Displacement Capacity:

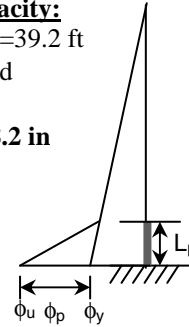
$L_p = 51.9 \text{ in (0.72D)}$, $H = 39.2 \text{ ft}$
 $\theta_p = (\phi_u - \phi_y)L_p = 0.036 \text{ rad}$
 $\Delta_y = H^2\phi_y/3 = 6.4 \text{ in}$
 $\Delta_p = \theta_p(H - l_p/2) = 16.0 \text{ in}$
 $\Delta_u = 22.4 \text{ in}$, $\mu_d = 3.5$



1. Constant plastic curvature

2. Displacement Capacity:

$L_p = 51.9 \text{ in (0.72D)}$, $H = 39.2 \text{ ft}$
 $\theta_p = (\phi_u - \phi_y)L_p = 0.036 \text{ rad}$
 $\Delta_y = H^2\phi_y/3 = 6.4 \text{ in}$
 $\Delta_p \sim (1/2)\theta_p(H - l_p/3) = 8.2 \text{ in}$
 $\Delta_u = 14.6 \text{ in}$, $\mu_d = 2.3$



2. Linear variation of curvature over plastic hinge length

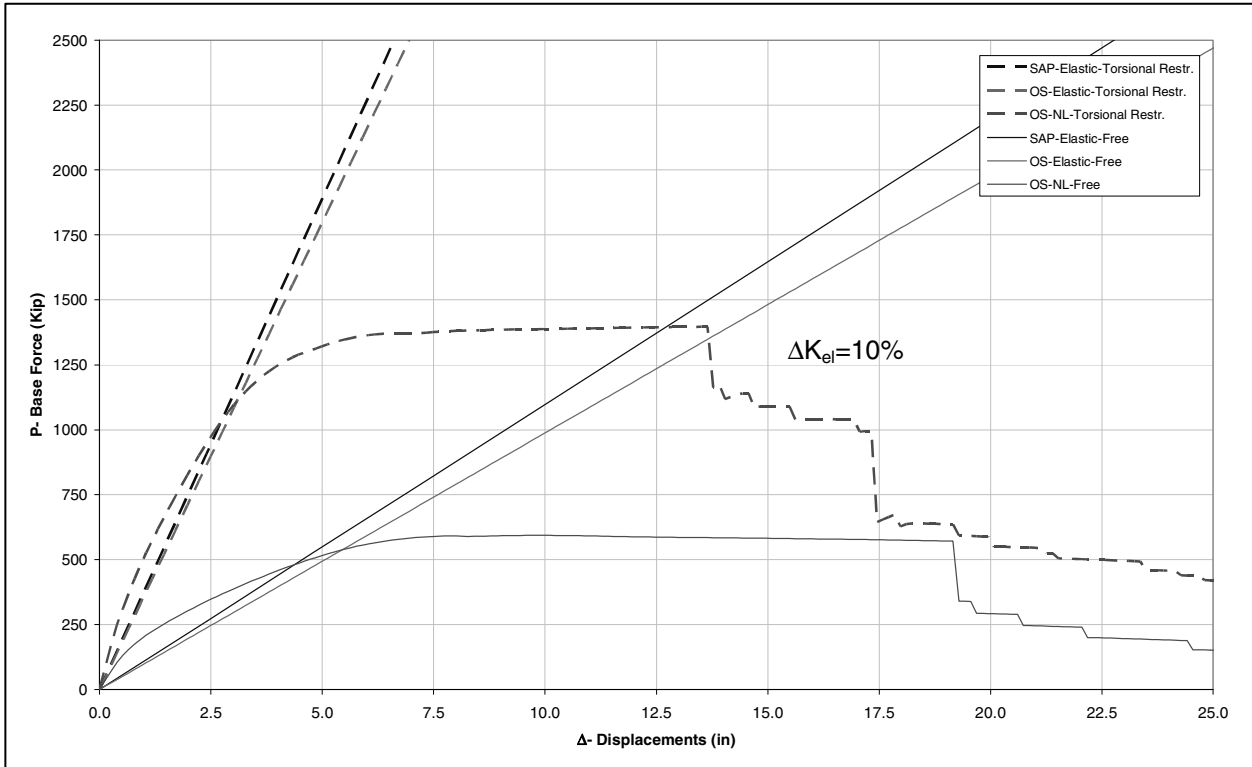


Fig. A.17 Pushover results for transverse direction.

With superstructure torsional restraint (NL results): $V_b=1380$ K, $\Delta_y=3.4$ in, $\Delta_u=13.6$ in, $\mu_d=4.0$ (~long. pushover). Free end (NL results): $V_b=593.1$ K, $\Delta_y=5.5$ in, $\Delta_u=19.2$ in, $\mu_d=3.5$ (similar to constant curvature estimation)

Effect of Cap Beam Torsional Stiffness

The correct torsional rigidity of the cap beam-superstructure system was modeled by adjusting the torsional resistance J of the cap beam element, thus obtaining the following results for a preliminary model of R14 Bridge:

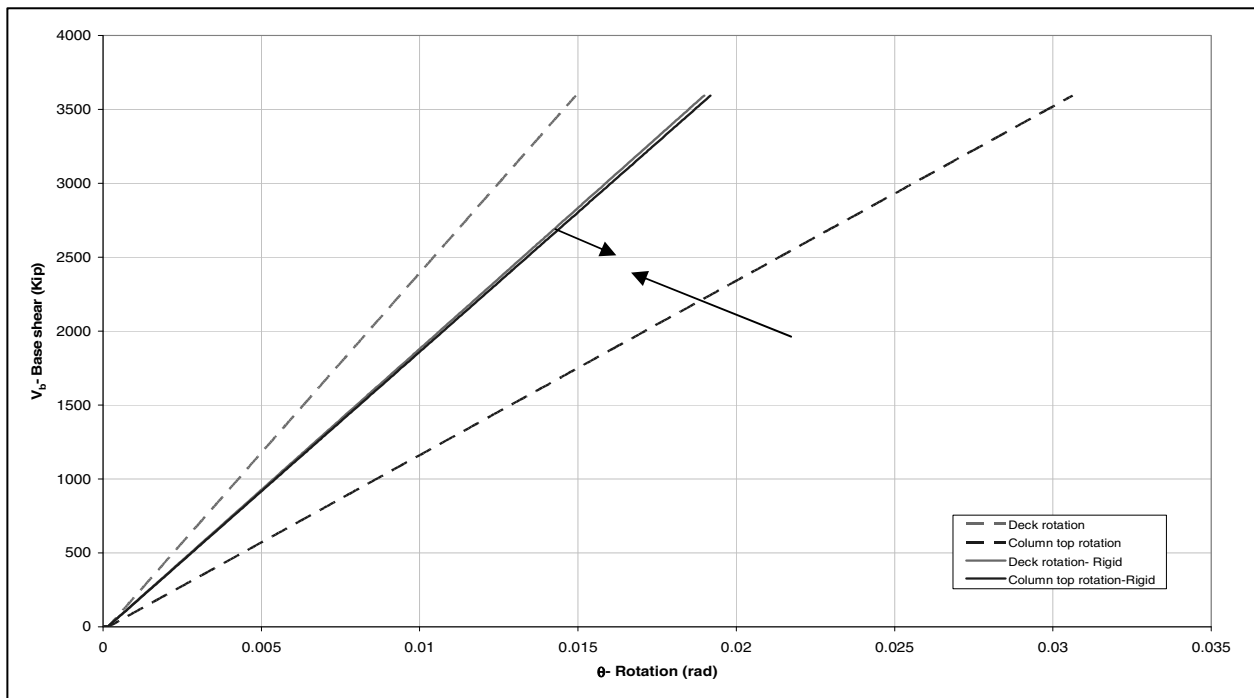


Fig. A.18 Effect of cap beam torsional stiffness on column top and superstructure rotation (pushover analysis in longitudinal direction).

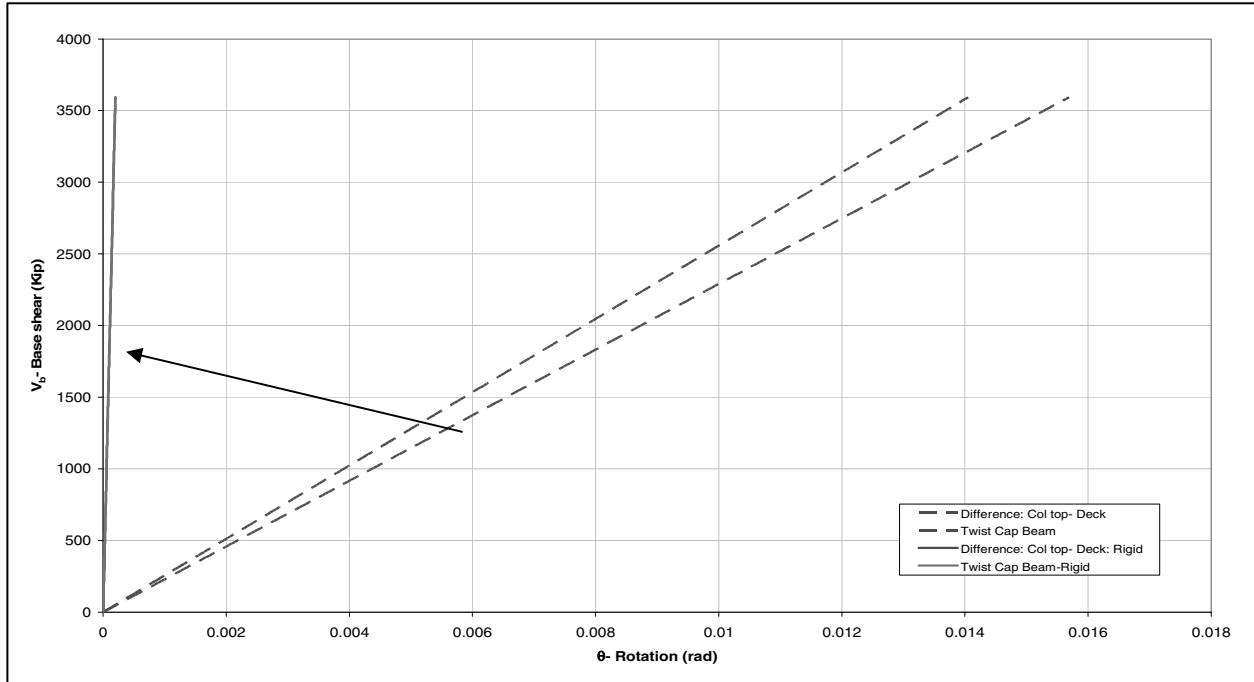


Fig. A.19 Effect of cap beam torsional stiffness on cap beam twist (pushover analysis in longitudinal direction).

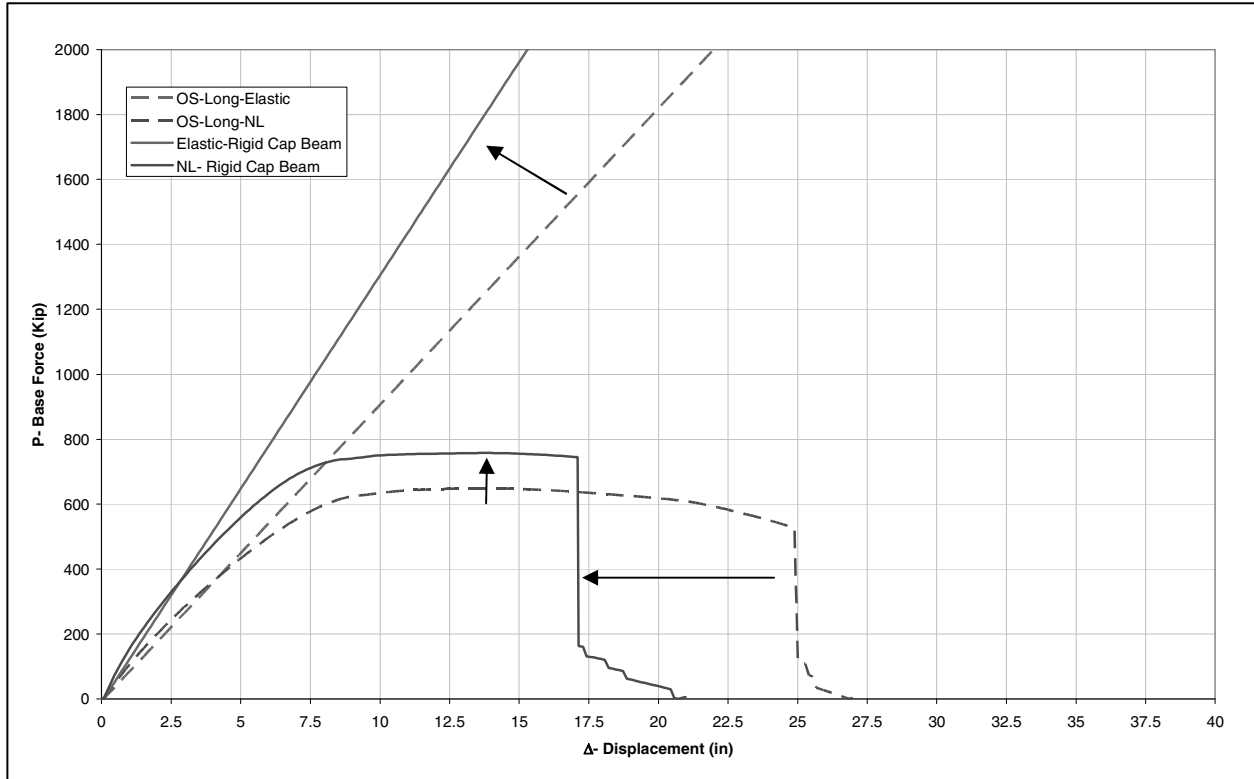


Fig. A.20 Effect of cap beam torsional stiffness on pushover curve in longitudinal direction.

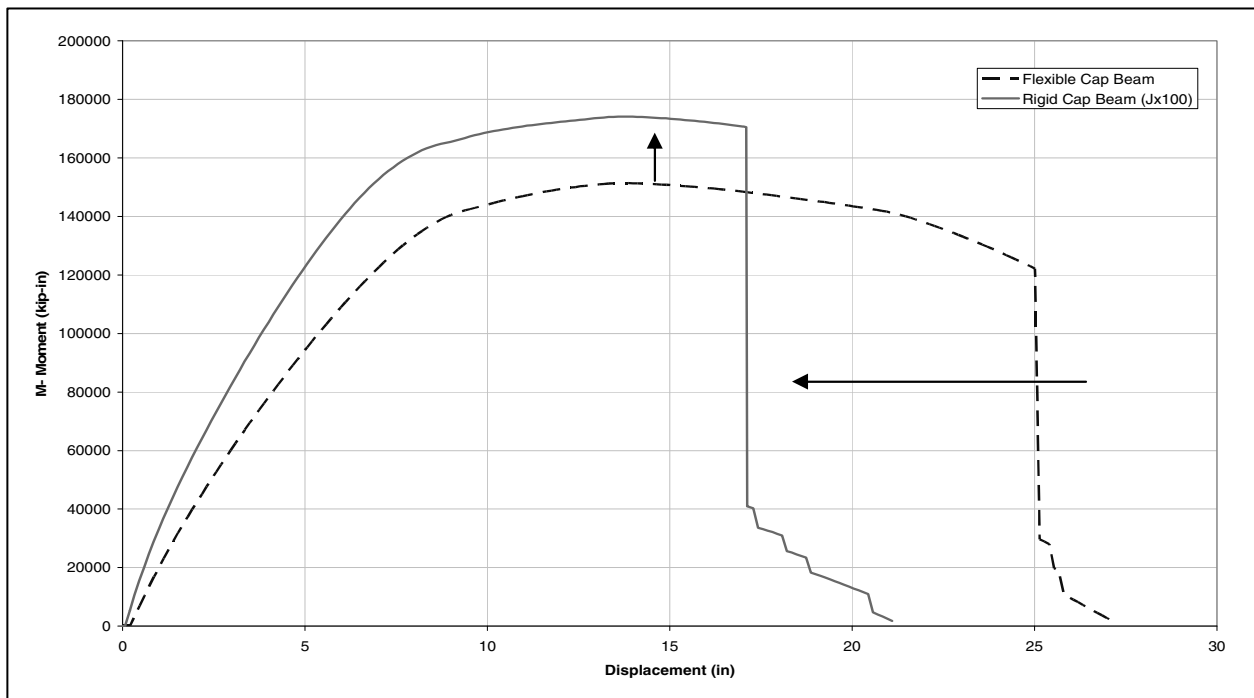


Fig. A.21 Effect of cap beam torsional stiffness on column top moment vs. superstructure displacement relationship for pushover analysis in longitudinal direction.

Using an approximation for rigid torsional stiffness ($J \times 100$) the following results were obtained:

- Significant reduction in column twist (R14: Resulting twist is 2% the value of the flexible model).
- Increase in column top fixity to superstructure and lateral stiffness of the bridge in the longitudinal direction (R14: 44% increase from $k_{\text{elastic}}=91.1$ K/in to 131.0 K/in).
- Reduction in period corresponding to the lateral translation mode (R14: 10% from $T_{\text{long}}=1.94$ sec to 1.76 sec), as well as global torsion of bridge. Insignificant reduction in modes corresponding to deformation of the deck (R14: 0–2% reduction in modal periods T_4, T_5).
- Increase in load demand and inelastic base shear (R14: 17% increase from $V_b=648.0$ K to 757.0 K).
- Reduction in displacement capacity and ductility (R14: 32% reduction in ultimate displacement from $\Delta_u=25.0$ in to 17.0 in, and ductility from $\mu_d=3.2$ to 2.5).
- For a certain level of displacements in the inelastic range, the column moment demand is higher for the case of the rigid cap beam (R14: 15% increase from $M_{\text{max}}=151411$ K-in to $M_{\text{max}}=174119$ K-in); however its ductility capacity is lower.

Abutment Models

Route 14 bridge model: Comparison of pushover curves for the longitudinal and transverse directions from SAP2000 and OpenSees bridge models using different abutment models. The fiber model is used for the plastic hinge zone for both SAP2000 and OpenSees bridge models. The roller abutment model corresponds to laterally unrestrained boundary conditions at the superstructure ends, while the simplified and spring abutment models provide lateral resistance to the superstructure ends from the embankment soil with a bilinear force-displacement relationship, among other components (see Section 2.7). Analysis results from Phase II.

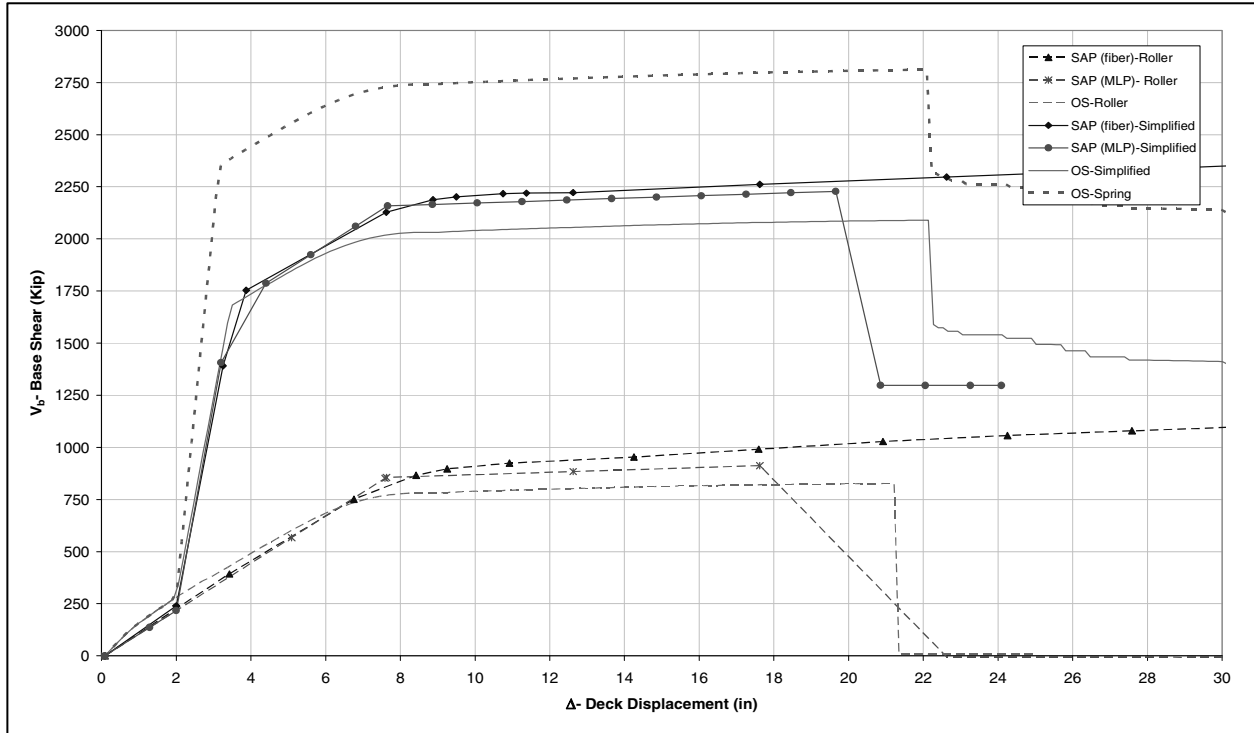


Fig. A.22 Pushover curve in longitudinal direction of R14 bridge using different abutment models.

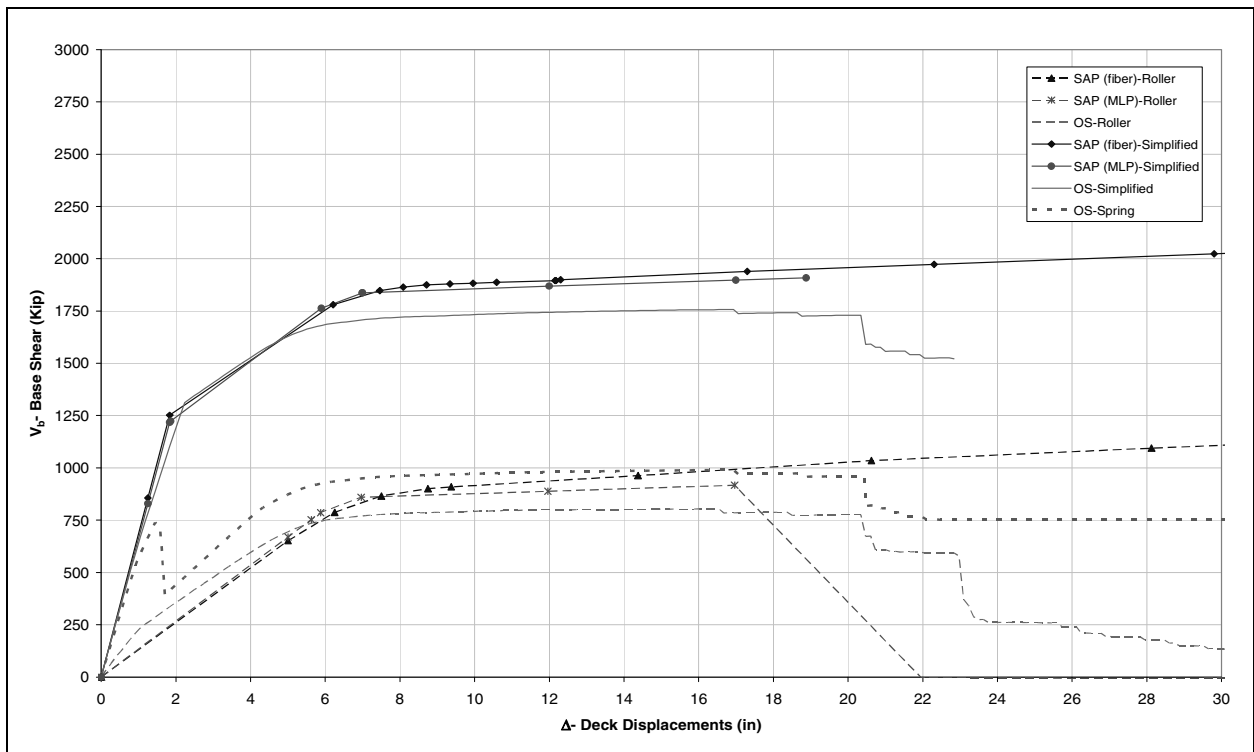


Fig. A.23 Pushover curve in transverse direction of R14 bridge using different abutment models.

The stiffness and ultimate base shear obtained from SAP2000 and OpenSees models for a specific abutment model match within 10%. The roller abutment model produces pushover curves with the lowest capacity, since the lateral resistance of the bridge consists primarily of the column bent capacity and frame action, for both the longitudinal and transverse directions of the bridge. The simplified abutment model accounts for the additional resistance obtained from the passive pressure developed behind the back wall, producing higher initial stiffness and an increase in the ultimate base shear (on the order of 100%, on average, for the transverse and longitudinal directions of the Route 14 bridge). For the longitudinal direction, the abutment resistance is introduced only after the closing of the gap.

The spring abutment model, implemented in OpenSees only, produces pushover curves that differ significantly from the response of the other two abutment models. In the longitudinal direction, after the closing of the gap, an additional resistance obtained from the passive pressure developed behind the wing wall, as well as the shear resistance of the distributed bearing pads, are accounted for in the lateral resistance of the bridge, producing an increase of 30% in the ultimate base shear and initial stiffness, for the case of the Route 14 bridge. In the transverse direction, the initial stiffness is increased similarly to the simplified abutment model, due to the soil embankment resistance. However, after the failure of the shear keys, the lateral resistance of the bridge consists primarily by the column bents, as well as a small contribution of the bearing pads shear resistance.

The following tables summarize the comparison between SAP2000 and OpenSees of elastic periods (first 5 mode shapes) for different abutment models (Route 14 bridge).

Table A.10 Elastic periods of R14 bridge, roller abutment.

Periods			Mode	Participating Mass Ratios			
OpenSees	SAP (fiber)	Δ (%)		UX- Longitudinal	UY- Transverse	UZ- Vertical	RZ- Torsion
11.110	10.586	4.7	Global torsion	0	0	0	100
1.867	1.860	0.4	Longitudinal	97.0	0	0	0
1.675	1.697	1.3	Transverse	0	99.0	0	0
0.555	0.552	0.5	Vertical super. deform. (S-shape)	2.0	0	0	0
0.410	0.401	2.2	Vertical super. deform. (W-shape)	0	0	72.8	0

The elastic periods match within 5% for the first five modes between the OpenSees and SAP2000 fiber models, using the roller abutment model. Also, the participating mass ratios demonstrate the low correlation between the first five natural mode shapes.

Table A.11 Elastic periods of R14 bridge, simplified abutment.

Periods			Mode	Participating Mass Ratios			
OpenSees	SAP (fiber)	Δ (%)		UX- Longitudinal	UY- Transverse	UZ- Vertical	RZ- Torsion
1.869	1.863	0.3	Longitudinal	96.1	0	0	0
0.765	0.765	0.0	Transverse	0	98.7	0	0
0.562	0.562	0.0	Vertical super. deform. (S-shape)	2.1	0	0	0
0.478	0.451	5.6	Global torsion	0	0	0	99.9
0.415	0.412	0.7	Vertical super. deform. (W-shape)	0	0	71.2	0

The elastic periods for the first five modes obtained from the OpenSees and SAP2000 fiber models still match within 5% using the simplified abutment model; however, the values computed for the periods of the transverse and torsional modes change considerably when using the simplified abutment model. The first mode period, longitudinal translation, conserves its value from the previous unrestrained abutment model due to the presence of the gap. The transverse mode is the second mode of vibration. Also, the participating mass ratios demonstrate the low correlation between the first five natural mode shapes.

Table A.12 Elastic periods of R14 bridge, spring abutment.

Periods			Mode	Participating Mass Ratios			
OpenSees	SAP (fiber)	Δ (%)		UX- Longitudinal	UY- Transverse	UZ- Vertical	RZ- Torsion
1.212	-	-	Longitudinal	96.1	0	0	0
0.769	-	-	Transverse	0	98.7	0	0
0.561	-	-	Vertical super. deform. (S-shape)	2.1	0	0	0
0.482	-	-	Global torsion	0	0	0	99.9
0.418	-	-	Vertical super. deform. (W-shape)	0	0	71.2	0

The spring abutment model was only implemented in OpenSees due its complexity, which consists of a combined parallel and series system behavior. The first mode, longitudinal translation, is affected considerably by the increase in the bridge stiffness, accounting for the distributed bearing pads shear resistance. The second mode, transverse translation, has the same period as the simplified abutment model, reflecting a similar initial stiffness. However, after the failure of the shear keys, the residual stiffness and strength is closer to the bridge behavior using the roller abutment model. The remaining modes, corresponding primarily to the deformation or vibration of the superstructure, are not affected by the abutment model and result in similar elastic periods. The participating mass ratios are similar to the simplified abutment model, demonstrating again the low correlation between the first five natural mode shapes of the bridge structure.

Nonlinear Time History Analysis Results: Preliminary Analysis of Phase II

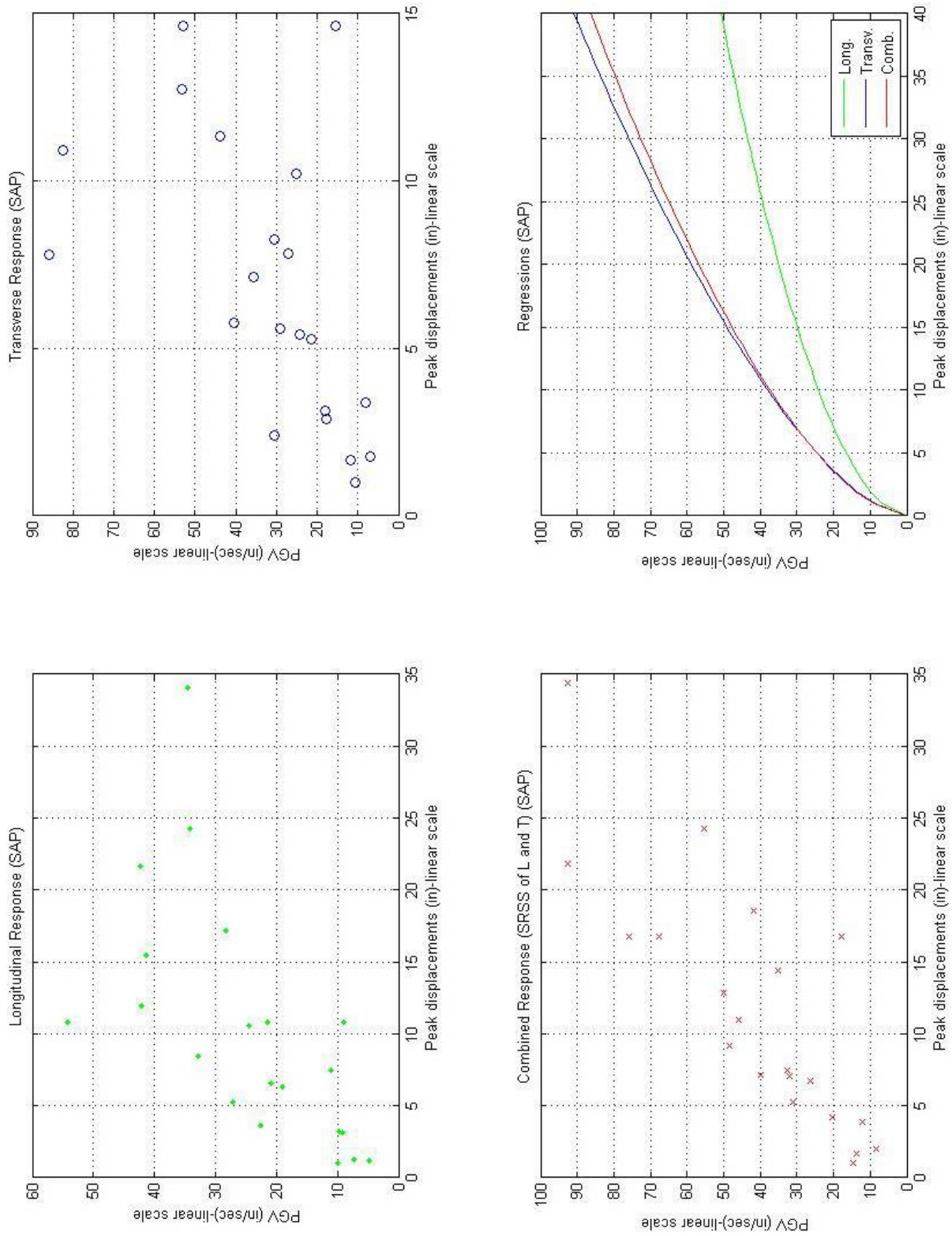


Fig. A.24 SAP2000 fiber model with roller abutment (linear scale): I880n ground motion set (Route 14 bridge).

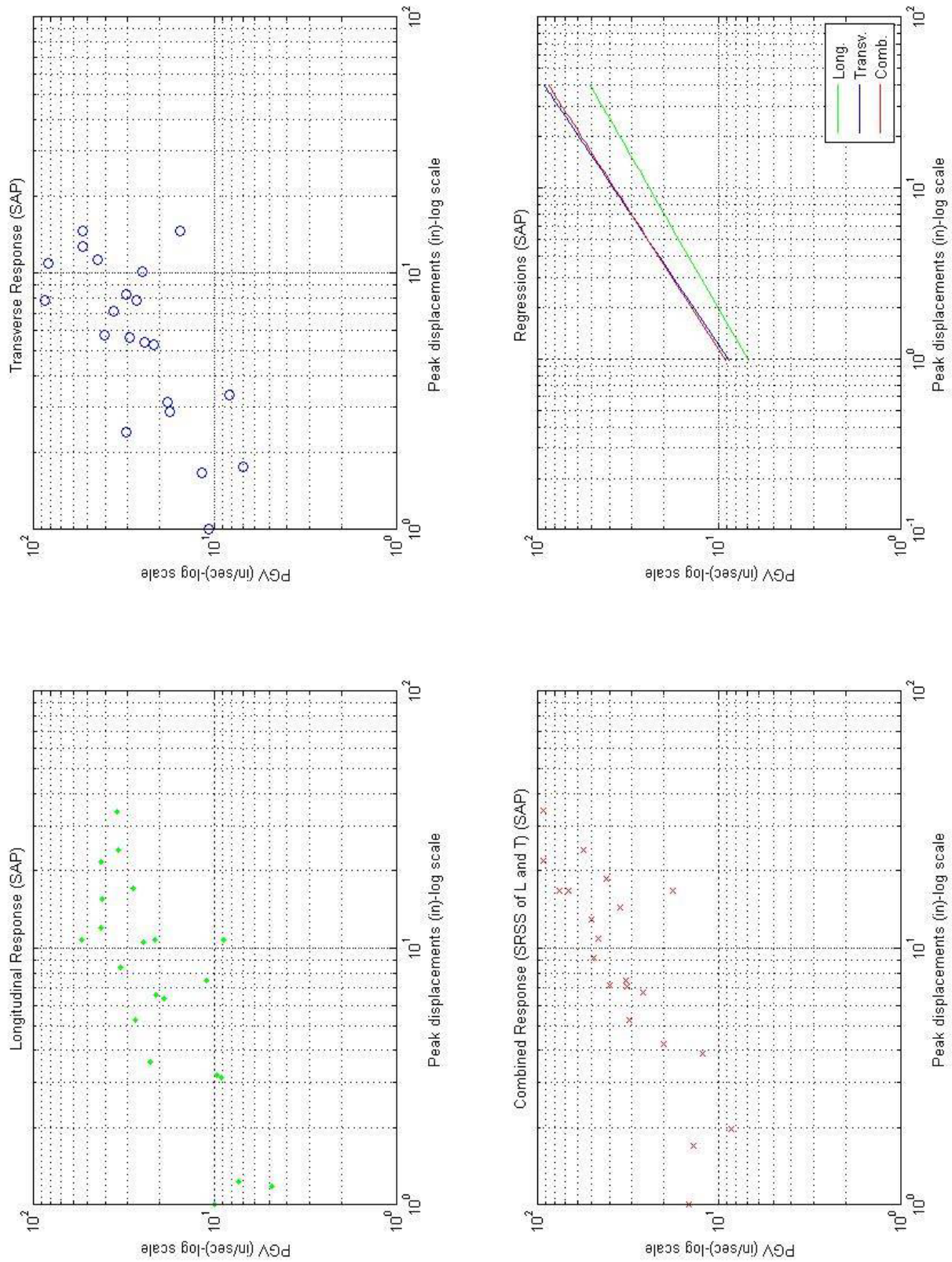


Fig. A.25 SAP2000 fiber model with roller abutment (log scale): I880n ground motion set (Route 14 bridge).

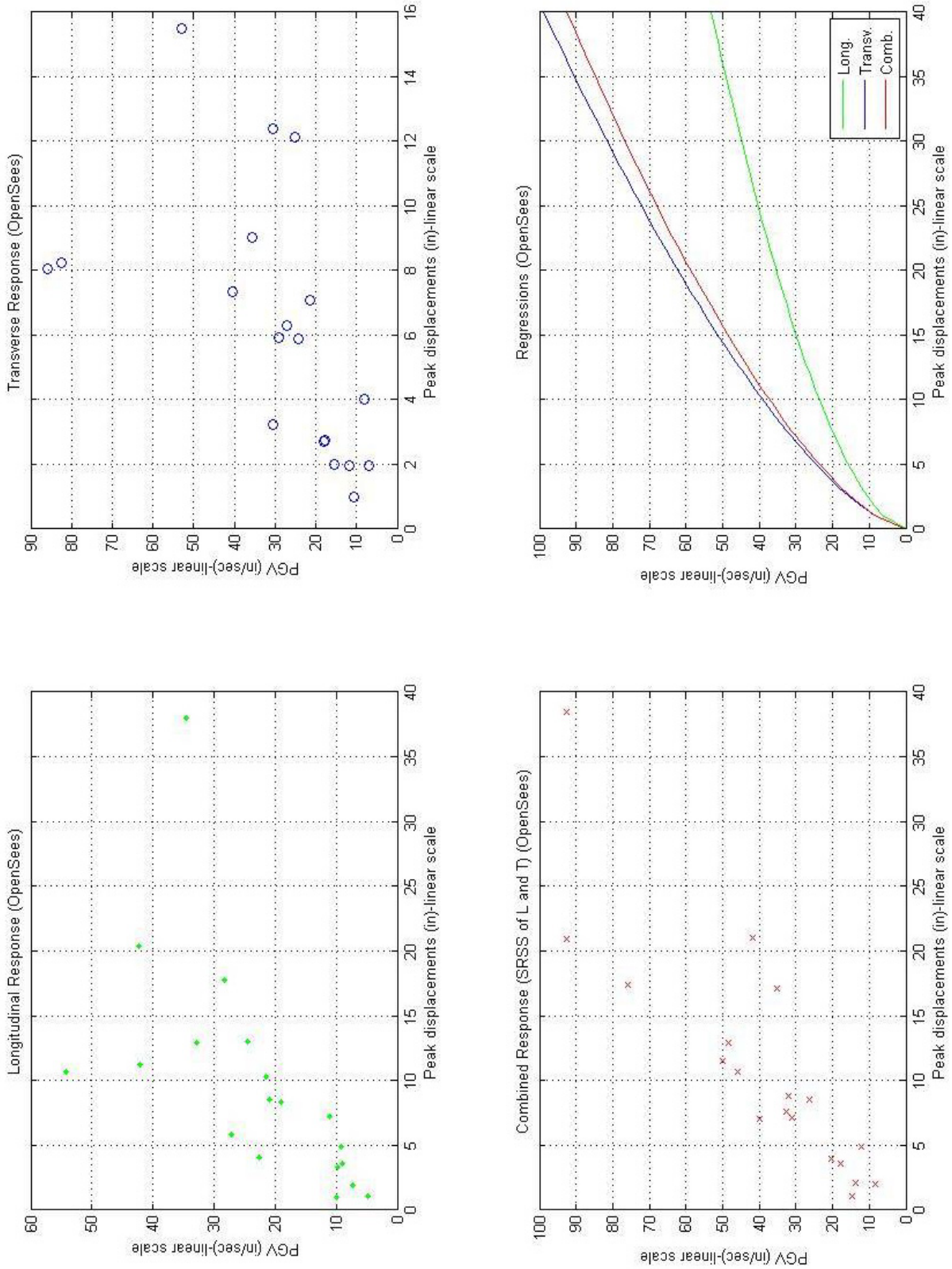


Fig. A.26 OpenSees fiber model with roller abutment (linear scale): I880n ground motion set (Route 14 bridge).

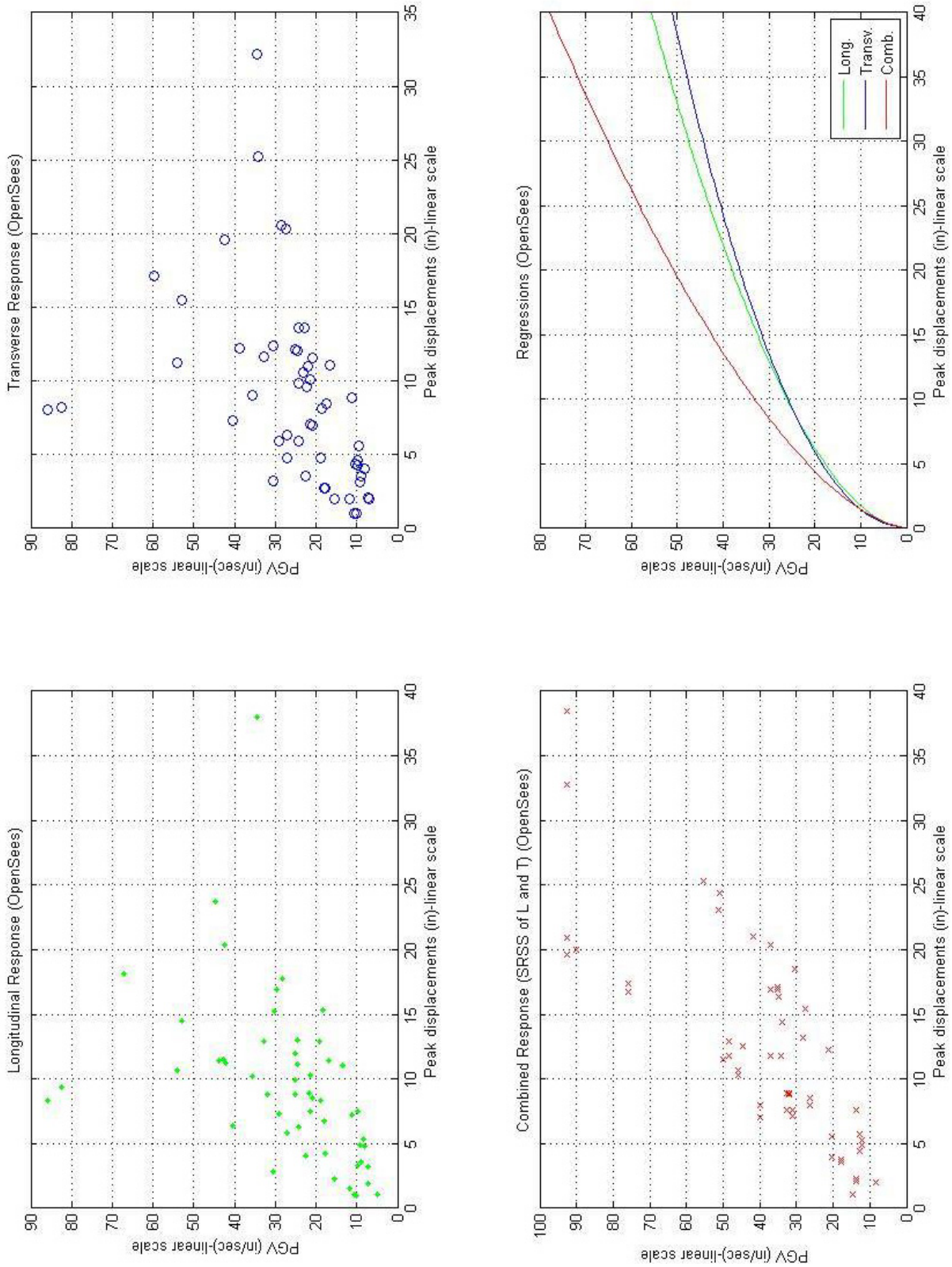


Fig. A.27 OpenSees fiber model with roller abutment (linear scale): 63 ground motions (Route 14 bridge).

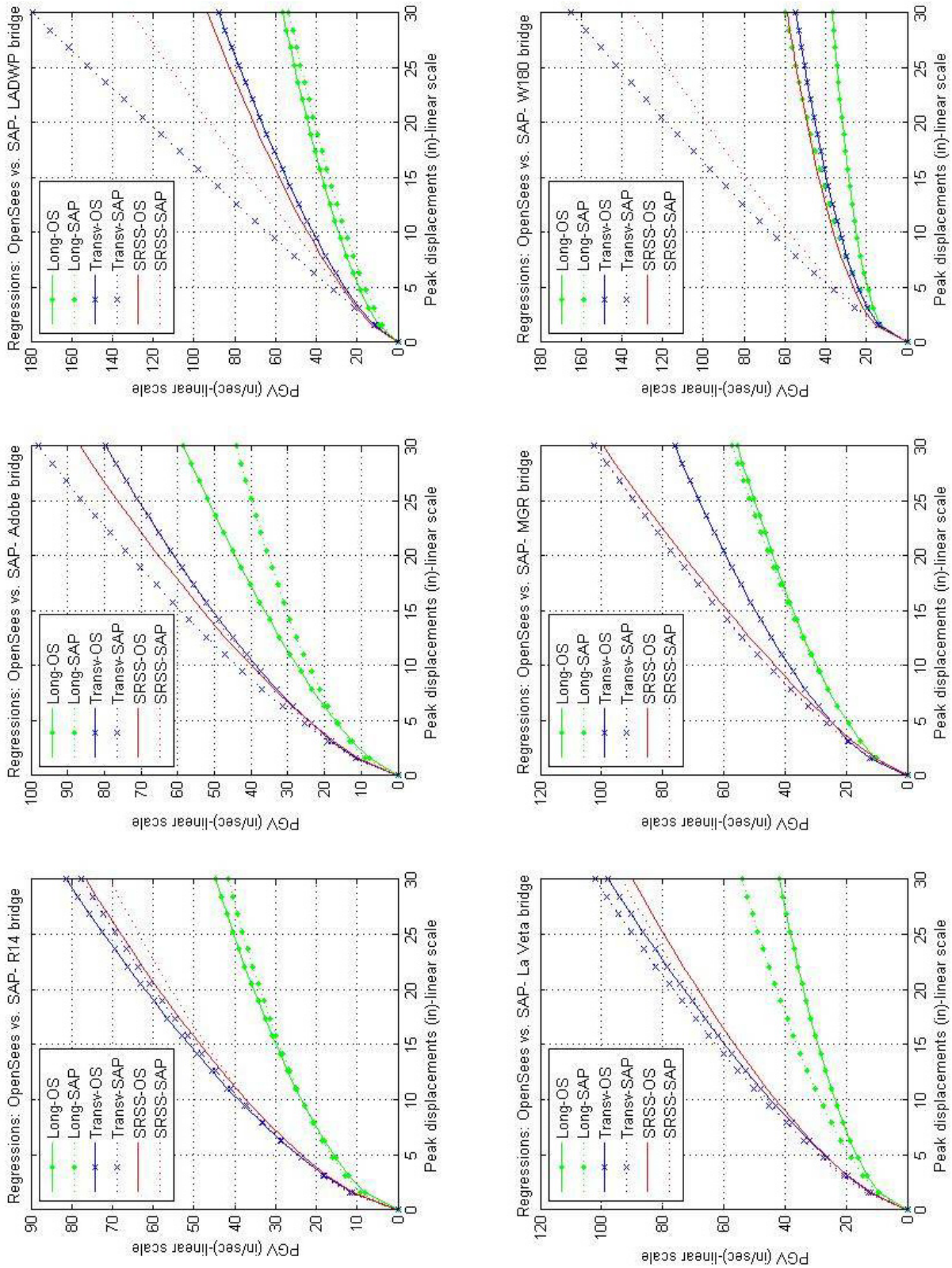


Fig. A.28 Comparison between SAP2000 and OpenSees fiber models: 6 bridges, roller abutment, linear scale, 23 ground motions.

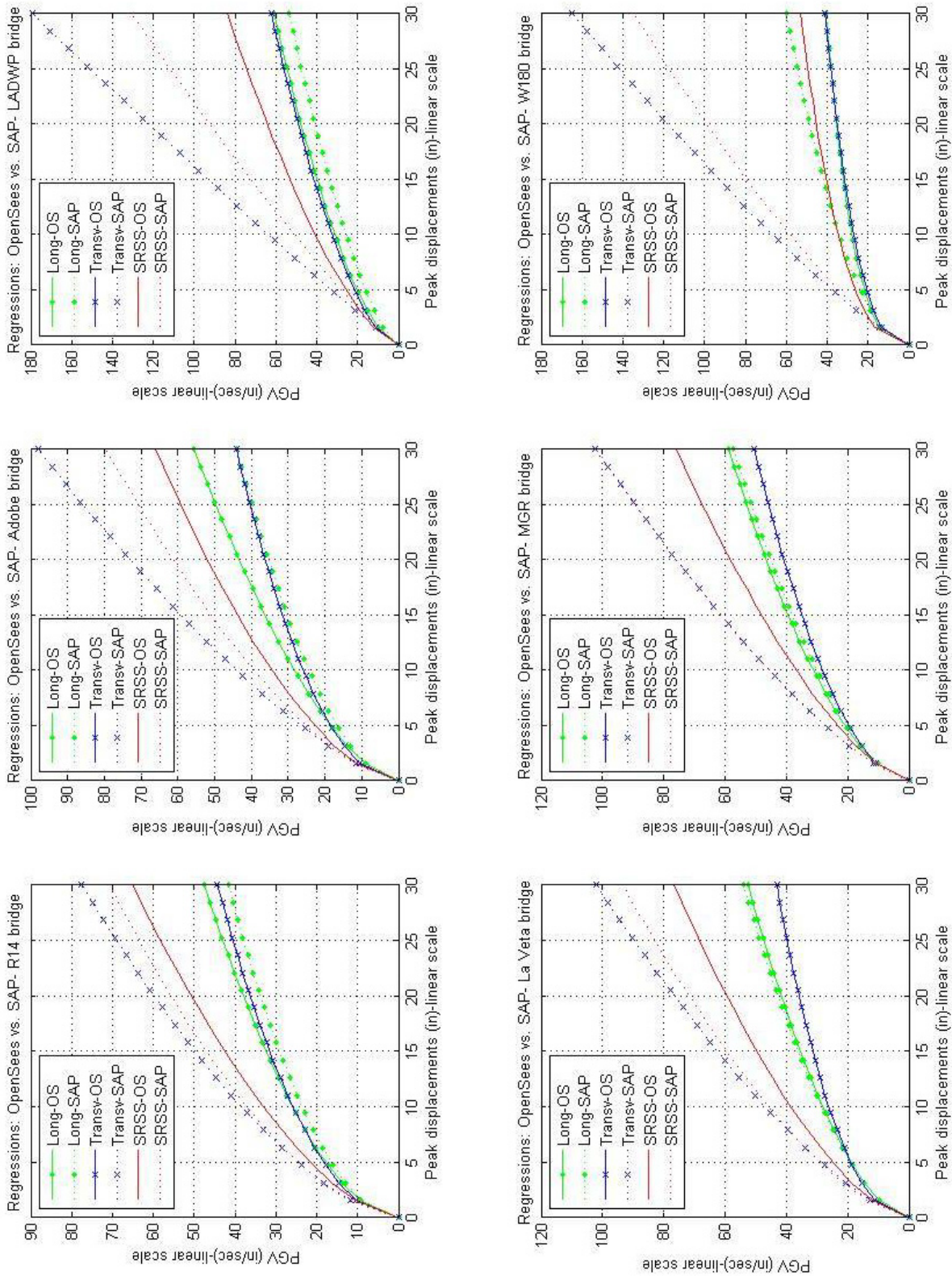


Fig. A.29 Comparison between SAP2000 and OpenSees fiber models: 6 bridges, roller abutment, linear scale, 23 records (SAP2000) vs. 63 records (OpenSees).

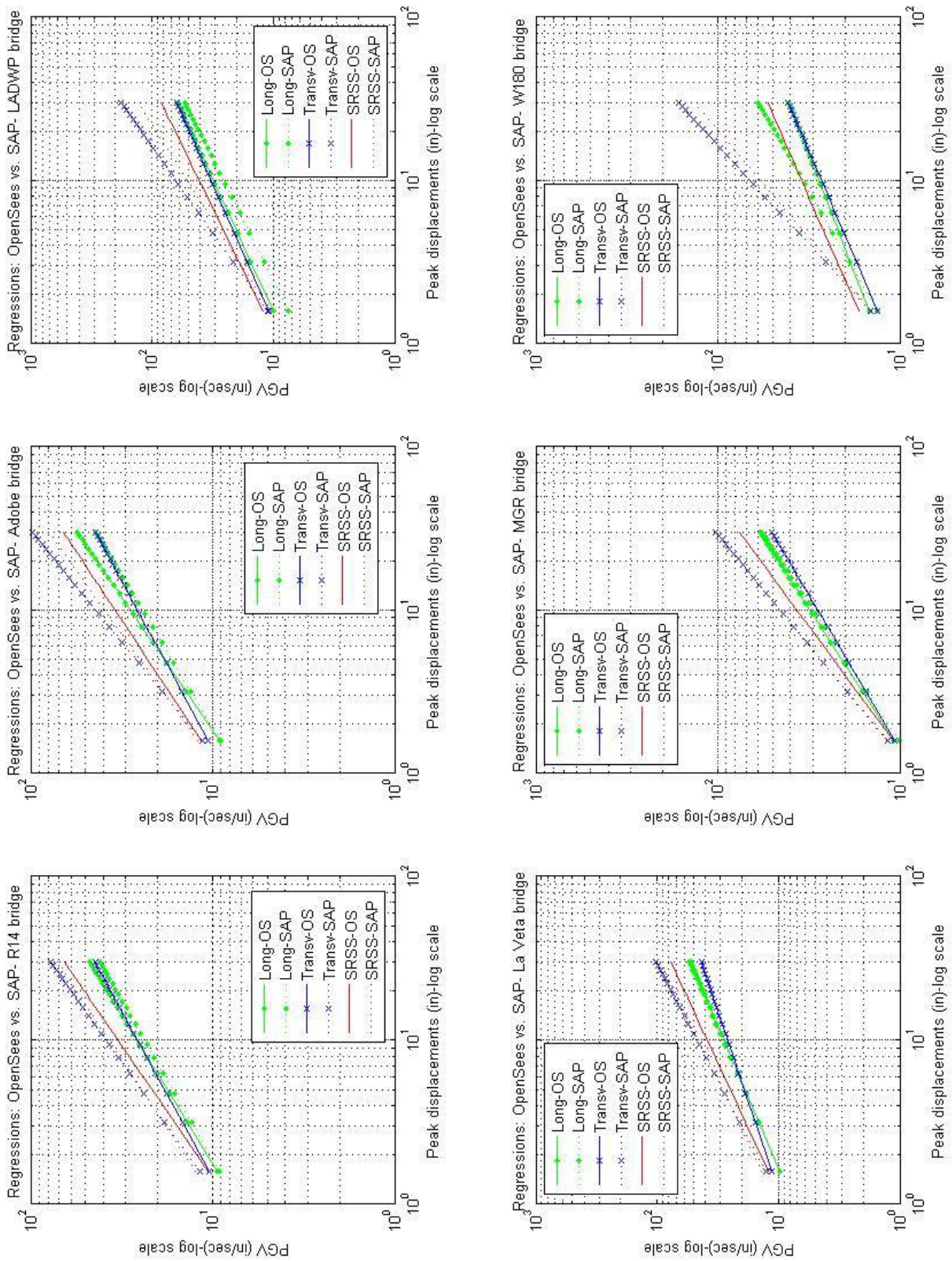


Fig. A.30 Comparison SAP2000 and OpenSees fiber models: 6 bridges, roller abutment, log scale, 23 records (SAP2000) vs. 63 records (OpenSees).

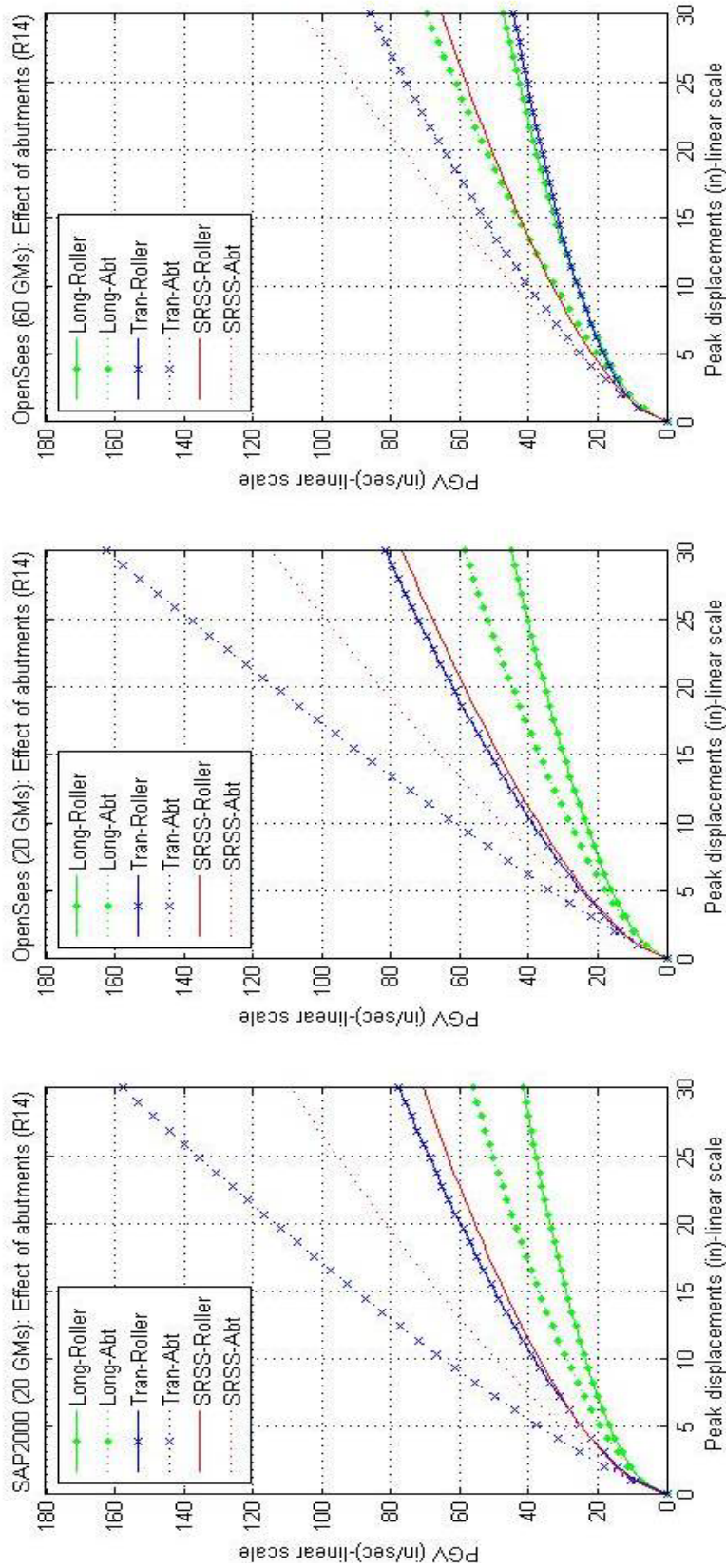


Fig. A.31 Roller vs. simplified abutment models, linear scale. Both OpenSees and SAP2000 models use fiber model for plastic hinge zone (Route 14 bridge).

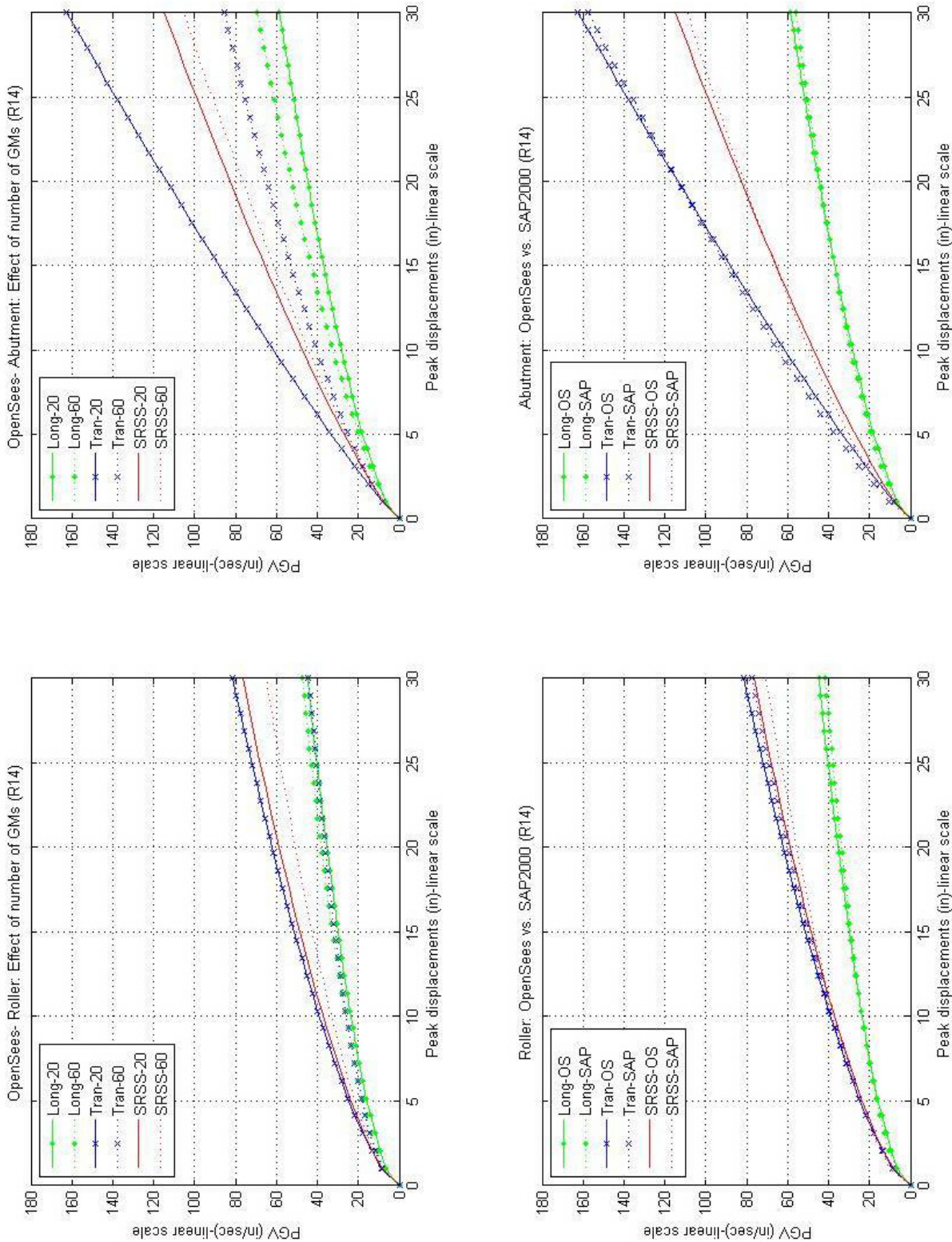


Fig. A.32 Comparison SAP2000 vs. OpenSees, Route 14 bridge: Effect of no. of records (linear scale). Fiber model for column plastic hinge zone is used in both programs.

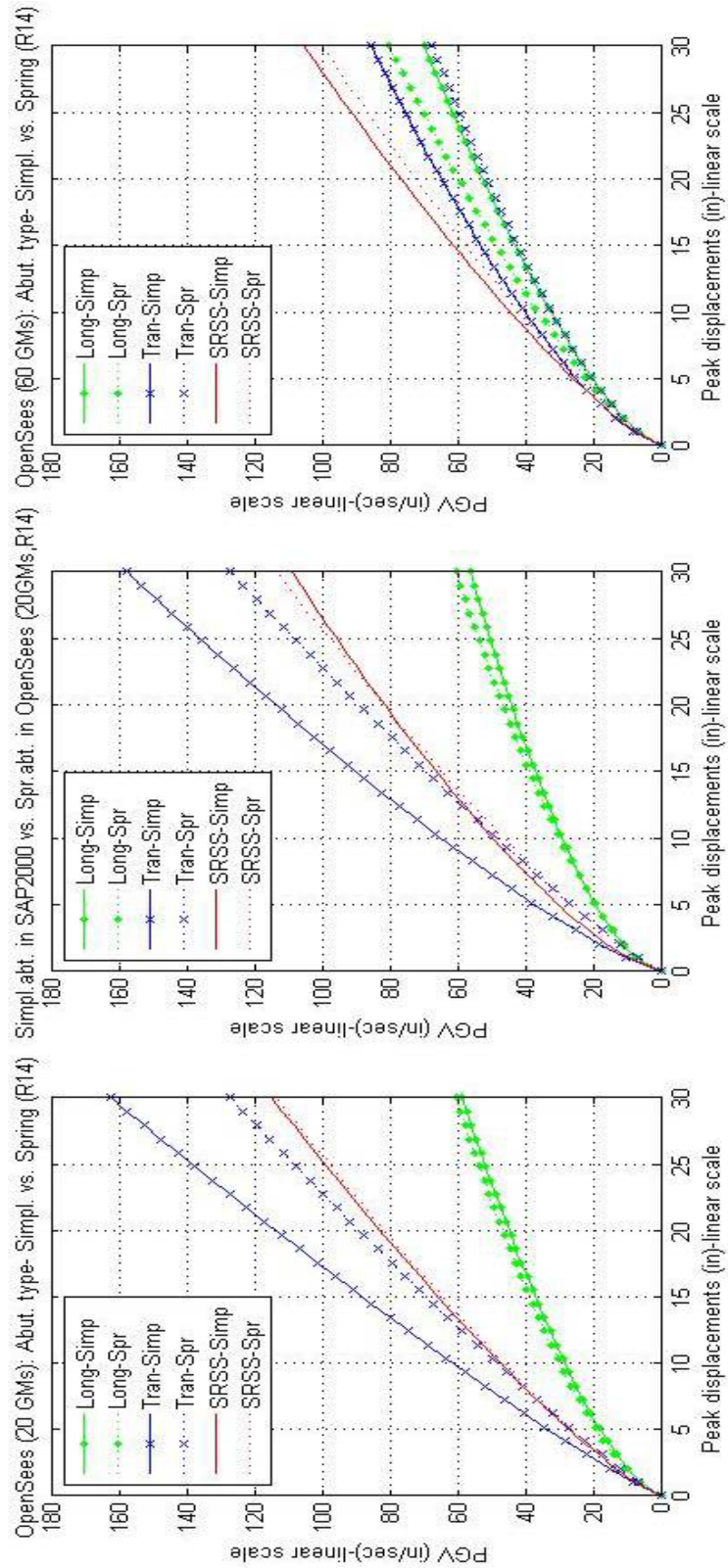


Fig. A.33 OpenSees model: comparison of simplified vs. spring abutment models (linear scale). Fiber model for column plastic hinge zone is used in both programs (Route 14 bridge).

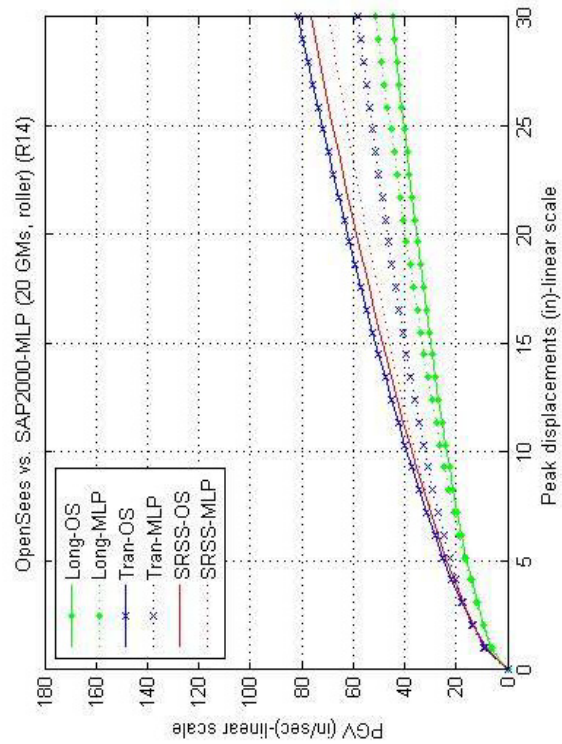
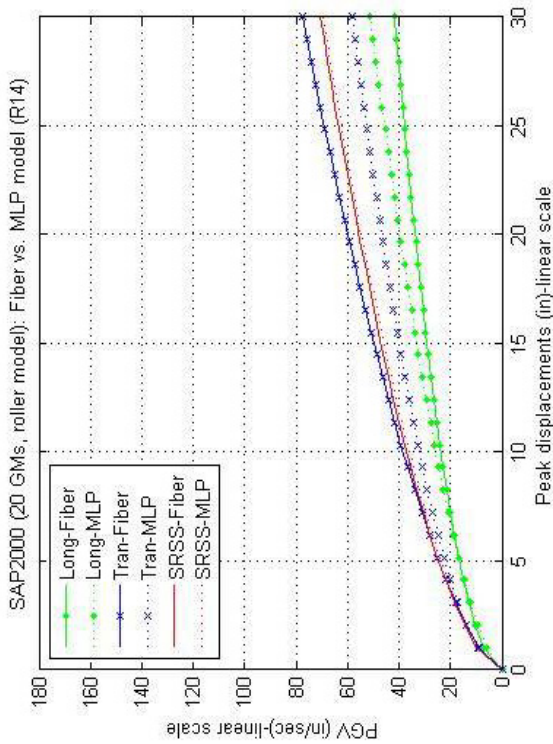
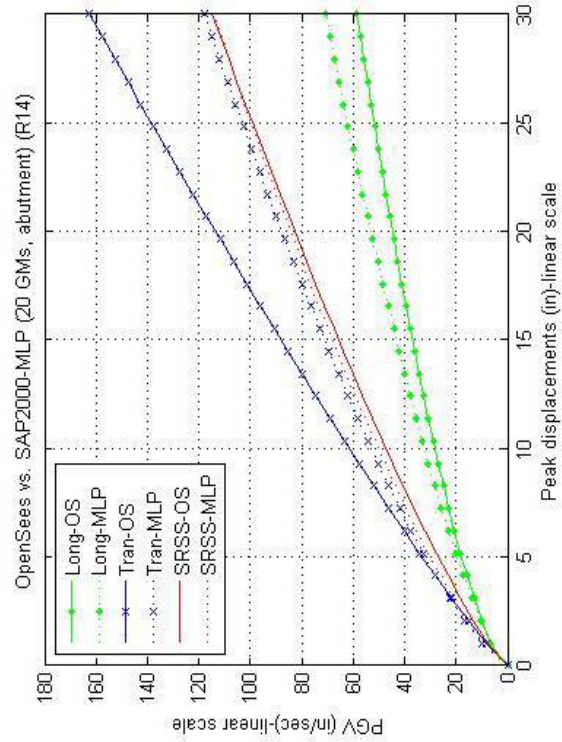
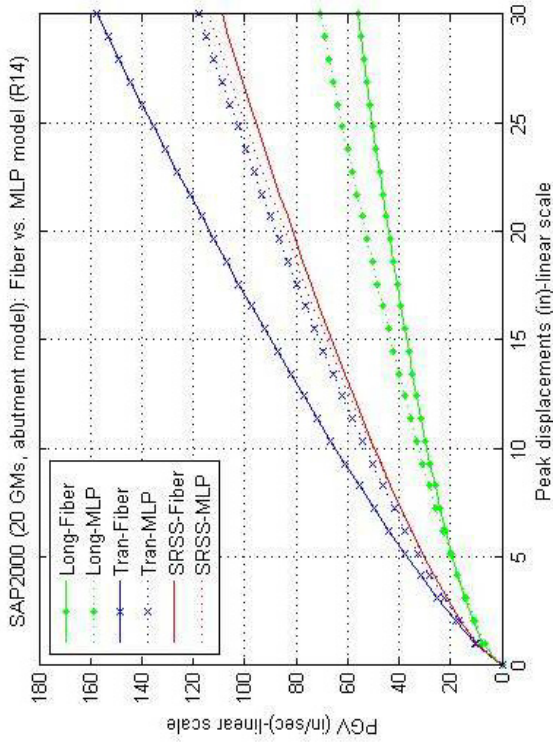


Fig. A.34 Comparison fiber vs. MLP models for plastic hinge zone in SAP2000 (linear scale), R14 bridge.

Nonlinear Time History Analysis: Preliminary Analysis of Phase II

Natural-Log Regression:

Table A.13 Regression coefficients (natural-log fit) for different bridges with roller abutment and fiber models: Peak ground velocity (PGV) vs. peak displacements, Phase II.

Bridge	Program	No. of records	Direction	β_1 - Y-axis intersection	β_2 - Slope
Route 14	SAP2000	23	Long.	1.9724	0.5166
			Transv.	2.1729	0.6405
			SRSS	2.2547	0.5890
	OpenSees	23	Long.	1.8127	0.5851
			Transv.	2.1225	0.6697
			SRSS	2.1022	0.6573
		63	Long.	1.9932	0.5488
			Transv.	2.1167	0.4923
			SRSS	2.0735	0.6183
Adobe	SAP2000	23	Long.	1.9553	0.5369
			Transv.	2.1048	0.7292
			SRSS	2.1918	0.6423
	OpenSees	23	Long.	1.7357	0.6855
			Transv.	2.1356	0.6590
			SRSS	2.0574	0.7072
		63	Long.	1.9283	0.6142
			Transv.	2.1362	0.4852
			SRSS	2.1718	0.5932
LADWP	SAP2000	23	Long.	1.7067	0.6686
			Transv.	1.9770	0.9445
			SRSS	1.9585	0.8568
	OpenSees	23	Long.	1.9707	0.6065
			Transv.	2.1616	0.6803
			SRSS	2.2163	0.6817
		63	Long.	2.0212	0.6146
			Transv.	2.1267	0.5894
			SRSS	2.1891	0.6584
La Veta	SAP2000	23	Long.	2.0079	0.5831
			Transv.	2.2157	0.7084
			SRSS	2.3187	0.6524
	OpenSees	23	Long.	1.9714	0.5179
			Transv.	2.1521	0.7144
			SRSS	2.2144	0.6715
		63	Long.	2.0045	0.5758
			Transv.	2.2104	0.4567
			SRSS	2.2000	0.6290
MGR	SAP2000	23	Long.	2.0423	0.5896
			Transv.	2.1201	0.7371
			SRSS	2.1316	0.7334
	OpenSees	23	Long.	2.0702	0.5719
			Transv.	2.2330	0.6166
			SRSS	2.0097	0.7618
		63	Long.	2.1124	0.5766
			Transv.	2.1213	0.5294
			SRSS	2.0818	0.6613

Table A.13—Continued

Bridge	Program	No. of records	Direction	β_1 - Y-axis intersection	β_2 - Slope
W180	SAP2000	23	Long.	2.3497	0.5120
			Transv.	2.2961	0.8259
			SRSS	2.3082	0.7629
	OpenSees	23	Long.	2.4109	0.3501
			Transv.	2.4368	0.4600
			SRSS	2.5576	0.4471
		63	Long.	2.5312	0.3452
			Transv.	2.4109	0.3828
			SRSS	2.6461	0.3896

Table A.14 Regression coefficients (natural-log fit) for Route 14 bridge: Peak displacements vs. peak ground velocity (PGV).

Program	Plastic hinge model	Abutment type	No. of records	Direction	β_1 - Y-axis intersection	β_2 - Slope
SAP2000	Fiber	Roller	23	Long.	1.9724	0.5166
				Transv.	2.1729	0.6405
				SRSS	2.2547	0.5890
		Simplified		Long.	1.9873	0.6002
				Transv.	2.3062	0.8098
				SRSS	2.2522	0.7169
	MLP	Roller		Long.	1.7986	0.6280
				Transv.	2.2285	0.5392
				SRSS	2.2125	0.5964
		Simplified		Long.	1.8300	0.7150
				Transv.	2.2964	0.7273
				SRSS	2.2002	0.7461
OpenSees	Fiber	Roller	23	Long.	1.8127	0.5851
				Transv.	2.1225	0.6697
				SRSS	2.1022	0.6573
			63	Long.	1.9932	0.5488
				Transv.	2.1167	0.4923
				SRSS	2.0735	0.6183
		Simplified	23	Long.	1.8095	0.6646
				Transv.	2.0794	0.8855
				SRSS	1.9977	0.8073
			63	Long.	1.8686	0.6987
				Transv.	2.0897	0.6943
				SRSS	1.9738	0.7892
		Spring	23	Long.	1.9090	0.6450
				Transv.	1.8500	0.8807
				SRSS	1.9575	0.8155
			63	Long.	1.9104	0.7267
				Transv.	1.9161	0.6745
				SRSS	1.8795	0.8017

Discussion of Results: Nonlinear Time History Analysis

Roller Abutment: (see Section 2.7.3.1)

- The bridge models using the NL-link multi-linear plastic model for the plastic hinge zone failed to converge for the intense ground motions that produced severe nonlinear action. Only the fiber models, which exhibited stable response, were considered in the comparison.
- Ground motion directivity effects included in the selected I880 set (20 records) produce larger displacements in one direction of the bridge due to higher intensity. The response in the longitudinal and transverse directions is therefore very distinct and the regression obtained from these values will depend on the orientation of a bridge.
- Using additional records (60+ records in total) and including near-fault (parallel and normal) directivity effects in each bridge direction, as well as far-fault records, the longitudinal and transverse response is very similar. The regressions relating the peak displacements to the intensity measure will be independent of the orientation of the bridge and will not include directivity effects.
- Using only 20 records, the displacement results in SAP2000 are underestimated in the transverse direction for some bridges ($T_{SAP} < T_{OS}$) and slightly overestimated in the longitudinal directions for other bridges ($L_{SAP} > L_{OS}$), with respect to the OpenSees results. There is no clear trend for so few records.
- Using 60 records for OpenSees, the displacement results in SAP2000 are clearly underestimated due to directivity effects in the transverse direction ($T_{SAP} \ll T_{OS}$) and similar in the longitudinal direction ($L_{SAP} > L_{OS}$), with respect to OpenSees.
- The parameters of the natural-logarithmic regression that need to be estimated are the slope (β_1), the intersection with Y-axis (β_2) and their standard deviation (σ_1, σ_2).
- The reliable estimation of the bias factors between SAP2000 and OpenSees of these regression parameters for the roller abutment models cannot be carried out using so few ground motions. The use of 60-100 ground motions is recommended as a minimum to capture trends over a range of intensities, including both near-fault and far-fault records of different hazard levels.
- The modeling of more realistic abutment behavior with lateral and longitudinal restraints at the superstructure ends has a significant effect on the bridge's response. The estimation

of bias factors (SAP vs. OpenSees) for unrestrained (laterally) roller abutment might not be necessary if the response of the bridge is controlled by the abutment nonlinear behavior.

Simplified and Spring Abutment Model: (see Sections 2.7.3.2 and 2.7.3.3)

- The abutment model with defined nonlinear behavior and lateral restraints reduces the displacements in both the longitudinal and transverse directions of the bridge, as expected, for both SAP2000 and OpenSees, independently of the number of ground motions used in the analysis.
- The response in the transverse and longitudinal directions of the bridge is different using the simplified abutment model, which defines distinct response behavior for each. The strong directivity effects included in some ground motions records also affects these differences.
- The bridge models with NL-Link element (MLP) representing column plastic hinge behavior failed to converge for intense ground motions with laterally unrestrained boundary conditions for the superstructure ends. However, the R14 bridge model presented stable results using the MLP and simplified abutment model. For this particular case, for both the restrained (simplified) and unrestrained (roller) models, the longitudinal displacements were underestimated and the transverse overestimated, with respect to the SAP2000 and OpenSees fiber models.
- Despite the uncoupled behavior of the NL-link element, the displacements obtained from the SRSS combination of longitudinal and transverse directions does not present a plus or minus bias, and is similar to both fiber models in SAP2000 and OpenSees.
- The remaining bridge models with MLP model and simplified abutment must be examined to determine their stability during high intensity ground motions and adequacy for nonlinear time history analysis.
- For the R14 bridge with a simplified abutment model, the nonlinear time history results using SAP2000 and OpenSees programs match well. However, for this particular bridge, the nonlinear time history results were matching using the unrestrained (roller) model. The abutment model behavior and overall bridge response had been previously compared through pushover curves.

- A similar analysis must be carried out for bridges displaying significant differences for the unrestrained (roller) model. The NL THA results using SAP2000 and OpenSees need to be compared for the remaining bridges in the study with the addition of the abutment model.
- The response of the bridge using the simplified and spring abutment model in OpenSees is significantly different, for both the longitudinal and transverse directions. The pushover curves of the two abutment models displayed distinct initial stiffness, ultimate capacity, and degradation of strength behavior, and these differences are strongly reflected in the NL THA results.
- The proper selection and modeling of realistic abutment conditions must be carried out, since evidently the abutment response dominates the bridge response for certain types of bridges.
- A larger catalog of motions must be used to assess the bias between SAP2000 and OpenSees results, in terms of an intensity measure such as the PGV (peak ground velocity). To increase the confidence level in the estimation of the corresponding parameters, different bridge geometries and hazard levels must be used in the analysis.
- The emphasis of this study has been on the column nonlinear behavior; however, other important nonlinearities must still be examined, including expansion joints, soil-structure interaction at the column base, and nonlinear superstructure effects, among others. These additional considerations could have a significant effect on the dynamic overall response of bridge structures.

Nonlinear Time History Analysis Results: Preliminary Analysis of Phase II

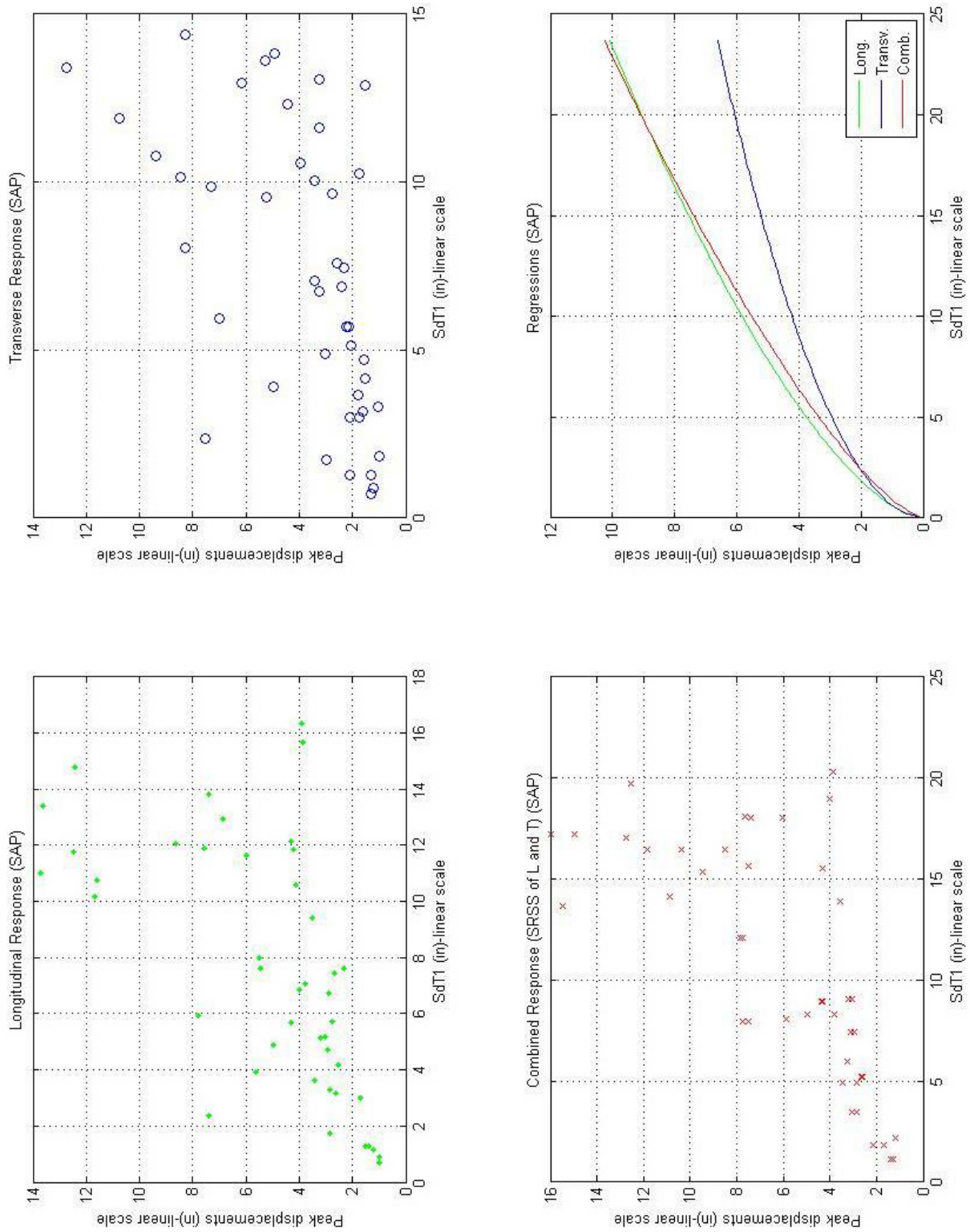


Fig. A.35 SAP2000 fiber model with simplified abutment model (linear scale): 63 ground motions (Route 14 bridge).

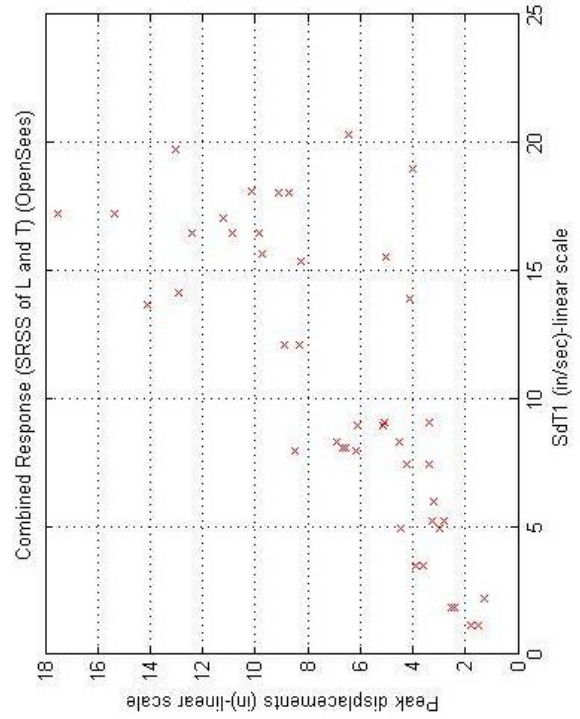
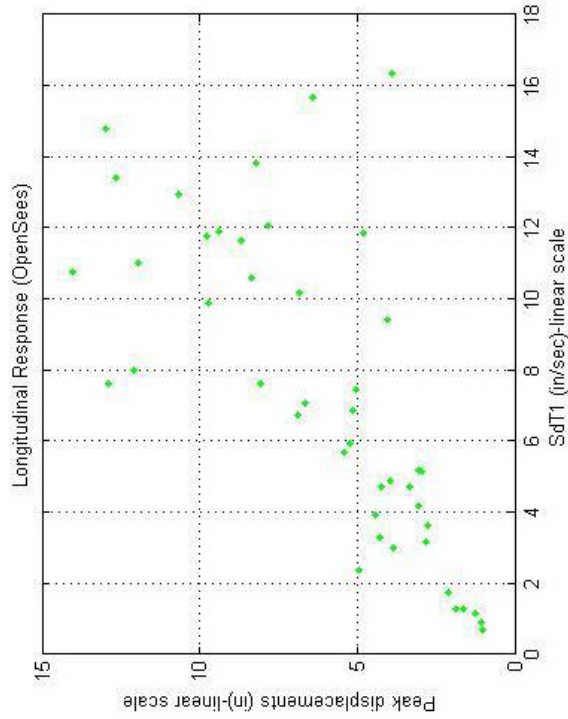
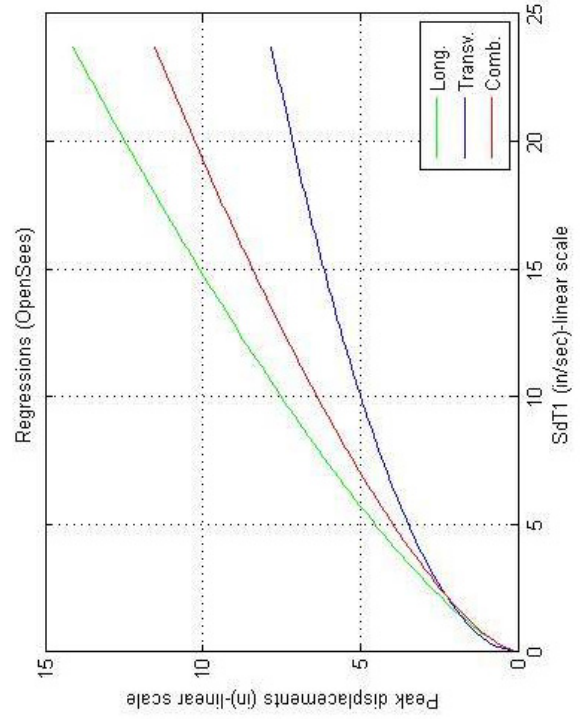
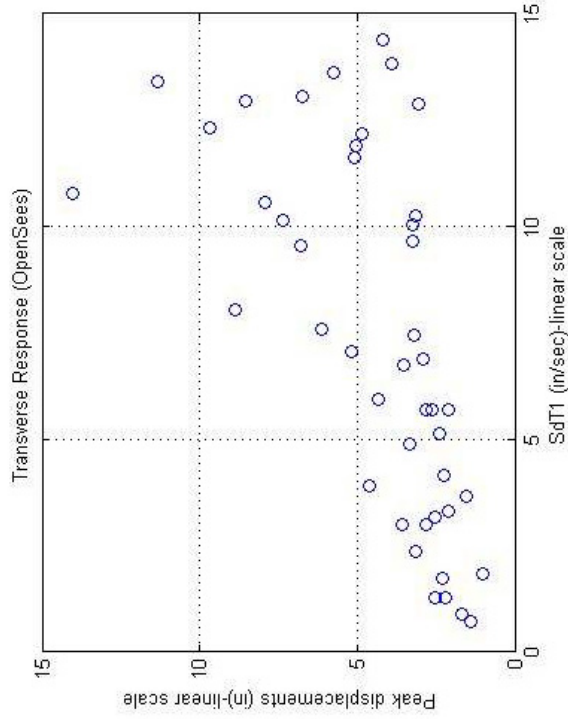


Fig. A.36 SAP2000 fiber model with simplified abutment model (logarithmic scale): 63 ground motions (Route 14 bridge).

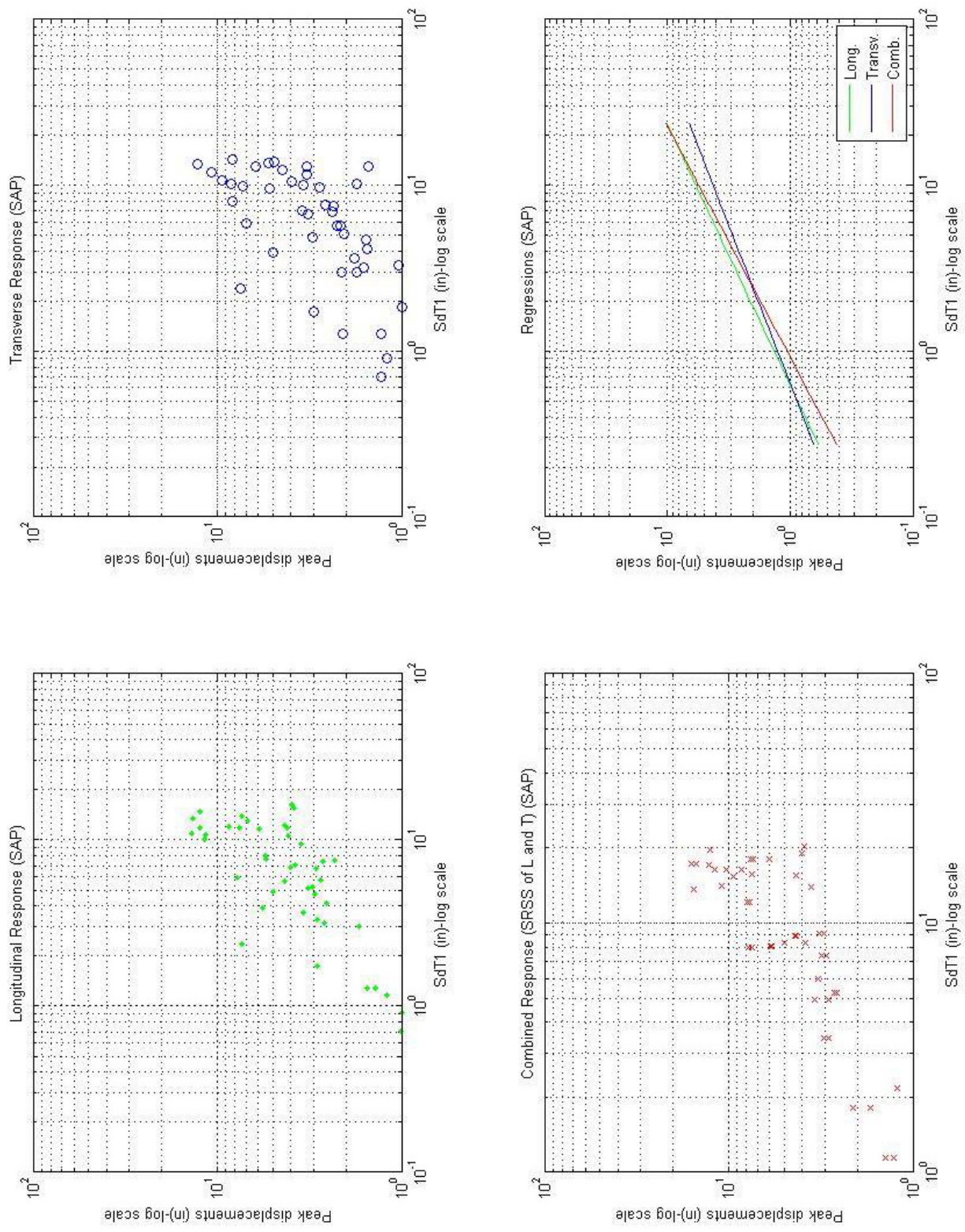


Fig. A.37 OpenSees fiber model with simplified abutment model (linear scale): 63 ground motions (Route 14 bridge).

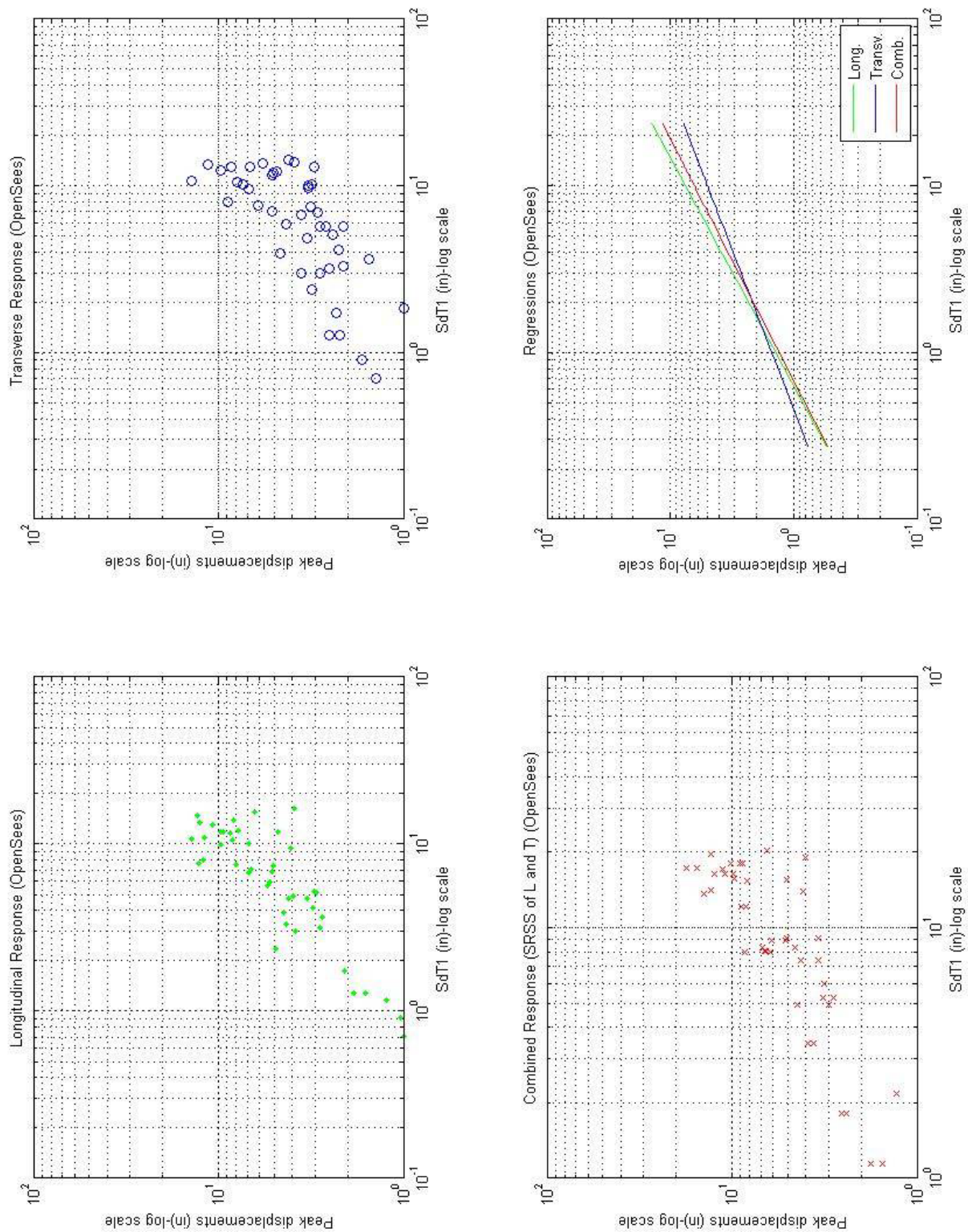


Fig. A.38 OpenSees fiber model with simplified abutment model (logarithmic scale): 63 ground motions (Route 14 bridge).

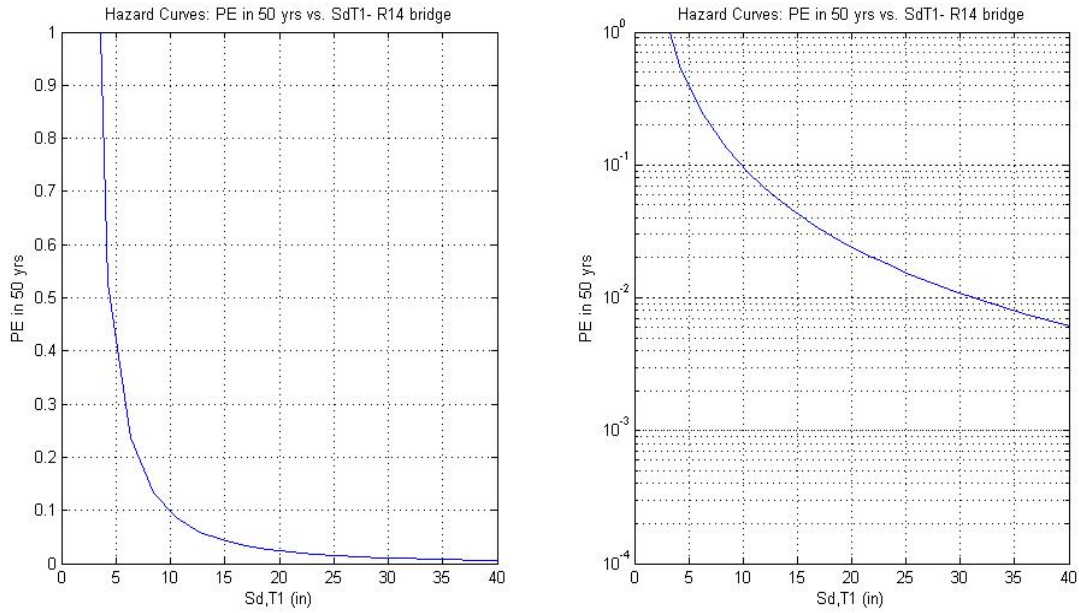


Fig. A.39 Hazard curve for Route 14 bridge: Probability of exceedance in 50 yrs vs. spectral displacements at first mode period.

The hazard curves were obtained through an exponential fit using the data obtained from USGS.

Table A.15 USGS data for R14 bridge.

Hazard: PE in 50 yrs	S _{d,T1} (in)
0.50	4.0893
0.10	11.4471
0.02	19.7349

Hazard curves: $H(s_d) = P[S_d \geq s_d] = k_o s_d^{-k}$. The results of the power-law fit are: $PE = k_o \cdot (S_{d,T1})^{-k}$, where $k_o=9.11$ and $b=1.98$.

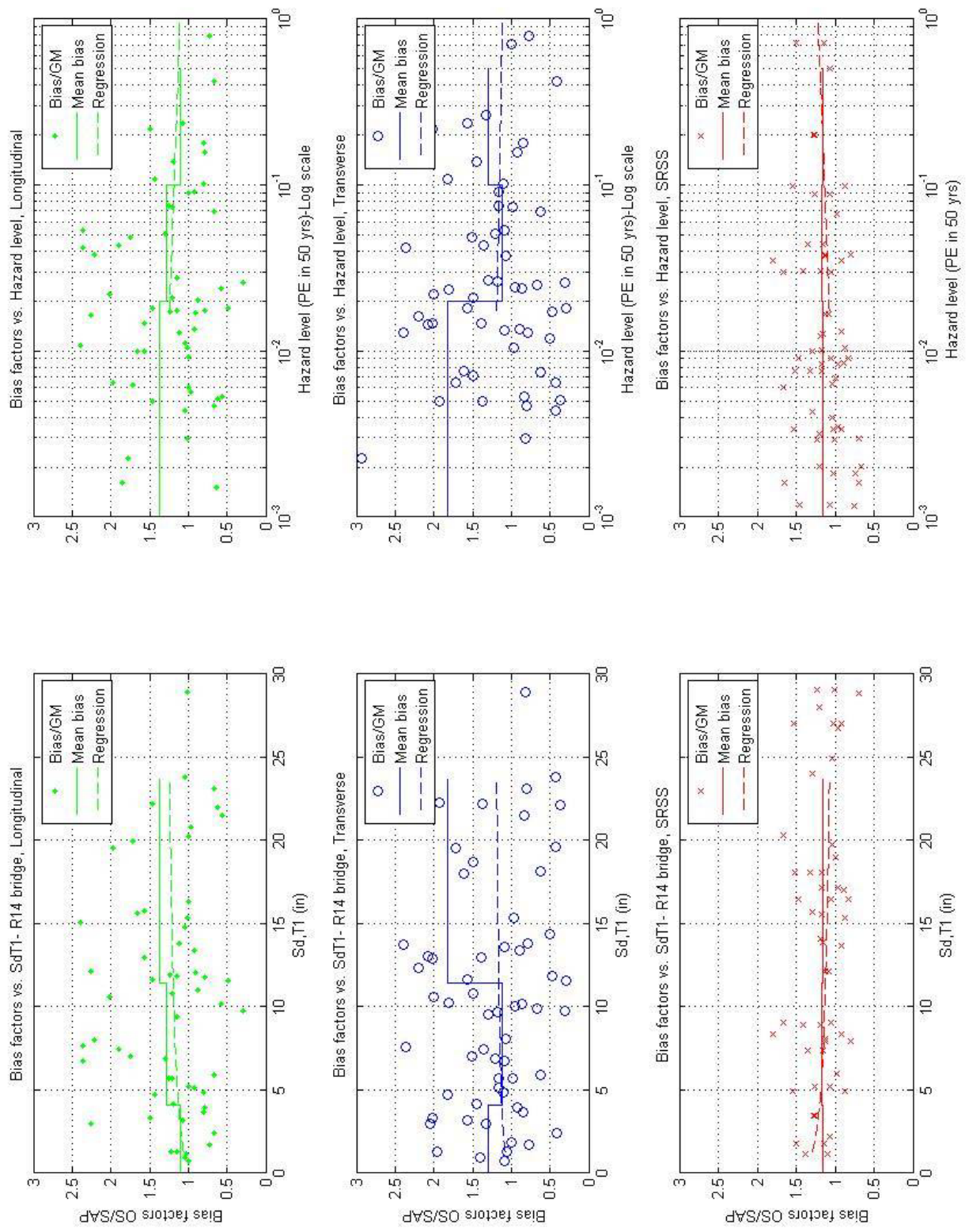


Fig. A.40 Ratio between OpenSees and SAP2000 nonlinear time history analysis results for R14 bridge, plotted for each direction of bridge.

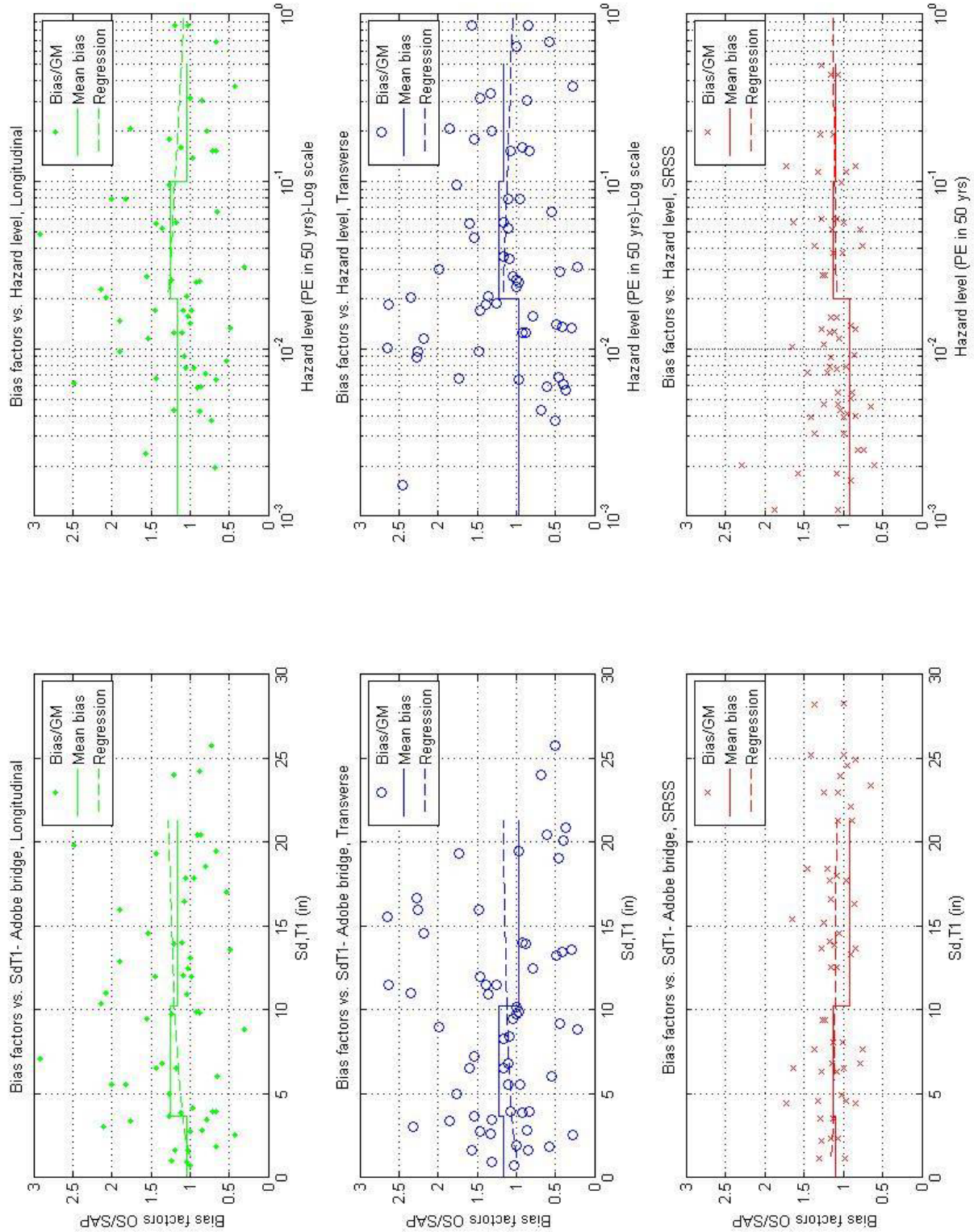


Fig. A.41 Ratio between OpenSees and SAP2000 nonlinear time history analysis results for Adobe Bridge, plotted for each direction of bridge.

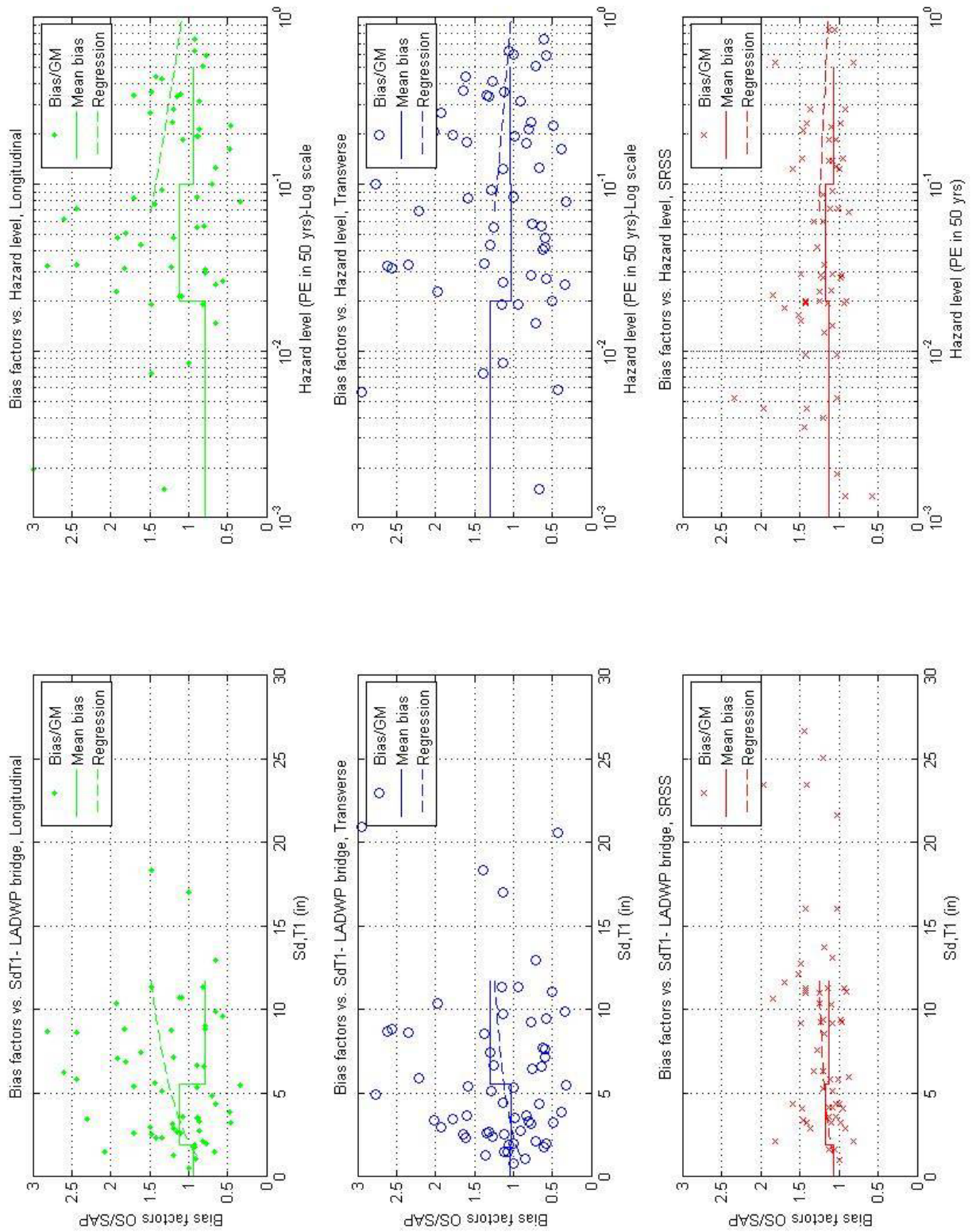


Fig. A.42 Ratio between OpenSees and SAP2000 nonlinear time history analysis results for LADWP bridge, plotted for each direction of bridge.

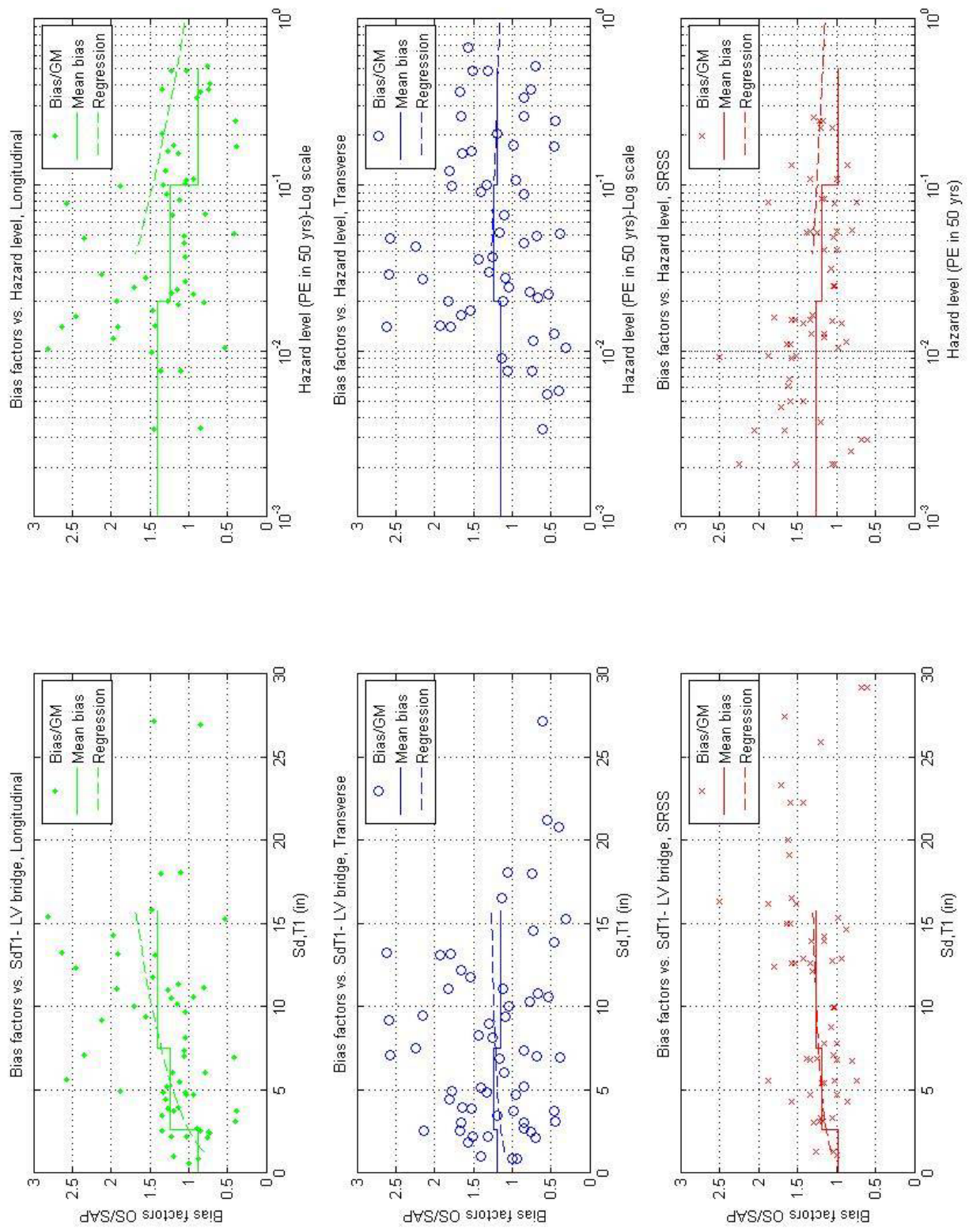


Fig. A.43 Ratio between OpenSees and SAP2000 nonlinear time history analysis results for La Veta bridge, plotted for each direction of bridge.

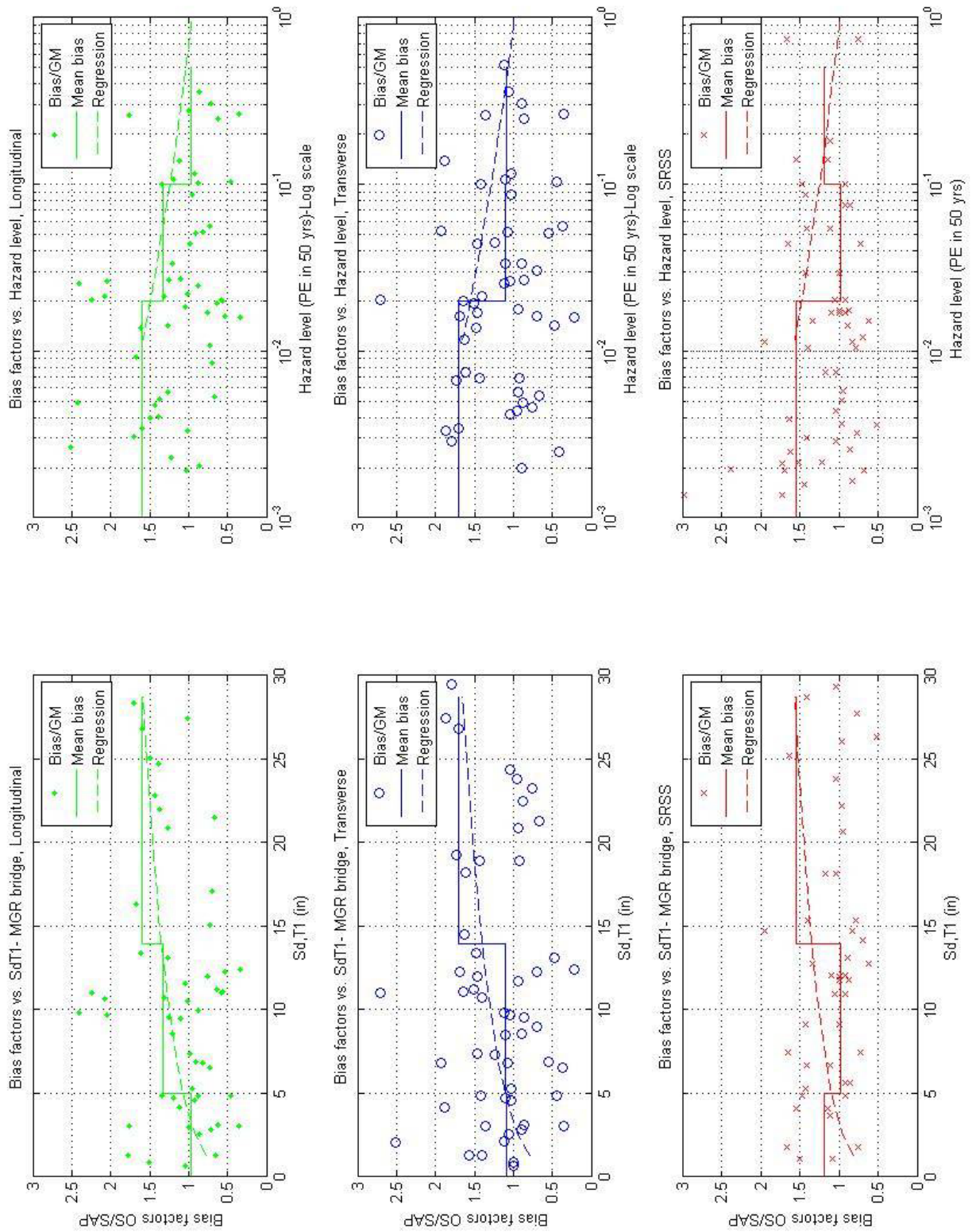


Fig. A.44 Ratio between OpenSees and SAP2000 nonlinear time history analysis results for MGR bridge, plotted for each direction of bridge.

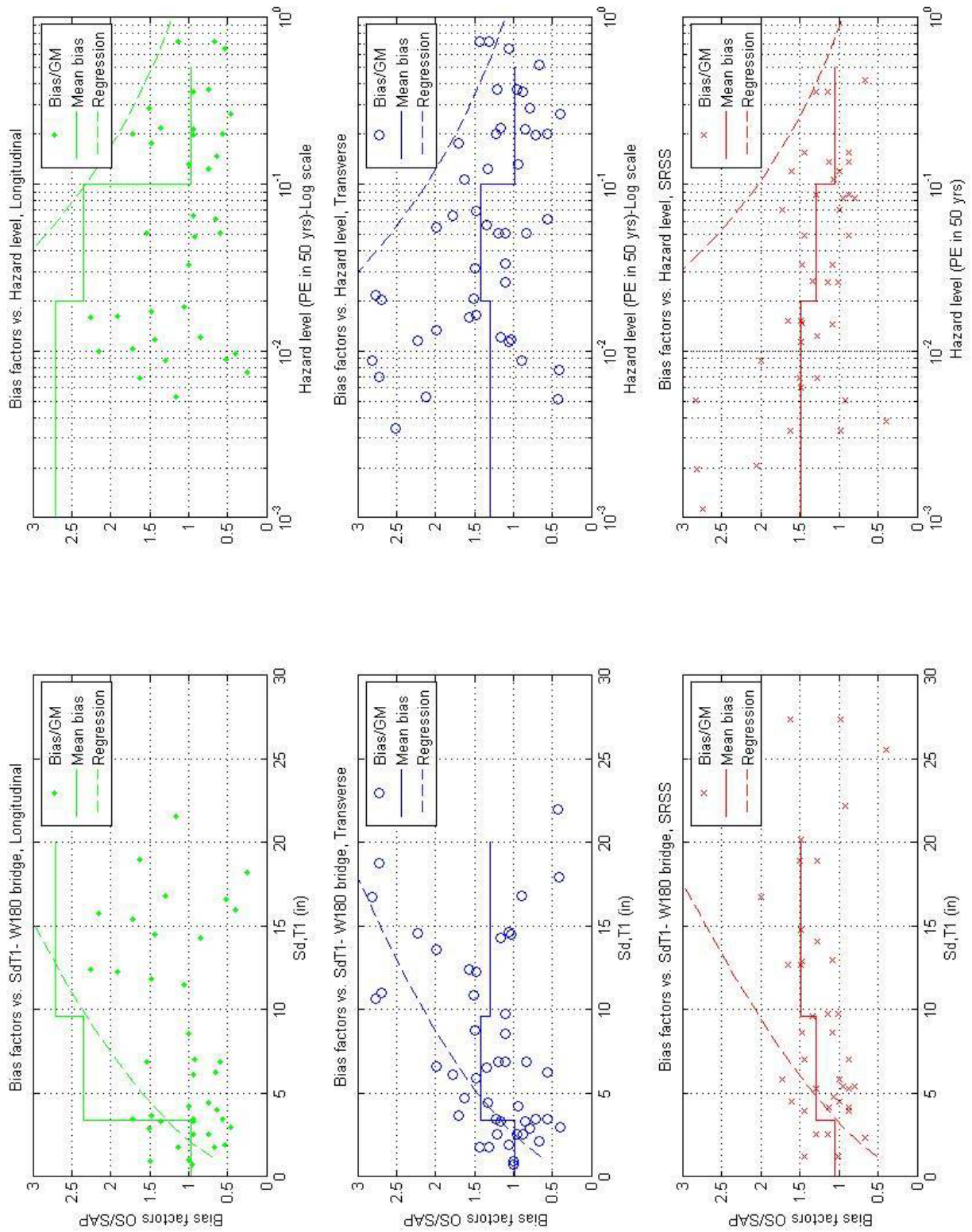


Fig. A.45 Ratio between OpenSees and SAP2000 nonlinear time history analysis results for W180 bridge, plotted for each direction of bridge.

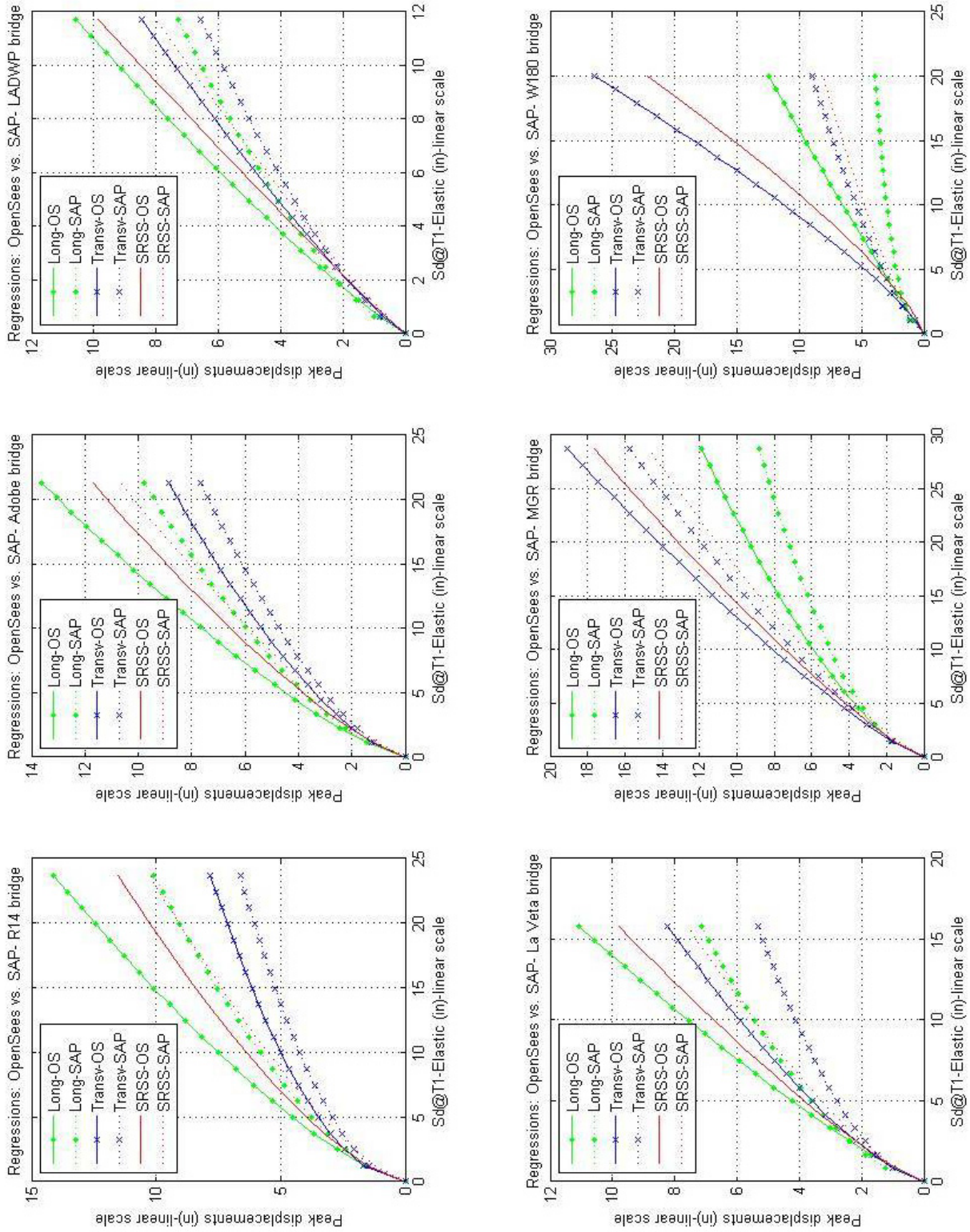


Fig. A.46 Comparison between SAP2000 and OpenSees fiber models: 6 bridges, simplified abutment model, linear scale, 63 records (linear scale).

Nonlinear Time History Analysis Results: Phase III

Natural-Log Regression

Table A.16 Regression coefficients (Natural-log fit) for different bridges with abutment type according to Table A.6 and fiber models: Spectral displacements ($s_{d,T1}$) vs. peak displacements, Phase III (63 ground motions).

Bridge	Program	Direction	β_1 - Y-axis intersection	β_2 - Slope
Route 14	SAP2000	Long.	0.3843	1.0397
		Transv.	0.9929	0.7557
		SRSS	0.5722	1.0243
	OpenSees	Long.	0.0774	1.0846
		Transv.	0.3414	1.1267
		SRSS	0.2719	1.1140
Adobe	SAP2000	Long.	0.2543	1.0807
		Transv.	0.9147	0.7532
		SRSS	0.4538	1.0485
	OpenSees	Long.	0.0733	1.0836
		Transv.	0.4971	0.9785
		SRSS	0.3202	1.0678
LADWP	SAP2000	Long.	0.1688	0.9769
		Transv.	0.4679	0.8279
		SRSS	0.1949	1.0891
	OpenSees	Long.	-0.1537	1.1199
		Transv.	0.2683	0.9161
		SRSS	0.0502	1.0850
La Veta	SAP2000	Long.	0.1799	1.1281
		Transv.	0.7785	0.8118
		SRSS	0.3714	1.1130
	OpenSees	Long.	0.1305	1.0367
		Transv.	0.4356	0.9295
		SRSS	0.3192	1.0233
MGR	SAP2000	Long.	0.7848	0.8969
		Transv.	0.3474	0.9676
		SRSS	0.3797	1.0591
	OpenSees	Long.	0.6153	0.9394
		Transv.	-0.0714	1.1739
		SRSS	-0.0031	1.2120
W180	SAP2000	Long.	1.1653	0.7301
		Transv.	0.4518	1.0030
		SRSS	0.5444	1.1015
	OpenSees	Long.	1.2341	0.5068
		Transv.	0.2781	1.0110
		SRSS	0.5405	0.9996

Bias Factors: Phase III

Method 1: Natural Log Regression

Table A.17 Bias factors computed for each bridge for different hazard levels, according to regression results.

Classification	Bridge	Direction	Hazard level		
			Low (50% in 50yr PE)	Moderate (10% in 50yr PE)	High (2% in 50yr PE)
Short (Simpl. Abtm.)	Route 14	Long.	1.18	1.30	1.37
		Transv.	1.18	1.18	1.18
		SRSS	1.19	1.15	1.13
		Mean	1.18	1.21	1.23
	Adobe	Long.	1.14	1.28	1.36
		Transv.	1.12	1.14	1.16
		SRSS	1.14	1.11	1.10
		Mean	1.13	1.18	1.21
	LADWP	Long.	1.03	1.26	1.40
		Transv.	1.00	1.16	1.26
		SRSS	1.10	1.18	1.22
		Mean	1.05	1.20	1.29
	La Veta	Long.	1.00	1.30	1.49
		Transv.	1.17	1.38	1.50
		SRSS	1.11	1.21	1.27
		Mean	1.09	1.30	1.42
Average- Short			1.11	1.22	1.29
Long (Roller Abtm.)	MGR	Long.	1.09	1.23	1.32
		Transv.	1.11	1.17	1.20
		SRSS	1.14	1.18	1.19
		Mean	1.12	1.19	1.24
	W180-N168	Long.	1.25	2.15	2.87
		Transv.	1.18	2.02	2.69
		SRSS	1.05	1.85	2.48
		Mean	1.16	2.01	2.68
Average- Long			1.14	1.60	1.96

Method 2: Pair-wise comparison and averaging

Table A.18 Bias factors computed for each bridge by pair-wise comparison for different hazard levels.

Classification	Bridge	Direction	Hazard level		
			Low (50% in 50yr PE)	Moderate (10% in 50yr PE)	High (2% in 50yr PE)
Short (Simpl. Abtm.)	Route 14	Long.	1.10	1.28	1.37
		Transv.	1.29	1.13	1.82
		SRSS	1.15	1.18	1.15
		Mean	1.18	1.20	1.45
		St.Dev.	0.36	0.57	0.51
	Adobe	Long.	1.04	1.26	1.16
		Transv.	1.17	1.23	0.96
		SRSS	1.09	1.13	0.92
		Mean	1.10	1.20	1.02
		St. Dev.	0.37	0.61	0.45
	LADWP	Long.	0.94	1.12	0.79
		Transv.	1.04	1.02	1.29
		SRSS	1.06	1.17	1.13
		Mean	1.01	1.10	1.07
		St. Dev.	0.25	0.42	0.52
	La Veta	Long.	0.88	1.23	1.40
		Transv.	1.19	1.24	1.14
		SRSS	0.98	1.19	1.26
		Mean	1.02	1.22	1.27
St. Dev.		0.35	0.44	0.51	
Average- Short			1.08	1.18	1.20
Long (Roller Abtm.)	MGR	Long.	0.97	1.33	1.60
		Transv.	1.09	1.10	1.71
		SRSS	1.19	0.98	1.55
		Mean	1.08	1.14	1.62
		St. Dev.	0.41	0.53	0.30
	W180-N168	Long.	0.97	2.34	2.71
		Transv.	0.98	1.41	1.30
		SRSS	1.06	1.29	1.49
		Mean	1.00	1.68	1.83
		St. Dev.	0.33	0.75	0.98
Average- Long			1.04	1.41	1.73

Method 3: Pair-wise comparison and natural log regression for bias

Table A.19 Regression coefficients (natural-log fit) relating bias factors between OpenSees and SAP2000 NL THA displacement results to intensity measure (spectral displacements $S_{d,T1}$).

Bridge	Direction	$\alpha_1 = (\beta_{1,OS} - \beta_{1,SAP})$	$\alpha_2 = (\beta_{2,OS} - \beta_{2,SAP})$
Route 14	Long.	0.0488	0.0531
	Transv.	0.0681	0.0331
	SRSS	0.2716	-0.0635
Adobe	Long.	-0.0200	0.0863
	Transv.	-0.0176	0.0562
	SRSS	0.1515	-0.0225
LADWP	Long.	-0.1722	0.2306
	Transv.	-0.1224	0.1367
	SRSS	0.0462	0.0729
La Veta	Long.	-0.2816	0.2902
	Transv.	0.0850	0.0549
	SRSS	0.0481	0.0785
MGR	Long.	-0.2952	0.2249
	Transv.	-0.2737	0.2308
	SRSS	-0.2466	0.2059
W180	Long.	-0.4408	0.5642
	Transv.	-0.5341	0.5653
	SRSS	-0.7709	0.6512

Table A.20 Bias factors computed for each bridge by regressions on bias obtained from pair-wise comparison.

Classification	Bridge	Direction	Hazard level		
			Low (50% in 50yr PE)	Moderate (10% in 50yr PE)	High (2% in 50yr PE)
Short (Simpl. Abtm.)	Route 14	Long.	1.13	1.20	1.23
		Transv.	1.12	1.16	1.18
		SRSS	1.20	1.12	1.09
		Mean	1.15	1.16	1.17
	Adobe	Long.	1.10	1.20	1.26
		Transv.	1.06	1.12	1.16
		SRSS	1.13	1.10	1.09
		Mean	1.09	1.14	1.17
	LADWP	Long.	0.98	1.25	1.42
		Transv.	0.97	1.12	1.21
		SRSS	1.10	1.19	1.24
		Mean	1.01	1.19	1.29
	La Veta	Long.	1.00	1.36	1.59
		Transv.	1.15	1.22	1.25
		SRSS	1.13	1.23	1.28
		Mean	1.09	1.27	1.38
Average- Short			1.09	1.19	1.25
Long (Roller Abtm.)	MGR	Long.	1.07	1.35	1.52
		Transv.	1.10	1.40	1.58
		SRSS	1.09	1.34	1.50
		Mean	1.09	1.36	1.54
	W180-N168	Long.	1.29	2.31	3.15
		Transv.	1.17	2.11	2.88
		SRSS	1.03	2.02	2.89
		Mean	1.16	2.15	2.97
Average- Long			1.13	1.75	2.25

Table A.21: Summary of bias factors results: regression and pair-wise comparison.

Bridge Type	Method	Hazard level		
		Low (50% in 50yr PE)	Moderate (10% in 50yr PE)	High (2% in 50yr PE)
Short	Regression	1.11	1.22	1.29
	Pair-wise, mean	1.08	1.18	1.20
	Pair-wise, reg.	1.09	1.19	1.25
Long	Regression	1.14	1.60	1.96
	Pair-wise, mean	1.04	1.41	1.73
	Pair-wise, reg.	1.13	1.75	2.25

Analysis of Results: Time History Analysis, Phase III

- Only the fiber models in SAP2000 and OpenSees programs, which exhibited stable response for the unrestrained (Roller) abutment model, were considered in this phase of the project. For the short bridges, the simplified abutment model was used, anticipating a significant contribution of the abutment response to the overall nonlinear behavior of the structure. For the long bridges analyzed, the roller abutment was selected, since the contribution of the abutment to the overall response is smaller.
- The complete set of 63 ground motions used for the nonlinear time history analysis of the six bridges includes far-field and near-field, fault-normal and fault-parallel, ground motions. Therefore, the effect of directivity is not represented by the computed bias factors.
- Different hazard levels were considered in the analysis, to determine the bias between SAP2000 and OpenSees programs for the elastic, moderately inelastic, and highly inelastic range of response of the different bridges. To guarantee that the bridges undergo excursion in the inelastic range for high intensity ground motions, a uniform scale factor of 2.0 was used for all the records.
- The (natural logarithmic) regression curves (method 1) relating peak displacements to the intensity measure obtained for each bridge in each direction of analysis have a similar shape and tendency for both SAP and OpenSees models.
- This regression method (method 1) shows a clear tendency for the bias between SAP2000 and OpenSees NL THA displacement results to increase with increasing intensity measure.
- The values shown in Table A.18 obtained through pair-wise comparison of OpenSees and SAP2000 displacement results are mean values at each hazard level. A large dispersion in the bias factors results was observed for individual records; however, on average (for the 63 ground motions), similar mean values are obtained for all 6 bridges and hazard levels.
- Since the average bias factor is greater than 1.0 for all cases (method 2), the nonlinear time history analysis displacement results obtained using OpenSees program are consistently higher than SAP2000 results.
- The (natural logarithmic) regressions computed for the bias factors also show a tendency to increase with increasing intensity measure or hazard level, for all bridges analyzed.

- For the low hazard level, the bridges remain essentially elastic. Since the modal periods computed for SAP2000 and OpenSees coincide within 5% for all 6 bridges analyzed, the nonlinear time history analysis displacement results should coincide as well. The average bias obtained for short and long bridges in the low hazard level range is around 10% using the 3 methods of bias computation.
- For the moderate hazard level, the bias factors computed using both methods of computation show a clear tendency for the OpenSees displacement results to exceed the SAP2000 nonlinear time history analysis displacement results. An average bias of 20% and 60% is computed for the short and long bridges, respectively.
- At the high hazard level, this tendency becomes more pronounced. Average bias of 25% and 100% are obtained for the short and long bridges, respectively.
- The natural log regressions relating elastic spectral displacements at the first mode period of each bridge (S_d, T_1) to the peak displacements observed for each ground motion are considered to be an adequate procedure to determine the overall relation between the intensity measure and expected bridge response (peak displacements) during time history analysis (Mackie 2003).
- All three methods (regression, pair-wise average, and pair-wise regression) for computing the bias factors are considered adequate. The bias factors obtained for the corresponding hazard levels using both methods are similar.
- Since only four and two bridges were used for the computation of the bias for the short and long bridges, respectively, the bias factors obtained using this procedure do not represent a sufficiently large and representative data set.
- In order to obtain reliable values, a larger number of bridges with different geometric configurations must be used to represent short and long bridges. An estimate of the dispersion of these results for different hazard levels must be obtained as well.

Appendix B: Modeling and Analysis Example of Standard Ordinary Bridge: Route 14 Bridge

This appendix presents all the major steps in constructing a complete three-dimensional bridge model using SAP2000 structural analysis program, which includes the geometry, cross sections, elements and materials, mass, boundary conditions and a simplified abutment model of the bridge. The steps and results of a moment-curvature analysis of the column cross section are also presented, as well as two nonlinear modeling options for the column plastic hinge. A brief explanation concerning the parameters used in the modal, gravity, pushover, and nonlinear time history analysis of the bridge is also offered at the end of the appendix.

1. Basic Geometry and Materials Data

The following table summarizes the principal characteristics of R14 bridge structure, required for the modeling phase.

Parameter	Value/ Description
General bridge description	Ordinary Standard multi-column bents bridge with 2 spans
Total length of the bridge (L_{Total})	286 ft
Number of spans and length of each deck span	2 spans: 145 and 141 ft
Total deck width (W_{deck})	53.7 ft
Deck depth (d_d)	5.74 ft
Deck cross-sectional geometry	$A=12816 \text{ in}^2$, $J=2.839 \times 10^7 \text{ in}^4$, $I_x=9.293 \times 10^6 \text{ in}^4$, $I_y=3.937 \times 10^8 \text{ in}^4$, $A_{vx}=3099.6 \text{ in}^2$, $A_{vy}=7795.6 \text{ in}^2$, $S_x=Z_x=2.698 \times 10^5 \text{ in}^3$, $S_y=Z_y=1.2218 \times 10^6 \text{ in}^3$.
Number and clear height of each column bent (H_{col})	2 columns: 35.1 ft
Column diameter (D_c)	5.42 ft
Deck centroid ($D_{c.g.}$)	34.0"
Length of cap beam to centroid of column bent (L_{cap})	11.96 ft
Cap beam dimensions ($B_{cap} \times d_d$)	7.55 x 5.74 ft
Location and size of expansion joints	No expansion joints specified
Support details for boundary conditions	Pinned foundations (reduction of column cross section)
Concrete material properties for concrete of superstructure (f_c , E_c)	Elastic deck: $f_c=5 \text{ ksi}$, $E_c=4030.5 \text{ ksi}$.
Concrete and reinforcing steel material properties of column bents	Concrete: 5 ksi, see figures below for σ - ϵ relation Steel: ASTM A706, see figure below for σ - ϵ relation
Reinforcement details of column bent cross section	Longitudinal reinforcement: 42#14 (bundles of 2), $\rho_l=2.848\%$ Transverse reinforcement: Spiral, #7@4.9", $\rho_s=0.803\%$
Foundation soil geotechnical properties	Rigid soil conditions assumed
Abutment general geometry	Simplified abutment model (see step 7)
Number and properties of abutment bearing pads	2 bearing pads considered, $k_v=1358.5 \text{ K/in.}$ (vertical stiffness)

Confined Concrete: Mander model (spreadsheet calculations of σ - ϵ relationship)

Data:

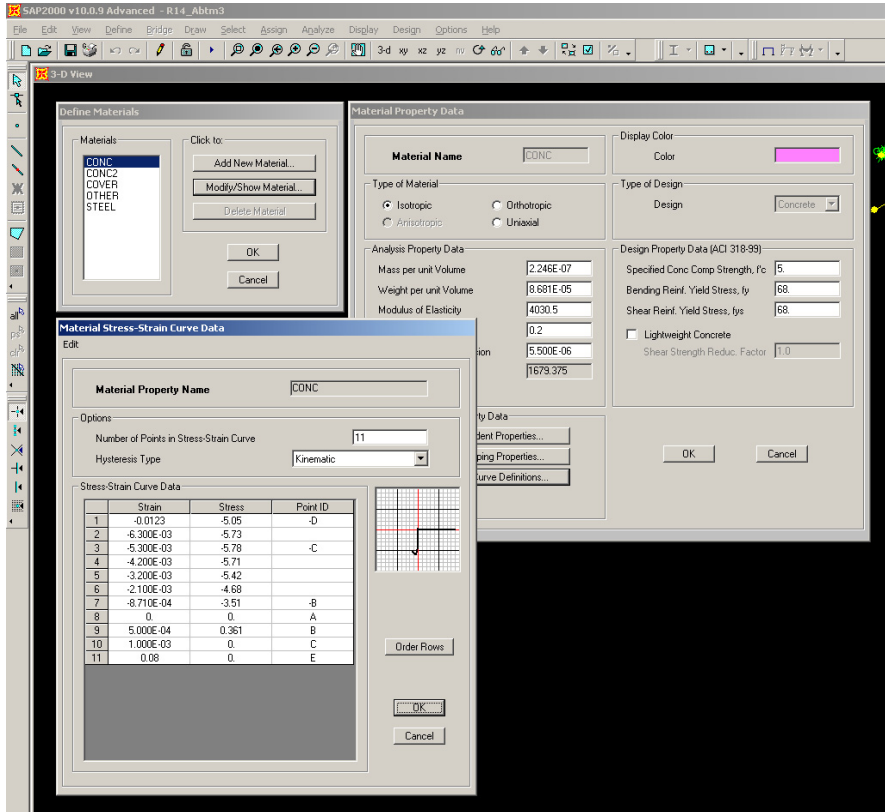
f_c (ksi)=	5
E_c (ksi)=	4030.5
ϵ_{co} =	0.002
ρ_l =	8.05E-03
f_{yt} (ksi)=	68
ϵ_{smax} =	0.06

Confined Concrete:

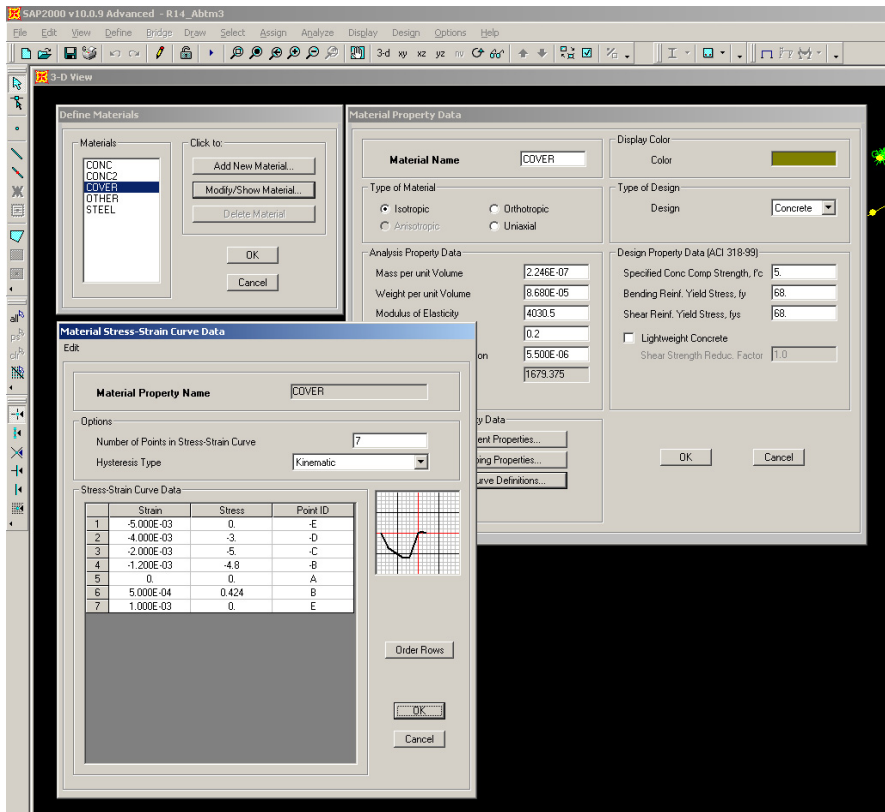
$r=E_c/(E_c-f_{cc}/\epsilon_{cc})$ =	1.454
$\epsilon_{cc}=\epsilon_{co}(1+5(f_{cc}/f_{co}-1))$ =	5.27E-03
$\epsilon_{cy}=0.7\epsilon_{cc}$ =	3.69E-03
f_{cc} (ksi)=	6.636
$\epsilon_{cmax}=0.004+0.1\rho_l f_y/f_c$ =	1.225E-02

Point	$x=\epsilon_c/\epsilon_{cc}$	ϵ_c	$f_c=f_{cc}x/(r-1+x^r)$ (ksi)
1	0.0	0.0000	0.00
2	0.2	0.0011	3.51
3	0.4	0.0021	5.38
4	0.6	0.0032	6.23
5	0.8	0.0042	6.56
6	1.0	0.0053	6.64
7	1.2	0.0063	6.59
8	1.4	0.0074	6.48
9	1.6	0.0084	6.34
10	1.8	0.0095	6.19
11	2.0	0.0105	6.04
12	2.3	0.0123	5.80

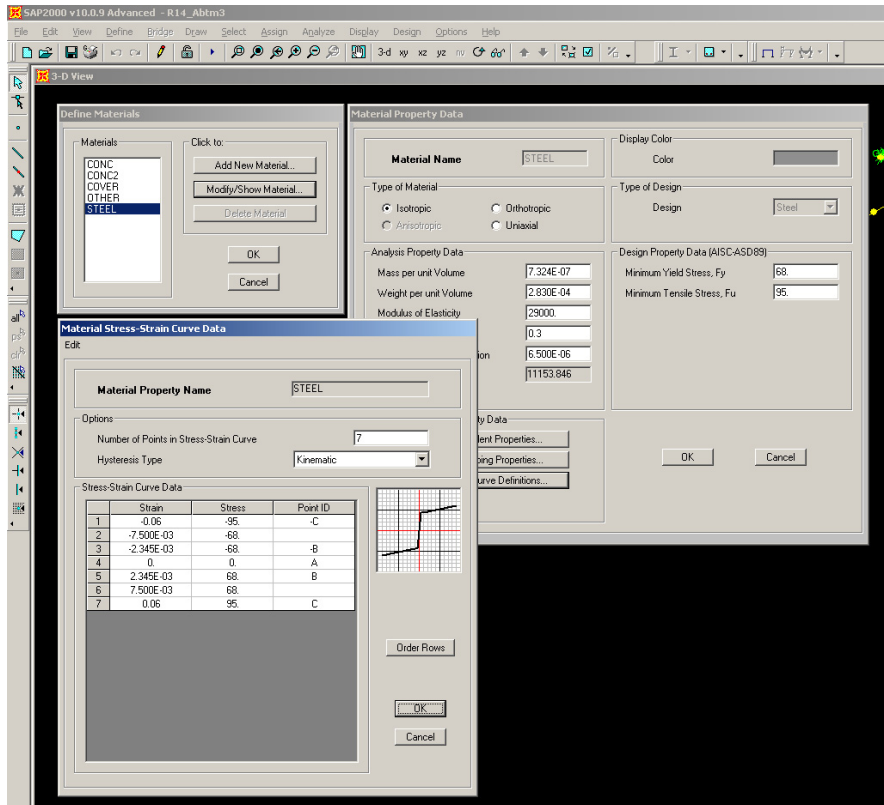
Confined concrete in SAP2000: Define →Material →Add New Material →CONC



Unconfined concrete in SAP2000: Define →Material →Add New Material →COVER



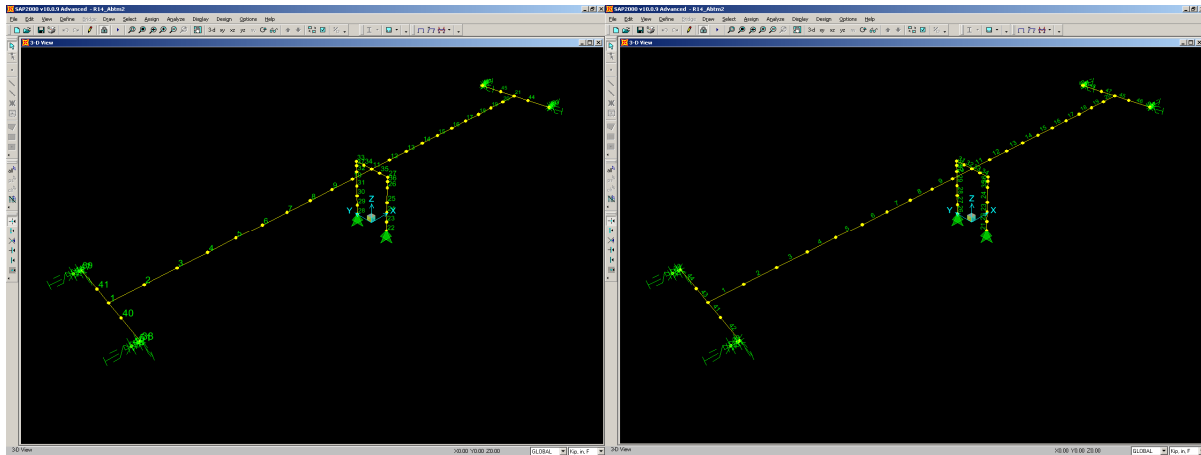
Reinforcing steel in SAP2000: Define → Material → Add New Material → STEEL



2. Geometry of the Bridge

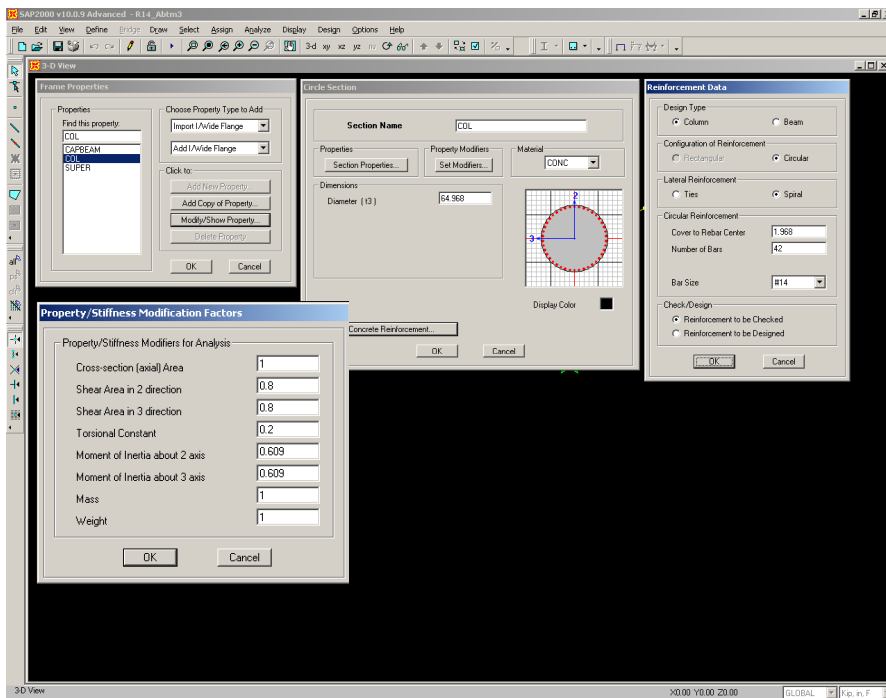
The construction of the bridge basic geometry is carried out according to the table in step 1. In this case, each span was discretized into 10 equal-length segments, each column into 5 segments, and the cap beam into 4 segments. The height of the deck was defined as $H_{col} + D_{c.g.} = 35.1 \times 12 + 34.0 = 455.16"$, a separate segment of $D_{c.g.}$ length was created at the column top with an end offset of the same length and a rigid zone factor of 1.0, to account for the rigidity of the joint. An additional segment below this was defined with the plastic hinge length: $L_p = 0.08L + 0.15f_{ye}d_{bl} = 0.08 \times 416.5 + 0.15 \times 68 \times 1.693 = 50.6"$. Notice the coordinate system used is according to section 2.1.2 of the guidelines.

Node and element numbering

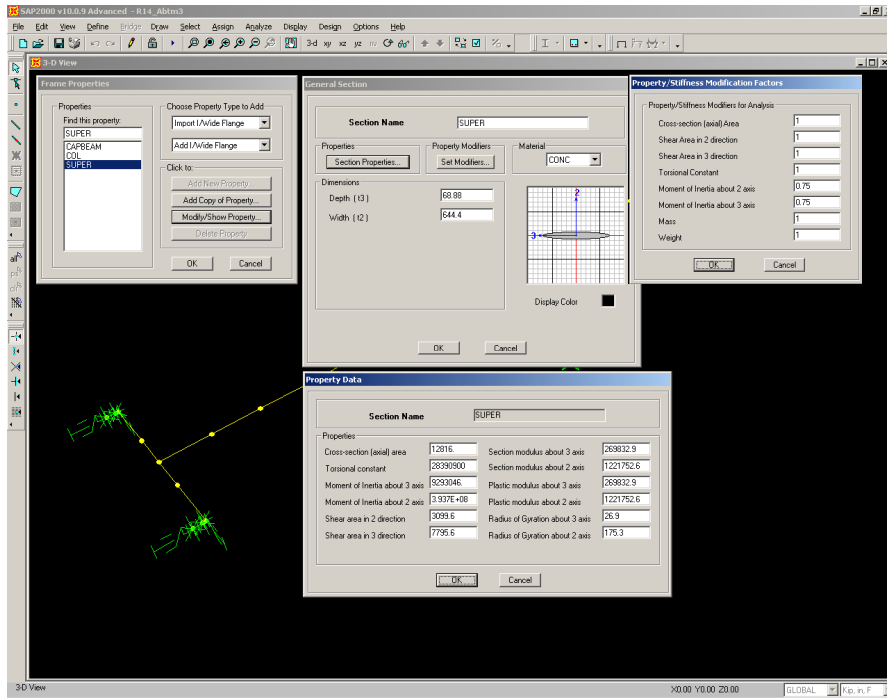


3. Definition of Section Properties

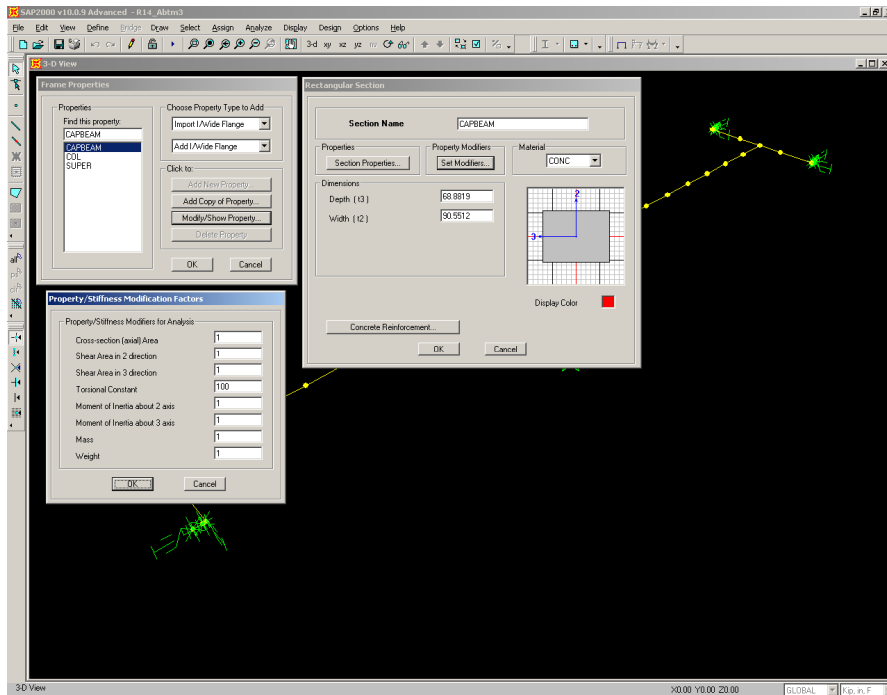
Concrete column in SAP2000: Define → Frame Sections → Add Circle



Superstructure in SAP2000: Define → Frame Sections → Add General



Cap beam in SAP2000: Define → Frame Sections → Add Rectangular



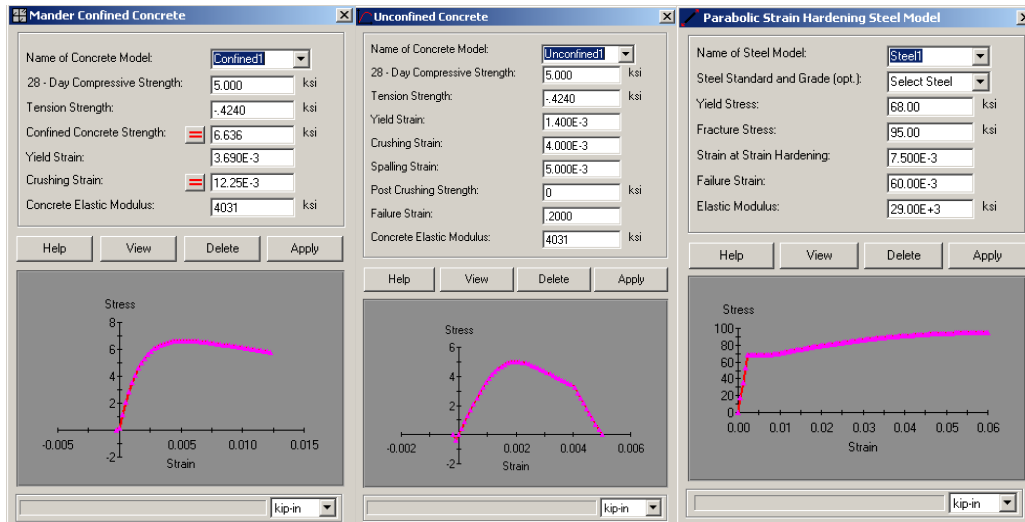
4. Mass Assignment

The translational mass of all elements is automatically computed in SAP2000; however, additional rotational mass is assigned (by the user) for the deck nodes, according to their tributary length and deck cross section characteristics. For example, for $L_{trib}=173.2$ in, we have:

$$M_{XX} = \frac{Ml^2}{12} = \frac{mA_{deck}L_{trib}d_w^2}{12} = \frac{4.471/(1000 \times 12^4) \times 12816 \times 173.2 \times (53.7 \times 12)^2}{12} = 16561.9 \text{ K} \cdot \text{in} \cdot \text{sec}^2$$

5. Moment-Curvature Analysis of Concrete Column Bent

The dead axial load is considered for the moment-curvature analysis of the column, obtained from Gravity analysis (see step 9) as $P_{col}=1247 \text{ K}$ ($7.51\%_c A_g$). The failure of the cross section is defined as the fracture of rebar or crushing of confined concrete. The reduced ultimate strain $\epsilon_{sur}=0.06$ in steel σ - ϵ relation, as well as the expected material strength for confined concrete and steel are used. The M - ϕ analysis was carried out using XTract by Imbsen.



XTRACT Material Report - Educational

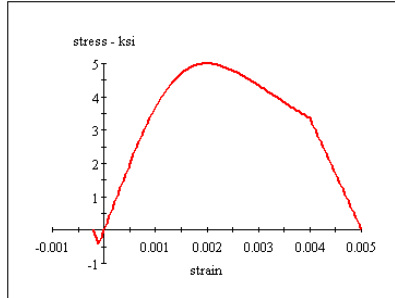
Imbsen & Associates, Inc. (Educatic
UCE

Material Name: Unconfined1
Material Type: Unconfined Concrete

2007-07-03
Col_R14_Caltrans
Col_R14
Page __ of __

Input Parameters:

Tension Strength: -.4240 ksi
28 Day Strength: 5.000 ksi
Post Crushing Strength: 0 ksi
Tension Strain Capacity: .1052E-3 Comp
Spalling Strain: 5.000E-3 Comp
Failure Strain: .2000 Comp
Elastic Modulus: 4031 ksi
Secant Modulus: 2500 ksi



Model Details:

For Strain - $\epsilon < 2 \cdot \epsilon_t$ $f_c = 0$

For Strain - $\epsilon < 0$ $f_c = \epsilon \cdot E_c$

For Strain - $\epsilon < \epsilon_{cu}$ $f_c = \frac{f_c \cdot r}{r - 1 + x^2}$

For Strain - $\epsilon < \epsilon_{sp}$ $f_c = f_{cu} + (f_{cp} - f_{cu}) \cdot \frac{(\epsilon - \epsilon_{cu})}{(\epsilon_{sp} - \epsilon_{cu})}$

$$x = \frac{\epsilon}{\epsilon_{cc}}$$

$$r = \frac{E_c}{E_c - E_{sec}}$$

$$E_{sec} = \frac{f_c}{\epsilon_{cc}}$$

ϵ = Concrete Strain

f_c = Concrete Stress

E_c = Elastic Modulus

E_{sec} = Secant Modulus

ϵ_t = Tension Strain Capacity

ϵ_{cu} = Ultimate Concrete Strain

ϵ_{cc} = Strain at Peak Stress = .002

ϵ_{sp} = Spalling Strain

f_c = 28 Day Compressive Strength

f_{cu} = Stress at ϵ_{cu}

f_{cp} = Post Spalling Strength

Material Color States:

- Tension strain after tension capacity
- Tension strain before tension capacity
- Initial state
- Compression before crushing strain
- Compression before end of spalling
- Compression after spalling

Reference:

Mander, J.B., Priestley, M. J. N., "Observed Stress-Strain Behavior of Confined Concrete", Journal of Structural Engineering, ASCE, Vol. 114, No. 8, August 1988, pp. 1827-1849

Comments:

User Comments

Moment Curvature Loading

General:

Loading Name:

On Section:

Applied First Step Loads:

Axial Load: kips

Mxx: kip-in

Myy: kip-in

Incrementing Loads:

Axial Load

Moment About the X-Axis (Mxx)

Moment About the Y-Axis (Myy)

Moment Rotation Options:

Calculate Moment Rotation

Plastic Hinge Length: in

Loading Direction:

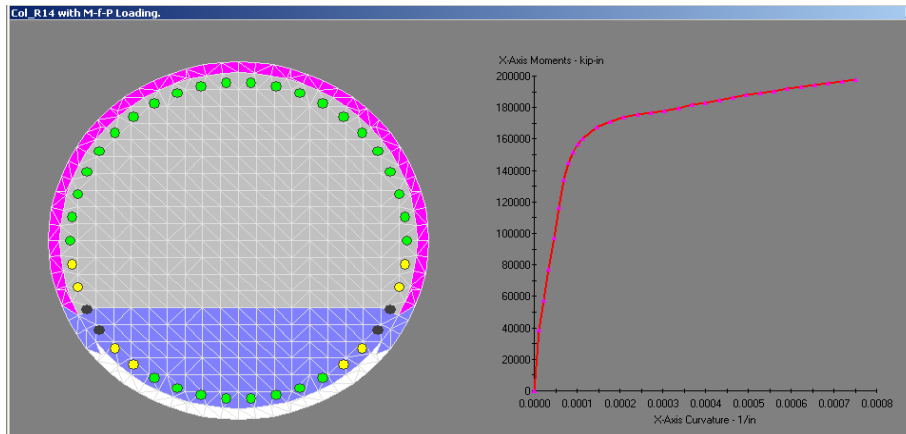
Positive Negative

Graphics Options:

Show Graph Show Animation

Solution Method
Delete
Cancel
Apply

Moment-Curvature Analysis results



The plastic curvature and capacity are defined between the ultimate and nominal, according to section 2.5.3 of the guidelines. The results of the $M-\phi$ analysis are ($L_p=50.6$ in. ($0.75D_c$), $H=35.1$ ft)

Nominal: $M_Y \approx 165,000$ K-in., $\phi_Y \approx 1.2 \times 10^{-4}$ in./in., $\theta_Y = \phi_Y L_p = 0.006$ rad, $\Delta_Y = H^2 \phi_Y / 3 = 7.3$ in.

Ultimate: $M_u \approx 190,000$ K-in., $\phi_u \approx 7.5 \times 10^{-4}$ in./in., $\theta_u = \phi_u L_p = 0.038$ rad, $\Delta_u = \Delta_Y + \Delta_p = 20.0$ in.

Plastic: $M_p = \{M_Y, M_u\} = 180,000$ K-in., $\phi_p = (\phi_u - \phi_Y) = 6.3 \times 10^{-4}$ in./in., $\theta_p = \phi_p L_p = 0.032$ rad, $\Delta_p = \theta_p (H - L_p / 2) = 12.7$ in.

The ultimate displacement capacity will be used to estimate the displacement demand used for the pushover analysis, defined as $1.5-2.0\Delta_u$, that is, about 30.0–40.0 in.

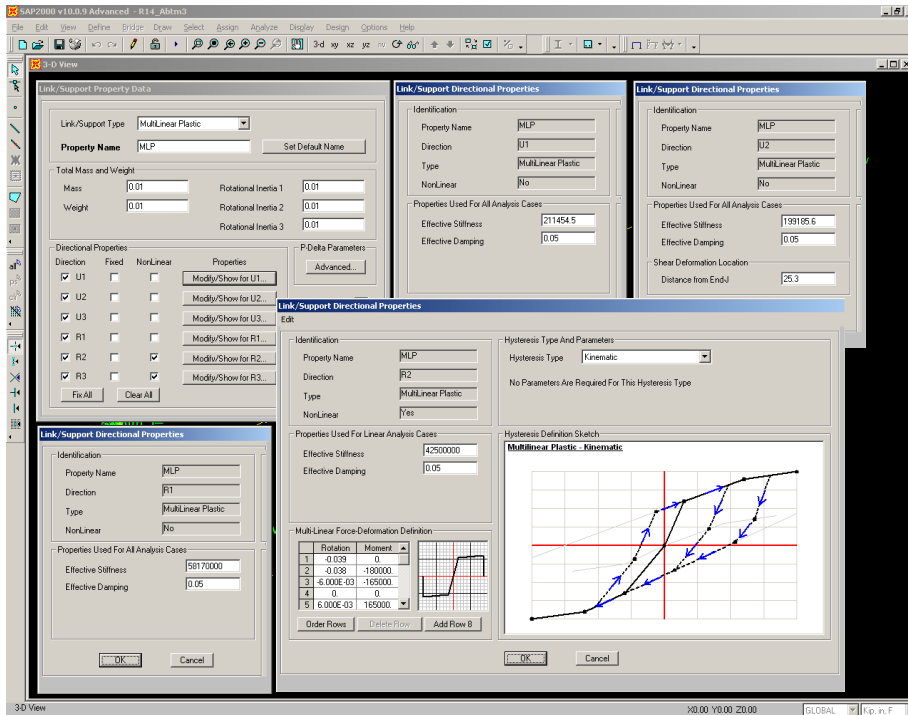
6. Definition of Column Plastic Hinge Models

- NL-Link: Multi-Linear Plastic (MLP)

The stiffness coefficients are computed as follows:

Stiff. Coeff.	Formula	Calculations
k_1 - Axial (U1)	EA/L	$4030.5 \times 0.8 \times 3315 / 50.6 = 2.114 \times 10^5$ K/in.
k_2, k_3 - Translation (U2, U3)	$12EI/L^3$	$12 \times 4030.5 \times 0.609 \times 874516.3 / (50.6)^3 = 1.988 \times 10^6$ K/in.
k_4 - Torsion (R1)	GJ/L	$1680 \times 1749032.5 / 50.6 = 5.817 \times 10^7$ K-in.
k_5, k_6 - Flexure (R2, R3)	EI/L	$4030.5 \times 0.609 \times 874516.3 / 50.6 = 4.25 \times 10^7$ K-in.

NL-Link (MLP) in SAP2000: Define ↪ Link/Support Property ↪ Multi-Linear Plastic



Due to biaxial symmetry of the column cross section, the properties defined for the translational degrees of freedom U2 and U3, as well as the rotational degrees of freedom R2 and R3 (bending) are the same. The inflection point of the NL-link segment for degrees of freedom U2 and U3 is defined at mid-height ($L_p/2$), assuming constant plastic curvature throughout the plastic hinge zone.

- Fiber Model (Spreadsheet calculations of fiber area and centroid)

Data:

D_{col} (in)=	65	Area	Calc
r_{col} (in)=	32.5	3318.307	3437.21
θ_{total} (rad)=	6.28		
θ_{total} (deg)=	360		
Cover (in)=	2		
A_b (in ²)=	2.25		
Bundle=	2		

Concrete Fibers:

n_r -inner=	2	Δ_r (in)=	7.63	no. fibers=	189
n_r -outer=	5	Δ_r (in)=	3.05		
n_r -cover=	2	Δ_r (in)=	1.00		
n_θ =	21	Δ_θ (rad)=	0.30		

$$A_{ij} = \Delta_r \Delta_\theta ((r_i - \Delta_r / 2) + (r_i + \Delta_r / 2))$$

No.	i: 1- n_r	j: 1- n_θ	$r_i = i \Delta_r$	$\theta_j = j \Delta_\theta$	A_{ij}	$x = r_i \cos(\theta_j)$	$y = r_i \sin(\theta_j)$
1	1	1	7.63	0.30	17.40	7.29	2.25
2	1	2	7.63	0.60	17.40	6.30	4.30
3	1	3	7.63	0.90	17.40	4.75	5.96

...

No.	i: 1-n _r	j: 1-n _θ	r _i =iΔ _r	θ _j =jΔ _θ	A _{ij}	x=r _i cos(θ _j)	y=r _i sin(θ _j)
43	1	1	18.30	0.30	16.70	17.49	5.39
44	1	2	18.30	0.60	16.70	15.12	10.31
45	1	3	18.30	0.90	16.70	11.41	14.31

...

No.	i: 1-n _r	j: 1-n _θ	r _i =iΔ _r	θ _j =jΔ _θ	A _{ij}	x=r _i cos(θ _j)	y=r _i sin(θ _j)
148	1	1	31.50	0.30	4.71	30.10	9.28
149	1	2	31.50	0.60	4.71	26.03	17.74
150	1	3	31.50	0.90	4.71	19.64	24.63

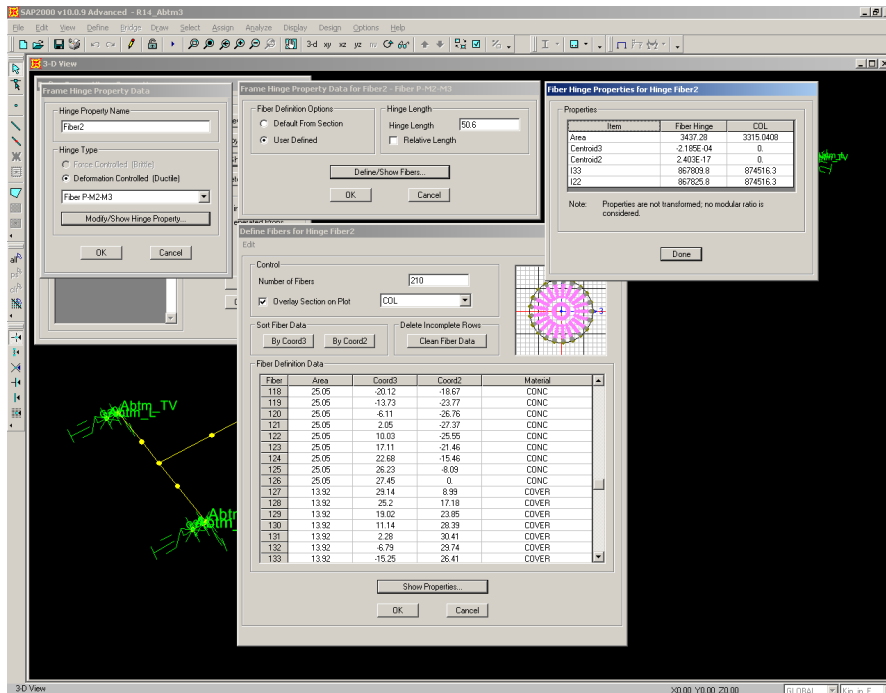
...

Reinforcement Fibers:

No.	i: 1-n _r	j: 1-n _θ	r _i =iΔ _r	θ _j =jΔ _θ	A _{ij}	x=r _i cos(θ _j)	y=r _i sin(θ _j)
1	1	1	30.50	0.30	4.50	29.14	8.99
2	1	2	30.50	0.60	4.50	25.20	17.18
3	1	3	30.50	0.90	4.50	19.02	23.85

...

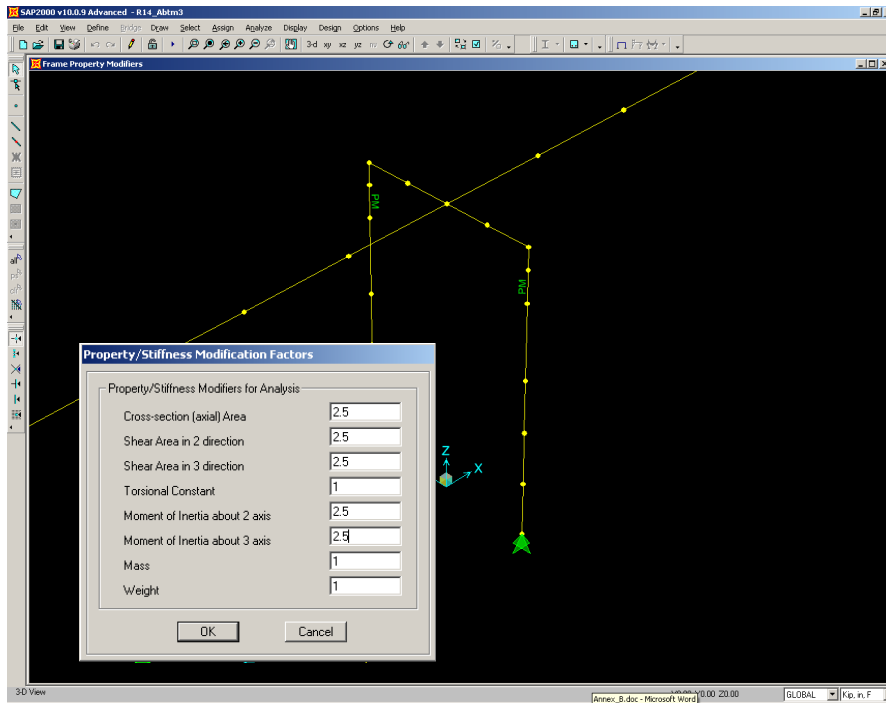
Fiber model in SAP2000: Define ↪ Hinge Properties ↪ Add New Property ↪ Deformation Controlled (Ductile) ↪ Fiber P-M2-M3 ↪ User Defined...



Notice that the column and fiber gross section properties match within 10% of each other. However, additional property modifiers must be assigned to the areas and inertias of the plastic hinge segment, since SAP2000 computes the effective stiffness of the segment as a series system

of the elastic section and hinge property. These modification factors, in the order of 1–3, are defined iteratively to match the elastic first mode period. In this case, a factor of 2.5 was assigned to the gross section areas and inertias.

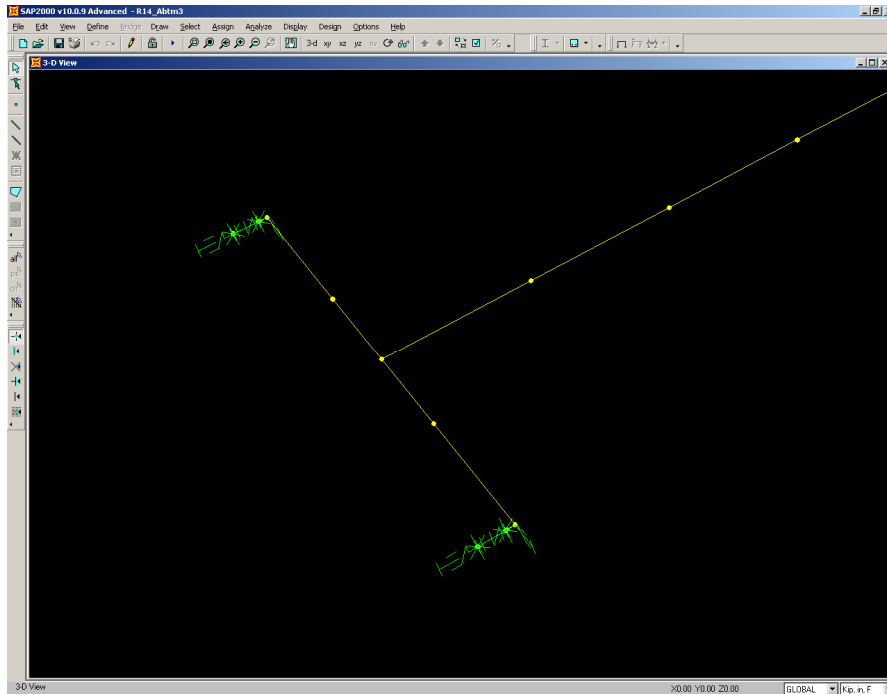
Modification factors in SAP2000: Assign ↪Frame/Cable/Tendon ↪Property Modifiers



7. Abutment Model

The abutment model used for the R14 bridge is the simplified abutment model, which general scheme is presented in section 2.7 of the guidelines. Using SAP2000, the general geometry of the abutment consists of a rigid element of length d_w (deck width), perpendicular to the longitudinal axis of the bridge (assuming no skew) and centered with respect to the deck centerline. The rigid element can be created by assigning any cross section (such as column or deck section) to the segment with additional property modifiers. These property modifiers consists of increasing all the gross section properties such as areas, inertias and torsional constant by a factor of 10^3 and ignoring the mass and weight of the element by assigning a zero factor to these quantities.

Simplified abutment model in SAP2000: General geometry



At each end of this rigid element, a zero-length (1 node) NL-Link element is defined with Multi-Linear plastic property to represent the transverse nonlinear behavior and vertical linear behavior assumed for the abutment. It is recommended to include a small rotational mass to the element, in the order of 10^{-3} , to increase the numerical stability of the model. The vertical response of the abutment is defined as an elastic spring with the bearing pads stiffness $k_v=1358.5$ K/in. In the transverse direction, an EPP (elastic-perfectly-plastic) model is defined, according to section 2.7 defined for the transverse direction with property modifiers $CW \times CL=(4/3) \times (2/3)$ and without a gap.

Transverse and longitudinal abutment response (spreadsheet calculation):

Data

K_i (K/in/ft)=	20
p_{max} (ksf)=	5
H- height factor (ft)=	5.5
CL=	0.67
CW=	1.33

Bridge	dw (in)	dd (ft)	wbw (in)	www (in)	Y (in)
R14	644.4	5.74	506.6	214.8	322.2
LV	906.0	6.23	756.5	302.0	453.0
Adobe	492.0	4.10	393.6	164.0	246.0
LADWP	499.2	4.27	396.7	166.4	249.6
MGR	507.6	6.23	358.1	169.2	253.8
W180	494.4	7.74	308.6	164.8	247.2

Longitudinal						
K_{abt} (K/in)	P_{bw} (K)	Δ_{gap} (in)	Δ_{eff} (in)	K_{eff} (K/in)	$P_{bw}/2$ (K)	$K_{eff}/2$ (K/in)
881.2	1264.6	2.0	3.44	368.1	632.3	184.1
1428.1	2224.3	2.0	3.56	625.3	1112.2	312.6
489.0	501.2	2.0	3.03	165.7	250.6	82.9
513.3	548.0	2.0	3.07	178.6	274.0	89.3
676.0	1052.9	2.0	3.56	296.0	526.4	148.0
723.9	1400.7	2.0	3.94	356.0	700.4	178.0

$$K_{abt} = K_i \times bw \times (dd/5.5) \quad \Delta_{eff} = \Delta_{gap} + P_{bw}/K_{abt}$$

$$P_{bw} = A_e \times 5.0 \times (dd/5.5) \quad K_{eff} = P_{bw}/\Delta_{eff}$$

$$A_e = dd \times bw$$

$$bw = dw - 2 \times dd$$

Transverse				
K_{abt} (K/in)	P_{bw} (K)	Δ_{eff} (in)	$P_{bw}/2$ (K)	$K_{eff}/2$ (K/in)
332.1	476.6	1.44	238.3	166.1
506.8	789.3	1.56	394.7	253.4
181.1	185.6	1.03	92.8	90.6
191.4	204.3	1.07	102.2	95.7
283.9	442.2	1.56	221.1	142.0
343.6	664.8	1.94	332.4	171.8

$$K_{abt} = K_i \times www \times (dd/5.5) \times 2/3 \times 4/3$$

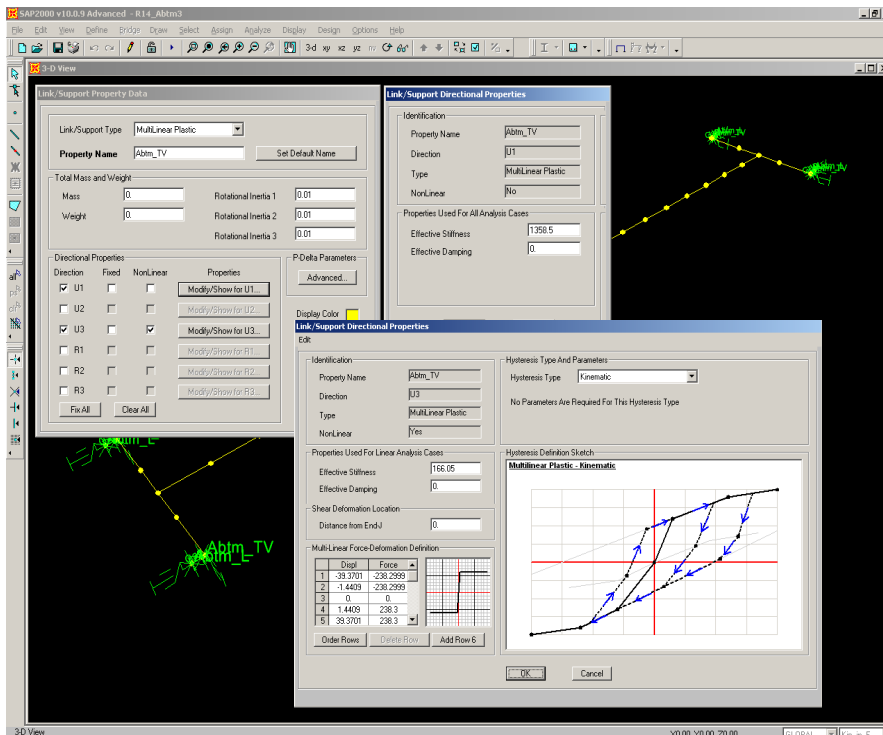
$$P_{bw} = A_e \times 5.0 \times (dd/5.5) \times 2/3 \times 4/3$$

$$A_e = dd \times www$$

$$www = dw/3$$

$$K_{eff} = K_{abt}$$

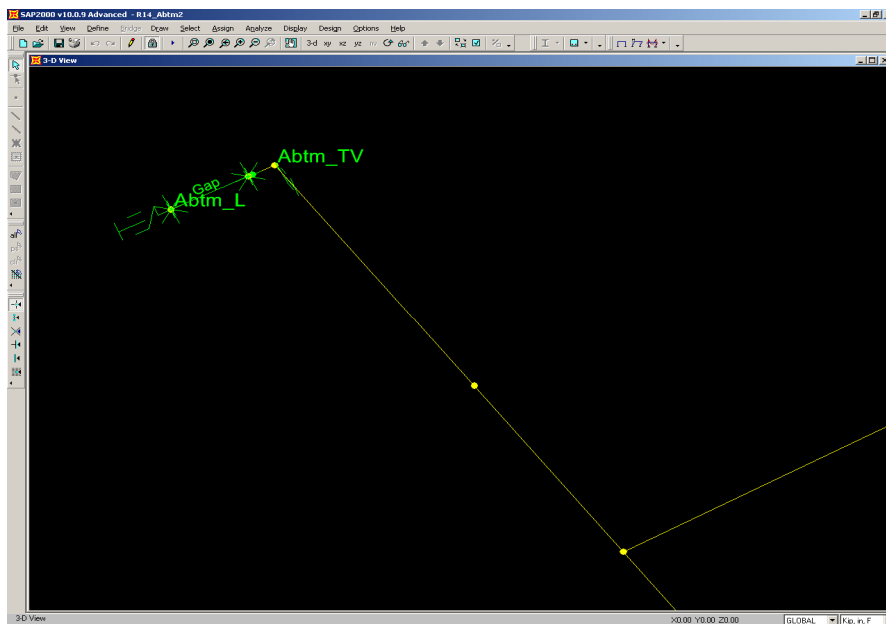
Transverse and vertical abutment response in SAP2000: Define \rightarrow Link/Support Property \rightarrow MultiLinear Plastic \rightarrow Abut_TV



In the longitudinal direction of the bridge, a series system is defined at each end of the rigid element, consisting of the following elements:

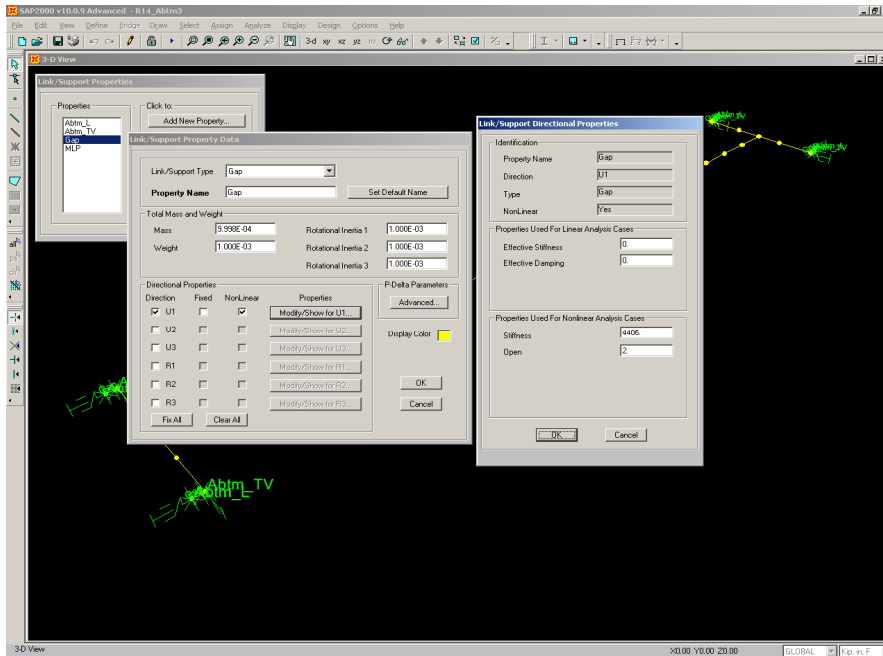
- Rigid element with shear and moment releases
- Boundary conditions: longitudinal translation allowed at each end of the gap element, the remaining degrees of freedom are fixed
- Gap element
- Zero-length NL-Link element with longitudinal backbone curve

Series system for longitudinal abutment response in SAP2000



The rigid element is again created assigning any cross section to the segment (such as column, superstructure, or cap beam) with property modifiers in the order of 10^3 to the gross section properties and 0 factors to the mass and weight of the section. The shear and moment releases are defined at the connection with the gap element. At the other end (connection with the first rigid element), a rigid connection is used.

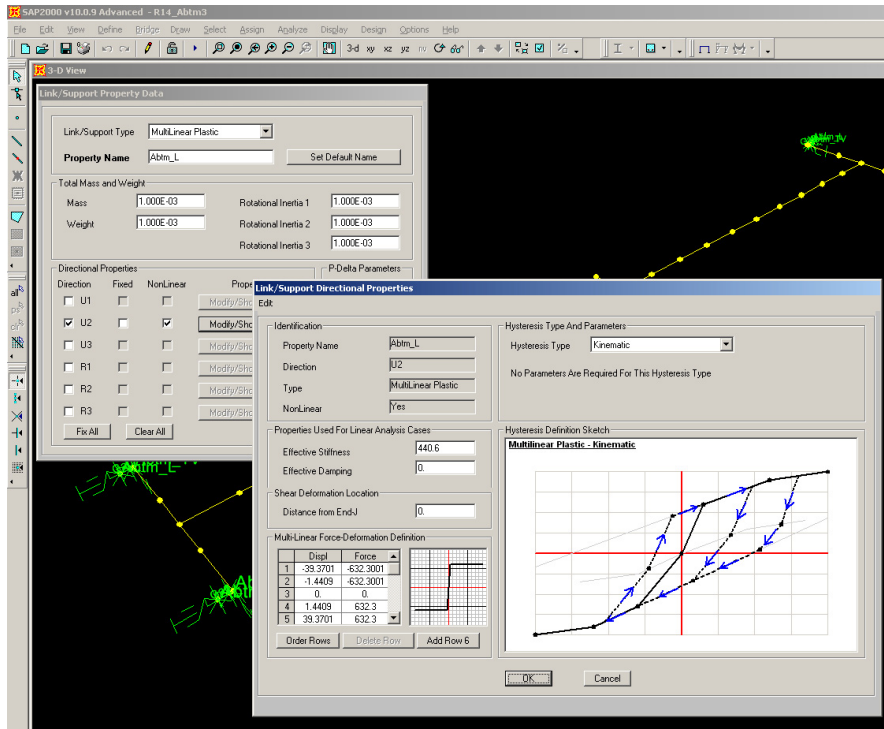
Gap element in SAP 2000: Define ↪ Link/Support Property ↪ Gap



The Gap element is defined as a finite length NL-Link element (2 nodes). The length of the gap, as defined below, does not affect the response of the system. The Gap element offered in SAP2000 requires the definition of properties used for linear and nonlinear analysis cases. For the linear analysis cases, a zero effective stiffness and zero effective damping are defined. For the nonlinear analysis cases, a term defined as “open” in SAP2000, corresponding to the gap size of 2”, is used with an infinite stiffness. It is recommended to use a stiffness value in the order of $10k_{abt}$ to avoid convergence problems. After the closing of the gap, the longitudinal behavior will be governed by the backbone curve assigned to the zero-length NL-link element.

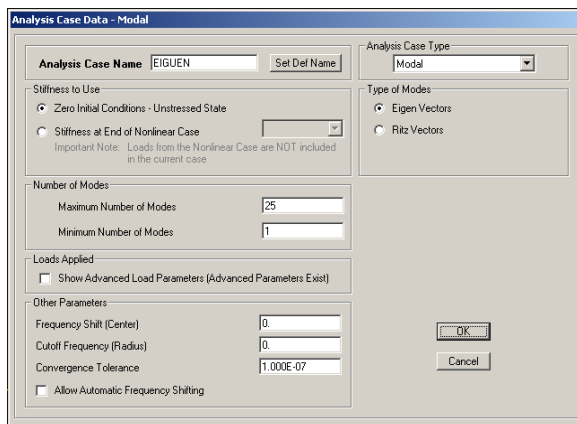
The zero-length (1 node) NL-Link element defined at the end of the Gap element is assigned a backbone curve corresponding to the EPP (elastic-perfectly-plastic) behavior defined according to section 7.8.1 of SDC 2004, corresponding to the nonlinear longitudinal abutment response.

Nonlinear longitudinal abutment behavior in SAP 2000: ↳Link/Support Property ↳ MultiLinear Plastic ↳ Abut_L



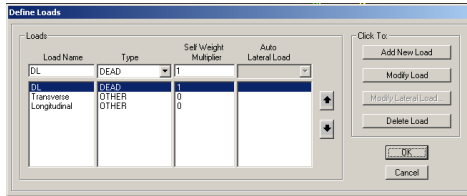
8. Modal Analysis

Eigenvector analysis in SAP2000: Define ↳ Analysis Case ↳ Modal ↳ Eigen Vector

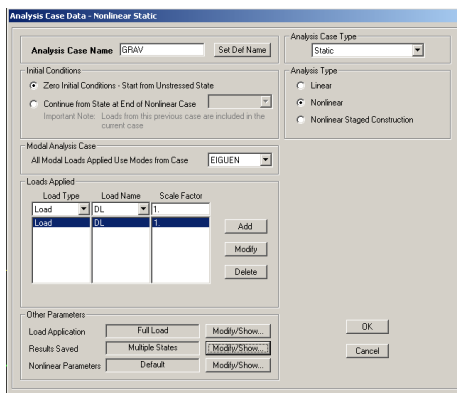


9. Dead Load Assignment (Self-Weight) and Gravity Analysis

Self-weight in SAP2000: Define ↪Loads



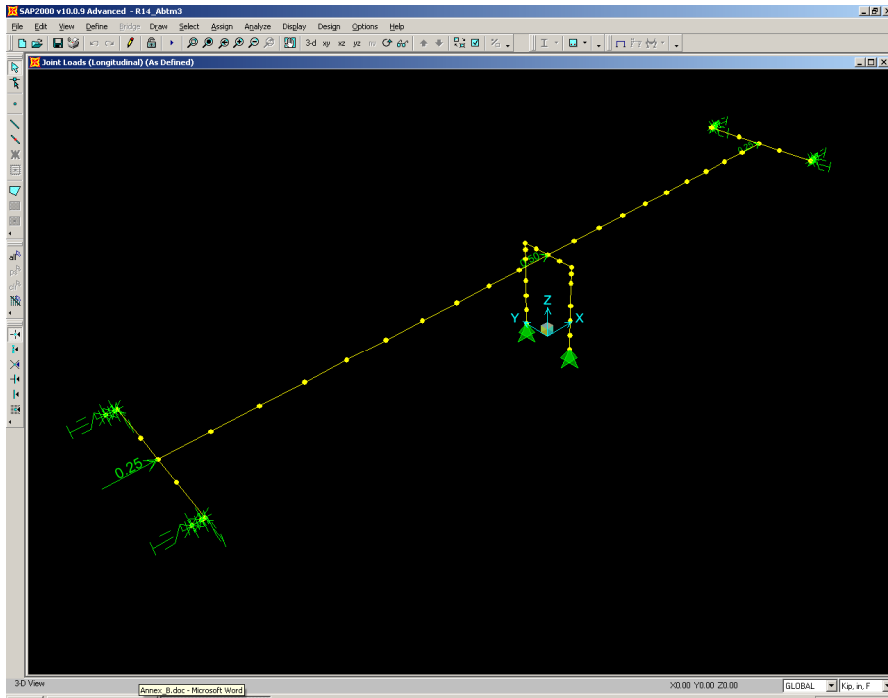
Gravity analysis in SAP2000: Define ↪Analysis Case ↪Static ↪Nonlinear ↪Full Load



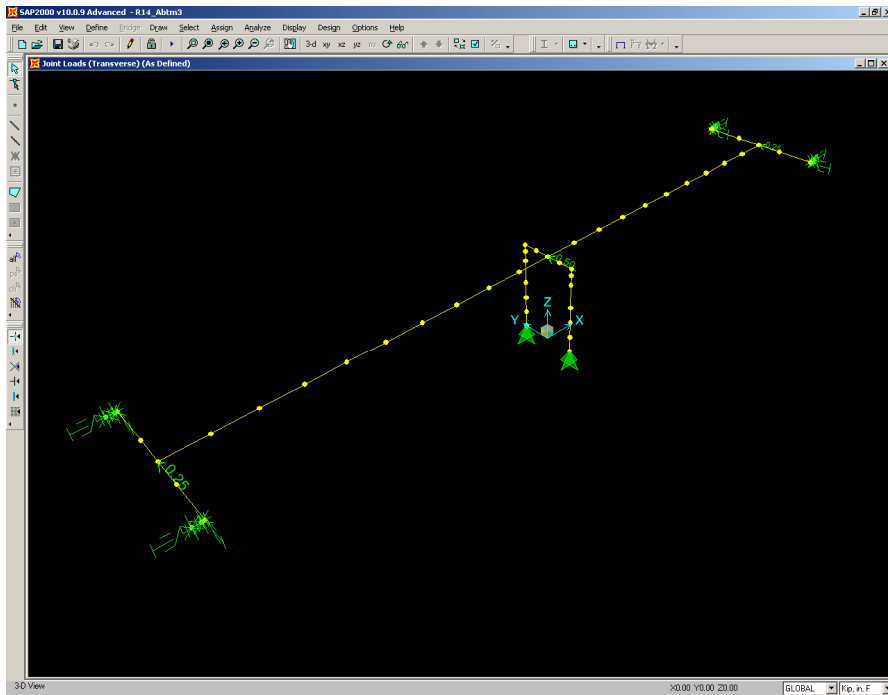
10. Pushover Analysis

The load pattern is defined according to the tributary mass. In this case, the deck center and ends were used as application points; however, additional nodes can be used throughout the deck span and at the two column tops. The mass of the abutment is not considered in the simplified abutment model, and therefore the load pattern is unmodified. Two separate load patterns for the transverse and longitudinal directions are defined. The magnitude of the loads is arbitrary; however, the proportion between the loads must be maintained.

Load pattern in the longitudinal direction (joint loads in SAP2000 in global direction U1).



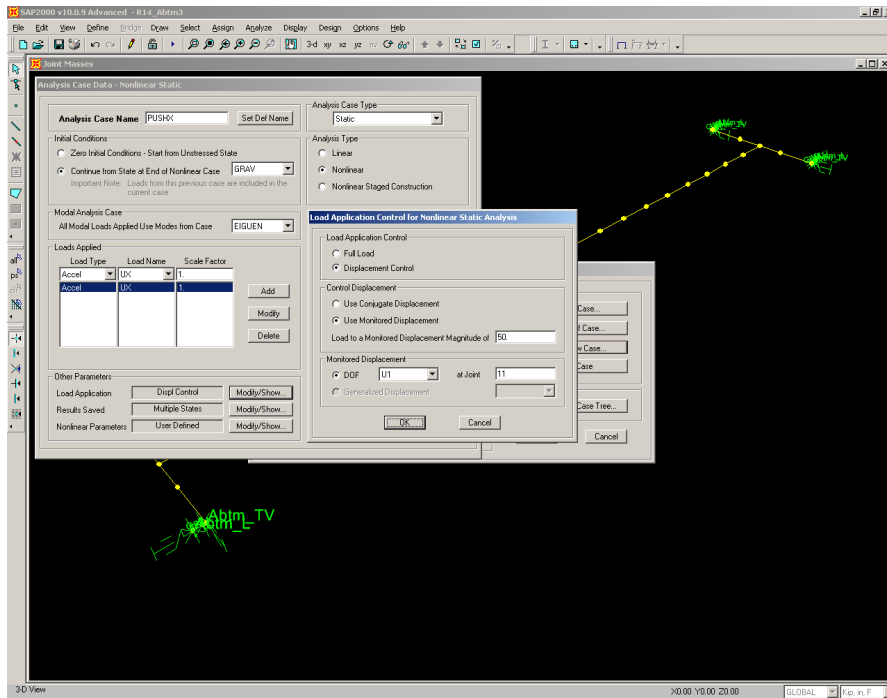
Load pattern in the transverse direction (joint loads in SAP2000 in global direction U2).



A separate pushover analysis case is also defined for the longitudinal and transverse directions. For both direction, the limiting displacement is defined as $1.5-2.0\Delta_u$. The monitored

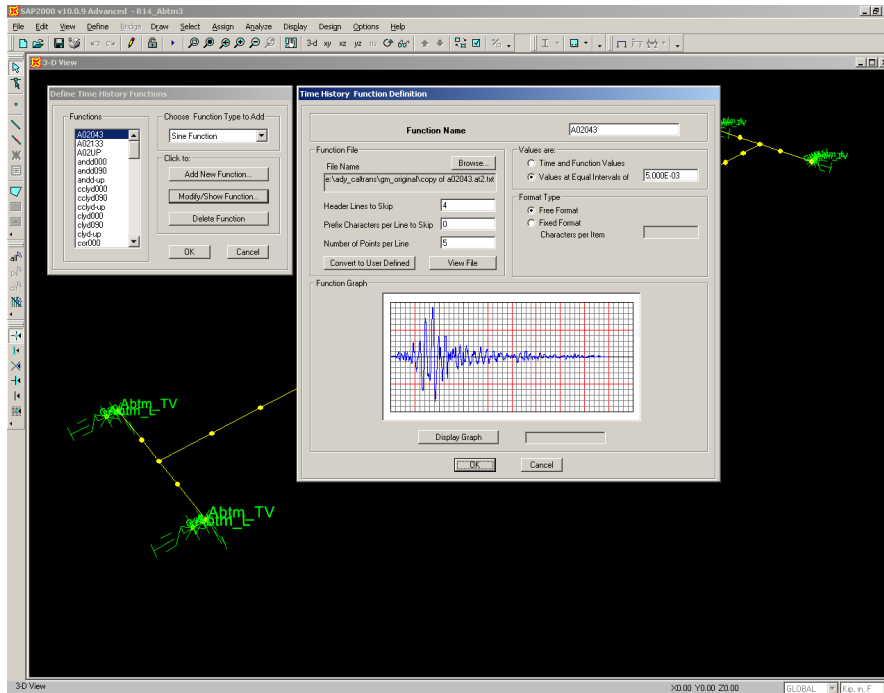
displacement is defined in this case for the intersection point between the deck and column top centerline.

Pushover analysis in SAP2000 with P-delta geometric nonlinearity: Define ↳ Analysis Case ↳ Static ↳ Nonlinear ↳ Displacement Control ↳ Multiple States



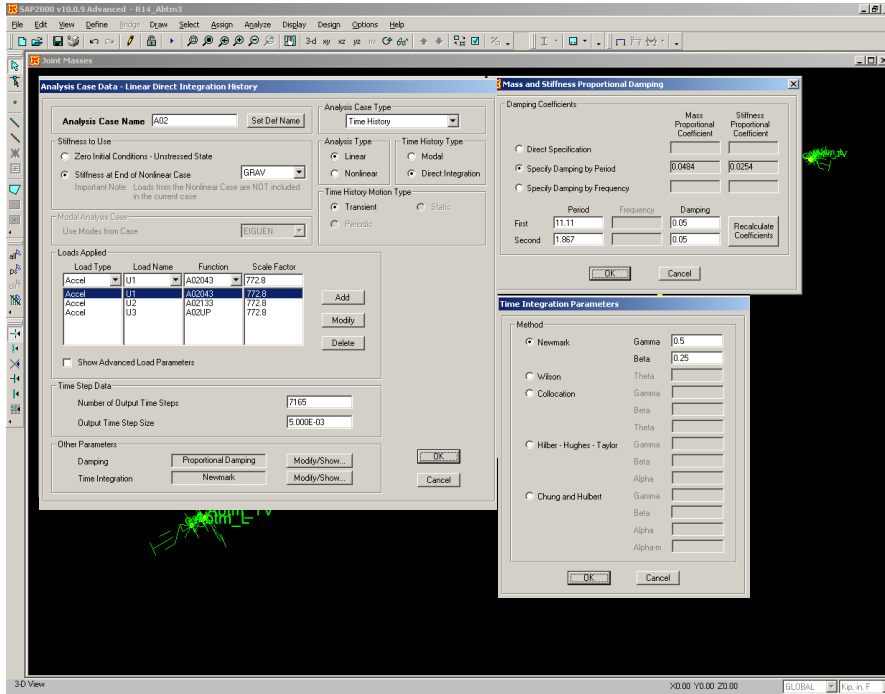
11. Time History Analysis

Ground motion input in SAP2000: Define → Functions → Time History → Functions From File

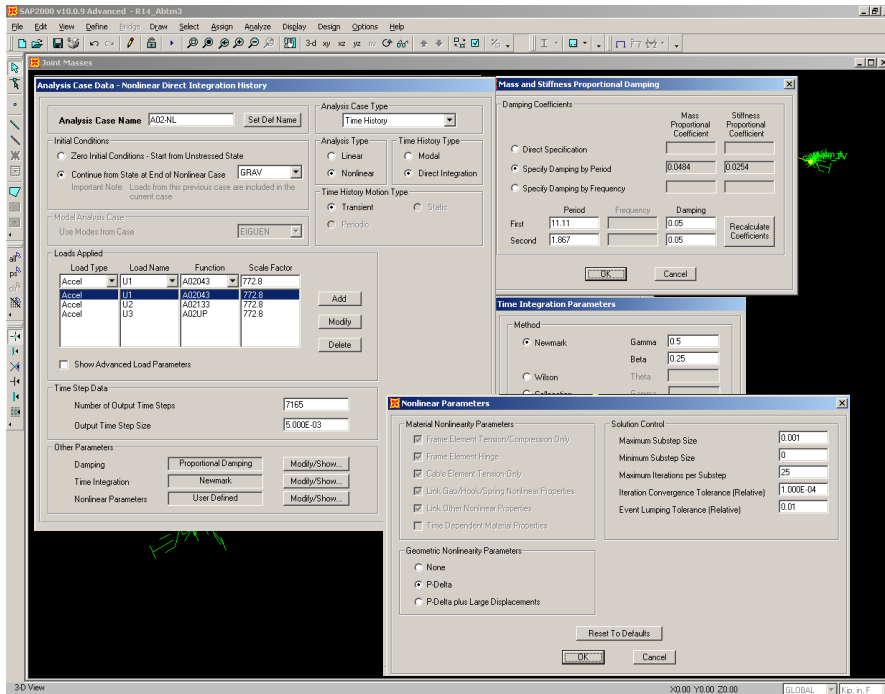


Since the seismic dynamic input provided is in the form of time history ground acceleration in units of g, a scale factor of 386.4 converts the record to in./sec² units. However, an additional scale factor of 2 is included to increase the intensity of the ground motion and guarantee nonlinear action of the bridge. Three components of the records are included, with the correct direction (U1, U2, and U3 corresponding to longitudinal, transverse, and vertical) assigned to each one. The Newmark constant acceleration method is used for both the linear and nonlinear time history analysis cases. If convergence problems result during the analysis, the HHT method should be used instead.

Linear time history in SAP2000: Define ↪ Analysis Case ↪ Time History ↪ Linear ↪ Direct Integration ↪ Transient



Nonlinear time history analysis in SAP2000: Define ↪ Analysis Case ↪ Time History ↪ Nonlinear ↪ Direct Integration ↪ Transient



Route 14 bridge has negligible skew and therefore the current ground motion input orientation is likely to produce the maximum displacement response in the principal orthogonal directions of the bridge. However, the maximum response of skew bridges could be produced using a different input orientation.

The modal, pushover and time history analysis results for Route 14 bridge are presented in Appendix A.

PEER REPORTS

PEER reports are available from the National Information Service for Earthquake Engineering (NISEE). To order PEER reports, please contact the Pacific Earthquake Engineering Research Center, 1301 South 46th Street, Richmond, California 94804-4698. Tel.: (510) 665-3405; Fax: (510) 665-3420.

- PEER 2008/03** *Guidelines for Nonlinear Analysis of Bridge Structures in California.* Ady Aviram, Kevin R. Mackie, and Božidar Stojadinović. August 2008.
- PEER 2008/02** *Treatment of Uncertainties in Seismic-Risk Analysis of Transportation Systems.* Evangelos Stergiou and Anne S. Kiremidjian. July 2008.
- PEER 2007/11** *Bar Buckling in Reinforced Concrete Bridge Columns.* Wayne A. Brown, Dawn E. Lehman, and John F. Stanton. February 2008.
- PEER 2007/10** *Computational Modeling of Progressive Collapse in Reinforced Concrete Frame Structures.* Mohamed M. Talaat and Khalid M. Mosalam. May 2008.
- PEER 2007/09** *Integrated Probabilistic Performance-Based Evaluation of Benchmark Reinforced Concrete Bridges.* Kevin R. Mackie, John-Michael Wong, and Božidar Stojadinović. January 2008.
- PEER 2007/08** *Assessing Seismic Collapse Safety of Modern Reinforced Concrete Moment-Frame Buildings.* Curt B. Haselton and Gregory G. Deierlein. February 2008.
- PEER 2007/07** *Performance Modeling Strategies for Modern Reinforced Concrete Bridge Columns.* Michael P. Berry and Marc O. Eberhard. April 2008.
- PEER 2007/06** *Development of Improved Procedures for Seismic Design of Buried and Partially Buried Structures.* Linda Al Atik and Nicholas Sitar. June 2007.
- PEER 2007/05** *Uncertainty and Correlation in Seismic Risk Assessment of Transportation Systems.* Renee G. Lee and Anne S. Kiremidjian. July 2007.
- PEER 2007/04** *Numerical Models for Analysis and Performance-Based Design of Shallow Foundations Subjected to Seismic Loading.* Sivapalan Gajan, Tara C. Hutchinson, Bruce L. Kutter, Prishati Raychowdhury, José A. Ugalde, and Jonathan P. Stewart. May 2008.
- PEER 2007/03** *Beam-Column Element Model Calibrated for Predicting Flexural Response Leading to Global Collapse of RC Frame Buildings.* Curt B. Haselton, Abbie B. Liel, Sarah Taylor Lange, and Gregory G. Deierlein. May 2008.
- PEER 2007/02** *Campbell-Bozorgnia NGA Ground Motion Relations for the Geometric Mean Horizontal Component of Peak and Spectral Ground Motion Parameters.* Kenneth W. Campbell and Yousef Bozorgnia. May 2007.
- PEER 2007/01** *Boore-Atkinson NGA Ground Motion Relations for the Geometric Mean Horizontal Component of Peak and Spectral Ground Motion Parameters.* David M. Boore and Gail M. Atkinson. May 2007.
- PEER 2006/12** *Societal Implications of Performance-Based Earthquake Engineering.* Peter J. May. May 2007.
- PEER 2006/11** *Probabilistic Seismic Demand Analysis Using Advanced Ground Motion Intensity Measures, Attenuation Relationships, and Near-Fault Effects.* Polsak Tothong and C. Allin Cornell. March 2007.
- PEER 2006/10** *Application of the PEER PBEE Methodology to the I-880 Viaduct.* Sashi Kunnath. February 2007.
- PEER 2006/09** *Quantifying Economic Losses from Travel Forgone Following a Large Metropolitan Earthquake.* James Moore, Sungbin Cho, Yue Yue Fan, and Stuart Werner. November 2006.
- PEER 2006/08** *Vector-Valued Ground Motion Intensity Measures for Probabilistic Seismic Demand Analysis.* Jack W. Baker and C. Allin Cornell. October 2006.
- PEER 2006/07** *Analytical Modeling of Reinforced Concrete Walls for Predicting Flexural and Coupled-Shear-Flexural Responses.* Kutay Orakcal, Loenardo M. Massone, and John W. Wallace. October 2006.
- PEER 2006/06** *Nonlinear Analysis of a Soil-Drilled Pier System under Static and Dynamic Axial Loading.* Gang Wang and Nicholas Sitar. November 2006.
- PEER 2006/05** *Advanced Seismic Assessment Guidelines.* Paolo Bazzurro, C. Allin Cornell, Charles Menun, Maziar Motahari, and Nicolas Luco. September 2006.
- PEER 2006/04** *Probabilistic Seismic Evaluation of Reinforced Concrete Structural Components and Systems.* Tae Hyung Lee and Khalid M. Mosalam. August 2006.
- PEER 2006/03** *Performance of Lifelines Subjected to Lateral Spreading.* Scott A. Ashford and Teerawut Juirnarongrit. July 2006.

- PEER 2006/02** *Pacific Earthquake Engineering Research Center Highway Demonstration Project.* Anne Kiremidjian, James Moore, Yue Yue Fan, Nesrin Basoz, Ozgur Yazali, and Meredith Williams. April 2006.
- PEER 2006/01** *Bracing Berkeley. A Guide to Seismic Safety on the UC Berkeley Campus.* Mary C. Comerio, Stephen Tobriner, and Ariane Fehrenkamp. January 2006.
- PEER 2005/16** *Seismic Response and Reliability of Electrical Substation Equipment and Systems.* Junho Song, Armen Der Kiureghian, and Jerome L. Sackman. April 2006.
- PEER 2005/15** *CPT-Based Probabilistic Assessment of Seismic Soil Liquefaction Initiation.* R. E. S. Moss, R. B. Seed, R. E. Kayen, J. P. Stewart, and A. Der Kiureghian. April 2006.
- PEER 2005/14** *Workshop on Modeling of Nonlinear Cyclic Load-Deformation Behavior of Shallow Foundations.* Bruce L. Kutter, Geoffrey Martin, Tara Hutchinson, Chad Harden, Sivapalan Gajan, and Justin Phalen. March 2006.
- PEER 2005/13** *Stochastic Characterization and Decision Bases under Time-Dependent Aftershock Risk in Performance-Based Earthquake Engineering.* Gee Liek Yeo and C. Allin Cornell. July 2005.
- PEER 2005/12** *PEER Testbed Study on a Laboratory Building: Exercising Seismic Performance Assessment.* Mary C. Comerio, editor. November 2005.
- PEER 2005/11** *Van Nuys Hotel Building Testbed Report: Exercising Seismic Performance Assessment.* Helmut Krawinkler, editor. October 2005.
- PEER 2005/10** *First NEES/E-Defense Workshop on Collapse Simulation of Reinforced Concrete Building Structures.* September 2005.
- PEER 2005/09** *Test Applications of Advanced Seismic Assessment Guidelines.* Joe Maffei, Karl Telleen, Danya Mohr, William Holmes, and Yuki Nakayama. August 2006.
- PEER 2005/08** *Damage Accumulation in Lightly Confined Reinforced Concrete Bridge Columns.* R. Tyler Ranf, Jared M. Nelson, Zach Price, Marc O. Eberhard, and John F. Stanton. April 2006.
- PEER 2005/07** *Experimental and Analytical Studies on the Seismic Response of Freestanding and Anchored Laboratory Equipment.* Dimitrios Konstantinidis and Nicos Makris. January 2005.
- PEER 2005/06** *Global Collapse of Frame Structures under Seismic Excitations.* Luis F. Ibarra and Helmut Krawinkler. September 2005.
- PEER 2005/05** *Performance Characterization of Bench- and Shelf-Mounted Equipment.* Samit Ray Chaudhuri and Tara C. Hutchinson. May 2006.
- PEER 2005/04** *Numerical Modeling of the Nonlinear Cyclic Response of Shallow Foundations.* Chad Harden, Tara Hutchinson, Geoffrey R. Martin, and Bruce L. Kutter. August 2005.
- PEER 2005/03** *A Taxonomy of Building Components for Performance-Based Earthquake Engineering.* Keith A. Porter. September 2005.
- PEER 2005/02** *Fragility Basis for California Highway Overpass Bridge Seismic Decision Making.* Kevin R. Mackie and Božidar Stojadinović. June 2005.
- PEER 2005/01** *Empirical Characterization of Site Conditions on Strong Ground Motion.* Jonathan P. Stewart, Yoojoong Choi, and Robert W. Graves. June 2005.
- PEER 2004/09** *Electrical Substation Equipment Interaction: Experimental Rigid Conductor Studies.* Christopher Stearns and André Filiatrault. February 2005.
- PEER 2004/08** *Seismic Qualification and Fragility Testing of Line Break 550-kV Disconnect Switches.* Shakhzod M. Takhirov, Gregory L. Fenves, and Eric Fujisaki. January 2005.
- PEER 2004/07** *Ground Motions for Earthquake Simulator Qualification of Electrical Substation Equipment.* Shakhzod M. Takhirov, Gregory L. Fenves, Eric Fujisaki, and Don Clyde. January 2005.
- PEER 2004/06** *Performance-Based Regulation and Regulatory Regimes.* Peter J. May and Chris Koski. September 2004.
- PEER 2004/05** *Performance-Based Seismic Design Concepts and Implementation: Proceedings of an International Workshop.* Peter Fajfar and Helmut Krawinkler, editors. September 2004.
- PEER 2004/04** *Seismic Performance of an Instrumented Tilt-up Wall Building.* James C. Anderson and Vitelmo V. Bertero. July 2004.
- PEER 2004/03** *Evaluation and Application of Concrete Tilt-up Assessment Methodologies.* Timothy Graf and James O. Malley. October 2004.
- PEER 2004/02** *Analytical Investigations of New Methods for Reducing Residual Displacements of Reinforced Concrete Bridge Columns.* Junichi Sakai and Stephen A. Mahin. August 2004.

- PEER 2004/01** *Seismic Performance of Masonry Buildings and Design Implications.* Kerri Anne Taeko Tokoro, James C. Anderson, and Vitelmo V. Bertero. February 2004.
- PEER 2003/18** *Performance Models for Flexural Damage in Reinforced Concrete Columns.* Michael Berry and Marc Eberhard. August 2003.
- PEER 2003/17** *Predicting Earthquake Damage in Older Reinforced Concrete Beam-Column Joints.* Catherine Pagni and Laura Lowes. October 2004.
- PEER 2003/16** *Seismic Demands for Performance-Based Design of Bridges.* Kevin Mackie and Božidar Stojadinović. August 2003.
- PEER 2003/15** *Seismic Demands for Nondeteriorating Frame Structures and Their Dependence on Ground Motions.* Ricardo Antonio Medina and Helmut Krawinkler. May 2004.
- PEER 2003/14** *Finite Element Reliability and Sensitivity Methods for Performance-Based Earthquake Engineering.* Terje Haukaas and Armen Der Kiureghian. April 2004.
- PEER 2003/13** *Effects of Connection Hysteretic Degradation on the Seismic Behavior of Steel Moment-Resisting Frames.* Janise E. Rodgers and Stephen A. Mahin. March 2004.
- PEER 2003/12** *Implementation Manual for the Seismic Protection of Laboratory Contents: Format and Case Studies.* William T. Holmes and Mary C. Comerio. October 2003.
- PEER 2003/11** *Fifth U.S.-Japan Workshop on Performance-Based Earthquake Engineering Methodology for Reinforced Concrete Building Structures.* February 2004.
- PEER 2003/10** *A Beam-Column Joint Model for Simulating the Earthquake Response of Reinforced Concrete Frames.* Laura N. Lowes, Nilanjan Mitra, and Arash Altoontash. February 2004.
- PEER 2003/09** *Sequencing Repairs after an Earthquake: An Economic Approach.* Marco Casari and Simon J. Wilkie. April 2004.
- PEER 2003/08** *A Technical Framework for Probability-Based Demand and Capacity Factor Design (DCFD) Seismic Formats.* Fatemeh Jalayer and C. Allin Cornell. November 2003.
- PEER 2003/07** *Uncertainty Specification and Propagation for Loss Estimation Using FOSM Methods.* Jack W. Baker and C. Allin Cornell. September 2003.
- PEER 2003/06** *Performance of Circular Reinforced Concrete Bridge Columns under Bidirectional Earthquake Loading.* Mahmoud M. Hachem, Stephen A. Mahin, and Jack P. Moehle. February 2003.
- PEER 2003/05** *Response Assessment for Building-Specific Loss Estimation.* Eduardo Miranda and Shahram Taghavi. September 2003.
- PEER 2003/04** *Experimental Assessment of Columns with Short Lap Splices Subjected to Cyclic Loads.* Murat Melek, John W. Wallace, and Joel Conte. April 2003.
- PEER 2003/03** *Probabilistic Response Assessment for Building-Specific Loss Estimation.* Eduardo Miranda and Hesameddin Aslani. September 2003.
- PEER 2003/02** *Software Framework for Collaborative Development of Nonlinear Dynamic Analysis Program.* Jun Peng and Kincho H. Law. September 2003.
- PEER 2003/01** *Shake Table Tests and Analytical Studies on the Gravity Load Collapse of Reinforced Concrete Frames.* Kenneth John Elwood and Jack P. Moehle. November 2003.
- PEER 2002/24** *Performance of Beam to Column Bridge Joints Subjected to a Large Velocity Pulse.* Natalie Gibson, André Filiatrault, and Scott A. Ashford. April 2002.
- PEER 2002/23** *Effects of Large Velocity Pulses on Reinforced Concrete Bridge Columns.* Greg L. Orozco and Scott A. Ashford. April 2002.
- PEER 2002/22** *Characterization of Large Velocity Pulses for Laboratory Testing.* Kenneth E. Cox and Scott A. Ashford. April 2002.
- PEER 2002/21** *Fourth U.S.-Japan Workshop on Performance-Based Earthquake Engineering Methodology for Reinforced Concrete Building Structures.* December 2002.
- PEER 2002/20** *Barriers to Adoption and Implementation of PBEE Innovations.* Peter J. May. August 2002.
- PEER 2002/19** *Economic-Engineered Integrated Models for Earthquakes: Socioeconomic Impacts.* Peter Gordon, James E. Moore II, and Harry W. Richardson. July 2002.
- PEER 2002/18** *Assessment of Reinforced Concrete Building Exterior Joints with Substandard Details.* Chris P. Pantelides, Jon Hansen, Justin Nadauld, and Lawrence D. Reaveley. May 2002.

- PEER 2002/17** *Structural Characterization and Seismic Response Analysis of a Highway Overcrossing Equipped with Elastomeric Bearings and Fluid Dampers: A Case Study.* Nicos Makris and Jian Zhang. November 2002.
- PEER 2002/16** *Estimation of Uncertainty in Geotechnical Properties for Performance-Based Earthquake Engineering.* Allen L. Jones, Steven L. Kramer, and Pedro Arduino. December 2002.
- PEER 2002/15** *Seismic Behavior of Bridge Columns Subjected to Various Loading Patterns.* Asadollah Esmaeily-Gh. and Yan Xiao. December 2002.
- PEER 2002/14** *Inelastic Seismic Response of Extended Pile Shaft Supported Bridge Structures.* T.C. Hutchinson, R.W. Boulanger, Y.H. Chai, and I.M. Idriss. December 2002.
- PEER 2002/13** *Probabilistic Models and Fragility Estimates for Bridge Components and Systems.* Paolo Gardoni, Armen Der Kiureghian, and Khalid M. Mosalam. June 2002.
- PEER 2002/12** *Effects of Fault Dip and Slip Rake on Near-Source Ground Motions: Why Chi-Chi Was a Relatively Mild M7.6 Earthquake.* Brad T. Agaard, John F. Hall, and Thomas H. Heaton. December 2002.
- PEER 2002/11** *Analytical and Experimental Study of Fiber-Reinforced Strip Isolators.* James M. Kelly and Shakhzod M. Takhirov. September 2002.
- PEER 2002/10** *Centrifuge Modeling of Settlement and Lateral Spreading with Comparisons to Numerical Analyses.* Sivapalan Gajan and Bruce L. Kutter. January 2003.
- PEER 2002/09** *Documentation and Analysis of Field Case Histories of Seismic Compression during the 1994 Northridge, California, Earthquake.* Jonathan P. Stewart, Patrick M. Smith, Daniel H. Whang, and Jonathan D. Bray. October 2002.
- PEER 2002/08** *Component Testing, Stability Analysis and Characterization of Buckling-Restrained Unbonded Braces™.* Cameron Black, Nicos Makris, and Ian Aiken. September 2002.
- PEER 2002/07** *Seismic Performance of Pile-Wharf Connections.* Charles W. Roeder, Robert Graff, Jennifer Soderstrom, and Jun Han Yoo. December 2001.
- PEER 2002/06** *The Use of Benefit-Cost Analysis for Evaluation of Performance-Based Earthquake Engineering Decisions.* Richard O. Zerbe and Anthony Falit-Baiamonte. September 2001.
- PEER 2002/05** *Guidelines, Specifications, and Seismic Performance Characterization of Nonstructural Building Components and Equipment.* André Filiatrault, Constantin Christopoulos, and Christopher Stearns. September 2001.
- PEER 2002/04** *Consortium of Organizations for Strong-Motion Observation Systems and the Pacific Earthquake Engineering Research Center Lifelines Program: Invited Workshop on Archiving and Web Dissemination of Geotechnical Data, 4–5 October 2001.* September 2002.
- PEER 2002/03** *Investigation of Sensitivity of Building Loss Estimates to Major Uncertain Variables for the Van Nuys Testbed.* Keith A. Porter, James L. Beck, and Rustem V. Shaikhutdinov. August 2002.
- PEER 2002/02** *The Third U.S.-Japan Workshop on Performance-Based Earthquake Engineering Methodology for Reinforced Concrete Building Structures.* July 2002.
- PEER 2002/01** *Nonstructural Loss Estimation: The UC Berkeley Case Study.* Mary C. Comerio and John C. Stallmeyer. December 2001.
- PEER 2001/16** *Statistics of SDF-System Estimate of Roof Displacement for Pushover Analysis of Buildings.* Anil K. Chopra, Rakesh K. Goel, and Chatpan Chintanapakdee. December 2001.
- PEER 2001/15** *Damage to Bridges during the 2001 Nisqually Earthquake.* R. Tyler Ranf, Marc O. Eberhard, and Michael P. Berry. November 2001.
- PEER 2001/14** *Rocking Response of Equipment Anchored to a Base Foundation.* Nicos Makris and Cameron J. Black. September 2001.
- PEER 2001/13** *Modeling Soil Liquefaction Hazards for Performance-Based Earthquake Engineering.* Steven L. Kramer and Ahmed-W. Elgamal. February 2001.
- PEER 2001/12** *Development of Geotechnical Capabilities in OpenSees.* Boris Jeremi . September 2001.
- PEER 2001/11** *Analytical and Experimental Study of Fiber-Reinforced Elastomeric Isolators.* James M. Kelly and Shakhzod M. Takhirov. September 2001.
- PEER 2001/10** *Amplification Factors for Spectral Acceleration in Active Regions.* Jonathan P. Stewart, Andrew H. Liu, Yoojoong Choi, and Mehmet B. Baturay. December 2001.
- PEER 2001/09** *Ground Motion Evaluation Procedures for Performance-Based Design.* Jonathan P. Stewart, Shyh-Jeng Chiou, Jonathan D. Bray, Robert W. Graves, Paul G. Somerville, and Norman A. Abrahamson. September 2001.

- PEER 2001/08** *Experimental and Computational Evaluation of Reinforced Concrete Bridge Beam-Column Connections for Seismic Performance.* Clay J. Naito, Jack P. Moehle, and Khalid M. Mosalam. November 2001.
- PEER 2001/07** *The Rocking Spectrum and the Shortcomings of Design Guidelines.* Nicos Makris and Dimitrios Konstantinidis. August 2001.
- PEER 2001/06** *Development of an Electrical Substation Equipment Performance Database for Evaluation of Equipment Fragilities.* Thalia Agnanos. April 1999.
- PEER 2001/05** *Stiffness Analysis of Fiber-Reinforced Elastomeric Isolators.* Hsiang-Chuan Tsai and James M. Kelly. May 2001.
- PEER 2001/04** *Organizational and Societal Considerations for Performance-Based Earthquake Engineering.* Peter J. May. April 2001.
- PEER 2001/03** *A Modal Pushover Analysis Procedure to Estimate Seismic Demands for Buildings: Theory and Preliminary Evaluation.* Anil K. Chopra and Rakesh K. Goel. January 2001.
- PEER 2001/02** *Seismic Response Analysis of Highway Overcrossings Including Soil-Structure Interaction.* Jian Zhang and Nicos Makris. March 2001.
- PEER 2001/01** *Experimental Study of Large Seismic Steel Beam-to-Column Connections.* Egor P. Popov and Shakhzod M. Takhirov. November 2000.
- PEER 2000/10** *The Second U.S.-Japan Workshop on Performance-Based Earthquake Engineering Methodology for Reinforced Concrete Building Structures.* March 2000.
- PEER 2000/09** *Structural Engineering Reconnaissance of the August 17, 1999 Earthquake: Kocaeli (Izmit), Turkey.* Halil Sezen, Kenneth J. Elwood, Andrew S. Whittaker, Khalid Mosalam, John J. Wallace, and John F. Stanton. December 2000.
- PEER 2000/08** *Behavior of Reinforced Concrete Bridge Columns Having Varying Aspect Ratios and Varying Lengths of Confinement.* Anthony J. Calderone, Dawn E. Lehman, and Jack P. Moehle. January 2001.
- PEER 2000/07** *Cover-Plate and Flange-Plate Reinforced Steel Moment-Resisting Connections.* Taejin Kim, Andrew S. Whittaker, Amir S. Gilani, Vitelmo V. Bertero, and Shakhzod M. Takhirov. September 2000.
- PEER 2000/06** *Seismic Evaluation and Analysis of 230-kV Disconnect Switches.* Amir S. J. Gilani, Andrew S. Whittaker, Gregory L. Fenves, Chun-Hao Chen, Henry Ho, and Eric Fujisaki. July 2000.
- PEER 2000/05** *Performance-Based Evaluation of Exterior Reinforced Concrete Building Joints for Seismic Excitation.* Chandra Clyde, Chris P. Pantelides, and Lawrence D. Reaveley. July 2000.
- PEER 2000/04** *An Evaluation of Seismic Energy Demand: An Attenuation Approach.* Chung-Che Chou and Chia-Ming Uang. July 1999.
- PEER 2000/03** *Framing Earthquake Retrofitting Decisions: The Case of Hillside Homes in Los Angeles.* Detlof von Winterfeldt, Nels Roselund, and Alicia Kitsuse. March 2000.
- PEER 2000/02** *U.S.-Japan Workshop on the Effects of Near-Field Earthquake Shaking.* Andrew Whittaker, ed. July 2000.
- PEER 2000/01** *Further Studies on Seismic Interaction in Interconnected Electrical Substation Equipment.* Armen Der Kiureghian, Kee-Jeung Hong, and Jerome L. Sackman. November 1999.
- PEER 1999/14** *Seismic Evaluation and Retrofit of 230-kV Porcelain Transformer Bushings.* Amir S. Gilani, Andrew S. Whittaker, Gregory L. Fenves, and Eric Fujisaki. December 1999.
- PEER 1999/13** *Building Vulnerability Studies: Modeling and Evaluation of Tilt-up and Steel Reinforced Concrete Buildings.* John W. Wallace, Jonathan P. Stewart, and Andrew S. Whittaker, editors. December 1999.
- PEER 1999/12** *Rehabilitation of Nonductile RC Frame Building Using Encasement Plates and Energy-Dissipating Devices.* Mehrdad Sasaki, Vitelmo V. Bertero, James C. Anderson. December 1999.
- PEER 1999/11** *Performance Evaluation Database for Concrete Bridge Components and Systems under Simulated Seismic Loads.* Yael D. Hose and Frieder Seible. November 1999.
- PEER 1999/10** *U.S.-Japan Workshop on Performance-Based Earthquake Engineering Methodology for Reinforced Concrete Building Structures.* December 1999.
- PEER 1999/09** *Performance Improvement of Long Period Building Structures Subjected to Severe Pulse-Type Ground Motions.* James C. Anderson, Vitelmo V. Bertero, and Raul Bertero. October 1999.
- PEER 1999/08** *Envelopes for Seismic Response Vectors.* Charles Menun and Armen Der Kiureghian. July 1999.
- PEER 1999/07** *Documentation of Strengths and Weaknesses of Current Computer Analysis Methods for Seismic Performance of Reinforced Concrete Members.* William F. Cofer. November 1999.

- PEER 1999/06** *Rocking Response and Overturning of Anchored Equipment under Seismic Excitations.* Nicos Makris and Jian Zhang. November 1999.
- PEER 1999/05** *Seismic Evaluation of 550 kV Porcelain Transformer Bushings.* Amir S. Gilani, Andrew S. Whittaker, Gregory L. Fenves, and Eric Fujisaki. October 1999.
- PEER 1999/04** *Adoption and Enforcement of Earthquake Risk-Reduction Measures.* Peter J. May, Raymond J. Burby, T. Jens Feeley, and Robert Wood.
- PEER 1999/03** *Task 3 Characterization of Site Response General Site Categories.* Adrian Rodriguez-Marek, Jonathan D. Bray, and Norman Abrahamson. February 1999.
- PEER 1999/02** *Capacity-Demand-Diagram Methods for Estimating Seismic Deformation of Inelastic Structures: SDF Systems.* Anil K. Chopra and Rakesh Goel. April 1999.
- PEER 1999/01** *Interaction in Interconnected Electrical Substation Equipment Subjected to Earthquake Ground Motions.* Armen Der Kiureghian, Jerome L. Sackman, and Kee-Jeung Hong. February 1999.
- PEER 1998/08** *Behavior and Failure Analysis of a Multiple-Frame Highway Bridge in the 1994 Northridge Earthquake.* Gregory L. Fenves and Michael Ellery. December 1998.
- PEER 1998/07** *Empirical Evaluation of Inertial Soil-Structure Interaction Effects.* Jonathan P. Stewart, Raymond B. Seed, and Gregory L. Fenves. November 1998.
- PEER 1998/06** *Effect of Damping Mechanisms on the Response of Seismic Isolated Structures.* Nicos Makris and Shih-Po Chang. November 1998.
- PEER 1998/05** *Rocking Response and Overturning of Equipment under Horizontal Pulse-Type Motions.* Nicos Makris and Yiannis Roussos. October 1998.
- PEER 1998/04** *Pacific Earthquake Engineering Research Invitational Workshop Proceedings, May 14–15, 1998: Defining the Links between Planning, Policy Analysis, Economics and Earthquake Engineering.* Mary Comerio and Peter Gordon. September 1998.
- PEER 1998/03** *Repair/Upgrade Procedures for Welded Beam to Column Connections.* James C. Anderson and Xiaojing Duan. May 1998.
- PEER 1998/02** *Seismic Evaluation of 196 kV Porcelain Transformer Bushings.* Amir S. Gilani, Juan W. Chavez, Gregory L. Fenves, and Andrew S. Whittaker. May 1998.
- PEER 1998/01** *Seismic Performance of Well-Confined Concrete Bridge Columns.* Dawn E. Lehman and Jack P. Moehle. December 2000.

ONLINE REPORTS

The following PEER reports are available by Internet only at http://peer.berkeley.edu/publications/peer_reports.html

PEER 2007/101 *Generalized Hybrid Simulation Framework for Structural Systems Subjected to Seismic Loading.* Tarek Elkhoraibi and Khalid M. Mosalam. July 2007.

PEER 2007/100 *Seismic Evaluation of Reinforced Concrete Buildings Including Effects of Masonry Infill Walls.* Alidad Hashemi and Khalid M. Mosalam. July 2007.